

COMPUTATION OF  
MOLECULAR WAVE FUNCTIONS IN TERMS  
OF LOCALISED MOLECULAR ORBITALS

by Colin John Matthews.

A thesis presented to the Faculty of  
Science of the University of London  
in candidature for the degree of  
Doctor of Philosophy.

The Bourne Laboratory,  
Royal Holloway College,  
(University of London),  
Egham Hill,  
Egham,  
Surrey  
TW20 OEX



August 1982.

ProQuest Number: 10097516

All rights reserved

INFORMATION TO ALL USERS

The quality of this reproduction is dependent upon the quality of the copy submitted.

In the unlikely event that the author did not send a complete manuscript and there are missing pages, these will be noted. Also, if material had to be removed, a note will indicate the deletion.



ProQuest 10097516

Published by ProQuest LLC(2016). Copyright of the Dissertation is held by the Author.

All rights reserved.

This work is protected against unauthorized copying under Title 17, United States Code.  
Microform Edition © ProQuest LLC.

ProQuest LLC  
789 East Eisenhower Parkway  
P.O. Box 1346  
Ann Arbor, MI 48106-1346

ABSTRACT

A preliminary investigation of a new Localised Molecular Orbital (LMO) method is presented and applied to the molecules HCN, CO, N<sub>2</sub>, H<sub>2</sub>O, NH<sub>3</sub> and CH<sub>4</sub>. The LMOs are called Perfectly Localised Molecular Orbitals (PLMOs) and are obtained in the one-determinant Hartree-Fock Molecular Orbital-Linear Combination of Atomic Orbitals (MO-LCAO) approximation in a minimal AO basis.

The PLMOs are obtained from a starting set of occupied Canonical Molecular Orbitals (CMOs) by applying a general orthogonal transformation to the sigma valence CMOs and by minimising the energy sacrificed in restricting the transformed MOs to basis AOs on one and two centres only. The atomic centres upon and between which the lone pair and bond PLMOs reside is decided largely by an energy criterion alone. The resulting set of PLMOs are non-orthogonal.

In the example molecules, the energy difference between the canonical wavefunction and that constructed from the PLMOs is found to be small. The PLMOs, expressed in terms of normalised hybrid atomic orbitals (HAOs) on each atom, are found to reflect a normal valence description of the molecules in which the overall level of hybridisation is low. This is possible because a substantial degree of non-orthogonality among the HAOs on each atom is found. The PLMOs yield satisfactory bond and lone pair moments and electronic populations, and are also shown to have a satisfactory behaviour at non-experimental geometries of the water molecule.

It is concluded that the small sacrifice in accuracy that results from completely localising LMOs by the PLMO method is outweighed by the advantages of dealing with one and two-centre LMOs. It is also suggested that the differences in the properties of LMOs generated by different orthogonal transformation criteria is dependent on the relative amounts of delocalisation from bond and lone pair LMOs.

ACKNOWLEDGEMENTS

The author is deeply indebted to his supervisor, Dr. D. Peters, for much help and encouragement both during and after his study at Royal Holloway College.

The work described in this thesis was supported by a Science Research Council Studentship grant. The author wishes to thank his friends and ex-colleagues in the Bourne Laboratory for their aid and co-operation and especially for their computing knowledge.

Finally, the author is also indebted to Joan Dunn for typing the thesis, and to his wife for her patience.

DEDICATION

To Hazel.

## CONTENTS

|  | page |
|--|------|
| List of Tables   | 12   |
| List of Figures  | 19   |
| <u>PART A INTRODUCTION</u>   | 21   |
| <u>Chapter One General Introduction</u>  | 22   |
| 1.1 Introductory Remarks   | 22   |
| 1.2 Molecular Orbital Theory and Local Regions<br>in Molecules                       | 26   |
| 1.3 Objectives of the Present Work   | 27   |
| 1.3(a) Generation of PLMOs   | 28   |
| 1.3(b) Desired properties of the PLMOs   | 30   |
| <u>Chapter Two Historical Survey: Existing LMO Methods</u>                           | 34   |
| 2.1 Introduction   | 34   |
| 2.2 Relocalisation Methods   | 34   |
| 2.2(a) Historical Introduction   | 34   |
| 2.2(b) Intrinsic Methods   | 35   |
| 2.2(c) "Cut-off" Methods   | 37   |
| 2.2(d) Population Methods  | 38   |
| 2.2(e) Projection Methods  | 38   |
| 2.2(f) Density Matrix Methods  | 39   |
| 2.3 Direct Methods   | 39   |
| 2.3(a) Introduction  | 39   |
| 2.3(b) Adams-Gilbert Formalism   | 40   |
| 2.3(c) Related Methods   | 41   |
| 2.4 Hybrid Methods   | 42   |
| 2.4(a) Introduction  | 42   |
| 2.4(b) Maximum Overlap Methods   | 43   |
| 2.4(c) Energy Optimisation Methods   | 44   |
| 2.4(d) Other Methods   | 46   |
| <u>Chapter Three Orthogonal and Non-Orthogonal Atomic<br/>and Molecular Orbitals</u> | 48   |
| 3.1 Molecular Orbitals   | 48   |
| 3.2 Hybrid Atomic Orbitals   | 53   |

|  | page |
|--|------|
| 3.2(a) Hybridisation   | 53   |
| 3.2(b) Orthogonality and the description of bonding  | 54   |
| 3.2(c) The Directional Properties of Hybrids   | 56   |
| <br>   |      |
| <u>PART B PLMO METHOD AND RESULTS</u>  | 58   |
| <br>   |      |
| <u>Chapter Four Illustration of PLMO Method - Example of HCN</u>   | 59   |
| 4.1 Introduction   | 59   |
| 4.1(a) Outline of Method   | 59   |
| 4.1(b) Investigation of HCN  | 60   |
| 4.2 Preliminaries  | 60   |
| 4.3 PLMO Method as Exemplified by HCN  | 62   |
| 4.3(a) Separation of CMOs  | 62   |
| 4.3(b) "Structure" specification   | 62   |
| 4.3(c) Orthogonal Transformation   | 65   |
| 4.3(d) Truncation  | 66   |
| 4.3(e) Orthonormalisation  | 66   |
| 4.3(f) Electronic Energy Calculation   | 66   |
| 4.3(g) Iteration to an energy minimum  | 67   |
| 4.4 Energy Diagrams and LMOs for HCN   | 67   |
| 4.5 Choosing the PLMO structure  | 77   |
| 4.6 Properties of the PLMOs  | 78   |
| 4.7 Comments on the Method   | 81   |
| 4.7(a) Separation of CMOs  | 81   |
| 4.7(b) Orthogonal Transformation and Truncation  | 82   |
| <br>   |      |
| <u>Chapter Five Examples of PLMO method - CO, N<sub>2</sub>, H<sub>2</sub>O, NH<sub>3</sub> &amp; CH<sub>4</sub></u> | 84   |
| 5.1 Introduction   | 84   |
| 5.2 Preliminaries  | 84   |
| 5.3 Energy Diagrams and LMOs   | 84   |
| 5.4 Choosing the PLMO Structures   | 97   |
| 5.5 PLMO Overlap Integrals   | 103  |
| 5.6 Summary  | 107  |



|  | page |
|--|------|
| <u>Chapter Six</u> <u>Electric Dipole Moment Analysis</u>          | 108  |
| 6.1 Introduction   | 108  |
| 6.2 Bond and Lone Pair Moments                                     | 108  |
| 6.3 Results for Example Molecules                                  | 111  |
| <br>   |      |
| <u>PART C</u> <u>DISCUSSION AND INTERPRETATION OF RESULTS -</u>    |      |
| <u>POPULATION ANALYSIS</u>   | 129  |
| <u>Chapter Seven</u> <u>Energy Diagrams</u>                        | 130  |
| 7.1 Introduction   | 130  |
| 7.2 Composition of the Diagrams                                    | 130  |
| 7.2(a) Significance of the Energies                                | 130  |
| 7.2(b) Overlaps with CMO Wavefunction                              | 132  |
| 7.3 PLMO Delocalisation Energy - Comparison to<br>Other Methods    | 133  |
| <br>   |      |
| <u>Chapter Eight</u> <u>Forms of PLMOs and Population Analysis</u> | 141  |
| 8.1 Electron Population Analysis                                   | 141  |
| 8.2 Hybridisation and Population Analysis of Molecules             | 142  |
| 8.2(a) HCN   | 142  |
| 8.2(b) CO  | 145  |
| 8.2(c) N <sub>2</sub>  | 147  |
| 8.2(d) H <sub>2</sub> O  | 147  |
| 8.2(e) NH <sub>3</sub>   | 151  |
| 8.2(f) CH <sub>4</sub>   | 151  |
| 8.2(g) Summary   | 154  |
| 8.3 PLMO Overlap Integrals   | 156  |
| 8.4 Discussion and Comparison with other Work                      | 157  |
| 8.4(a) Overall Significance of PLMO Results                        | 157  |
| 8.4(b) Comparison of PLMOs to LMOs Obtained<br>by Other Methods    | 158  |
| 8.4(b)(i) Forms of LMOs  | 158  |
| 8.4(b)(ii) Summary   | 168  |
| 8.4(b)(iii) "Bent" bonds   | 170  |
| 8.4(c) Hybridisation Trends  | 171  |
| 8.4(d) PLMO Overlap Integrals                                      | 178  |
| <br>   |      |
| <u>Chapter Nine</u> <u>Bond and Lone Pair Moments</u>              | 182  |
| 9.1 Total Dipole Moments and PLMO Components                       | 182  |
| 9.2 Comparison to Other Authors                                    | 189  |



|   | page |
|---|------|
| I.2(a) Definitions and Properties                                     | 234  |
| I.2(b) Expansion of Density Functions in Terms<br>of an Orbital Basis | 237  |
| I.2(b)(i) Spin-Orbital Basis  | 237  |
| I.2(b)(ii) Doubly Occupied MO Basis                                   | 239  |
| I.2(b)(iii) Non-Orthogonal Atomic Orbital<br>Basis                    | 239  |
| I.3 Energy of a Closed Shell System                                   | 240  |
| I.4 SCF Solutions to Schrodingers Equation                            | 242  |
| I.4(a) Hartree-Fock MOs   | 242  |
| I.4(b) LCAO-MO Approximation  | 243  |
| I.4(c) The Forms of the Atomic Orbitals                               | 245  |
| I.5 Dipole Moments  | 247  |
| I.6 Electron Population Analysis                                      | 251  |
| I.7 Methods of Orthogonalisation                                      | 253  |
| <br>  |      |
| <u>Appendix II</u> <u>Computational Details</u>                       | 257  |
| II.1 Gaussian Seventy   | 257  |
| II.2 ENLOC7   | 258  |
| II.2(a) Preliminaries   | 258  |
| II.2(b) Energy Minimisation   | 261  |
| II.2(b)(i) Transformation, Truncation<br>and Testing                  | 262  |
| II.2(b)(ii) Energy Calculation  | 263  |
| II.2(c) Endpoint LMOs   | 264  |
| II.2(d) Computing Time  | 265  |
| II.3 Bond and Angle Deformation in Water                              | 266  |
| <br>  |      |
| <u>Appendix III</u> <u>Abbreviations and Symbols Used</u>             | 268  |
| <br>  |      |
| <u>References</u>   | 275  |

LISTS OF TABLES AND FIGURES

LIST OF TABLES

- 4.1 Geometry and co-ordinate system for HCN
- 4.2 Occupied CMOs and eigenvalues for HCN (STO-3G basis)
- 4.3 Occupied CMOs and eigenvalues for HCN (STO-5G basis)
- 4.4 Inner shells, pi orbitals and LMOs for low energy structures for HCN (STO-3G basis)
- 4.5 Inner shells, pi orbitals and LMOs for low energy structures for HCN (STO-5G basis)
- 4.6 Inner shells (truncated), pi orbitals and LMOs for low energy structures for HCN (STO-3G basis)
- 4.7 Absolute values of overlap integrals between sigma PLMOs (inc. inner shells) for HCN and  $\Delta$  function (STO-3G basis)
- 4.8 Absolute values of overlap integrals between sigma PLMOs (inc. inner shells) for HCN and  $\Delta$  function (STO-5G basis)
- 4.9 Absolute values of overlap integrals between sigma PLMOs (inc. truncated inner shells) for HCN and  $\Delta$  function (STO-3G basis)
  
- 5.1 Geometry and co-ordinate system for CO
- 5.2 Geometry and co-ordinate system for N<sub>2</sub>
- 5.3 Geometry and co-ordinate system for H<sub>2</sub>O
- 5.4 Geometry and co-ordinate system for NH<sub>3</sub>
- 5.5 Geometry and co-ordinate system for CH<sub>4</sub>

- 5.6 Occupied CMOs and eigenvalues for CO (STO-3G basis)
- 5.7 Occupied CMOs and eigenvalues for N<sub>2</sub> (STO-3G basis)
- 5.8 Occupied CMOs and eigenvalues for H<sub>2</sub>O (STO-3G basis)
- 5.9 Occupied CMOs and eigenvalues for NH<sub>3</sub> (STO-3G basis)
- 5.10 Occupied CMOs and eigenvalues for CH<sub>4</sub> (STO-3G basis)
- 5.11 Inner shells, pi orbitals and LMOs for low energy structures for CO (STO-3G basis)
- 5.12 Inner shells, pi orbitals and LMOs for low energy structures for N<sub>2</sub> (STO-3G basis)
- 5.13 Inner shells, pi orbitals and LMOs for low energy structures for H<sub>2</sub>O (STO-3G basis)
- 5.14 Inner shell and LMOs for low energy structures for NH<sub>3</sub> (STO-3G basis)
- 5.15 Inner shell and LMOs for low energy structures for CH<sub>4</sub> (STO-3G basis)
- 5.16 Absolute values of overlap integrals between sigma PLMOs (inc. inner shells) of CO and Δ function (STO-3G basis)
- 5.17 Absolute values of overlap integrals between sigma PLMOs (inc. inner shells) of N<sub>2</sub> and Δ function (STO-3G basis)
- 5.18 Absolute values of overlap integrals between sigma PLMOs (inc. inner shells) of H<sub>2</sub>O and Δ function (STO-3G basis)
- 5.19 Absolute values of overlap integrals between sigma PLMOs (inc. inner shells) of NH<sub>3</sub> and Δ function (STO-3G basis)

- 5.20 Absolute values of overlap integrals between sigma PLMOs (inc. inner shells) of  $\text{CH}_4$  and  $\Delta$  function (STO-3G basis)
- 6.1 Dipole moment analysis in terms of PLMOs for HCN (STO-3G basis)
- 6.2 Dipole moment analysis in terms of PLMOs for HCN (STO-5G basis)
- 6.3 Dipole moment analysis in terms of PLMOs for HCN (inner shells truncated) (STO-3G basis)
- 6.4 Dipole moment analysis in terms of PLMOs for CO (STO-3G basis)
- 6.5 Dipole moment analysis in terms of PLMOs for  $\text{N}_2$  (STO-3G basis)
- 6.6 Dipole moment analysis in terms of PLMOs for  $\text{H}_2\text{O}$  (z component) (STO-3G basis)
- 6.7 Dipole moment analysis in terms of PLMOs for  $\text{H}_2\text{O}$  (x component) (STO-3G basis)
- 6.8 Dipole moment analysis in terms of PLMOs for  $\text{NH}_3$  (z component) (STO-3G basis)
- 6.9 Dipole moment analysis in terms of PLMOs for  $\text{NH}_3$  (x component) (STO-3G basis)
- 6.10 Dipole moment analysis in terms of PLMOs for  $\text{NH}_3$  (y component) (STO-3G basis)
- 6.11 Dipole moment analysis in terms of PLMOs for  $\text{CH}_4$  (z component) (STO-3G basis)

- 6.12 Dipole moment analysis in terms of PLMOs for  $\text{CH}_4$  (x component) (STO-3G basis)
- 6.13 Dipole moment analysis in terms of PLMOs for  $\text{CH}_4$  (y component) (STO-3G basis)
- 7.1 Comparison of PLMO delocalisation energy in HCN with that sacrificed in other methods that yield one and two-centre LMOs
- 7.2 Comparison of PLMO delocalisation energy in CO with that sacrificed in other methods that yield one and two-centre LMOs.
- 7.3 Comparison of PLMO delocalisation energy in  $\text{H}_2\text{O}$  with that sacrificed in other methods that yield one and two-centre LMOs
- 7.4 Comparison of PLMO delocalisation energy in  $\text{NH}_3$  with that sacrificed in other methods that yield one and two-centre LMOs.
- 7.5 Comparison of PLMO delocalisation energy in  $\text{CH}_4$  with that sacrificed in other methods that yield one and two-centre LMOs
- 8.1 Electron populations of AOs in PLMOs for HCN (STO-3G basis)
- 8.2 Electron populations of AOs in PLMOs for CO (STO-3G basis)
- 8.3 Electron populations of AOs in PLMOs for  $\text{N}_2$  (STO-3G basis)



- 8.4 Electron populations of AOs in PLMOs for H<sub>2</sub>O  
(STO-3G basis)
- 8.5 Electron populations of AOs in PLMOs for NH<sub>3</sub>  
(STO-3G basis)
- 8.6 Electron populations of AOs in PLMOs for CH<sub>4</sub>  
(STO-3G basis)
- 8.7 Comparison of valence sigma PLMOs of HCN  
(STO-3G basis) to LMOs of other methods
- 8.8 Comparison of valence sigma PLMOs of CO  
(STO-3G basis) to LMOs of other methods.
- 8.9 Comparison of valence sigma PLMOs of N<sub>2</sub>  
(STO-3G basis) to LMOs of other methods.
- 8.10 Comparison of valence sigma PLMOs of H<sub>2</sub>O  
(STO-3G basis) to LMOs of other methods.
- 8.11 Comparison of valence sigma PLMOs of NH<sub>3</sub>  
(STO-3G basis) to LMOs of other methods.
- 8.12 Comparison of valence sigma PLMOs of CH<sub>4</sub>  
(STO-3G basis) to LMOs of other methods.
- 8.13 Absolute values of overlap integrals between  
normalised Valence HAOs on the same atom  
for the example molecules.
- 8.14 "Bent bonds" in water and ammonia from different  
LMO methods
- 8.15 Comparison of bond PLMOs in CH<sub>4</sub>, NH<sub>3</sub> and H<sub>2</sub>O
- 8.16 Comparison of lone pair PLMOs in CO and N<sub>2</sub>
- 8.17 Comparison of bonding HAOs in CO and N<sub>2</sub>

- 9.1 Non-zero total dipole moments of the example molecules (STO-3G basis)
- 9.2 Contributions to the total dipole moments of the PLMO wavefunctions of the example molecules (STO-3G basis)
- 9.3 Sum of absolute values of diagonal and off-diagonal electronic contributions to the dipole moments of the PLMO wavefunctions of the example molecules (STO-3G basis)
- 9.4 Comparison of PLMO bond and lone pair moments of HCN to those of other methods.
- 9.5 Comparison of PLMO bond and lone pair moments of CO to those of other methods
- 9.6 Comparison of PLMO bond and lone pair moments of H<sub>2</sub>O to those of other methods.
- 9.7 Comparison of PLMO bond and lone pair moments of NH<sub>3</sub> to those of other methods.
- 9.8 Comparison of PLMO bond moments of CH<sub>4</sub> to those of other methods.
  
- 10.1 Truncated and renormalised inner shell CMOs of the example molecules (STO-3G basis)
- 10.2 Lone pair PLMOs of the example molecules (STO-3G basis)
- 10.3 C-H bond PLMOs in the example molecules (STO-3G basis)
- 10.4 Bonding nitrogen HAOs in N<sub>2</sub> and HCN (STO-3G basis)

- 11.1 Positions and values of energy minima in the CMO and PLMO wavefunctions of  $H_2O$  (STO-3G basis)
  - 11.2 Force constants for bond and angle deformation in  $H_2O$  (STO-3G basis)
  - 11.3 PLMOs and PLMO moments during stretch of  $O-H_1$  bond in  $H_2O$  (STO-3G basis)
  - 11.4 PLMOs and PLMO moments during angle deformation in  $H_2O$  (STO-3G basis)
  - 11.5 Molecular dipole moment during stretch of  $O-H_1$  bond in  $H_2O$  (STO-3G basis)
  - 11.6 Molecular dipole moment and direction of bonding hybrids during angle deformation in  $H_2O$  (STO-3G basis)
- 
- II.1 Processing resources required to obtain an energy minimum for the PLMOs of each molecule.

LIST OF FIGURES

- 4.1 Energy diagram for LMO structures in sigma frame of HCN (STO-3G basis)
- 4.2 Energy diagram for LMO structures in sigma frame of HCN (STO-5G basis)
- 4.3 Energy diagram for LMO structures in sigma frame of HCN with inner shells truncated (STO-3G basis)
- 5.1 Energy diagram for LMO structures in sigma frame of CO (STO-3G basis)
- 5.2 Energy diagram for LMO structures in sigma frame of N<sub>2</sub> (STO-3G basis)
- 5.3 Energy diagram for LMO structures in sigma frame of H<sub>2</sub>O (STO-3G basis)
- 5.4 Energy diagram for LMO structures in sigma frame of NH<sub>3</sub> (STO-3G basis)
- 5.5 Energy diagram for LMO structures in sigma frame of CH<sub>4</sub> (STO-3G basis)
- 6.1 Bond and lone pair moments for HCN (STO-3G basis)
- 6.2 Bond and lone pair moments for CO (STO-3G basis)
- 6.3 Bond and lone pair moments for N<sub>2</sub> (STO-3G basis)
- 6.4 Bond and lone pair moments for H<sub>2</sub>O (STO-3G basis)
- 6.5 Bond and lone pair moments for NH<sub>3</sub> (STO-3G basis)
- 6.6 Bond moments for CH<sub>4</sub> (STO-3G basis)

- 8.1 Direction of bonding hybrids of oxygen in water
  - 8.2 Direction of bonding hybrids of nitrogen in ammonia
  - 8.3 Valence sigma HAOs in the PLMOs of the example molecules.
- 
- II.1 Flow-diagram of ENLOC7
  - II.2 Flow-diagram of subroutine FUNCT

PART A

INTRODUCTION

CHAPTER ONEGENERAL INTRODUCTION1.1 INTRODUCTORY REMARKS

The electronic structure and properties of any molecule may be determined in principle by solution of Schrodinger's (time-independent) equation.<sup>1</sup> The wavefunction, which describes the electronic state of the molecule and is a solution of Schrodinger's equation is a function of the co-ordinates of all the nuclei and electrons in the molecule. In order to actually compute solutions of the Schrodinger equation for most molecules a number of well documented approximations have to be made, and methods of describing the electronic structure of molecules (such as the Molecular Orbital and Valence Bond Methods) are well known. What is ultimately of interest to chemists however, is that the electronic distribution in molecules may be determined by quantum mechanical means and that the structure and reactivity of molecules can be understood in terms of this electron distribution. It is fortunate therefore, that it is not necessary to understand the intricacies of the construction of elaborate wavefunctions in order to describe the physical situation in a molecule. The physically essential features of an electron distribution may be understood in terms of a small number of density functions<sup>2-8</sup> of which the most familiar is simply the electron density. Thus for many (but not all) purposes the electron distribution may be treated as a 'charge cloud' without loss of rigour.

From a quantum mechanical point of view, each molecular calculation, even those on slightly different conformations of the same molecule, are entirely independent. Also, the electron density obtained from such calculations is found to be 'smeared out' over the entire

molecule - the electrons appear like an unstructured sea surrounding the fixed nuclei. In contrast to this, in chemistry, some molecules are considered to be related in structure (e.g. a homologous series of hydrocarbons) and the properties of molecules are understood not in isolation, but in relation to other molecules that are thought of as having a similar structure or organisation. Hence a molecular system in chemistry is understood in terms of its parts: chemical bonds and functional groups which are often believed to behave in a similar manner in different molecules i.e. to be transferable from molecule to molecule.

These two approaches to the description of molecular structure may be resolved by a quantum mechanical picture of a molecule in which the total electron density is broken up into parts. In this way the quantum chemist may search for subunits of a molecular wavefunction with which to identify standard molecular components such as bonds e.g. carbon-hydrogen bonds, lone pairs, e.g. on N in Ammonia, and functional groups e.g. carboxylic groups, and hence make a bridge between classical chemical ideas and quantum mechanics.<sup>9</sup> This bridge is attempted in a number of different 'local' theories, each one of which attempts in a different way, and at differing levels of mathematical rigour, to promote the understanding of local regions in molecules. Some of these methods can be briefly mentioned at this point.

Bader and co-workers<sup>10-16</sup> have developed a method of partitioning a molecule into regions defined by saddle points in the electron density, where each such region satisfies the virial theorem and is quantum mechanically separable from its environment. Such 'virial



fragments' can be used to characterise the type of bonding in an isoelectronic series<sup>10</sup> and to interpret the charge and energy changes in nucleophilic displacement reactions<sup>15</sup> for example. Another, related<sup>17</sup> method of testing the localisability of electrons is the Loge theory.<sup>18</sup> Here, the three dimensional space of the molecule is portioned into non-overlapping volumes or 'loges' defined by the minimisation of a missing information function. The 'best' loges are generally found to be those which localise pairs of electrons in regions of space associated with core, bonded and non-bonded electrons and are hence labelled 'core', 'bond', and 'lone pair loges'.

A molecular wavefunction may be expressed in terms of the molecules' constituent electron groups by the use of 'Generalised Product functions' (or 'Group functions').<sup>19</sup> In this method each electron group is described by its own antisymmetric wavefunction and the molecular wavefunction, in turn, may be expressed in terms of these 'group functions'. If an intelligent choice of the electrons comprising each group can be made and the groups are only weakly interacting then an antisymmetric product of group functions may represent quite an accurate wavefunction for the molecule. Such an 'intelligent' choice of groups for a molecule with a well-defined valence structure may be found to be inner shell, bonding and non-bonding electron pair functions or 'geminals'.

The theory of 'group functions' contains within it the more familiar Molecular Orbital Theory (see Appendix I) as a special case. In an MO (Molecular Orbital) treatment each 'group' consists of a single electron described by a spin-orbital, and the molecular wavefunction at the Hartree-Fock level of approximation, consists of an anti-

symmetrised product (or determinant) of variationally optimised spin-orbitals. These MOs, which are obtained as solutions to an eigenvalue equation, are not uniquely defined however and the standard delocalised canonical molecular orbitals (CMOs) may be transformed into localised molecular orbitals (LMOs) which can represent in the MO approximation the inner shells, bonds and lone pairs already defined. Alternatively, LMOs for many molecules can be built up from atomic orbitals without reference to any previously obtained CMOs by simply using chemical intuition and experience as starting points in a number of simpler procedures.

Finally, the Valence Bond (VB) theory of molecular structure<sup>22,20</sup> - which was historically one of the earliest theories to be developed<sup>21</sup> - is closely tied to chemical ideas of structure. It has, as its basis, the idea that molecular formation arises from the bringing together of complete atoms which are then allowed to interact. Thus the stabilising electron density between 'bonded' atoms in a molecule is obtained by the association of valence orbitals on adjacent atoms in pairs, the electrons, being of antiparallel spin. This clearly reflects, in a mathematical sense, the chemical idea of a two-centre bond largely independent of all but the two atoms concerned. VB methods of various sorts have been developed over the years but have lost in popularity to MO methods. Valence Bond calculations can still be used successfully however to investigate the properties of local regions in molecules.<sup>23,24</sup>

To summarise the above comments, it is clear that there are a number of different but related approaches to the understanding of chemical concepts through quantum mechanics. Of those mentioned, the most popular and well-developed is probably the method of molecular orbitals and it is that method which is used as a basis of this work. The theory of localised molecular orbitals is introduced in the next part of this chapter.

## 1.2 MOLECULAR ORBITAL THEORY AND LOCAL REGIONS IN MOLECULES

The two main viewpoints of the electron organisation in a molecule that were mentioned in the previous section are mirrored within molecular orbital (MO) theory itself. The delocalised nature of a molecular electronic distribution is reflected in the canonical MOs (CMOs) while the alternative local picture is given by localised MOs (LMOs). The method of MOs at the Hartree-Fock level in the one-determinant approximation, and the method of solution of the Hartree-Fock eigenvalue equation yielding CMOs in Linear Combination of Atomic Orbital (LCAO) form are given in Appendix I.

The CMOs belong to irreducible representations of the molecular symmetry group and are in general delocalised over the entire molecule. In other words, in the LCAO form the delocalised CMOs have significant contributions from atomic orbitals on atoms in all parts of the molecule. Some properties of molecules are most usefully interpreted in terms of the CMOs, for example those properties which relate to the molecule as a whole. The common examples are ionization and electronic excitation phenomena.<sup>25,26</sup> In the former case the electron removed by ionization may be considered to be removed from the CMO with the highest orbital energy and the excited states of a molecule are sometimes found to correspond to electron excitations from occupied to 'virtual' ground state CMOs. This last point cannot be demonstrated formally but it is sometimes true in an approximate sense.

For other chemical properties however, which are essentially understood in terms of local regions in molecules such as two-centre bonds, the delocalised CMOs do not provide the necessary analytical basis and these properties may be understood instead within the MO

theory in terms of LMOs. LMOs, in contrast to CMOs, only have appreciable amplitudes in small, well-defined regions of a molecule. In LCAO form an LMO usually has significant contributions from atomic orbitals on one or two atoms, representing a lone pair of electrons or a two-centre bond respectively. Besides corresponding to classical chemical concepts, LMOs serve as a theoretical basis for the analysis of bond energies,<sup>27-30</sup> rotational barriers,<sup>31</sup> NMR coupling constants,<sup>32</sup> bond moments,<sup>33</sup> and the transferability of structural subunits between similar molecules.<sup>34</sup> Moreover, LMOs can be used as intermediate functions in more complicated quantum mechanical calculations such as those involved with Configuration Interaction (CI).<sup>35</sup>

The many different methods by which LMOs may be obtained: from CMOs, or directly from modified eigenvalue equations, or by combination of hybrid atomic orbitals, are outlined in the next chapter. This great variety of different methods implies that no one method is generally accepted or is clearly satisfactory, particularly in the sense of being free from arbitrariness. The generation of unique LMOs by a new, simple prescription forms the basis of the rest of this work.

### 1.3 OBJECTIVES OF THE PRESENT WORK

In this work is presented a preliminary investigation of a new LMO method. The development and interpretation of the method has been undertaken from a chemical viewpoint rather than a mathematical one. The objective has not been to treat a chemistry problem by a mathematically exact method with maximal accuracy but instead to attribute a deeper meaning and justification to the concepts and models chemistry has already developed. What follows therefore is a test of the applicability of the chemical concepts of lone pairs, two-centre bonds

and directed valence to LMO theory. The work's objective may be formally stated as: To investigate the extent to which the electronic structure of simple molecules - obtained via the one-determinant Hartree-Fock MO-LCAO scheme in a minimal basis - may be expressed in terms of two-centre bond and one-centre lone pair PLMOs.

### 1.3(a) Generation of PLMOs

The new LMO method presented in this work is that of Perfectly Localised Molecular Orbitals (PLMOs) and it is explained in detail in Part B. The essential elements of the procedure are outlined here.

The PLMOs are constrained to be perfectly localised in LCAO form by Atomic Orbital (AO) basis truncation. The localised orbitals are not obtained as solutions to an eigenvalue equation but are generated, from a set of previously determined CMOs, as an endpoint to an energy minimisation procedure. The method is applied only to the sigma CMOs, the pi molecular orbitals are left in their canonical form. Given a geometrical arrangement of atoms in a molecule (the experimental equilibrium geometry), the atomic centres upon and between which lone pair and bond LMOs are generated are not fixed by a priori assumptions about the electronic structure, but instead many different distributions ('structures') of lone pairs and bonds are considered and are rejected or accepted as suitable representations of electron organisation in a molecule largely by an energy criterion alone. In order to keep the link with chemical valence concepts, the final PLMOs are expressed in terms of normalised hybrids on each atom. Unlike the starting set of CMOs, the PLMOs and their constituent Hybrid Atomic Orbitals (HAOs) are not constrained to be mutually orthogonal.

This lack of orthogonality in the PLMOs is an important aspect of the method. The problem of non-orthogonality is dealt with in detail in Chapter 3 but here it should be mentioned that the reason that the PLMOs are non-orthogonal is that it is not usually possible in a minimal AO basis to simultaneously impose perfect localisation and LMO orthogonality.<sup>36-38</sup> Relaxing the orthogonality requirement (whilst maintaining linear independence) allows the manufacture of PLMOs from the CMOs but not usually without loss of accuracy in the molecular wavefunction. This loss of accuracy is to be expected since the presence of a certain amount of delocalisation of electron density out of one-centre lone pairs and two-centre bonds must be taken as given.<sup>39</sup> In orthogonal LMOs this electron delocalisation beyond the primary atomic centres participating in a bond or lone pair is manifested in small AO contributions on secondary atomic centres which are often termed LMO 'tails'. In the PLMOs these 'tails' are denied existence by AO basis truncation and here the slight electron delocalisation is reflected in the overlap integral between PLMOs and/or in a resultant loss of accuracy in the molecular wavefunction.

Generally, the localisation of MOs in molecules is only expected to be possible when the valence structure of the molecule is well defined.<sup>39-41</sup> When this is not the case - in Valence Bond language 'resonance' between structures is important - any LMOs generated tend to be ambiguous or non-classical in character.<sup>41-43</sup> For this reason molecules chosen as a first test of the PLMO method are Hydrogen Cyanide, Nitrogen, Carbon Monoxide, Water, Ammonia and Methane. These simple molecules have well recognised valence structures and serve as a good basis for comparison with other LMO methods.

The connection between a well defined valence description of a molecule and the ability to obtain LMOs unambiguous in character is a straightforward reflection of the relation between the localisability of electrons and the localisability of orbitals shown in a note by Daudel.<sup>44</sup> Simply, when electrons are easily localisable (i.e. the electron density may be portioned easily into well defined parts) the LMOs generated to describe them will also be well localised and vice versa. As Daudel concludes<sup>44</sup> 'To obtain information on the localisability of electrons we must therefore express the wavefunction in terms of the most localised orbitals. The defect of localisability of the orbitals gives a lower bound of the localisability of electrons.' Hence no three-centre sigma bonding is considered in this work (though in some molecules it may be important)<sup>45</sup> and amongst all the possible combinations of two-centre sigma bonds and lone pairs that may be generated in a molecule we must search for the most localised LMOs not precluded on energetic grounds. In other words, if it is not found possible for a particular molecule to select clearly a single bond and lone pair 'structure' on energy grounds as a PLMO description, the structure within a group of similar energy having its LMOs most localised is to be chosen in order to get a lower bound to electron localisability.

### 1.3(b) Desired Properties of the PLMOs

To test the success of the PLMO method, it is helpful to summarise here the desirable properties of the PLMOs in the trial molecules.

Firstly, a small energy sacrifice relative to the canonical wavefunction is desirable. As was mentioned in the previous sub-section, constraining the LMOs to be perfectly localised is generally expected -

even with non-orthogonal PLMOs chosen to be at an energy minimum - to introduce inaccuracies into the wavefunction. This inaccuracy may be measured by the energy sacrificed in going from the wavefunction constructed from the CMOs (the Canonical wavefunction) to that constructed from the PLMOs (the PLMO wavefunction). If the PLMOs are to be considered as reasonable candidates for a description of the electron distribution in a particular molecule, this energy sacrifice should be as small as possible.

Secondly, the PLMOs for a molecule via their expression in terms of normalised hybrids are hoped to have a close connection to the classical valence concepts developed over the years. Although a new LMO method should be expected to give new insights into electronic structure; where these ideas differ widely from the well-trusted semi-empirical results built up by years of chemical experience they should be viewed with suspicion.

Thirdly, it is hoped that some evidence to support the idea of transferability in the PLMOs can be found. As was mentioned in Section 1.1 the idea that different molecules are constructed from essentially similar structural subunits underlies most of chemistry. This is reflected in LMO work by the search for similarities in the forms of bond and lone pair LMOs formed by the same atoms in corresponding chemical environments in different molecules. In this way it may prove possible to transfer localised orbitals (or Fock matrix elements) of small molecular subunits from one molecule to another<sup>34</sup> and/or to build up the wavefunction of a large molecule by using the transferred parts from smaller prototype molecules ('the building block approach').<sup>34</sup> Clearly, nothing on this scale is possible in this



work but it may nevertheless be possible to identify similarities in lone pairs or the bonding behaviour of atoms in the few cases where comparable chemical environments occur in the molecules studied. This would be of particular interest in view of the suggestion of Adams<sup>46</sup> and the experience of others<sup>47-49</sup> that the LMOs most suited for transfer are those which are non-orthogonal and have no delocalisation 'tails' in the region of other LMOs - properties satisfied by the PLMOs.

Fourthly, any one-electron properties attributable to the individual PLMOs should have 'sensible' values. In fact, properties of individual LMOs (or MOs) are not usually directly observable but may be related to differences in expectation values of different states or systems.<sup>50</sup> The one-electron property calculated in this work is the dipole moment, and individual bond and lone pair moments have a wide utility in chemistry (see Chapter 6). A discussion of the values of the PLMO bond and lone pair moments is carried out in Chapter 9.

Lastly, while it is admitted that the PLMOs are to be non-orthogonal it is to be hoped that they are not too far from orthogonal. The attributes of non-orthogonal orbitals are discussed in Chapter 3 but two points may be mentioned here:

- a) LMOs with large overlap integrals can give rise to computational difficulties since it is a requirement of the one-determinant Hartree-Fock MO theory that the MOs be linearly independent.
- b) Orthogonal LMOs can have appreciable spatial overlap<sup>51</sup> but they do remain distinct in a mathematical sense. For example, any one-electron molecular property can be expressed as an exact sum of MO contributions provided they are chosen mutually orthogonal - for non-

orthogonal orbitals there is a contribution to the one-electron property arising from orbital overlap. Hence, in order to be able to decompose such a molecular property as nearly as possible into non-orthogonal orbital contributions, the orbitals must have low overlap integrals i.e. be as close as possible to orthogonal.

The desired properties of the PLMOs listed above are by no means exhaustive, but they should help in assessing the success or failure of the attempt to express the wavefunction of the trial molecules in terms of a single determinant of perfectly localised molecular orbitals (PLMOs).

## CHAPTER TWO

### HISTORICAL SURVEY: EXISTING LMO METHODS

#### 2.1 INTRODUCTION

It is not possible to review in critical detail all the available LMO methods in the literature. Instead, this chapter contains a brief summary of the main developments in the generation of LMOs.

LMOs may be generated in many different ways<sup>52,53</sup> representing different uses, applications and levels of mathematical rigour and computational efficiency. Broadly speaking however, the methods of generation can be divided into three groups. In the first group (section 2.2) the molecular wavefunction (or density matrix) constructed from the CMOs needs to be previously known. The LMOs are often obtained via an orthogonal transformation of the previously determined CMOs, hence exploiting the non-uniqueness of the solutions to the Hartree-Fock equations (Appendix I). In the second group of methods (section 2.3) no previous calculation of the molecular wavefunction is necessary. Instead, LMOs are obtained directly as solutions to a modified eigenvalue equation through appropriate changes in the Hartree-Fock operator,  $\hat{F}$  (section I-4). The third group of methods (section 2.4) comprises the generation of LMOs from hybrid atomic orbitals (HAOs) by various criteria (maximum HAO overlap, energy minimisation and so on). These LMO methods are briefly described in the rest of this chapter with some of the key references to the literature.

#### 2.2 RELOCALISATION METHODS

##### 2.2(a) Historical Introduction

The invariance of determinantal wavefunctions to an orthogonal transformation was first pointed out by Fock.<sup>54</sup> Hund<sup>55,56</sup> was the

first to formulate MO wavefunctions (for  $H_2O$ ) in terms of localised orbitals. Later, Coulson<sup>57</sup> demonstrated how to transform the CMOs of methane into LMOs in different ways including one in which non-orthogonal two-centre bond orbitals were obtained that fitted a predetermined hybridisation scheme. In a wider discussion of the localised nature of chemical bonds, Coulson<sup>58</sup> pointed out the equivalence of Mulliken's delocalised CMOs and LMOs. Lennard-Jones<sup>59,60</sup> gave the first full discussion of the relationship between LMOs (termed 'equivalent orbitals' due to the high symmetry of many of the example molecules) and the 'standard' or canonical MOs through the determinantal invariance. This work was continued by Lennard-Jones and co-workers.<sup>61-69</sup> The criterion fixing the orthogonal transformation of the CMOs was thus far based almost exclusively on symmetry requirements in highly symmetric molecules, and where this was not sufficient, by extra ad hoc constraints. With the sophistication of electronic computers however, it became possible to impose more wide-ranging requirements on the construction of transforming matrices and the variety of localising criteria thereby increased dramatically.

#### 2.2(b) Intrinsic Methods

The type of criterion used to derive a matrix transformation is called 'intrinsic'<sup>70</sup> if the criterion arises from an extremum condition on a numerical quantity which does not explicitly require localisation in any pre-determined region of a molecule but is instead a property of the function space in which the calculation is undertaken. Such 'intrinsic methods' are among the most popular LMO methods yet devised.

Foster & Boys<sup>71</sup> introduced a criterion on the orthogonal transformation of the CMOs which imposes maximal separation of the centroids of charge of the LMOs. This yields a set of 'exclusive orbitals' which are found to be localised. A reformulation of the mathematical definition of 'maximal separation' was given by Boys.<sup>72</sup> The procedure soon proved popular<sup>73-76</sup> and has been widely used since.<sup>77</sup>

Following a suggestion by Lennard-Jones & Pople<sup>62</sup> that the 'equivalent orbitals' simultaneously maximise the sum of coulombic self-repulsion terms and minimise the 'non-classical' off-diagonal exchange terms in the electronic interaction energy expression, Edmiston & Ruedenberg developed a method of transforming CMOs to 'energy localised' MOs with this criterion as its basis.<sup>70,83-85</sup> This method is rigorously applicable to both atomic and molecular systems. The method received immediate attention and application by the original authors themselves and by others<sup>50, 86-95</sup> and has been used in countless applications since.

A third intrinsic criterion to fix the orthogonal transformation of the CMOs, which was originally suggested by Edmiston & Ruedenberg,<sup>70,83</sup> has been developed by Von Niessen.<sup>96-98</sup> This method Von Niessen calls 'density localisation' since the criterion physically corresponds to the minimisation of the sum of the charge density overlap integrals of different MOs. In fact all three of these intrinsic criteria yield LMOs that are very similar (see Chapter 8) and although the Edmiston & Ruedenberg procedure is often held to be superior because of the attractiveness of its criterion, the Boys method is often preferred due to the fact that it avoids some of the computation of polycentre integrals required in the Edmiston & Ruedenberg method.

### 2.2(c) "Cut-Off" Methods

An orthogonal transformation of CMOs may often be fixed by ensuring that one or more of the resultant LMOs do not contain any delocalisations. This is normally achieved in a LCAO approximation by constraining "secondary" atomic orbitals that are not primarily involved in a two-centre bond or one-centre lone pair to have a zero coefficient. Such methods may be termed "cut-off" methods<sup>53</sup> and these are the oldest and simplest of the transformation procedures. Such procedures were often used in early work to localise MOs as an "afterthought" in standard MO calculations. Examples of the method are given by Sahni,<sup>99</sup> Pople,<sup>100</sup> Ellison & Shull,<sup>101</sup> Burnelle & Coulson<sup>102</sup> and Duncan.<sup>103</sup> The method was generalised by Peters<sup>104-113</sup> who showed the applicability of the method to many molecules and also the usefulness of the LMOs obtained. Later, Polak<sup>114</sup> used a similar criterion to fix the coefficients of hybrid atomic orbitals in LMOs in simple organic molecules. A more recent method proposed by Verwoerd<sup>115</sup> owes much to these techniques. In this procedure, non-orthogonal LMOs are obtained that are each a linear combination of a starting set of CMOs and which minimise the "non-local content" (expressed in terms of LCAO coefficients on secondary centres) of the LMOs. The method has been applied by Claxton.<sup>116</sup>

A related criterion to that of requiring certain LCAO coefficients to be zero or a minimum is to require that bonding HAOs on an atom (usually in a non-linear molecule) point directly at other bonding atoms. This constraint on the values of LCAO coefficients has been used to fix a transformation of the CMOs by Pople,<sup>63</sup> Duncan & Pople<sup>117</sup> and Peters<sup>106</sup> for example.

### 2.2(d) Population Methods

An electron population analysis<sup>118-123</sup> based on LCAO coefficients has been used by Magnasco & Perico<sup>124,125</sup> as the basis for another criterion fixing the orthogonal transformation of CMOs that generates LMOs. Local populations - corresponding to two-centre bonds and one-centre lone pairs - are defined in particular parts of a molecule and when an orthogonal transformation of the CMOs is found that simultaneously maximises the sum of the local populations and minimises the "residual populations" on secondary atomic centres, the resulting MOs are the "uniformly localised" MOs. The form of these LMOs in many molecules correspond quite closely to those obtained by intrinsic methods (see Chapter 8).

### 2.2(e) Projection Methods

The use of projection operator techniques is well known in quantum chemistry<sup>19</sup> and the use of these in the generation of LMOs is now well described. Methods which require previous knowledge of the molecular wavefunction (or more accurately in this context an associated density matrix) are considered here.

Polak<sup>36, 126-131</sup> has developed a method for finding "strictly localised orbitals" (SLOs) where each is composed of one or two valence hybrid atomic orbitals and has maximum projection onto the space spanned by the occupied CMOs. Since the SLOs of maximum projection yield the maximum value of an "occupation number" the localised orbitals are also termed "localised natural orbitals". Similar projection techniques are employed by Roby,<sup>132</sup> in a paper that gives localised orbitals by a variety of different projection criteria. In one method (which in the Hartree-Fock approximation is equivalent to

to that of Polak's,<sup>133</sup> except that no orthogonality constraint is imposed on the atomic hybrids) Roby searches for optimum HAOs on one or two centres that have maximum projection onto the occupied CMO manifold. In a second method, LMOs in the space spanned by the CMOs are sought that have maximum projection onto the subspaces formed from the AOs of one atom (to form lone pairs) and from the AOs of two adjacent atoms (to form a two-centre bond). Both methods are applied to CO,<sup>132</sup> the latter method yielding especially interesting results in the context of this work (see Chapter 8).

#### 2.2(f) Density Matrix Methods

The previously described projection methods owe much to the nature of the first order density matrix in an orbital basis. The possibility of generating localised orbitals from a molecular density matrix was recognised by McWeeny,<sup>5</sup> but in practice difficulties arise. If LMOs could be completely localised then they could be obtained by diagonalising subunits of the density matrix and selecting those orbitals with eigenvalues of 2. The smallest portioning into subunits for which this is possible would then represent maximum localisation. However, in practice the eigenvalues are slightly less than 2 (due to inherent delocalisations) and problems occur with degenerate eigenvalues. Successful methods based on this procedure have nevertheless been proposed and applied to various molecules.<sup>134</sup>

### 2.3 DIRECT METHODS

#### 2.3(a) Introduction

It is obviously desirable to obtain LMOs directly, without previous solution of any MO-LCAO equations. One type of method which has had many variants and many applications is to obtain the required



localised orbitals as solutions to an eigenvalue equation. Such an equation often uses a Hartree-Fock operator that has been specifically modified in such a way so as to produce eigenfunctions which have a localised nature.

2.3(b) Adams-Gilbert Formalism

Adams<sup>135,136</sup> exploited the freedom to use non-orthogonal (but linearly independent) one-electron functions satisfying the Hartree-Fock equations in order to derive an eigenvalue equation that yields localised orbitals for model subsystems of an electronic system. In this method, each subsystem has its own eigenvalue equation, the operator of which is modified by a uniquely defined hermitian potential - a "screening potential" - which describes the interaction of the model subgroup of electrons with the rest of the system. An application of the method to a selection of molecules was published some years later.<sup>137</sup>

Gilbert<sup>138</sup> derived equations of a more generalised form to those of Adams, wherein the modification of the Hartree-Fock operator was now due to an arbitrary hermitian "localising potential" of which the one found by Adams was a special case. Different types of localised orbitals may be obtained as eigenfunctions by different choices of the localising potential. The equations of Adams and of Gilbert were discovered more or less independently by the two authors. The resulting set of equations which are of general application are often called Adams-Gilbert (AG) equations.

Anderson<sup>139,140</sup> extended and simplified the AG equations by admitting the possibility of a non-hermitian potential (pseudopotential) being introduced into the operator of the eigenvalue equations and by no longer limiting himself to the Hartree-Fock manifold.<sup>141</sup> These

modifications to the AG equations began their application to the field of solid state physics where interest has been widespread,<sup>142</sup> and also to multi-configuration wavefunctions.<sup>143</sup>

More recent variations on the general Adams-Gilbert formalism, relating to molecular systems, have been published by Kambara<sup>144,145</sup> Matsuoka<sup>146</sup> and Mehler.<sup>147,148</sup> These latter two authors are of particular interest in the context of this work as they have both used a modified form of the AG equations which generates localised orbitals which are expanded only in basis functions belonging to each separate subsystem. This allows the dimensionality of the expansion problem to be reduced since different secular equations of small dimension are now solved for different subsystems.

### 2.3(c) Related Methods

Other authors have presented eigenfunction methods for directly determining LMOs that are less closely related to those of Adams and Gilbert.

Peters<sup>149,150</sup> has presented a method in which an eigenvalue problem is solved for each of  $N$  LMOs in a subspace (comprising a single occupied orbital and all the virtual orbitals) that is orthogonal to the space spanned by a pre-selected  $(N-1)$  localised orbitals. The procedure is repeated for each LMO in turn until self-consistency is obtained. This method has been taken up and applied in other work by Wilhite & Whitten<sup>151</sup> and Carpenter & Peters.<sup>152</sup>

Stoll & Preuss et al.<sup>153,154</sup> directly determine LMOs by the addition of a localisation operator to the Hartree-Fock operator. They further approximate the interaction between orbital groups belonging to different localisation centres in order to reduce the computational complexity of the method. The method has been applied to a

number of small prototype molecules<sup>154</sup> and the evaluation of observables from the resultant non-orthogonal localised orbitals is performed with the help of many-body corrections.

Payne<sup>43</sup> has introduced a method which yields optimised non-orthogonal LMOs in the one-determinant approximation, expressed in a basis set of AOs which involves only one atomic centre for lone pairs and two atomic centres for bonds. The LMOs are optimal in the sense that they minimise the electronic energy. By applying the variational procedure to the non-orthogonal orbitals of the constrained form, Payne obtains an eigenvalue equation of reduced dimension which each LMO satisfies. The equation that results is similar in form to the Matsuoka<sup>146</sup> modification of the AG equations. Most recently, Stoll et al.<sup>38</sup> have improved the equations derived in Payne's method and have retrieved non-orthogonal LMOs from the eigenvalue equations by two different computational procedures. The energy sacrificed in obtaining one and two-centre LMOs in the example molecules is found to be very small.<sup>38</sup>

## 2.4 HYBRID METHODS

### 2.4(a) Introduction

The general problems of the electronic structure of molecules have for many years been successfully described in terms of hybrid atomic orbitals (HAOs).<sup>155-157</sup> Thus, when discussing valence concepts in terms of LMOs - generated by one of the above methods for example - it is often useful to express each LMO as a linear combination of normalised HAOs. Alternatively it is possible to build up one and two-centre LMOs from previously determined HAOs by various criteria. This latter approach is almost always computationally simpler than the

previously described ab-initio procedures. This is because where energy calculations are used at all (many variations of a "maximum overlap" method for example have no energy calculation) they are normally of reduced complexity. Such semi-empirical HAO methods have been developed largely independently of the above LMO methods, though some localisation criteria have been usefully applied to both approaches.<sup>83,132,181</sup>

#### 2.4(b) Maximum Overlap Methods

The notion that the "best" hybrids for a molecule can be approximated by those having maximum overlap is originally due to Slater<sup>155</sup> and Pauling.<sup>156</sup> This approach has been widely applied and developed since for a number of systems,<sup>158</sup> though the basic idea - that the overlap integral between hybrids is a measure of bond strength - has no firm basis in theory<sup>158</sup> and is by no means always demonstrable in practice.<sup>159</sup> Despite this, a variety of different methods have been proposed and applied to a large number of different molecules.

Murrell<sup>160</sup> proposed a method for determining maximum overlap hybrids in molecules of type  $XY_n$  which was applicable to cases of little or no symmetry. This method was generalised by Golebiewski<sup>161</sup> and by Lykos et al,<sup>162, 163</sup> who showed that the hybrids could be obtained by direct matrix diagonalisation, thus making hybrid construction into an eigenvalue problem of wide applicability. Pelikan & Valko<sup>164</sup> later extended the approach so as to construct hybrid orbitals for a central atom and ligands simultaneously.

Another approach was introduced by Del Re<sup>165,166</sup> in which the hybrids were chosen so as to factorise the overlap matrix as closely as possible into a set of 2 x 2 diagonal blocks. The results of this

method when applied to certain cycloalkanes were similar to those of Coulson & Goodwin<sup>167</sup> who used a numerical maximum overlap technique. Del Re's procedure was modified later to improve the description of atoms with lone pairs.<sup>168</sup>

A simple method involving a "stepwise use of maximum overlap" was introduced by Stamper & Trinajstić<sup>169</sup> which has been applied with success to a number of simple molecules.<sup>169,170</sup> More recently, Boca et al.<sup>171-175</sup> have continued the use of maximum overlap procedures by the formulation of their "extended maximum overlap approximation" (EMOA). In this method HAOs are obtained iteratively by maximizing a sum of hybrid overlaps which are weighted by parameters reflecting empirical binding energies. The HAOs are then combined to form localised bond orbitals.

#### 2.4(c) Energy Optimisation Methods

These methods generally require greater computational effort than the maximum overlap approach but they have a firmer theoretical basis. In these methods the forms of the atomic hybrids, from which localised orbitals are built, are determined by optimising disposable parameters such that the electronic energy (or certain of its components) is an extremum. In many cases if the localisation conditions are relaxed to the extent that the optimum hybrids may be delocalised over a number of atomic centres, the full ab-initio results are reproduced.

The method of McWeeny & Del Re<sup>176</sup> was an example of this. In this method the first order density matrix is transformed as closely as possible to 2 x 2 block diagonal form (as in Del Re's analogous factorisation of the overlap matrix<sup>165</sup>) while simultaneously minimising

the associated electronic energy. The calculation was undertaken at three levels of approximation which were a) non-polar calculation, b) polarisation of bonds admitted and c) delocalisation of optimum hybrids found in b) allowed. The full self-consistent field (SCF) results for each molecule were reproduced in approximation c).

Letcher & Dunning<sup>177</sup> introduced a method for obtaining completely localised sigma orbitals (built from HAOs) in a non-orthogonal AO basis. Disposable parameters in an orthogonal transformation matrix, linking an orthogonal AO basis with orthogonal localised orbitals, were fixed by requiring that the energy be a minimum. The final localised orbitals were obtained by applying an analogous transformation to the non-orthogonal AO basis. The method was later applied to molecules containing pi bonds<sup>178</sup> and adapted to cater for extended basis sets.<sup>179</sup>

Hoyland<sup>47</sup> has formed two-centre localised orbitals in a series of paraffins from energy optimised, symmetrically orthogonalised, combinations of tetrahedral  $sp^3$  carbon hybrids and 1s hydrogen AOs. The intermediate non-orthogonal bond functions obtained in methane were taken over for analogous calculations on higher paraffins (ethane and propane) to test the transferable nature of the localised orbitals. Later<sup>48</sup> an improved procedure was published in which the carbon hybrids were also energy optimised.

Single determinant MO wavefunctions have been constructed for a variety of polyatomic molecules by Petke & Whitten<sup>180</sup> in a minimal AO basis. Localised orbitals representing two-centre bonds and one-centre lone pairs were obtained by minimising the total energy of the wavefunction with respect to all hybridisation and bond polarity parameters whilst maintaining the orthogonality of HAOs on the same atom. More recently Aufderheide<sup>181</sup> has obtained HAOs (called

Localised AOs-LAOs) on each atom in a molecule by an orthogonal intra-atomic transformation with MO invariance of a starting set of Slater-type AOs. The transformation is fixed by requiring that the intra-atomic sum of orbital exchange energy elements be a maximum for the LAOs of the atom. This criterion for the LAOs is analogous to the Edmiston & Ruedenberg criterion for "energy localised MOs".<sup>83</sup> The method has been applied<sup>182</sup> to numerous molecules of 1st Row atoms previously treated by Edmiston & Ruedenberg.

#### 2.4(d) Other Methods

Besides obtaining hybrids by optimising the electronic energy of a molecule - a procedure justified by the variational principle - it is possible to define hybrids in localised orbitals by optimising other mathematical functions.

Flygare & Weiss<sup>183</sup> for example constructed a set of one and two-centre LMOs for formaldehyde from a set of hybrid Slater-type orbitals in a minimal basis. The disposable parameters left in the LCAO description were optimised such that the standard deviation between the sums of experimental and calculated values of ten one-electron operators was minimised. Another method involving the electric dipole moment is that of Del Re<sup>184</sup> who has shown how it is possible to construct HAOs in a truncated basis by imposing conditions on those AOs. One set of conditions is that the AOs should be such that the electric dipole moment of a polyatomic molecule, described in terms of a semi-empirical bond orbital scheme, should be expressed as the dipole moment of the system of bond charges located at the nuclei.

Weinstein & Pauncz<sup>185,186</sup> have obtained LMOs by optimising a series of electron populations in previously fixed parts of a molecule. The local populations that were optimised were the same as those defined

by Magnasco & Perico<sup>124</sup> previously described. The difference to the work of Magnasco & Perico is that the starting set of orbitals in this case were the maximum overlap orbitals of Lykos & Schmeising.<sup>163</sup> It was found that the final LMOs were an improvement on this starting set.

"Natural Hybrid Orbitals" have recently been obtained from semi-empirical molecular wavefunctions by Foster & Weinhold<sup>187</sup> and from ab-initio SCF wavefunctions by Rives & Weinhold.<sup>188</sup> These orthonormal hybrid orbitals are obtained by diagonalising subunits of the first order density matrix in a procedure closely related to that of McWeeny & Del Re<sup>176</sup> but without any energy criterion.



### CHAPTER THREE

#### ORTHOGONAL AND NON-ORTHOGONAL ATOMIC AND MOLECULAR ORBITALS

As was mentioned in Chapter 1, the LMOs generated in this work - the PLMOs - are not constrained to be mutually orthogonal; neither are the hybrid orbitals on each atomic centre in terms of which the PLMOs are expressed. An interpretation of the forms of the PLMOs will be made in Chapter 8 where a comparison will be made to LMOs generated by other methods in which an orthonormality constraint - either on the LMOs or HAOs - is maintained. The purpose of this chapter is to lay the foundations for some of the discussion of chapter 8 and also to clarify some general points regarding orbital orthogonality.

#### 3.1. MOLECULAR ORBITALS

The basis of one-determinant Hartree-Fock MO theory is outlined in the first Appendix (I-1 to I-4). It is shown there that the only constraint on the MOs comprising the wavefunction is that they are all linearly independent, so it might seem that it is simply a matter of choice whether the MOs are chosen to be mutually orthogonal or not. Nevertheless imposing the constraint that the MOs be orthogonal does confer certain advantages. These are:

a) The expansion of the one and two-electron density functions in terms of an MO basis take on simpler forms (equations I.41 and I.43 ). This simplifies the expression for the electronic energy (equation I.54 ) hence yielding the Hartree-Fock equations in their usual form (equation I.59 ), and also simplifies the expressions for other molecular properties. In particular, one-electron

properties such as the dipole moment become a simple sum over the MOs (equations I.84 and I.85).

b) The antisymmetry requirement of the wavefunction is easily translated into the requirement that the MOs satisfy the Pauli Exclusion principle. It is considered that each MO can be occupied by two electrons, one of  $\alpha$  spin and one of  $\beta$  spin.

c) The physical interpretation of the results is very much simpler if the MOs are orthogonal. The MOs are usually considered distinct and exclusive both mathematically and physically.

For these reasons the "standard" solutions to the Hartree equation (the CMOs) are those in which MO orthogonality has been imposed. Similarly, when these CMOs are to be transformed into LMOs an orthogonal transformation is often used so that the LMOs are also mutually orthogonal. This means that one-electron properties for example may now be expressed as a simple sum over bonds and lone pairs which the LMOs represent.

These advantages may be qualified however, by noting the following:

a) The orthonormality property of the MOs

$$S_{ij} = \int \phi_i^*(r_1) \phi_j(r_1) dr_1 = \delta_{ij} \quad \text{all } i, j \quad (3.1)$$

is a mathematical property. While it makes MOs (or LMOs) distinct in a mathematical sense, they are not necessarily distinct in a physical or spatial sense.<sup>51</sup> Orthogonal LMOs still have spatial overlap which is not apparent from the overlap integral (equation 3.1) due to the phase cancellations between AOs.<sup>51</sup>

b) While the Pauli Exclusion principle is easily understood in terms of orthogonal MOs, the overall requirement that a wavefunction be antisymmetric in no way implies or requires that the MOs be orthogonal.<sup>189</sup> It is true that in simple wavefunctions consisting of a Hartree Product of MOs an orthogonality constraint can mimic the full antisymmetry requirement,<sup>189-191</sup> but in a determinantal wavefunction the linear independence of the constituent MOs is the essential requirement.

c) It proves to be the case that mutually orthogonal LMOs are in general slightly delocalised and hence have non-local "tails" on secondary atomic centres. As was mentioned in Chapter 1, it is not generally possible to remove these "tails" by constraining the LMOs to be completely localised around their "primary" atoms and to maintain orthogonality.

Many of the LMO methods described in the previous chapter employ non-orthogonal orbitals for this last reason, though other advantages may be ascribed to non-orthogonal LMOs. For example:

- 1) Since an orthogonal LMO representing a particular bond or lone pair (say a C-H bond) will have its "tail" on different "overflow atoms" in different molecules, and also because strictly localised (hence non-orthogonal) LMOs may be thought better localised than those with "tails", it is often considered that orbital non-orthogonality is necessary in order to yield LMOs that are most nearly transferable from one molecule to another.<sup>47-49</sup> Thus Adams has speculated on the properties expected of "molecularly invariant orbitals".<sup>46</sup>

- 2) Removing the orthogonality constraint on LMOs allows them to take up the optimum form consistent with their method of generation. In certain methods, orthogonality requirements may be considered to stand in opposition to the variation principle since LCAO coefficients are kept from assuming those values which would minimise molecular energy.<sup>37</sup>

There are also points to be made against the use of non-orthogonal LMOs:

- 1) The delocalised "tails", which are encountered in the orthogonal LMOs generated by some of the relocalisation methods of the previous chapter, are still apparent when the LMOs are allowed to become non-orthogonal.<sup>189,192</sup> Hence it is possible that the imposition of orthogonality is not a severe restriction for the localisation process in these cases and that the appearance of "tails" is only a property of the particular localisation criterion chosen.
- 2) The similarity of LMOs and their properties in corresponding chemical environments in different molecules, has been demonstrated for orthogonal orbitals as well as for non-orthogonal orbitals.<sup>193-198</sup> In these cases the nature of the "overflow atom" influences the degree of similarity between molecules.<sup>195-197</sup> Hence, when synthesising LMOs of a large molecule by transferring LMO fragments from smaller prototype molecules, standard "tail" contributions have to be included.<sup>198</sup>

- 3) Non-orthogonal LMOs of optimum form may cause interpretational problems if their overlap integrals are large. In the limit the orbitals may "collapse" to a single function, thus making the LMO set linearly dependent and invalidating the determinantal wavefunction constructed from them. Linear dependence can always be avoided by using orthogonal MOs, though other techniques can be used such as the use of a "penalty function" in the minimisation of an energy functional.<sup>189</sup>

In summary then, there are advantages and disadvantages to both orthogonal and non-orthogonal orbitals and it cannot be said whether orthogonal or non-orthogonal LMOs serve as better descriptions of the electronic structure of molecules. The two approaches complement one another by attempting to explain molecular structure in different, but equally enlightening ways. An example of this duality is shown in the investigation of the conformational behaviour of molecules in terms of localised orbitals. The interaction between the electron density in mutually rotating groups in a molecule may be expressed via LMOs in two different ways.

One approach<sup>30,199</sup> is based on the use of "Energy Localised MOs".<sup>83,84</sup> Here, the interaction is explained in terms of variations in the one-electron, two-centre interference energy<sup>200</sup> within a given LMO representing a bond or lone pair. This is possible because the energy localised MOs of one group of atoms generally have delocalisation "tails" on the other, interacting group. These "tails" therefore are not considered simply by-products of orbital orthogonality, but become central to an explanation of electron interaction in this view.

The second approach however, is based on the view that short range interactions between molecular groups - especially their orientation dependence - is best described by non-orthogonal functions.<sup>201-210</sup> In this case<sup>211</sup> the internal rotation barrier is investigated in terms of bonds and lone pairs represented by strictly localised non-orthogonal orbitals each extending over only one or two nuclei and hence devoid of any delocalisation "tails". The barrier is now simply explained in terms of the penetration (overlap) between localised orbitals on the mutually rotating groups.

### 3.2 HYBRID ATOMIC ORBITALS

#### 3.2(a) Hybridisation

The PLMOs obtained in this work are expressed in terms of normalised Hybrid Atomic Orbitals (HAOs) on each atom (see Part B). In this way LMOs found from quantum mechanical calculations may be understood using the concept of hybridisation which has been developed over many years<sup>155-157</sup> and has been invaluable in explaining and systematising chemical concepts in terms now familiar to chemists.<sup>40,212-214</sup>

The idea of hybridisation stems from the assumption that an atom retains its identity within a molecule and makes only slight adjustments to the molecular environment. This assumption implies that the molecular wavefunction may be represented in terms of orbitals formed by combination of atomic functions. In such a LCAO-MO procedure each atom then has s, p etc. orbitals unambiguously associated with it, making it possible to define s and p electronic populations. A definition of the wavefunction in terms of atomic orbitals is essential for any discussion of hybridisation. Wavefunctions expressed in terms of a one-centre expansion for example cannot be understood by

specifying hybridisation at individual atoms. The approach used in this work, that of using normalised HAOs to analyse LMOs, follows the example of most LMO methods. However, that hybridisation is more than simply an analytical tool can be judged by the success of methods that build wavefunctions directly from atomic hybrids in some way (see previous chapter).

The HAOs at each atomic centre are not constrained to be mutually orthogonal in the PLMO method. This point is in contradiction to the properties of the AOs in an isolated atom, to the original work of Slater and Pauling<sup>155-157</sup> and to much standard chemistry since.<sup>214</sup> However, by analogy with the previous section, a number of advantages and disadvantages may be associated with the presence or absence of orthogonality constraints between HAOs at an atomic centre in a molecule, and these will be discussed here.

### 3.2(b) Orthogonality and the description of bonding

Orthogonal hybrids may be considered distinct both mathematically and physically. Thus at a simple level - in Valence Bond terms "the Perfect Pairing Approximation" - the valence electrons of an atom may be assigned unambiguously to orthogonal HAOs in order to be paired individually with the hybrids on attached groups to form bonds or to form non-bonding pairs of electrons. The electron density of an atom therefore becomes a simple superimposition of the densities of the HAOs at that atom.

Orthogonality also provides a simplification to the mathematical problem of constructing HAOs on an atom in a molecule. The restrictions on the relative values of AO coefficients that orthogonality represents,

especially in molecules of high symmetry such as methane or water, significantly reduces the number of disposable parameters in the problem. These may then be fixed by some simple prescription such as a requirement that bonding hybrids point directly towards another atom. It is clear then that the imposition of hybrid orthogonality is both intuitively and mathematically appealing.

In spite of this, most LMO methods do not restrict atomic hybrids to be mutually orthogonal. This is due to the fact that in the more accurate MO theory, electronic delocalisation - and hence the inadequacy of the perfect pairing approximation - has to be admitted. In LMO methods that involve an orthogonal transformation of the CMOs such as those of Edmiston & Ruedenberg,<sup>83-85</sup> Boys and Peters,<sup>71,72, 104-106</sup> the orthogonality requirement on the HAOs is replaced by the mutual orthogonality of the slightly delocalised LMOs containing the hybrids. This replacement in the Peters method has been discussed in the literature<sup>215</sup> and the effect on the actual level of hybridisation in the HAOs of water has been demonstrated in a note by Coulson.<sup>216</sup> In LMO methods that generate non-orthogonal LMOs, constituent HAOs may or may not be mutually orthogonal at each atomic centre. Some authors exploit the computational simplification that results from the use of orthogonal HAOs (many of the "Hybrid methods" of section 2.4) while others consider orthogonality a restriction that moves HAOs away from their optimum form.<sup>132</sup> In both cases, when LMOs are constrained to one or two centres i.e. to mimic the perfect pairing approximation, a sacrifice in the accuracy of the wavefunction has to be made in most molecules.

For these reasons, when the electronic structure of some molecules are expressed in terms of LMOs, contradictions may seem to arise with the corresponding description in classical valence terms.<sup>42</sup> However,



by analysing such LMO descriptions in terms of orthogonal HAOs one atom at a time, violations of the normal valence rules - such as the octet rule - are shown to be apparent rather than real.<sup>217</sup>

### 3.2(c) The Directional Properties of Hybrids

The orthogonality conditions between HAOs at an atom effect the relative values of the AO coefficients. These in turn effect the direction in which an atomic hybrid points. Thus the directional properties of hybrids - in particular the VSEPR model of molecular geometry and the phenomenon of "bent" bonds - will be discussed here.

It is often considered that the Valence Shell Electron Pair Repulsion (VSEPR) model of molecular geometry<sup>218-220</sup> requires the use of orthogonal HAOs at atomic centres in a molecule. This is not actually so. In fact, the model is most profitably explained in terms of electron pairs spatially correlated by the antisymmetry requirement without reference to HAOs at all.<sup>220</sup> If a description in terms of directed hybrids on a central atom is required however, what is important is a minimum of spatial overlap between them. The distinction between no overlap in a mathematical sense and in a spatial sense has already been made in the discussion of LMOs.<sup>51</sup> It is true that the electron correlation imposed by the Pauli exclusion principle, and the energetic interactions between electron pairs, are most easily understood in terms of doubly occupied mutually orthogonal hybrids at a central atom, but this description is not actually necessary. What ultimately determines molecular geometry is the position of the minimum in an energy surface, and the hybrids used to describe the area of space most probably occupied by electron pairs is largely a matter of taste.

To obtain bonding hybrids from both LMO and VB calculations on non-linear molecules that are not exactly directed towards a bonded atom, is the rule rather than the exception.<sup>24</sup> Such "bent" bonds are obtained with non-orthogonal HAOs of varying degrees<sup>85,98,102,103,106,125</sup> and also with orthogonal bonding hybrids optimised in different ways.<sup>126,180</sup> A discussion of the "bent" bonds obtained from orthogonal hybrids by a maximum overlap criterion has been given as well.<sup>166,168</sup> It is clear that the removal of hybrid orthogonality may allow HAOs to be directed at angles unobtainable with orthogonal hybrids (and may lead in certain cases to roughly equivalent hybrid angles in similar molecules<sup>93</sup>) but there is apparently little correlation between the non-orthogonality of HAOs and the appearance of "bent" bonds.

The best conclusion that may be drawn from the above discussion is essentially the same as was reached in section 3.1. While orthogonal and non-orthogonal hybrids each have their own advantages - and valence rules have historically been formulated in terms of orthogonal HAOs<sup>212,213</sup> they are really equally acceptable alternatives. The two approaches offer complementary viewpoints.

The approach taken in this work is not to impose any orthogonality constraints on the HAOs. Thus "we do not set out with any preconceived ideas about the condition of the atom in the molecule. This will emerge from the results".<sup>215</sup>

PART B

PLMO METHOD AND RESULTS

CHAPTER FOURILLUSTRATION OF PLMO METHOD - EXAMPLE OF HCN4.1 INTRODUCTION4.1(a) Outline of Method

In this chapter is presented the method used to generate sets of non-orthogonal Perfectly Localised Molecular Orbitals (PLMOs) in a LCAO approximation. The PLMOs were not found by finding SCF solutions to eigenvalue equations but by searching an energy surface for a minimum by standard techniques. The energy surface was constructed by the simple technique of transforming a starting set of CMOs, truncating the resulting MOs so that they were perfectly localised, forming a specific set of lone pairs and two-centre bonds ("a structure") and then computing the total electronic energy of the resulting many-electron wavefunction. The electronic energy was hence a function of the parameters defining the transformation of the CMOs.

A minimum of energy and a corresponding set of LMOs was obtained for each set of lone pairs and bonds that were generated for a given molecule. Such a set of strictly localised LMOs does not generally span the Hartree-Fock manifold and hence corresponds to an energy higher than that calculated from the CMOs. This "energy sacrifice" was smaller for some arrangements of lone pairs and bonds than for others. Those "structures" of lowest energy were hence candidates for an approximate description of the electronic structure of the molecule. The final set of PLMOs were chosen from among these low energy "structures" by selecting the most "localised" set, in line with the argument in Chapter one (1.3(a)). The computational details are set

out in Appendix II.

#### 4.1(b) Investigation of HCN

In order to illustrate the PLMO method by an explicit example, the results of applying the procedure to HCN are presented in this chapter. Three different investigations were carried out.

In the first investigation, the starting set of CMOs was expressed in a STO-3G minimal basis of AOs. (see Appendix I, Section 4(c) for an explanation of terms). In the second case a more accurate STO-5G AO basis was used. In the third investigation the basis AOs were again of STO-3G quality but the inner shell CMOs were truncated and renormalised and hence had AO contributions from one centre only. By comparing the results in the three cases it was possible to test the effect of changing the quality of the starting CMOs and of altering the treatment of the inner shells.

#### 4.2 PRELIMINARIES

The geometry and co-ordinate system used for HCN is shown in Table 4.1. The same construction was used for all three investigations.

For each molecule considered a starting set of CMOs expressed in LCAO form were required. Since the electronic energy had to be calculated and also, at a later stage, the dipole moment, various integrals over atomic orbitals were also needed. A convenient source both for the CMOs and also the necessary integrals over AOs was found in Gaussian 70.<sup>222</sup> This performed a standard Hartree-Fock SCF MO-LCAO calculation of the sort described in Appendix I. A minimal basis set was used where each Slater-type AO (STO) was approximated by a linear combination of  $k$  gaussian orbitals (STO- $kG$ ). As the number  $k$  increases the representation of each STO becomes more accurate and the energy calculated from the CMOs (the canonical energy) decreases.<sup>223</sup> The effect of this on the PLMOs may be gauged by comparing the results for the STO-3G and STO-5G calculations.

TABLE 4.1. GEOMETRY<sup>221</sup> AND CO-ORDINATE SYSTEM FOR HCN

| R(C-N) = 1.153 Å |                             | R(C-H) = 1.066 Å |        | ∠HCN = 180° |
|------------------|-----------------------------|------------------|--------|-------------|
| Atom             | Co-ordinates (atomic units) |                  |        |             |
|                  | x                           | y                | z      |             |
| H                | 0.0                         | 0.0              | -2.014 |             |
| C                | 0.0                         | 0.0              | 0.0    |             |
| N                | 0.0                         | 0.0              | 2.179  |             |

The occupied CMOs and the orbital eigenvalues for HCN, calculated by Gaussian 70 using standard STO exponents,<sup>224</sup> are shown in Tables 4.2 and 4.3.

#### 4.3 PLMO METHOD AS EXEMPLIFIED BY HCN

##### 4.3(a) Seperation of CMOs

Some of the CMOs of each molecule were regarded as already localised and these were therefore separated from the CMOs to be transformed. In HCN the carbon and nitrogen inner shells ( $k_C$  and  $k_N$ ) were predominantly  $1s_C$  and  $1s_N$  in nature and hence regarded as localised onto their respective atomic centres. These inner shells could either be left in their canonical form or truncated and renormalised so that only AOs on the relevant atom made contributions to the MO. Both cases were considered for HCN. The  $\pi$  MOs ( $\pi_1$  and  $\pi_2$ ) were considered as localised C-N bonds and therefore set aside with the inner shells. This left three sigma CMOs ( $\sigma_3$ ,  $\sigma_4$  and  $\sigma_5$ ) with appreciable AO contributions from all the atomic centres in the molecule. These CMOs,  $\phi$ , generally R in number, were to be transformed.

##### 4.3(b) "Structure" Specification

A fixed arrangement of lone pairs or two-centre bonds in a molecule was termed a "structure". This was specified by simply denoting which AO coefficients in the MOs would be set to zero at a later, truncation stage. If all but the AO coefficients arising from one atom (say atom a) were set to zero in a MO, that MO was considered a lone pair on that atom (symbol  $\lambda_a$ ). If all but the AO coefficients arising from two atoms (say atoms a and b) were set to zero in a MO, that MO was considered a bond between those atoms (symbol  $\mu_{ab}$ ). In HCN the many possible structures described by the three  $\sigma$ MOs include  $\lambda_N$   $\lambda_C$   $\mu_{CN}$ ,  $\lambda_H$   $\mu_{CH}$   $\mu_{CN}$ ,  $2\mu_{CN}$   $\mu_{NH}$  and so on.

TABLE 4.2 OCCUPIED CMOs AND EIGENVALUES FOR HCN (STO-3G BASIS)

| (a)<br>CMO     | Basis AOs       |                 |                 |                  |                  |                  |                 |                 |                  |                  |                  | Eigenvalue <sup>(b)</sup><br>(H) |
|----------------|-----------------|-----------------|-----------------|------------------|------------------|------------------|-----------------|-----------------|------------------|------------------|------------------|----------------------------------|
|                | 1s <sub>H</sub> | 1s <sub>C</sub> | 2s <sub>C</sub> | 2p <sub>xC</sub> | 2p <sub>yC</sub> | 2p <sub>zC</sub> | 1s <sub>N</sub> | 2s <sub>N</sub> | 2p <sub>xN</sub> | 2p <sub>yN</sub> | 2p <sub>zN</sub> |                                  |
| k <sub>N</sub> | -0.0005         | 0.0004          | -0.0106         | -                | -                | -0.0076          | 0.9940          | 0.0298          | -                | -                | -0.0088          | -15.3851                         |
| k <sub>C</sub> | -0.0059         | 0.9929          | 0.0311          | -                | -                | 0.0019           | -0.0005         | -0.0068         | -                | -                | 0.0016           | -11.0801                         |
| σ <sub>3</sub> | 0.0669          | -0.1656         | 0.3563          | -                | -                | 0.2024           | -0.2011         | 0.6275          | -                | -                | -0.2263          | - 1.1822                         |
| σ <sub>4</sub> | -0.4495         | 0.1458          | -0.4655         | -                | -                | 0.4001           | -0.0812         | 0.2800          | -                | -                | 0.0460           | - 0.7504                         |
| σ <sub>5</sub> | -0.1561         | -0.0734         | 0.2155          | -                | -                | 0.3173           | 0.1319          | -0.6898         | -                | -                | -0.6740          | - 0.4933                         |
| π <sub>1</sub> | -               | -               | -               | 0.5204           | -0.3225          | -                | -               | -               | 0.5395           | -0.3343          | -                | - 0.4420                         |
| π <sub>2</sub> | -               | -               | -               | 0.3225           | 0.5204           | -                | -               | -               | 0.3343           | 0.5394           | -                | - 0.4420                         |

(a) The CMOs are: k - inner shell CMO

σ - valence sigma CMO

π - pi CMO

(b) The eigenvalue in Hartrees (H)



TABLE 4.3 OCCUPIED CMOs AND EIGENVALUES FOR HCN (STO-5G BASIS)

| (a)<br>CMO     | Basis AOs       |                 |                 |                  |                  |                  |                 |                 |                  |                  |                  |          | (b)<br>Eigenvalue (H) |
|----------------|-----------------|-----------------|-----------------|------------------|------------------|------------------|-----------------|-----------------|------------------|------------------|------------------|----------|-----------------------|
|                | 1s <sub>H</sub> | 1s <sub>C</sub> | 2s <sub>C</sub> | 2p <sub>xC</sub> | 2p <sub>yC</sub> | 2p <sub>zC</sub> | 1s <sub>N</sub> | 2s <sub>N</sub> | 2p <sub>xN</sub> | 2p <sub>yN</sub> | 2p <sub>zN</sub> |          |                       |
| k <sub>N</sub> | -0.0006         | 0.0003          | -0.0073         | -                | -                | -0.0057          | 0.9963          | 0.0197          | -                | -                | -0.0068          | -15.5732 |                       |
| k <sub>C</sub> | -0.0038         | 0.9954          | 0.0210          | -                | -                | 0.0020           | -0.0005         | -0.0050         | -                | -                | 0.0015           | -11.2250 |                       |
| σ <sub>3</sub> | 0.0643          | -0.1595         | 0.3526          | -                | -                | 0.1995           | -0.1932         | 0.6320          | -                | -                | -0.2272          | - 1.1887 |                       |
| σ <sub>4</sub> | -0.4494         | 0.1402          | -0.4648         | -                | -                | 0.4010           | -0.0777         | 0.2794          | -                | -                | 0.0507           | - 0.7549 |                       |
| σ <sub>5</sub> | -0.1563         | -0.0718         | 0.2144          | -                | -                | 0.3158           | 0.1220          | -0.6840         | -                | -                | -0.6758          | - 0.4982 |                       |
| π <sub>1</sub> | -               | -               | -               | 0.0361           | -0.6113          | -                | -               | -               | 0.0374           | -0.6335          | -                | - 0.4462 |                       |
| π <sub>2</sub> | -               | -               | -               | 0.6113           | 0.0361           | -                | -               | -               | 0.6335           | 0.0374           | -                | - 0.4462 |                       |

(a) The CMOs are: k - inner shell CMO

σ - valence sigma CMO

π - pi CMO

(b) The eigenvalue in Hartrees (H)



with the notation of equation (4.2).

Transforming the delocalised CMOs,  $\underline{\phi}$ , by the orthogonal matrix  $\underline{T}$  gave a new set of R orthogonal MOs  $\underline{\phi}^R$

$$\underline{\phi}^R = \underline{\phi} \cdot \underline{T} \quad (4.4)$$

#### 4.3(d) Truncation

The transformed orthogonal MOs,  $\underline{\phi}^R$ , were now truncated and renormalised so that they only had contributions from one or two atomic centres. The "structure" so obtained was that specified at an earlier stage (Section 4.3(b)). The truncated and renormalised set,  $\underline{\phi}^T$ , were now no longer mutually orthogonal.

#### 4.3(e) Orthonormalisation

The R truncated MOs and the other occupied CMOs were next brought together and tested to ensure they were linearly independent. Linear dependencies would occur in structures where more bonds or lone pairs were created on or between atoms than there were appropriate basis AOs. A regular example was two or more hydrogen lone pairs on the same hydrogen atom.

In acceptable structures, a copy of the linearly independent truncated MOs were orthonormalised by the Schmidt procedure (Section I-7). This was done so that the computation of the electronic energy exploited the simpler equations for orthogonal MOs. As has already been explained, the one-determinant wavefunction is, of course, unchanged for computational purposes by such an orthonormalisation of its constituent MOs.

#### 4.3(f) Electronic Energy Calculation

The electronic energy was calculated from the 1st order density matrix in the atomic orbital basis and the one and two-electron

integrals, essentially using equation (I.58 ). For computational details see Appendix II.

#### 4.3(g) Iteration to an energy minimum

The electronic energy of the wavefunction constructed from the truncated MOs (including the inner shells and  $\pi$  orbitals) is hence a function of the  $\frac{1}{2}R(R - 1)$  independent parameters used in constructing a general orthogonal transforming matrix (Section 4.3(c)). For a particular "structure" these parameters were varied until an energy minimum was found. The non-orthogonal but linearly independent MOs corresponding to this minimum were hence the final LMOs for this structure. This procedure was repeated for every possible arrangement of bonds and lone pairs, so that a long series of "structures" with corresponding energies and LMOs were obtained.

In order to test the uniqueness of the LMOs and associated energies, several different arbitrary starting values of the transformation parameters were used in the energy minimisations. This test of uniqueness for functions has been used by other workers using other localising methods.<sup>92,97</sup> In fact, each structure's LMOs were found to be unique in all cases except where there was more than one lone pair on an atom or more than one sigma bond between a pair of atoms.

#### 4.4 ENERGY DIAGRAMS AND LMOs FOR HCN

For HCN a total of 56 different structures were considered by the method of the previous section, (216 if the 3 transformed MOs were permuted amongst the lone pairs and bonds) not all of which gave rise to linearly independent truncated MOs. The lowest energy structures

for HCN are exhibited in Figures 4.1, 4.2 and 4.3. In Figure 4.1 are the results using a STO-3G basis, in figure 4.2 are shown the results corresponding to a STO-5G basis and in figure 4.3 are the results for a STO-3G basis but with the inner shells truncated and renormalised. Also exhibited in the figures is the overlap between the canonical wavefunction and that constructed from the endpoint LMOs,  $\langle \Psi_{\text{CMO}} / \Psi_{\text{LMO}} \rangle$ . The structures are shown both by symbols and in diagrammatic form. In the diagrams, a single line between two atoms denotes a sigma bond, two wavy lines between atoms denotes a pair of sigma bonds and a pair of crosses beside an atom represents a lone pair on that atom (positioning has no significance).

All the structures are seen to correspond to energies higher than that of the canonical MOs. The difference is the energy which must be sacrificed when restricting the LMOs generated by the above method, to only one or two atomic centres. Obviously, the lower the energy associated with a structure, the closer will that structure be to the CMO description of the ground state. This can be confirmed by noting the general trend of the overlaps of the LMO wavefunctions with that of the SCF CMO wavefunction in the diagrams. Hence the lower energy structures will give the more accurate description of the electronic arrangement in the molecule in terms of lone pairs and two-centre bonds. For this reason, when looking for such a description of the molecule it is only necessary to consider the structures at the bottom end of the energy scale in figures 4.1, 4.2 and 4.3.

The three lowest such structures are the same in all three figures and the LMOs for these cases, along with the inner shells and  $\pi$  MOs are shown in Tables 4.4, 4.5 and 4.6. Only the unique LMOs

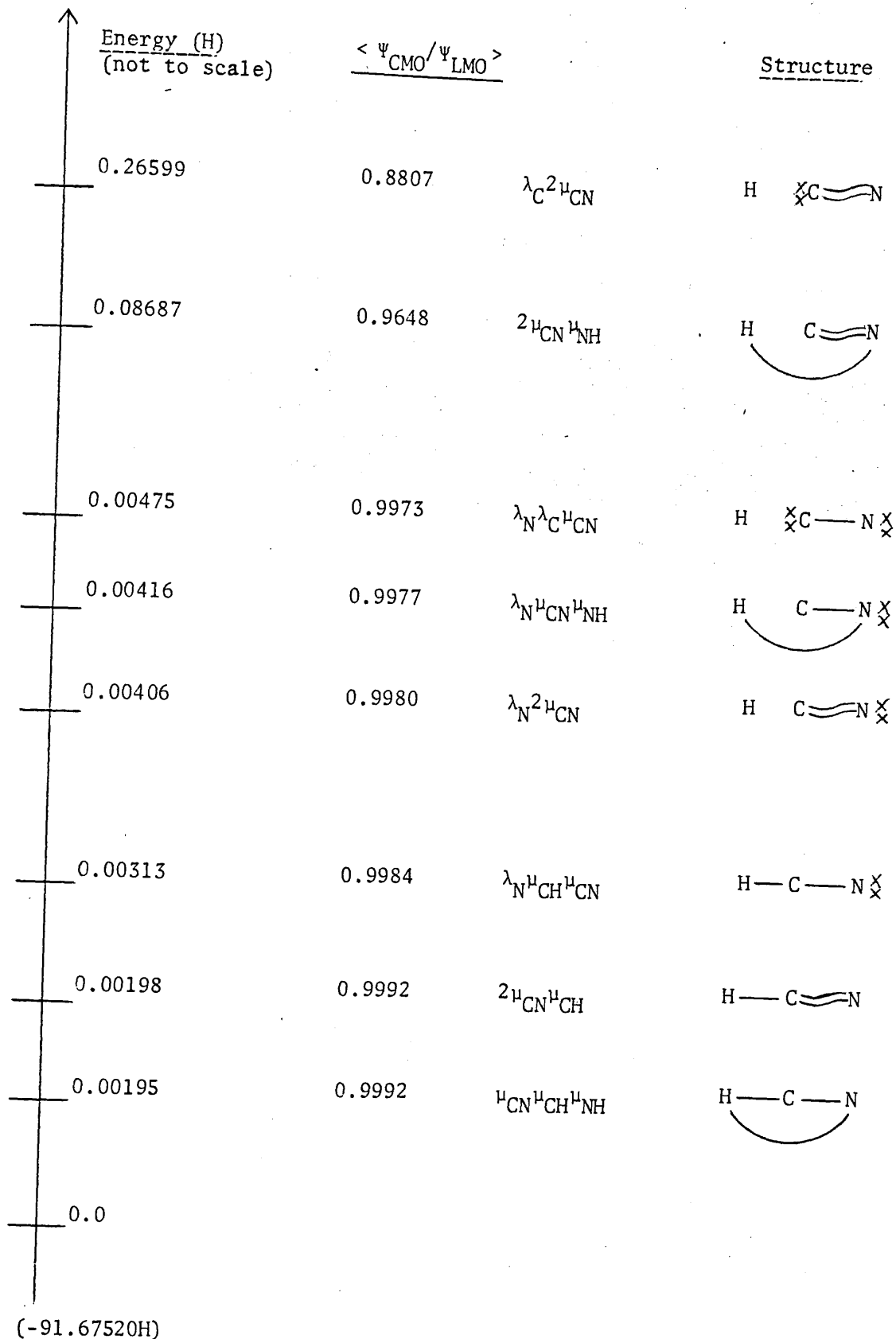


Figure 4.1 Energy diagram for LMO structures in sigma frame of HCN  
(STO-3G basis)  
(for expansion of symbols see narrative)

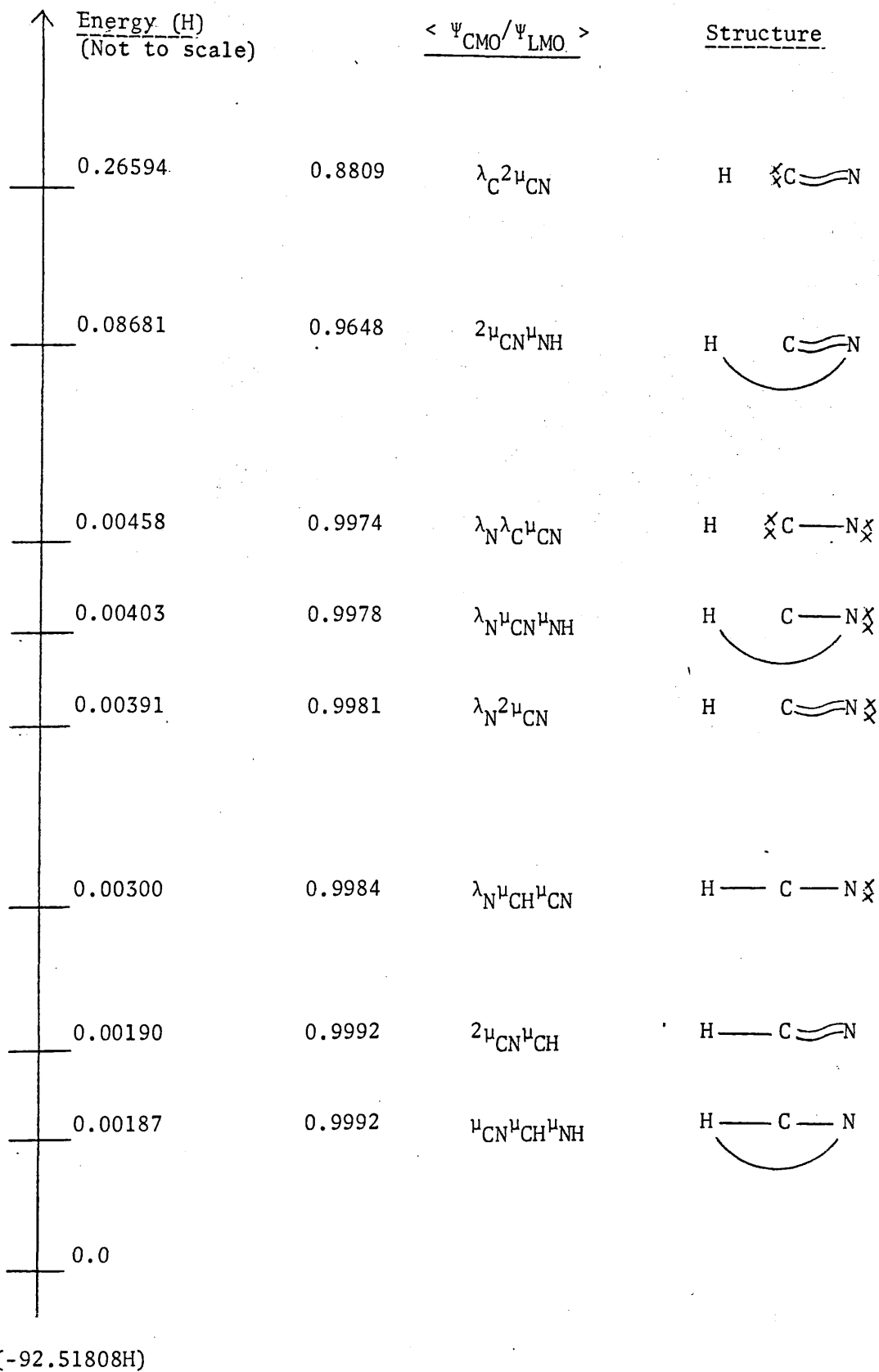


Figure 4.2 Energy diagram for LMO structures in sigma frame of HCN  
(STO-5G basis)  
(for explanation of symbols see narrative)

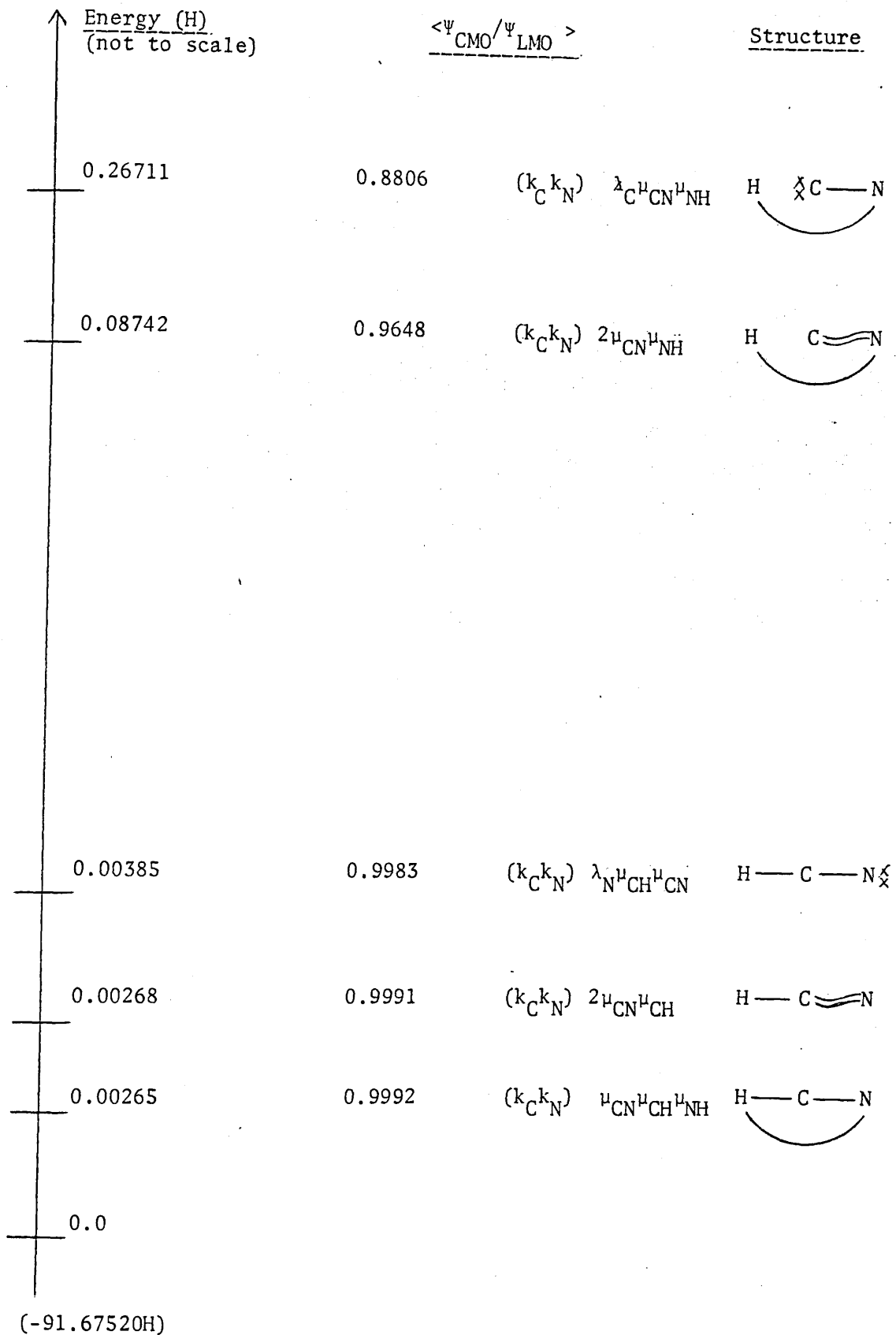


Figure 4.3 Energy diagram for LMO structures in sigma frame of HCN  
with inner shells truncated (STO-3G basis)  
 (for explanation of symbols see narrative)



TABLE 4.4 INNER SHELLS, PI ORBITALS AND LMOs FOR LOW ENERGY STRUCTURES FOR HCN (STO-3G BASIS)

(For explanation, see narrative)

| Structure | LMO             | 1s <sub>H</sub> | 1s <sub>C</sub>  | 2s <sub>C</sub> <sup>or</sup> | 2p <sub>zC</sub> | 1s <sub>N</sub> | 2s <sub>N</sub> <sup>or</sup> | 2p <sub>zN</sub> |                  |
|-----------|-----------------|-----------------|------------------|-------------------------------|------------------|-----------------|-------------------------------|------------------|------------------|
| All       | k <sub>N</sub>  | -0.0005         | -0.0022          | -0.0099                       | -0.0076          | 1.0010          | 0.0290                        | -0.0088          |                  |
|           | k <sub>C</sub>  | -0.0059         | 1.0006           | 0.0302                        | 0.0019           | -0.0021         | -0.0066                       | 0.0016           |                  |
|           | λ <sub>N</sub>  |                 |                  |                               |                  | -0.0187         | 0.9442                        | 0.3288           |                  |
|           | μ <sub>CH</sub> | 0.4729          | (-0.0611)        | 0.7388                        | (-0.6711)        |                 |                               |                  |                  |
|           | μ <sub>CN</sub> | 0.5411          | (-0.1281)        | 0.7343                        | 0.6666)          | 0.6329          | (-0.0935                      | -0.0453          | (-0.9946)        |
|           | μ <sub>CH</sub> | 0.4765          | (-0.0639)        | 0.7306                        | (-0.6798)        |                 |                               |                  |                  |
|           | μ <sub>CN</sub> | 0.5418          | (-0.1294)        | 0.7440                        | 0.6556)          | 0.6307          | (-0.0939                      | -0.0404          | (-0.9948)        |
|           | μ <sub>CH</sub> | 0.4737          | (-0.0597)        | 0.7311                        | 0.6796)          |                 |                               |                  |                  |
|           | μ <sub>NH</sub> | 0.0505          |                  |                               |                  | 0.9969          | (-0.0185                      | 0.9435           | 0.3309)          |
|           | Structure       | MO              | 2p <sub>xC</sub> |                               | 2p <sub>yC</sub> |                 | 2p <sub>xN</sub>              |                  | 2p <sub>yN</sub> |
| All       | π <sub>1</sub>  | 0.6122          | ( 0.8500         |                               | -0.5268)         | 0.6347          | ( 0.8500                      | -0.5267)         |                  |
|           | π <sub>2</sub>  | 0.6122          | ( 0.5268         |                               | 0.8500)          | 0.6347          | ( 0.5268                      | 0.8500)          |                  |

TABLE 4.5 INNER SHELLS, PI ORBITALS AND LMOs FOR LOW ENERGY STRUCTURES FOR HCN (STO-5G BASIS)

(For explanation see narrative)

| Structure                         | LMO         | $1s_H$          | $1s_C$    | $2s_C^{or}$     | $2p_{zC}$ | $1s_N$    | $2s_N^{or}$ | $2p_{zN}$ |
|-----------------------------------|-------------|-----------------|-----------|-----------------|-----------|-----------|-------------|-----------|
| All                               | $k_N$       | -0.0006         | -0.0015   | -0.0071         | -0.0057   | 1.0008    | 0.0192      | -0.0068   |
|                                   | $k_C$       | -0.0038         | 1.0006    | 0.0204          | 0.0020    | -0.0016   | -0.0049     | 0.0015    |
| $\lambda_N$ $\mu_{CH}$ $\mu_{CN}$ | $\lambda_N$ |                 |           |                 |           | -0.0118   | 0.9446      | 0.3278    |
|                                   | $\mu_{CH}$  | 0.4728          | (-0.0545) | 0.7341          | (-0.6769) |           |             |           |
|                                   | $\mu_{CN}$  | 0.5362          | (-0.1249) | 0.7413          | 0.6594    | (-0.0920) | -0.0420     | (-0.9949) |
| $2\mu_{CN}$ $\mu_{CH}$            | $\mu_{CH}$  | 0.4764          | (-0.0573) | 0.7259          | (-0.6854) |           |             |           |
|                                   | $\mu_{CN}$  | 0.5377          | (-0.1255) | 0.7501          | 0.6493    | (-0.0920) | -0.0365     | (-0.9951) |
| $\mu_{CN}$ $\mu_{CH}$ $\mu_{NH}$  | $\mu_{CH}$  | 0.4736          | (-0.0535) | 0.7263          | (-0.6852) |           |             |           |
|                                   | $\mu_{NH}$  | 0.0495          |           |                 |           | (-0.0115) | 0.9439      | 0.3301    |
| Structure                         | MO          | $2p_{xC}$       | $2p_{yC}$ | $2p_{xN}$       | $2p_{yN}$ |           |             |           |
| All                               | $\pi_1$     | 0.6124 ( 0.0590 | -0.9983)  | 0.6346 (0.0590  | -0.9983)  |           |             |           |
|                                   | $\pi_2$     | 0.6124 ( 0.9983 | 0.0590)   | 0.6346 ( 0.9983 | 0.0590)   |           |             |           |

TABLE 4.6 INNER SHELLS (TRUNCATED), PI ORBITALS AND LMOs FOR LOW ENERGY STRUCTURES FOR HCN (STO-3G BASIS)

(For explanation see narrative)

| Structure                                       | LMO             | 1s <sub>H</sub> | 1s <sub>C</sub>  | 2s <sub>C</sub> <sup>or</sup> | 2p <sub>zC</sub> | 1s <sub>N</sub>  | 2s <sub>N</sub> <sup>or</sup> | 2p <sub>zN</sub> |
|---|-----------------|-----------------|------------------|-------------------------------|------------------|------------------|-------------------------------|------------------|
| All   | k <sub>N</sub>  |                 |                  |                               |                  | 0.9995           | 0.0290                        | -0.0088          |
|   | k <sub>C</sub>  |                 | 0.9995           | 0.0301                        | 0.0019           |                  |                               |                  |
| λ <sub>N</sub> <sup>μ</sup> CH <sup>μ</sup> CN  | λ <sub>N</sub>  | 0.4730          | 0.6140           | 0.7388                        | -0.6712)         | - 0.0187         | 0.9443                        | 0.3286           |
|   | μ <sub>CH</sub> |                 | (-0.0611         |                               |                  |                  |                               |                  |
|   | μ <sub>CN</sub> | 0.5410          | (-0.1283         | 0.7344                        | 0.6665)          | (-0.0935         | -0.0454                       | (-0.9946)        |
| 2 <sup>μ</sup> <sub>CN</sub> <sup>μ</sup> CH    | μ <sub>CH</sub> | 0.4766          | (-0.0639         | 0.7304                        | -0.6801)         |                  |                               |                  |
|   | μ <sub>CN</sub> |                 | (-0.1292         | 0.7443                        | 0.6552)          | (-0.0937         | -0.0407                       | (-0.9948)        |
| μ <sub>CN</sub> <sup>μ</sup> CH <sup>μ</sup> NH | μ <sub>CH</sub> | 0.4737          | (-0.0597         | 0.7308                        | -0.6800)         |                  |                               |                  |
|   | μ <sub>NH</sub> | 0.0509          |                  |                               |                  | 0.9969           | 0.9435                        | 0.3309)          |
| Structure                                       | MO              |                 | 2p <sub>xC</sub> | 2p <sub>yC</sub>              |                  | 2p <sub>xN</sub> | 2p <sub>yN</sub>              |                  |
| All   | π <sub>1</sub>  |                 |                  |                               |                  |                  |                               |                  |
|   | π <sub>2</sub>  |                 |                  |                               |                  |                  |                               |                  |

As Table 4.4

are shown for each structure, thus the form of the C-H bond is the sole representative in the  $2\mu_{\text{CN}}^{\mu_{\text{CH}}}$  case. In order to show the forms of the orbitals more clearly the nodeless 2s Slater-type AO has been replaced by a  $2s^{\text{or}}$  AO, Schmidt-orthogonalised to the 1s AO. The 1s and  $2s^{\text{or}}$  AO coefficients become altered accordingly. The LMOs and  $\pi$  MOs (and inner shells in Table 4.6) are shown as a normalised hybrid atomic orbital (HAO) on each centre with a corresponding coefficient (polarity parameter). The HAOs on each atom are not constrained to be mutually orthogonal. A more detailed analysis of the localised orbitals is reserved for Part C, here it is sufficient to point out that the orbital forms for the three investigations (Tables 4.4, 4.5 and 4.6) are very similar. In other words, increasing the accuracy of the basis set from STO-3G to STO-5G, or truncating and renormalising the inner shells makes little difference to the end-point LMOs.

The greatest difference between the three sets of results occurs in the energy diagrams, figures 4.1, 4.2 and 4.3. It should be noted first that the origin of the energy scale (the canonical energy) for the STO-5G case (fig. 4.2) is some 0.84 Hartree lower than in the STO-3G case (fig. 4.1 and 4.3). This is a very large energy difference, and at first sight would appear to invalidate the STO-3G approximation. However, the energies relative to the origin in the two cases are very similar. The effect of the 5G basis being to reduce all energies relative to the origin by only about 0.0001 Hartree and the closeness of the LMOs obtained has already been pointed out. In fact although the total energy converges slowly towards the pure STO value with increasing length of gaussian expansion, other

values such as atomisation energy, atomic populations and dipole moments are quite well represented by a STO-3G expansion.<sup>223, 226</sup>

The most noticeable disparity in the three energy diagrams is evident when the inner shells are truncated. For most structures the net result is an increase of about 0.0007 H compared with the untruncated STO-3G case. However, the three structures between 0.00406 H and 0.00475 H in Fig. 4.1 are missing in Fig. 4.3. The structures in this case were found at energies just above the top of the scale in Fig. 4.3. The general forms of the LMOs in the two cases give a clue as to the reason for this difference in energy. The carbon lone pair in the  $\lambda_N \lambda_C \mu_{CN}$  structure and the nitrogen lone pairs in the other two structures are very different in character in the two examples. In Fig. 4.1 the lone pairs show a very large 1s contribution and hence a very large overlap ( $>0.995$ ) with the corresponding inner shell MO. In the second case, when the inner shells no longer have small AO contributions from secondary centres, the lone pairs are more familiar in appearance with a large 2s contribution. From these observations it seems that the relevant lone pair orbitals in these structures will "collapse" into the atomic core and become indistinguishable from the inner shell MOs, when allowed the freedom to do so. When the inner shells are left with their canonical delocalisations this freedom is present, and the result is an orbital overlap very large but slightly less than unity. When the inner shells are strictly localised like the lone pairs however, such a "collapse" would force the overlap integral to unity and hence to the rejection of that MO set due to linear dependence. Thus the lone pair MOs in this case are forced to take on a more usual form with a corresponding

energy sacrifice.

With this exception, truncating the inner shell MOs or using a longer gaussian expansion to represent the STO basis set, makes little difference to the relative energies of the different structures or to the corresponding LMOs. With this in mind, and since this work represents only a preliminary investigation of the PLMO method, all other molecules were investigated using a STO-3G basis and with the inner shells left untruncated for simplicity.

#### 4.5 CHOOSING THE PLMO STRUCTURE

The problem of deciding which of the low energy structures will be considered the basic valence description of HCN, and hence yielding the PLMOs for this molecule, still remains. The three lowest energy structures are common to all three figures and are therefore considered appropriate candidates.

The argument presented in Chapter 1 (section 1.3(a)) determines that the  $\lambda_{\text{N}}^{\mu}\text{CH}^{\mu}\text{CN}$  structure be chosen, since the LMOs are localised onto fewer atomic centres in this set than in the other two. Thus the extent to which the electronic structure of HCN may be expressed in terms of two-centre bonds and one-centre lone pairs is tested more rigorously by selecting this arrangement. In fact, by comparing the forms of the LMOs in the three structures, the PLMOs can be seen to lead to the LMOs of the other two arrangements by allowing the nitrogen lone pair to delocalise first onto the carbon atom, and secondly onto the distant hydrogen atom. Hence the N-H bond in the second case is lone pair-like at the nitrogen atom and has only a small hydrogen coefficient, while the two C-N bonds present in the first case are no longer unique.

#### 4.6 PROPERTIES OF THE PLMOs

A particular arrangement of lone pairs and bonds, to be considered the basic simple valence approximation to the electronic structure of HCN, and a corresponding set of PLMOs has thus been found. Besides yielding a description of the electronic organisation of the molecule directly, the PLMOs may be used to calculate observables and other useful functions for the molecule. In this work, the dipole moment is calculated for all the molecules investigated in Chapter 6 and the results of a Mulliken Population analysis<sup>118-123</sup> is presented in Chapter 8. It is appropriate at this stage however, to show the overlap integrals between the sigma PLMOs.

The absolute values of the overlap integrals are shown for the three cases of HCN in Tables 4.7, 4.8 and 4.9. The pi orbitals are orthogonal to all the sigma PLMOs by symmetry. Also exhibited in the figures is a measure of non-orthogonality of the  $\sigma$  PLMOs,  $\Delta$ . This is the root mean square value of the off-diagonal elements of the sigma overlap integral matrix and is defined by:

$$\Delta = \left( \frac{1}{n\sigma(n\sigma - 1)} \sum_{i=1}^{n\sigma} \sum_{\substack{j=1 \\ (i \neq j)}}^{n\sigma} \langle \phi_i / \phi_j \rangle^2 \right)^{\frac{1}{2}} \quad (4.5)$$

where  $n\sigma$  is the number of  $\sigma$  PLMOs (including inner shells). A discussion of these values is undertaken in Chapter 8 but it may be noted here that the overlap integrals shown are very similar in the three tables. This is simply a reflection of the similarity of the PLMOs already noted.

TABLE 4.7 ABSOLUTE VALUES OF OVERLAP INTEGRALS BETWEEN SIGMA PLMOs  
(INC. INNER SHELLS) OF HCN AND  $\Delta$  FUNCTION<sup>(a)</sup> (STO-3G BASIS)

|             | $k_N$  | $k_C$  | $\lambda_N$ | $\mu_{CH}$        | $\mu_{CN}$ |
|-------------|--------|--------|-------------|-------------------|------------|
| $k_N$       | 1.0    |        |             |                   |            |
| $k_C$       | 0.0000 | 1.0    |             | $\Delta = 0.0334$ |            |
| $\lambda_N$ | 0.0001 | 0.0279 | 1.0         |                   |            |
| $\mu_{CH}$  | 0.0108 | 0.0076 | 0.0104      | 1.0               |            |
| $\mu_{CN}$  | 0.0002 | 0.0041 | 0.0060      | 0.1002            | 1.0        |

(a) For definition of  $\Delta$  see narrative

TABLE 4.8 ABSOLUTE VALUES OF OVERLAP INTEGRALS BETWEEN SIGMA PLMOs  
(INC. INNER SHELLS) OF HCN AND  $\Delta$  FUNCTION<sup>(a)</sup> (STO-5G BASIS)

|             | $k_N$  | $k_C$  | $\lambda_N$ | $\mu_{CH}$        | $\mu_{CN}$ |
|-------------|--------|--------|-------------|-------------------|------------|
| $k_N$       | 1.0    |        |             |                   |            |
| $k_C$       | 0.0000 | 1.0    |             | $\Delta = 0.0330$ |            |
| $\lambda_N$ | 0.0000 | 0.0268 | 1.0         |                   |            |
| $\mu_{CH}$  | 0.0115 | 0.0076 | 0.0122      | 1.0               |            |
| $\mu_{CN}$  | 0.0002 | 0.0040 | 0.0053      | 0.0990            | 1.0        |

(a) For definition of  $\Delta$  see narrative



TABLE 4.9 ABSOLUTE VALUES OF OVERLAP INTEGRALS BETWEEN SIGMA PLMOs  
(INC. TRUNCATED INNER SHELLS) OF HCN AND FUNCTION<sup>(a)</sup>  
(STO-3G BASIS)

|             | $k_N$  | $k_C$  | $\lambda_N$ | $\mu_{CH}$        | $\mu_{CN}$ |
|-------------|--------|--------|-------------|-------------------|------------|
| $k_N$       | 1.0    |        |             |                   |            |
| $k_C$       | 0.0048 | 1.0    |             | $\Delta = 0.0344$ |            |
| $\lambda_N$ | 0.0058 | 0.0338 | 1.0         |                   |            |
| $\mu_{CH}$  | 0.0082 | 0.0133 | 0.0103      | 1.0               |            |
| $\mu_{CN}$  | 0.0108 | 0.0080 | 0.0062      | 0.1002            | 1.0        |

(a) For definition of  $\Delta$  see narrative.

#### 4.7 COMMENTS ON THE METHOD

The LMO method presented here is a new one. The PLMOs are generated by a straightforward procedure based on the requirement that the delocalisation energy of one and two-centre LMOs be a minimum. It is perhaps surprising that such a simple technique has not been exploited before. In the next chapter the results of applying the method to other molecules besides HCN are given. In this section some comments on particulars of the PLMO method, not already given in this chapter, are presented.

##### 4.7(a) Separation of CMOs

The inner shell and pi CMOs were separated from the sigma valence CMOs at the very beginning of the procedure (Section 4.3(a)). The inner shells were not included in the localising process because they were considered to be already localised onto their atomic centres. This assertion is well founded. It is well known that the core orbitals in a molecule - represented by the Slater 1s AOs in HCN - are almost identical with those of the free atom, while the valence MOs contain the essential part of the chemical information. This separation of core and valence regions (electrons)<sup>227</sup> forms the basis for the successful application of pseudopotential methods<sup>228</sup> in molecular calculations, which are only slightly less accurate than corresponding ab-initio procedures.<sup>228,229</sup>

The two pi orbitals in HCN were separated from the sigma valence MOs which were used to form localised bonds and lone pairs. The sigma-pi description of the C-N multiple bond that results from this separation may be contrasted to the three C-N "banana bonds" that are generated by other LMO methods.<sup>71,83</sup> These two alternative

descriptions of multiple bonds in general are of course equivalent,<sup>69,212</sup> and if the "banana bond" description is required in HCN (or in CO or N<sub>2</sub> (next chapter)) then an appropriate 3 x 3 linear transformation of the sigma PLMO and pi CMOs may be simply applied. The reduction in computational complexity that results from sigma-pi separation may also be used to advantage in molecules with a number of multiple bonds, where the delocalisation of the pi electron system need not invalidate an examination of the sigma electrons in terms of localised orbitals.<sup>42,230</sup>

#### 4.7(b) Orthogonal Transformation and Truncation

The energy minimum found for each structure (including the PLMO structure) does not fix the associated LMOs completely. Any linear combination of the final LMOs for a structure would yield an identical energy, and provided such a linear combination did not change the structure specification (e.g. by generating three-centre bonds or by turning a one-centre LMO into a two-centre LMO), the resulting LMOs would be equally acceptable solutions, on an energy criterion, for that structure. Clearly, since the PLMO method gives a unique set of LMOs for each structure (provided there is not more than one sigma bond between a pair of atoms or more than one sigma lone pair on an atom) the full freedom afforded the LMOs by the requirement that they be linearly independent and normalised, is not exploited by the orthogonal transformation and truncation steps in this method. In other words, the search for an energy minimum for each structure does not occur within the whole function space available, but is constrained to the direction of convergence imposed by the orthogonal transformation of the CMOs. This can be most easily seen in the

structures at the CMO energy for  $N_2$  and CO (next chapter) where because the CMOs and other LMOs occur at the same energy they must be linked by a linear transformation. In these examples the number of disposable parameters used to construct the orthogonal transforming matrix, and in terms of which the energy functional is minimised,  $(\frac{1}{2}R(R-1))$  (Section 4.3(c)), is less than the number that would be required to construct a general linear transformation matrix which still maintains the linear independence of the transformed CMOs  $(\frac{1}{2}R(R+1))$ . The one and two-centre LMOs selected by the PLMO method for any structure are hence those in the space of a truncation of an orthogonal transformation of the CMOs in which the energy sacrificed is a minimum. How severe this restriction on the PLMO wavefunctions of the example molecules proves to be, might be judged by comparing the size of the energy sacrifice in the PLMO wavefunction to one and two-centre LMO wavefunctions obtained by other methods. Such a comparison will be undertaken in Chapter 7.

The success or failure of the PLMO method must be judged by an analysis of the results (Part C). However, an advantage of the PLMO procedure, besides yielding unique LMOs, is that it should ensure that when the energy sacrifice is low, i.e. when only small AO coefficients have been deleted by the truncation, the final LMOs are not far from orthogonal. This is true of the PLMO structure in HCN (Tables 4.7, 4.8 and 4.9).

## CHAPTER FIVE

### EXAMPLES OF PLMO METHOD - CO, N<sub>2</sub>, H<sub>2</sub>O, NH<sub>3</sub> & CH<sub>4</sub>

#### 5.1 INTRODUCTION

The general method of obtaining PLMOs, outlined in the previous chapter, was applied to the molecules carbon monoxide, nitrogen, water, ammonia and methane. A STO-3G basis was used and the inner shells were left untruncated. Neither of these simplifications are expected to influence the results to any great extent as the comparisons made in chapter 4 show. The results for these molecules are displayed in this chapter in the same format as the HCN results of the preceding chapter.

#### 5.2 PRELIMINARIES

The molecular geometry and the atomic co-ordinates used are shown in Tables 5.1 to 5.5.

The starting sets of CMOs and integrals over AOs were obtained from the Gaussian 70 package as with HCN. The occupied CMOs and the orbital energies are shown in Tables 5.6 to 5.10. The pi CMOs for each molecule,  $\pi_1$  and  $\pi_2$  in CO,  $\pi_1$  and  $\pi_2$  in N<sub>2</sub>, and  $\pi_1$  in H<sub>2</sub>O, and the inner shells, were considered as already localised and hence separated from the remaining sigma CMOs which were to be transformed. The inner shells of the nitrogen molecule (Table 5.7) were delocalised onto both atomic centres due to symmetry, but by taking a renormalised sum and difference of the CMOs the inner shells become localised onto the atomic centres (Table 5.12).

#### 5.3 ENERGY DIAGRAMS AND LMOs

Some structures and associated energies for the example molecules, obtained by application of the PLMO procedure, are shown in Figures 5.1 to 5.5. The notation used is the same as for HCN.

TABLE 5.1 <sup>231</sup> GEOMETRY AND CO-ORDINATE SYSTEM FOR CO

| $R(C - O) = 1.1282\text{\AA}$ |                             |     |        |
|-------------------------------|-----------------------------|-----|--------|
| Atom                          | Co-ordinates (atomic units) |     |        |
|                               | x                           | y   | z      |
| C                             | 0.0                         | 0.0 | 0.0    |
| O                             | 0.0                         | 0.0 | 2.1320 |

TABLE 5.2 <sup>232</sup> GEOMETRY AND CO-ORDINATE SYSTEM FOR N<sub>2</sub>

| $R(N - N) = 1.0976\text{\AA}$ |                             |     |        |
|-------------------------------|-----------------------------|-----|--------|
| Atom                          | Co-ordinates (atomic units) |     |        |
|                               | x                           | y   | z      |
| N <sub>1</sub>                | 0.0                         | 0.0 | 0.0    |
| N <sub>2</sub>                | 0.0                         | 0.0 | 2.0742 |

TABLE 5.3 <sup>233</sup> GEOMETRY AND CO-ORDINATE SYSTEM FOR H<sub>2</sub>O

| $R(O - H) = 0.9572\text{\AA}$ $\angle HOH = 104.52^\circ$ |                             |     |         |
|---|-----------------------------|-----|---------|
| Atom  | Co-ordinates (atomic units) |     |         |
|   | x                           | y   | z       |
| O   | 0.0                         | 0.0 | 0.0     |
| H <sub>1</sub>  | 1.4305                      | 0.0 | -1.1072 |
| H <sub>2</sub>  | -1.4305                     | 0.0 | -1.1072 |

TABLE 5.4 GEOMETRY<sup>232</sup> AND CO-ORDINATE SYSTEM FOR NH<sub>3</sub>

| $R(N - H) = 1.008 \text{ \AA} \quad \angle HNH = 107.3^\circ$ |                             |        |        |
|---|-----------------------------|--------|--------|
| Atom  | Co-ordinates (atomic units) |        |        |
|   | x                           | y      | z      |
| N   | 0.0                         | 0.0    | 0.0    |
| H <sub>1</sub>  | 1.772                       | 0.0    | -0.700 |
| H <sub>2</sub>  | -0.886                      | 1.534  | -0.700 |
| H <sub>3</sub>  | -0.886                      | -1.534 | -0.700 |

TABLE 5.5 GEOMETRY<sup>232</sup> AND CO-ORDINATE SYSTEM FOR CH<sub>4</sub>

| $R(C - H) = 1.091 \text{ \AA} \quad \angle HCH = 109.63^\circ$ |                             |        |        |
|--|-----------------------------|--------|--------|
| Atom   | Co-ordinates (atomic units) |        |        |
|  | x                           | y      | z      |
| C  | 0.0                         | 0.0    | 0.0    |
| H <sub>1</sub>   | 1.189                       | -1.189 | 1.189  |
| H <sub>2</sub>   | -1.189                      | 1.189  | 1.189  |
| H <sub>3</sub>   | -1.189                      | -1.189 | -1.189 |
| H <sub>4</sub>   | 1.189                       | 1.189  | -1.189 |

TABLE 5.6 OCCUPIED CMOs AND EIGENVALUES FOR CO (STO-3G BASIS)

| CMO<br>(a)     | 1s <sub>C</sub> | 2s <sub>C</sub> | 2p <sub>xC</sub> | 2p <sub>yC</sub> | 2p <sub>zC</sub> | 1s <sub>O</sub> | 2s <sub>O</sub> | 2p <sub>xO</sub> | 2p <sub>yO</sub> | 2p <sub>zO</sub> | Eigenvalue (H)<br>(b) |
|----------------|-----------------|-----------------|------------------|------------------|------------------|-----------------|-----------------|------------------|------------------|------------------|-----------------------|
| k <sub>O</sub> | 0.0004          | -0.0087         | -                | -                | -0.0074          | 0.9941          | 0.0278          | -                | -                | -0.0068          | -20.4242              |
| k <sub>C</sub> | 0.9936          | 0.0263          | -                | -                | 0.0070           | -0.0002         | -0.0069         | -                | -                | 0.0010           | -11.0934              |
| σ <sub>3</sub> | -0.1265         | 0.2403          | -                | -                | 0.1669           | -0.2224         | 0.7664          | -                | -                | -0.2180          | -1.4599               |
| σ <sub>4</sub> | -0.1660         | 0.5387          | -                | -                | 0.0679           | 0.1320          | -0.6459         | -                | -                | -0.6277          | -0.6995               |
| π <sub>1</sub> | -               | -               | 0.0336           | 0.4443           | -                | -               | -               | 0.0597           | 0.7887           | -                | -0.5511               |
| π <sub>2</sub> | -               | -               | -0.4443          | 0.0336           | -                | -               | -               | -0.7887          | 0.0597           | -                | -0.5511               |
| σ <sub>5</sub> | -0.1671         | 0.7609          | -                | -                | -0.5728          | 0.0011          | 0.0382          | -                | -                | 0.4341           | -0.4465               |

a) The CMOs are: k - inner shell CMO

σ - valence sigma CMO

π - pi CMO

b) The eigenvalue in Hartrees (H)



TABLE 5.7 OCCUPIED CMOs AND EIGENVALUES FOR N<sub>2</sub> (STO-3G BASIS)

| CMO (a)        | 1s <sub>N1</sub> | 2s <sub>N1</sub> | 2p <sub>xN1</sub> | 2p <sub>yN1</sub> | 2p <sub>zN1</sub> | 1s <sub>N2</sub> | 2s <sub>N2</sub> | 2p <sub>xN2</sub> | 2p <sub>yN2</sub> | 2p <sub>zN2</sub> | Eigenvalue (H) (b) |
|----------------|------------------|------------------|-------------------|-------------------|-------------------|------------------|------------------|-------------------|-------------------|-------------------|--------------------|
| k <sub>1</sub> | 0.7031           | 0.0128           | -                 | -                 | 0.0021            | 0.7031           | 0.0128           | -                 | -                 | -0.0021           | -15.5180           |
| k <sub>2</sub> | 0.7028           | 0.0269           | -                 | -                 | 0.0099            | -0.7028          | -0.0269          | -                 | -                 | 0.0099            | -15.5161           |
| σ <sub>3</sub> | -0.1758          | 0.4888           | -                 | -                 | 0.2401            | -0.1758          | 0.4888           | -                 | -                 | -0.2401           | -1.4427            |
| σ <sub>4</sub> | -0.1711          | 0.7420           | -                 | -                 | -0.2642           | 0.1711           | -0.7420          | -                 | -                 | -0.2642           | -0.7225            |
| π <sub>1</sub> | -                | -                | 0.4867            | 0.3919            | -                 | -                | -                | 0.4867            | 0.3919            | -                 | -0.5730            |
| π <sub>2</sub> | -                | -                | 0.3919            | -0.4867           | -                 | -                | -                | 0.3919            | -0.4867           | -                 | -0.5730            |
| σ <sub>5</sub> | -0.0690          | 0.4081           | -                 | -                 | -0.6038           | -0.0690          | 0.4081           | -                 | -                 | -0.6038           | -0.5395            |

a) The CMOs are: k - inner shell CMO

σ - valence sigma CMO

π - pi CMO

b) The eigenvalue in Hartrees (H)

TABLE 5.8 OCCUPIED CMOs AND EIGENVALUES FOR H<sub>2</sub>O (STO-3G BASIS)

| CMO<br>(a)     | 1s <sub>O</sub> | 2s <sub>O</sub> | 2p <sub>xO</sub> | 2p <sub>yO</sub> | 2p <sub>zO</sub> | 1s <sub>H<sub>1</sub></sub> | 1s <sub>H<sub>2</sub></sub> | Eigenvalue (H)<br>(b) |
|----------------|-----------------|-----------------|------------------|------------------|------------------|-----------------------------|-----------------------------|-----------------------|
| k <sub>0</sub> | 0.9941          | 0.0266          | 0.0000           | -                | -0.0043          | -0.0060                     | -0.0060                     | -20.2417              |
| σ <sub>2</sub> | -0.2328         | 0.8335          | 0.0000           | -                | -0.1296          | 0.1587                      | 0.1587                      | -1.2684               |
| σ <sub>3</sub> | 0.0000          | 0.0000          | -0.6064          | -                | 0.0000           | -0.4450                     | 0.4450                      | -0.6179               |
| σ <sub>4</sub> | 0.1032          | -0.5369         | 0.0000           | -                | -0.7767          | 0.2778                      | 0.2778                      | -0.4530               |
| π <sub>1</sub> | -               | -               | -                | 1.0000           | -                | -                           | -                           | -0.3912               |

- a) The CMOs are: k - inner shell CMO  
σ - valence sigma CMO  
π - pi CMO

b) The eigenvalue in Hartrees (H)

TABLE 5.9 OCCUPIED CMOs AND EIGENVALUES FOR  $\text{NH}_3$  (STO-3G BASIS)

| CMO<br>(a) | $1s_N$  | $2s_N$ | $2p_{xN}$ | $2p_{yN}$ | $2p_{zN}$ | $1s_{H_1}$ | $1s_{H_2}$ | $1s_{H_3}$ | Eigenvalue (H)<br>(b) |
|------------|---------|--------|-----------|-----------|-----------|------------|------------|------------|-----------------------|
| $k_N$      | 0.9934  | 0.0322 | 0.0000    | 0.0000    | -0.0049   | -0.0067    | -0.0067    | -0.0067    | -15.3027              |
| $\sigma_2$ | -0.2197 | 0.7346 | 0.0000    | 0.0000    | -0.1345   | 0.1602     | 0.1602     | 0.1602     | -1.0909               |
| $\sigma_3$ | 0.0000  | 0.0000 | -0.5927   | 0.0000    | 0.0000    | -0.4945    | 0.2472     | 0.2472     | -0.5751               |
| $\sigma_4$ | 0.0000  | 0.0000 | 0.0000    | -0.5927   | 0.0000    | 0.0000     | -0.4282    | 0.4282     | -0.5751               |
| $\sigma_5$ | -0.0870 | 0.4375 | 0.0000    | 0.0000    | 0.8980    | -0.1184    | -0.1184    | -0.1184    | -0.3510               |

a) The CMOs are:  $k$  - inner shell CMO $\sigma$  - valence sigma CMO

b) The eigenvalue in Hartrees (H)

TABLE 5.10 OCCUPIED CMOs AND EIGENVALUES FOR CH<sub>4</sub> (STO-3G BASIS)

| CMO (a)        | 1s <sub>C</sub> | 2s <sub>C</sub> | 2p <sub>xC</sub> | 2p <sub>yC</sub> | 2p <sub>zC</sub> | 1s <sub>H<sub>1</sub></sub> | 1s <sub>H<sub>2</sub></sub> | 1s <sub>H<sub>3</sub></sub> | 1s <sub>H<sub>4</sub></sub> | Eigenvalue (H) (b) |
|----------------|-----------------|-----------------|------------------|------------------|------------------|-----------------------------|-----------------------------|-----------------------------|-----------------------------|--------------------|
| k <sub>C</sub> | 0.9920          | 0.0380          | 0.0000           | 0.0000           | 0.0000           | -0.0069                     | -0.0069                     | -0.0069                     | -0.0069                     | -11.0303           |
| σ <sub>2</sub> | -0.2212         | 0.6295          | 0.0000           | 0.0000           | 0.0000           | 0.1808                      | 0.1808                      | 0.1808                      | 0.1808                      | -0.9085            |
| σ <sub>3</sub> | 0.0000          | 0.0000          | 0.0000           | 0.0000           | -0.5711          | -0.3015                     | -0.3015                     | 0.3015                      | 0.3015                      | -0.5177            |
| σ <sub>4</sub> | 0.0000          | 0.0000          | 0.0000           | -0.5711          | 0.0000           | 0.3015                      | -0.3015                     | 0.3015                      | -0.3015                     | -0.5177            |
| σ <sub>5</sub> | 0.0000          | 0.0000          | -0.5711          | 0.0000           | 0.0000           | -0.3015                     | 0.3015                      | 0.3015                      | -0.3015                     | -0.5177            |

a) The CMOs are: k - inner shell CMO

σ - valence sigma CMO

b) The eigenvalue in Hartrees (H)

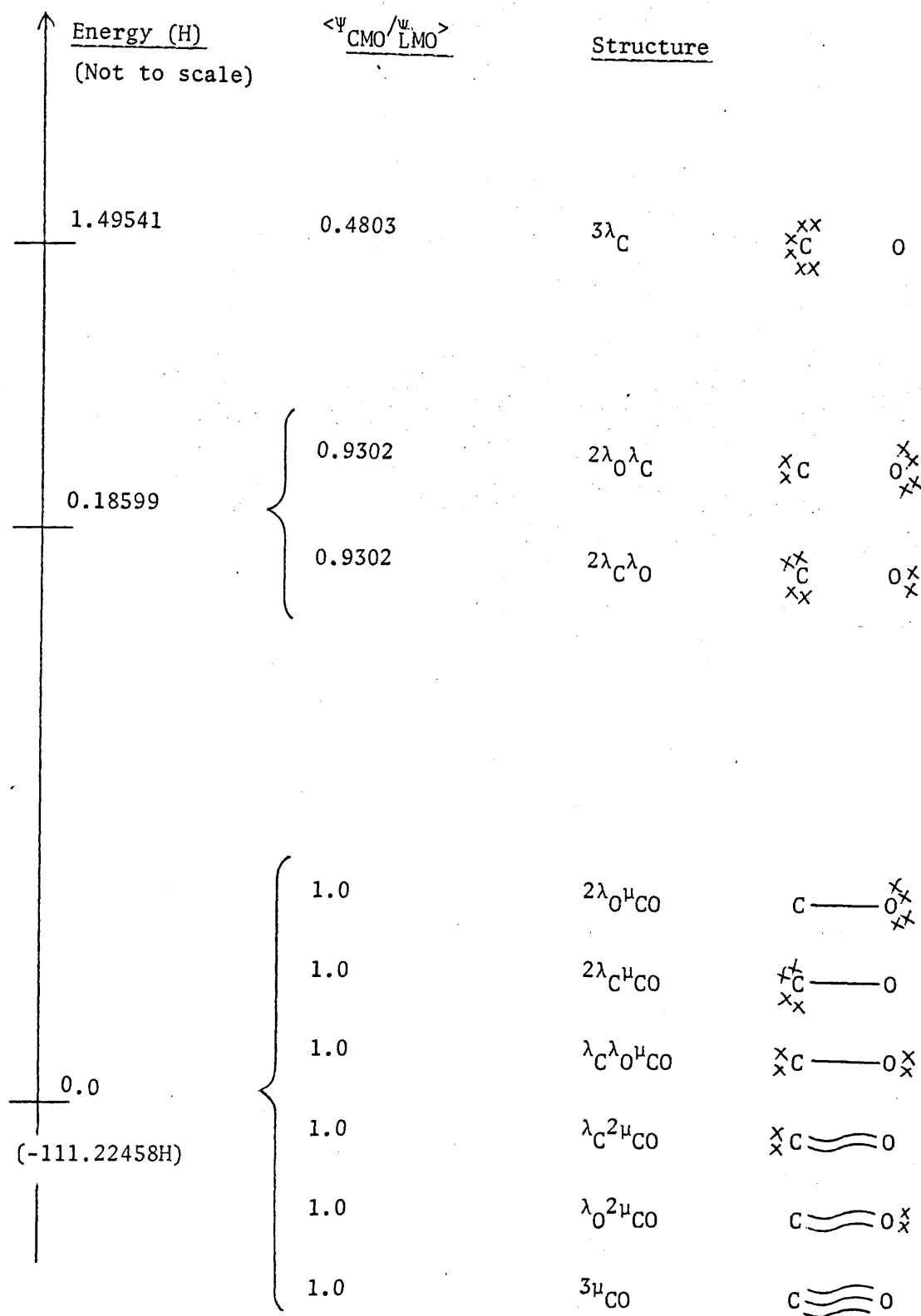


Figure 5.1 Energy diagram for LMO structures in sigma frame of CO  
 (STO-3G basis)  
 (For explanation of symbols see narrative)

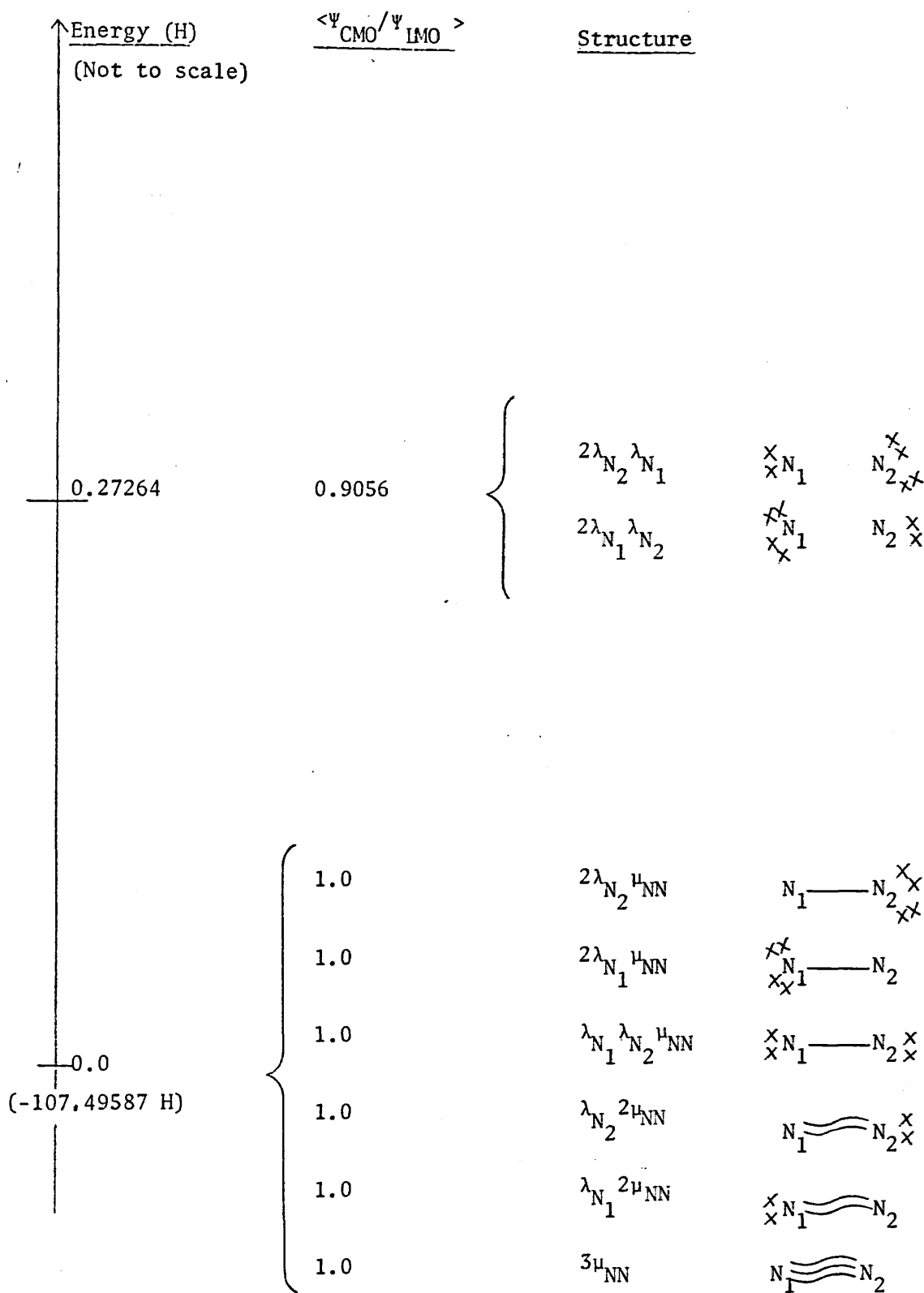


Figure 5.2 Energy diagram for LMO structures in sigma frame of  $N_2$   
(STO-3G basis)  
(For explanation of symbols see narrative)

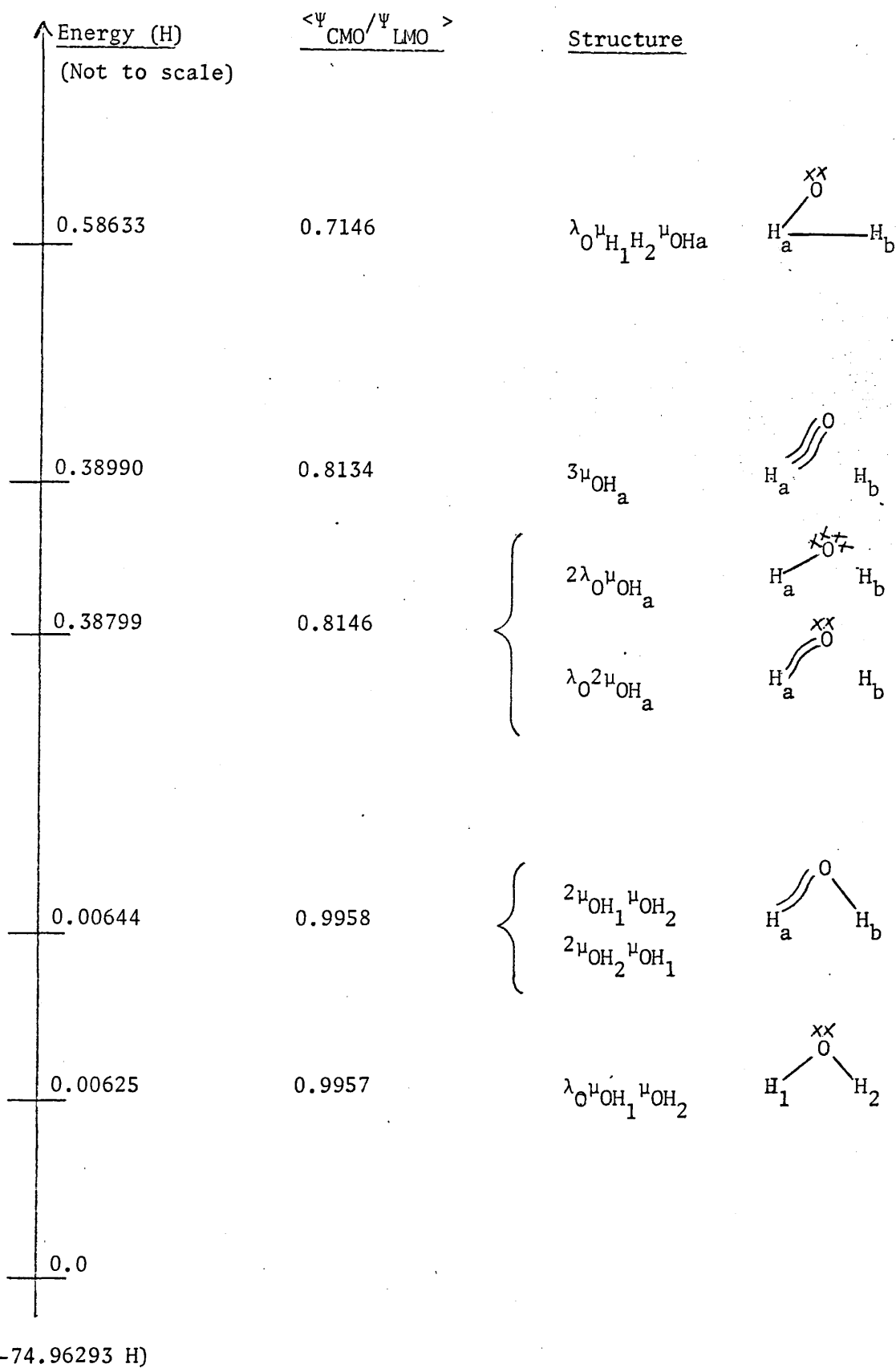


Figure 5.3 Energy diagram for LMO structures in sigma frame of  $\text{H}_2\text{O}$   
(STO-3G basis)  
(For explanation of symbols see narrative.)

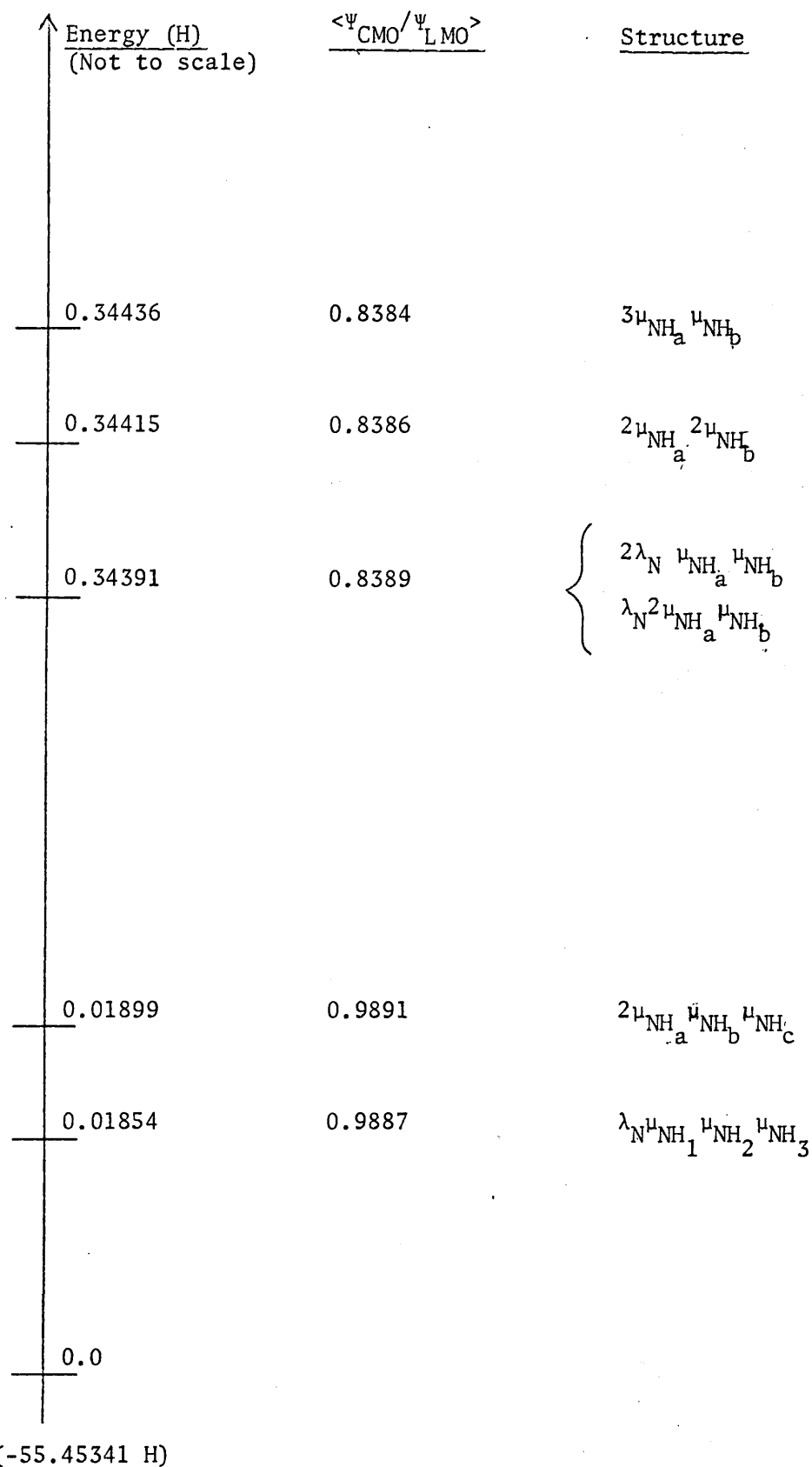


Figure 5.4 Energy diagram for LMO structures in sigma frame of  $\text{NH}_3$   
 (STO-3G basis)  
 (For explanation of symbols see narrative)



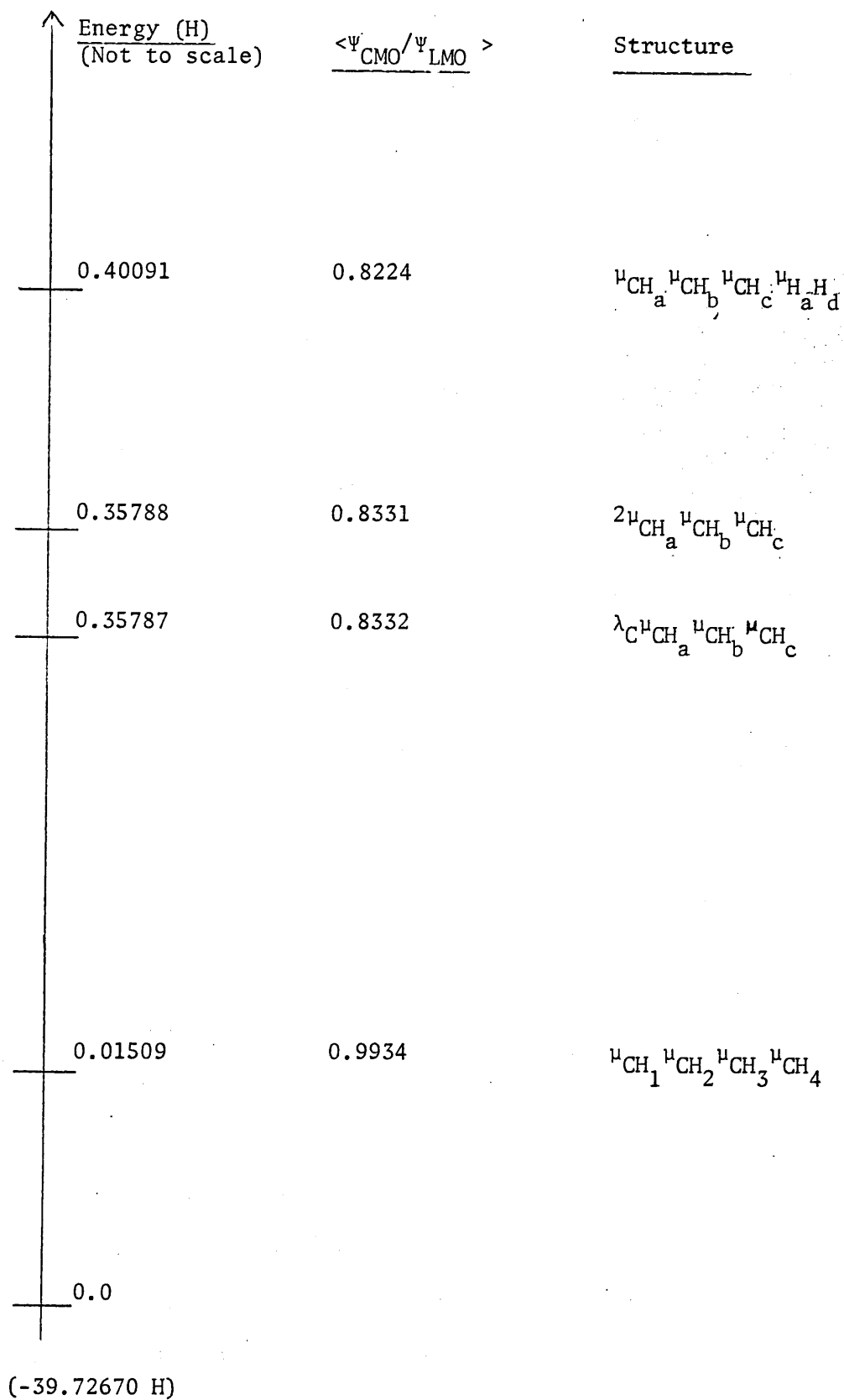


Figure 5.5 Energy diagram for LMO structures in sigma frame of CH<sub>4</sub>  
 (STO-3G basis)  
 (For explanation of symbols see narrative)

The number of different arrangements of lone pairs and bonds possible for a molecule, increases dramatically as the number of atoms and/or the number of delocalised CMOs increases. The energy diagrams for carbon monoxide and nitrogen, Figures 5.1 and 5.2 contain almost all the structures possible for the three transformed and truncated MOs; while for water, ammonia and methane, Figures 5.3 5.4 and 5.5, only those structures in the very bottom section of the energy scale are shown. In these latter three molecules there are many equivalent structures differing only in the hydrogen atom labels. These structures were all separately investigated (or a selection of them in methane) and an energy minimum obtained. Equivalent structures at the same energy are represented in the figures by labelling the hydrogen atoms algebraically with letters rather than explicitly with numbers.

The LMOs corresponding to the structures near the bottom of each of the energy diagrams are shown in Tables 5.11 to 5.15. Again, an orthogonalised 2s AO has been used, with a resulting alteration to the 1s and 2s<sup>OR</sup> AO coefficients. Only the unique LMOs are shown for each structure. The LMOs are expressed in the form of a normalised hybrid on each atom and a polarity parameter.

#### 5.4 CHOOSING THE PLMO STRUCTURES

For the diatomic molecules CO and N<sub>2</sub> it is not possible to resolve using an energy criterion, a number of different structures (Figures 5.1 and 5.2). The reason is that, if one of the three transformed MOs remains untruncated, i.e. represents a N-N or C-O bond and the inner shells are left untruncated, the LMOs span the Hartree-Fock manifold and therefore yield the canonical energy and wavefunction.

TABLE 5.11. INNER SHELLS, PI ORBITALS AND LMOs FOR LOW ENERGY STRUCTURES FOR CO (STO-3G BASIS)

(for explanation see narrative)

| Structure | LMO                             | 1s <sub>C</sub>  | 2s <sub>C</sub> <sup>or</sup> | 2p <sub>zC</sub>         | 1s <sub>O</sub>  | 2s <sub>O</sub> <sup>or</sup> | 2p <sub>zO</sub> |          |
|-----------|---------------------------------|------------------|-------------------------------|--------------------------|------------------|-------------------------------|------------------|----------|
| All       | k <sub>O</sub>                  | -0.0018          | -0.0084                       | -0.0074                  | 1.0007           | 0.0270                        | -0.0068          |          |
|           | k <sub>C</sub>                  | 1.0001           | 0.0255                        | 0.0070                   | -0.0019          | -0.0067                       | 0.0010           |          |
|           | λ <sub>C</sub>                  | -0.0201          | 0.9227                        | -0.3851                  |                  |                               |                  |          |
|           | λ <sub>O</sub>                  |                  |                               |                          | -0.0161          | 0.9642                        | 0.2647           |          |
|           | μ <sub>CO</sub>                 | 0.4638           | (-0.1496                      | 0.0688                   | 0.7486           | (-0.0553                      | 0.0231           | -0.9982) |
|           | 2λ <sub>O</sub> μ <sub>CO</sub> |                  |                               |                          |                  |                               |                  |          |
|           | 2λ <sub>C</sub> μ <sub>CO</sub> |                  |                               |                          |                  |                               |                  |          |
|           | λ <sub>O</sub> 2μ <sub>CO</sub> |                  |                               |                          |                  |                               |                  |          |
|           | λ <sub>C</sub> 2μ <sub>CO</sub> |                  |                               |                          |                  |                               |                  |          |
|           |                                 |                  | as λ <sub>C</sub> above       |                          |                  |                               |                  |          |
|           |                                 |                  |                               | as μ <sub>CO</sub> above |                  |                               |                  |          |
|           |                                 |                  |                               |                          |                  | as λ <sub>O</sub> above       |                  |          |
| Structure | MO                              | 2p <sub>xC</sub> | 2p <sub>yC</sub>              | 2p <sub>xC</sub>         | 2p <sub>yO</sub> | 2p <sub>xO</sub>              | 2p <sub>yO</sub> |          |
| All       | π <sub>1</sub>                  | ( 0.0754         | 0.9972)                       | 0.7910                   | ( 0.0755         | 0.9971)                       |                  |          |
|           | π <sub>2</sub>                  | (-0.9972         | 0.0754)                       | 0.7910                   | (-0.9971         | 0.0755)                       |                  |          |

TABLE 5.12 INNER SHELLS, PI ORBITALS AND LMOs FOR LOW ENERGY STRUCTURES FOR N<sub>2</sub> (STO-3G BASIS)

(for explanation see narrative)

| Structure  | LMO  | 1s <sub>N<sub>1</sub></sub>  | 2s <sub>N<sub>1</sub></sub> <sup>or</sup> | 2p <sub>zN<sub>1</sub></sub> | 1s <sub>N<sub>2</sub></sub>  | 2s <sub>N<sub>2</sub></sub> <sup>or</sup> | 2p <sub>zN<sub>2</sub></sub> |
|--|--|------------------------------|---|------------------------------|------------------------------|---|------------------------------|
| A11  | k <sub>N<sub>1</sub></sub><br>k <sub>N<sub>2</sub></sub> | 1.0007<br>-0.0022            | 0.0273<br>-0.0097                         | 0.0084<br>-0.0055            | -0.0022<br>1.0007            | -0.0097<br>0.0273                         | 0.0055<br>-0.0084            |
| λ <sub>N<sub>1</sub></sub> <sup>μ<sub>NN</sub></sup><br>λ <sub>N<sub>2</sub></sub> <sup>μ<sub>NN</sub></sup>   | λ <sub>N<sub>1</sub></sub>                               | -0.0181                      | 0.9386                                    | -0.3444                      |                              |   |                              |
|  | λ <sub>N<sub>2</sub></sub>                               |                              |   |                              | -0.0181                      | 0.9386                                    | 0.3444                       |
| 2λ <sub>N<sub>1</sub></sub> <sup>μ<sub>NN</sub></sup><br>2λ <sub>N<sub>2</sub></sub> <sup>μ<sub>NN</sub></sup> | μ <sub>NN</sub>  | 0.6122                       | 0.0408                                    | 0.9942                       | 0.6122                       | 0.0408                                    | -0.9942                      |
|  | μ <sub>NN</sub>  |                              |   |                              | (-0.0905                     |   | (-0.9942)                    |
| λ <sub>N<sub>1</sub></sub> <sup>2μ<sub>NN</sub></sup><br>λ <sub>N<sub>2</sub></sub> <sup>2μ<sub>NN</sub></sup> | λ <sub>N<sub>1</sub></sub>                               |                              | as λ <sub>N<sub>2</sub></sub> above       |                              |                              | as λ <sub>N<sub>1</sub></sub> above       |                              |
|  | λ <sub>N<sub>2</sub></sub>                               |                              |   |                              |                              |   |                              |
| Structure  | MO   | 2p <sub>xN<sub>1</sub></sub> | 2p <sub>yN<sub>1</sub></sub>              | 2p <sub>xN<sub>2</sub></sub> | 2p <sub>yN<sub>2</sub></sub> | 2p <sub>xN<sub>2</sub></sub>              | 2p <sub>yN<sub>2</sub></sub> |
| A11  | π <sub>1</sub><br>π <sub>2</sub>                         | ( 0.7789<br>( 0.6272         | 0.6249<br>-0.7789                         | 0.6249<br>( 0.6272           | ( 0.7789<br>( 0.6272         | 0.6249<br>-0.7789                         | 0.6272<br>-0.7789            |

TABLE 5.13 INNER SHELL, PI ORBITAL AND LMOs FOR LOW ENERGY STRUCTURES FOR  $H_2O$  (STO-3G BASIS)  
(For explanation see narrative)

| Structure     | LMO                | $1s_O$    | $2s_O$ or | $2p_{xO}$ | $2p_{zO}$ | $1s_{H_1}$ | $1s_{H_2}$ |
|---------------|--------------------|-----------|-----------|-----------|-----------|------------|------------|
| All           | $k_O$              | 1.0004    | 0.0258    | 0.0000    | -0.0043   | -0.0060    | -0.0060    |
| $2\mu_{OH_2}$ | $\mu_{OH_1}^{(a)}$ | 0.6857    | -0.1092   | 0.6210    | -0.7753   | 0.5379     |            |
| $\lambda_O$   | $\mu_{OH_1}$       | -0.0212   | 0.9712    | 0.0000    | 0.2375    |            |            |
|               | $\mu_{OH_1}$       | 0.6841    | -0.1038   | 0.6240    | -0.7735   | 0.5382     |            |
|               | $\mu_{OH_2}$       | 0.6841    | -0.1038   | -0.6240   | -0.7735   |            | 0.5382     |
| Structure     | MO                 | $2p_{yO}$ |           |           |           |            |            |
| All           | $\pi_1$            | 1.0000    |           |           |           |            |            |

a) The  $\mu_{OH_2}$  PLMO of the  $2\mu_{OH_1}$   $\mu_{OH_2}$  structure is equivalent to the  $\mu_{OH_1}$  LMO shown.

TABLE 5.14 INNER SHELL AND LMOs FOR LOW ENERGY STRUCTURES FOR NH<sub>3</sub> (STO-3G BASIS)  
(For explanation see narrative)

| Structure  | LMO                     | 1s <sub>N</sub> | 2s <sub>N</sub> or | 2p <sub>xN</sub> | 2p <sub>yN</sub> | 2p <sub>zN</sub> | 1s <sub>H<sub>1</sub></sub> | 1s <sub>H<sub>2</sub></sub> | 1s <sub>H<sub>3</sub></sub> |
|--|-------------------------|-----------------|--------------------|------------------|------------------|------------------|-----------------------------|-----------------------------|-----------------------------|
| All  | k <sub>N</sub>          | 1.0009          | 0.0313             | 0.0000           | 0.0000           | -0.0049          | -0.0067                     | -0.0067                     | -0.0067                     |
| 2 $\mu_{\text{NH}_1}$ $\mu_{\text{NH}_2}$ $\mu_{\text{NH}_3}$                    | (a) $\mu_{\text{NH}_2}$ | 0.6452          | (-0.0391)          | 0.1748           | -0.3664          | 0.6403           | -0.6509                     | 0.5096                      |                             |
|  | $\mu_{\text{NH}_3}$     | 0.6452          | (-0.0391)          | 0.1748           | -0.3664          | -0.6403          | -0.6509                     |                             | 0.5096                      |
| $\lambda_{\text{N}}$ $\mu_{\text{NH}_1}$ $\mu_{\text{NH}_2}$ $\mu_{\text{NH}_3}$ | $\lambda_{\text{N}}$    | -0.0232         | 0.8347             | 0.0000           | 0.0000           | 0.5501           |                             |                             |                             |
|  | $\mu_{\text{NH}_1}$     | 0.6450          | (-0.0389)          | 0.1729           | 0.7397           | 0.0000           | -0.6492                     | 0.5100                      |                             |
|  | $\mu_{\text{NH}_2}$     | 0.6450          | (-0.0389)          | 0.1729           | -0.3698          | 0.6406           | -0.6492                     | 0.5100                      |                             |
|  | $\mu_{\text{NH}_3}$     | 0.6450          | (-0.0389)          | 0.1729           | -0.3698          | -0.6406          | -0.6492                     |                             | 0.5100                      |

a) The unique LMOs for 2 $\mu_{\text{NH}_2}$   $\mu_{\text{NH}_1}$   $\mu_{\text{NH}_3}$  and for 2 $\mu_{\text{NH}_3}$   $\mu_{\text{NH}_1}$   $\mu_{\text{NH}_2}$  structures are equivalent to the  $\mu_{\text{NH}_2}$  and  $\mu_{\text{NH}_3}$  LMOs shown.

TABLE 5.15 INNER SHELL AND LMOs FOR LOW ENERGY STRUCTURE FOR CH<sub>4</sub> (STO-3G BASIS)

(for explanation see narrative)

| Structure                    | LMO                          | 1s <sub>C</sub> | 2s <sup>or</sup> <sub>C</sub> | 2p <sub>x</sub> C | 2p <sub>y</sub> C | 2p <sub>z</sub> C | 1s <sub>H1</sub> | 1s <sub>H2</sub> | 1s <sub>H3</sub> | 1s <sub>H4</sub> |
|------------------------------|------------------------------|-----------------|-------------------------------|-------------------|-------------------|-------------------|------------------|------------------|------------------|------------------|
| All                          | k <sub>C</sub>               | 1.0014          | 0.0368                        | 0.0000            | 0.0000            | 0.0000            | -0.0069          | -0.0069          | -0.0069          | -0.0069          |
| <sup>μ</sup> CH <sub>1</sub> | <sup>μ</sup> CH <sub>1</sub> | 0.5694          | 0.5239                        | 0.4909            | -0.4907           | 0.4907            | 0.5311           |                  |                  |                  |
| <sup>μ</sup> CH <sub>2</sub> | <sup>μ</sup> CH <sub>2</sub> | 0.5694          | 0.5239                        | -0.4909           | 0.4907            | 0.4907            |                  | 0.5311           |                  |                  |
| <sup>μ</sup> CH <sub>3</sub> | <sup>μ</sup> CH <sub>3</sub> | 0.5694          | 0.5239                        | -0.4909           | -0.4907           | -0.4907           |                  |                  | 0.5311           |                  |
| <sup>μ</sup> CH <sub>4</sub> | <sup>μ</sup> CH <sub>4</sub> | 0.5694          | 0.5239                        | 0.4909            | 0.4907            | -0.4907           |                  |                  |                  | 0.5311           |

From among these six structures for each molecule it is now necessary to choose the sets which are most localised. This procedure selects any one of three structures in each case involving one two-centre bond and two one-centre lone pairs. The final choice must therefore be made by more empirical means.

Since a unique sigma bond,  $\mu_{CO}$  or  $\mu_{NN}$ , and unique lone pairs  $\lambda_O$ ,  $\lambda_C$  and  $\lambda_{N_1}$ ,  $\lambda_{N_2}$ , are identical in all the structures at the canonical energy - the exception as usual being where there is more than one lone pair on the same atom or more than one sigma bond between the pair of atoms - the structures containing all these three orbitals (the only completely unique structures) are to be chosen. Thus  $\lambda_C$ ,  $\lambda_O$ ,  $\mu_{CO}$  and  $\lambda_{N_1}$ ,  $\lambda_{N_2}$ ,  $\mu_{NN}$  are to be considered the basic valence descriptions yielding the PLMOs.

In both water and ammonia (Figures 5.3 and 5.4) there are two structures at nearly the same energy at the bottom of the energy level diagrams. The most localised structure in each case is to be selected, so that the valence descriptions are  $\lambda_O$ ,  $\mu_{OH_1}$ ,  $\mu_{OH_2}$  for water and  $\lambda_N$ ,  $\mu_{NH_1}$ ,  $\mu_{NH_2}$ ,  $\mu_{NH_3}$  for ammonia. In methane (Figure 5.5) all structures but one are precluded on energy grounds. This is  $\mu_{CH_1}$ ,  $\mu_{CH_2}$ ,  $\mu_{CH_3}$ ,  $\mu_{CH_4}$ .

### 5.5 PLMO OVERLAP INTEGRALS

The absolute values of the overlap integrals between the PLMOs for each molecule are shown in Tables 5.16 to 5.20. Also shown is the function,  $\Delta$ , defined in the previous chapter as a measure of the total non-orthogonality of the orbitals.



TABLE 5.16 ABSOLUTE VALUES OF OVERLAP INTEGRALS BETWEEN SIGMA  
 PLMOs (INC. INNER SHELLS) of CO AND  $\Delta$  FUNCTION <sup>(a)</sup> (STO-3G BASIS)

|             | $k_O$  | $k_C$  | $\lambda_C$ | $\lambda_O$       | $\mu_{CO}$ |
|-------------|--------|--------|-------------|-------------------|------------|
| $k_O$       | 1.0    |        |             |                   |            |
| $k_C$       | 0.0000 | 1.0    |             | $\Delta = 0.0452$ |            |
| $\lambda_C$ | 0.0150 | 0.0006 | 1.0         |                   |            |
| $\lambda_O$ | 0.0025 | 0.0307 | 0.1389      | 1.0               |            |
| $\mu_{CO}$  | 0.0000 | 0.0000 | 0.0003      | 0.0002            | 1.0        |

a) For definition of  $\Delta$  see narrative (Chapter 4)

TABLE 5.17 ABSOLUTE VALUES OF OVERLAP INTEGRALS BETWEEN SIGMA  
 PLMOs (INC. INNER SHELLS) of  $N_2$  AND  $\Delta$  FUNCTION <sup>(a)</sup> (STO-3G BASIS)

|                 | $k_{N_1}$ | $k_{N_2}$ | $\lambda_{N_1}$ | $\lambda_{N_2}$   | $\mu_{NN}$ |
|-----------------|-----------|-----------|-----------------|-------------------|------------|
| $k_{N_1}$       | 1.0       |           |                 |                   |            |
| $k_{N_2}$       | 0.0000    | 1.0       |                 | $\Delta = 0.0489$ |            |
| $\lambda_{N_1}$ | 0.0002    | 0.0227    | 1.0             |                   |            |
| $\lambda_{N_2}$ | 0.0227    | 0.0002    | 0.1513          | 1.0               |            |
| $\mu_{NN}$      | 0.0000    | 0.0000    | 0.0003          | 0.0003            | 1.0        |

a) For definition of  $\Delta$  see narrative (Chapter 4)

TABLE 5.18 ABSOLUTE VALUES OF OVERLAP INTEGRALS BETWEEN SIGMA  
 PLMOs (INC. INNER SHELL) OF H<sub>2</sub>O AND Δ FUNCTION <sup>(a)</sup> (STO-3G BASIS)

|              | $k_O$  | $\lambda_O$ | $\mu_{OH_1}$      | $\mu_{OH_2}$ |
|--------------|--------|-------------|-------------------|--------------|
| $k_O$        | 1.0    |             |                   |              |
| $\lambda_O$  | 0.0020 | 1.0         | $\Delta = 0.0559$ |              |
| $\mu_{OH_1}$ | 0.0053 | 0.0231      | 1.0               |              |
| $\mu_{OH_2}$ | 0.0053 | 0.0231      | 0.1329            | 1.0          |

a) For definition of  $\Delta$  see narrative (Chapter 4)

TABLE 5.19 ABSOLUTE VALUES OF OVERLAP INTEGRALS BETWEEN SIGMA PLMOs  
 (INC. INNER SHELL) OF NH<sub>3</sub> AND Δ FUNCTION <sup>(a)</sup> (STO-3G BASIS)

|              | $k_N$  | $\lambda_N$ | $\mu_{NH_1}$      | $\mu_{NH_2}$ | $\mu_{NH_3}$ |
|--------------|--------|-------------|-------------------|--------------|--------------|
| $k_N$        | 1.0    |             |                   |              |              |
| $\lambda_N$  | 0.0064 | 1.0         | $\Delta = 0.0865$ |              |              |
| $\mu_{NH_1}$ | 0.0115 | 0.0289      | 1.0               |              |              |
| $\mu_{NH_2}$ | 0.0115 | 0.0289      | 0.1549            | 1.0          |              |
| $\mu_{NH_3}$ | 0.0115 | 0.0289      | 0.1549            | 0.1549       | 1.0          |

a) For definition of  $\Delta$  see narrative (Chapter 4)

TABLE 5.20 ABSOLUTE VALUES OF OVERLAP INTEGRALS BETWEEN SIGMA PLMOs  
(INC. INNER SHELL) OF CH<sub>4</sub> AND Δ FUNCTION<sup>(a)</sup> (STO-3G BASIS)

|              | $k_C$  | $\mu_{CH_1}$ | $\mu_{CH_2}$      | $\mu_{CH_3}$ | $\mu_{CH_4}$ |
|--------------|--------|--------------|-------------------|--------------|--------------|
| $k_C$        | 1.0    |              |                   |              |              |
| $\mu_{CH_1}$ | 0.0124 | 1.0          | $\Delta = 0.1033$ |              |              |
| $\mu_{CH_2}$ | 0.0124 | 0.1330       | 1.0               |              |              |
| $\mu_{CH_3}$ | 0.0124 | 0.1330       | 0.1330            | 1.0          |              |
| $\mu_{CH_4}$ | 0.0124 | 0.1330       | 0.1330            | 0.1330       | 1.0          |

a) For definition of  $\Delta$  see narrative (Chapter 4).

## 5.6 SUMMARY

The PLMO procedure has been applied to the occupied CMOs of the example molecules and a unique set of non-orthogonal PLMOs have been obtained in each case. These PLMOs may now be used to obtain bond and lone pair moments (Chapter 6) and their properties may be discussed and investigated both in isolation and in relation to other LMO methods in what follows (Chapters 7, 8, 9, 10 and 11).

## CHAPTER 6

ELECTRIC DIPOLE MOMENT ANALYSIS6.1 INTRODUCTION

For a molecule in a particular state (normally the ground state) described by a wavefunction  $\Psi$ , first order properties can be written as the expectation value of an appropriate operator. For example, for the electric dipole moment:

$$\langle \underline{D} \rangle = \langle \Psi | \hat{D} | \Psi \rangle \quad (6.1)$$

The computation of dipole moments and other one-electron properties is often routinely carried out in computer programs for calculating Hartree-Fock SCF-MO wavefunctions,<sup>234</sup> and these may be compared with the dipole moments obtained from experiment.<sup>235,236</sup> For various reasons - including the inaccuracy of a one-determinant wavefunction expressed in an incomplete set of basis functions, and environmental factors - such calculated dipole moments rarely agree closely with experimental values. These calculations, however, can still lead to a better understanding of electronic structure in molecules. One particular approach is outlined below.

6.2 BOND AND LONE PAIR MOMENTS

While total molecular properties are of value to chemists, the division of the total amongst the constituent bonds and lone pairs of classical valence theory can be of equal, or greater utility,<sup>30</sup> and so bond and lone pair moments are of considerable chemical interest. Applications in chemistry include the interpretation of Infra Red gas phase absorption intensities in terms of dipole moment derivatives with respect to symmetry co-ordinates,<sup>237-240</sup> reactive substitution, and internal rotation barriers in molecules.<sup>241,242</sup> Further, if it is accepted that bonds and lone pairs may be transferred between similar chemical environments in different molecules, then the bond

and lone pair moments should be also. Thus by assigning local moments to small prototype molecules it should be possible in theory to predict the molecular properties of a large molecule by vectorial addition of its constituent bond and lone pair moments.

One way in which such local moments may be calculated from LMOs and associated partitioned nuclear changes is outlined in section 5 of Appendix I. Some of that development with some of the relevant equations are reproduced here.

The electric dipole moment  $\underline{D}$  (equation 6.1) may be divided into electronic and nuclear contributions both of which may be further divided into x, y and z components. The z component (for example) of the electronic part of the dipole moment for a molecule described by a one-determinant MO wavefunction may be expressed in terms of non-orthogonal MOs thus:

$$-\langle D_z \rangle_{\text{elec.}} = 2 \sum_{i=1}^n \sum_{j=1}^n \langle \phi_i / z / \phi_j \rangle (\underline{S}^{-1})_{ji} \quad (6.1)$$

where n - number of doubly occupied MOs

$\phi_i, \phi_j$  - MOs

$\langle \phi_i / z / \phi_j \rangle$  - z component dipole moment integral over MOs

$(\underline{S}^{-1})_{ji}$  - (j,i) element of the inverse of the matrix of MO overlap integrals.

Equation (6.2) may be rewritten:

$$-\langle D_z \rangle_{\text{elec.}} = 2 \sum_{i=1}^n \langle \phi_i / z / \phi_i \rangle (\underline{S}^{-1})_{ii} + 4 \sum_{i=1}^n \sum_{\substack{j=1 \\ (i < j)}}^n \langle \phi_i / z / \phi_j \rangle (\underline{S}^{-1})_{ji} \quad (6.3)$$

In equation (6.3) the first sum may be called "the diagonal terms" and the second (double) sum "the off-diagonal terms". As written, each pair of MOs contribute only once to the off-diagonal terms. For orthogonal MOs the off-diagonal terms vanish (since the MO overlap matrix and its inverse are both the unit matrix) and the electronic component of the dipole moment becomes an exact sum of MO contributions  $z^i_{elec}$ .

$$-\langle D_z \rangle_{elec} = \sum_{i=1}^n z^i_{elec} = \sum_{i=1}^n 2\langle \phi_i / z / \phi_i \rangle . \quad (6.4)$$

In order to put the expression for non-orthogonal MOs (equation 6.3) into this form, the contribution from each MO,  $z^i_{elec}$ , needs to be defined by:

$$z^i_{elec} = 2\langle \phi_i / z / \phi_i \rangle (\underline{S}^{-1})_{ii} + 2 \sum_{\substack{j=1 \\ (j \neq i)}}^n \langle \phi_i / z / \phi_j \rangle (\underline{S}^{-1})_{ji} \quad (6.5)$$

Where now the off-diagonal terms of equation (6.3) have been allocated among the diagonal terms such that the overlap contribution arising from two MOs has been divided equally between them. The x and y components may be defined entirely analogously.

It is also possible to partition the nuclear contribution to each component of the dipole moment among the constituent MOs of the molecule, hence yielding total MO dipole moment contributions (section I-5). When the MOs are LMOs that represent bonds and lone pairs, the dipole moment contributions arising from each MO are hence the bond and lone pair moments introduced at the beginning of this section.

### 6.3 RESULTS FOR EXAMPLE MOLECULES

The non-orthogonal PLMOs of each molecule studied were used to calculate total molecular electric dipole moments and to analyse the totals in terms of bond and lone pair moments using the method of Appendix I section 5. The relevant dipole moment integrals for each molecule were available from the Gaussian 70 package<sup>222</sup> (see Appendix II). The results are shown in Tables 6.1 to 6.13. The co-ordinate systems used are those already exhibited (Tables 4.1 and 5.1 to 5.5). The tables are best understood in terms of equations (6.3) and (6.5).

Each table refers to one component of the total dipole moment of each molecule. For HCN, CO and N<sub>2</sub> only the z component to the dipole is needed. For H<sub>2</sub>O the x and z, and for NH<sub>3</sub> and CH<sub>4</sub> the x, y and z components are required. Each table is divided into two parts. In the upper part, each PLMO in the first column is assigned a total dipole moment component in the last (seventh) column. The columns in between these, and the data in the lower part of the table show how the contributions to the total bond or lone pair moments arise. The second column in the upper part of each table shows the co-ordinate dipole moment integral for each PLMO times the conversion factor from atomic units to Debyes. The third column exhibits the multiplication factor needed to obtain the diagonal electronic contribution for each PLMO (fourth column) as in the first term of equation (6.5). The lower part of the table shows in an analogous fashion the significant off-diagonal electronic contributions arising from each PLMO pair, and the total, using the last term of equation (6.3). These off-diagonal contributions



TABLE 6.1 DIPOLE MOMENT ANALYSIS IN TERMS OF PLMOs FOR HCN (STO-3G BASIS) (a)

(For explanation see narrative)

| PLMO<br>( $\phi_i$ ) | $\langle \phi_i / z / \phi_i \rangle$ | $2(\underline{S}^{-1})_{ii}$ | Diagonal<br>Contribution | Re-alloc.<br>Contribution | Nuclear<br>Contribution | PLMO<br>Moment |
|----------------------|---------------------------------------|------------------------------|--------------------------|---------------------------|-------------------------|----------------|
| k <sub>N</sub>       | 5.5357                                | 2.0002                       | -11.0725                 | -11.0716                  | 11.0753                 | 0.0037         |
| k <sub>C</sub>       | 0.0006                                | 2.0017                       | -0.0012                  | -0.0012                   | -                       | -0.0012        |
| $\lambda_N$          | 6.7150                                | 2.0018                       | -13.4421                 | -13.4574                  | 11.0753                 | -2.3821        |
| $\mu_{CH}$           | -3.3890                               | 2.0208                       | 6.8485                   | 6.8577                    | -5.1198                 | 1.7379         |
| $\mu_{CN}$           | 3.4108                                | 2.0204                       | -6.8912                  | -6.8926                   | 5.5377                  | -1.3549        |
| $\pi_1$              | 2.8958                                | 2.0000                       | -5.7916                  | -5.7917                   | 5.5377                  | -0.2540        |
| $\pi_2$              | 2.8958                                | 2.0000                       | -5.7916                  | -5.7917                   | 5.5377                  | -0.2540        |
|                      |                                       |                              |                          |                           | Total Dipole            | -2.5046        |

| PLMO<br>( $\phi_i$ ) | PLMO<br>( $\phi_j$ ) | $\langle \phi_i / z / \phi_j \rangle$ | $4(\underline{S}^{-1})_{ji}$ | Off-Diagonal<br>Contribution |
|----------------------|----------------------|---------------------------------------|------------------------------|------------------------------|
| k <sub>N</sub>       | $\mu_{CH}$           | -0.0568                               | 0.0438                       | 0.0024                       |
| k <sub>N</sub>       | $\mu_{CN}$           | -0.1269                               | -0.0052                      | -0.0006                      |
| k <sub>C</sub>       | $\lambda_N$          | 0.0138                                | -0.1116                      | 0.0016                       |
| k <sub>C</sub>       | $\mu_{CH}$           | -0.1039                               | -0.0282                      | -0.0030                      |
| k <sub>C</sub>       | $\mu_{CN}$           | 0.1144                                | -0.0128                      | 0.0014                       |
| $\lambda_N$          | $\mu_{CH}$           | -0.1246                               | -0.0388                      | -0.0048                      |
| $\lambda_N$          | $\mu_{CN}$           | -1.3812                               | -0.0198                      | -0.0274                      |
| $\mu_{CH}$           | $\mu_{CN}$           | 0.0589                                | -0.4046                      | 0.0238                       |
|                      |                      |                                       |                              | -0.0066                      |

a) All units in Debyes.

TABLE 6.2 DIPOLE MOMENT ANALYSIS IN TERMS OF PLMOs FOR HCN (STO-5G BASIS) (a)

(For explanation see narrative)

| PLMO<br>( $\phi_i$ ) | $\langle \phi_i / z / \phi_i \rangle$ | $2(\underline{S}^{-1})_{ii}$ | Diagonal<br>Contribution | Re-alloc.<br>Contribution | Nuclear<br>Contribution | PLMO<br>Moment |
|----------------------|---------------------------------------|------------------------------|--------------------------|---------------------------|-------------------------|----------------|
| $k_N$                | 5.5361                                | 2.0003                       | -11.0739                 | -11.0756                  | 11.0755                 | -0.0001        |
| $k_C$                | 0.0006                                | 2.0016                       | -0.0012                  | -0.0011                   | -                       | -0.0011        |
| $\lambda_N$          | 6.7110                                | 2.0018                       | -13.4341                 | -13.4477                  | 11.0755                 | -2.3722        |
| $\mu_{CH}$           | -3.3937                               | 2.0204                       | 6.8566                   | 6.8564                    | -5.1199                 | 1.7365         |
| $\mu_{CN}$           | 3.4193                                | 2.0198                       | -6.9063                  | -6.9113                   | 5.5378                  | -1.3735        |
| $\pi_1$              | 2.8961                                | 2.0000                       | -5.7922                  | -5.7922                   | 5.5378                  | -0.2544        |
| $\pi_2$              | 2.8961                                | 2.0000                       | -5.7922                  | -5.7922                   | 5.5378                  | -0.2544        |
| Total Dipole         |                                       |                              |                          |                           |                         | -2.5192        |

| PLMO<br>( $\phi_i$ )    | PLMO<br>( $\phi_j$ ) | $\langle \phi_i / z / \phi_j \rangle$ | $4(\underline{S}^{-1})_{ji}$ | Off-diagonal<br>Contribution |
|-------------------------|----------------------|---------------------------------------|------------------------------|------------------------------|
| $k_N$                   | $\mu_{CH}$           | -0.0612                               | -0.0466                      | -0.0028                      |
| $k_N$                   | $\mu_{CN}$           | -0.1248                               | -0.0054                      | -0.0006                      |
| $k_C$                   | $\lambda_N$          | 0.0144                                | -0.1070                      | 0.0016                       |
| $k_C$                   | $\mu_{CH}$           | -0.1031                               | -0.0280                      | -0.0028                      |
| $k_C$                   | $\mu_{CN}$           | 0.1098                                | -0.0124                      | 0.0014                       |
| $\lambda_N$             | $\mu_{CH}$           | -0.1354                               | -0.0466                      | -0.0064                      |
| $\lambda_N$             | $\mu_{CN}$           | -1.3884                               | -0.0162                      | -0.0224                      |
| $\mu_{CH}$              | $\mu_{CN}$           | 0.0290                                | -0.3996                      | 0.0116                       |
| (a) All units in Debyes |                      |                                       |                              |                              |
| -0.0204                 |                      |                                       |                              |                              |

TABLE 6.3 DIPOLE MOMENT ANALYSIS IN TERMS OF PLMOs FOR HCN (INNER SHELLS TRUNCATED) (STO-3G BASIS) (a)

(For explanation see narrative)

| PLMO<br>( $\phi_i$ ) | $\langle \phi_i / z / \phi_i \rangle$ | $2(\underline{S}^{-1})_{ii}$ | Diagonal<br>Contribution | Re-alloc.<br>Contribution | Nuclear<br>Contribution | PLMO<br>Moment |
|----------------------|---------------------------------------|------------------------------|--------------------------|---------------------------|-------------------------|----------------|
| k <sub>N</sub>       | 5.5343                                | 2.0005                       | -11.0714                 | -11.0718                  | 11.0753                 | 0.0035         |
| k <sub>C</sub>       | 0.0009                                | 2.0028                       | -0.0018                  | -0.0018                   | -                       | -0.0018        |
| $\lambda_N$          | 6.7145                                | 2.0026                       | -13.4465                 | -13.4583                  | 11.0753                 | -2.3830        |
| $\mu_{CH}$           | -3.3895                               | 2.0210                       | 6.8502                   | 6.8561                    | -5.1198                 | 1.7363         |
| $\mu_{CN}$           | 3.4106                                | 2.0207                       | -6.8918                  | -6.8945                   | 5.5377                  | -1.3568        |
| $\pi_1$              | 2.8958                                | 2.0000                       | -5.7916                  | -5.7916                   | 5.5377                  | -0.2539        |
| $\pi_2$              | 2.8958                                | 2.0000                       | -5.7916                  | -5.7916                   | 5.5377                  | -0.2539        |
| Total Dipole         |                                       |                              |                          |                           |                         | -2.5096        |

| PLMO<br>( $\phi_i$ ) | PLMO<br>( $\phi_j$ ) | $\langle \phi_i / z / \phi_j \rangle$ | $4(\underline{S}^{-1})_{ji}$ | Off-diagonal<br>Contribution |         |
|----------------------|----------------------|---------------------------------------|------------------------------|------------------------------|---------|
| k <sub>N</sub>       | $\lambda_N$          | 0.0826                                | -0.0226                      | 0.0019                       |         |
| k <sub>N</sub>       | $\mu_{CH}$           | -0.0594                               | 0.0380                       | 0.0023                       |         |
| k <sub>N</sub>       | $\mu_{CN}$           | -0.1062                               | -0.0468                      | -0.0050                      |         |
| k <sub>C</sub>       | $\lambda_N$          | 0.0470                                | -0.1346                      | 0.0063                       |         |
| k <sub>C</sub>       | $\mu_{CH}$           | -0.1285                               | -0.0492                      | -0.0095                      |         |
| k <sub>C</sub>       | $\mu_{CN}$           | 0.1214                                | -0.0262                      | 0.0032                       |         |
| $\lambda_N$          | $\mu_{CH}$           | -0.1249                               | -0.0378                      | -0.0047                      |         |
| $\lambda_N$          | $\mu_{CN}$           | -1.3806                               | -0.0196                      | -0.0271                      |         |
| $\mu_{CH}$           | $\mu_{CN}$           | 0.0582                                | -0.4048                      | 0.0236                       |         |
| Total Dipole         |                      |                                       |                              |                              | -0.0090 |

(a) All units in Debyes

TABLE 6.4 DIPOLE MOMENT ANALYSIS IN TERMS OF PLMOs FOR CO (STO-3G BASIS) (a)

(for explanation see narrative)

| PLMO<br>( $\phi_i$ ) | $\langle \phi_i / z / \phi_i \rangle$ | $2(\underline{S}^{-1})_{ii}$ | Diagonal<br>Contribution | Re-alloc.<br>Contribution | Nuclear<br>Contribution | PLMO<br>Moment |
|----------------------|---------------------------------------|------------------------------|--------------------------|---------------------------|-------------------------|----------------|
| kO                   | 5.4172                                | 2.0005                       | -10.8371                 | -10.8347                  | 10.8375                 | 0.0028         |
| kC                   | 0.0025                                | 2.0020                       | -0.0049                  | -0.0048                   | -                       | -0.0048        |
| $\lambda$ O          | 6.2577                                | 2.0414                       | -12.7741                 | -12.6475                  | 10.8375                 | -1.8100        |
| $\lambda$ C          | -1.5293                               | 2.0401                       | 3.1200                   | 3.2476                    | -                       | 3.2476         |
| $\mu$ CO             | 3.5724                                | 2.0000                       | -7.1448                  | -7.1440                   | 5.4187                  | -1.7253        |
| $\pi_1$              | 3.9494                                | 2.0000                       | -7.8988                  | -7.8988                   | 8.1281                  | 0.2293         |
| $\pi_2$              | 3.9494                                | 2.0000                       | -7.8988                  | -7.8988                   | 8.1281                  | 0.2293         |
| Total Dipole         |                                       |                              |                          |                           |                         | 0.1689         |

| PLMO<br>( $\phi_i$ ) | PLMO<br>( $\phi_j$ ) | $\langle \phi_i / z / \phi_j \rangle$ | $4(\underline{S}^{-1})_{ji}$ | Off-diagonal<br>Contribution |
|----------------------|----------------------|---------------------------------------|------------------------------|------------------------------|
| kO                   | $\lambda$ C          | 0.0776                                | -0.0632                      | 0.0049                       |
| kC                   | $\lambda$ O          | 0.0203                                | -0.1189                      | 0.0024                       |
| kC                   | $\lambda$ C          | -0.0813                               | -0.0272                      | -0.0022                      |
| $\lambda$ O          | $\lambda$ C          | 0.4420                                | -0.5674                      | 0.2508                       |
| $\lambda$ C          | $\mu$ CO             | 1.0362                                | -0.0015                      | 0.0016                       |
| Total Dipole         |                      |                                       |                              | 0.2575                       |

(a) All units in Debyes

TABLE 6.5 DIPOLE MOMENT ANALYSIS IN TERMS OF PLMOs FOR  $N_2$  (STO-3G BASIS) (a)  
(for explanation see narrative)

| PLMO<br>( $\phi_i$ ) | $\langle \phi_i / z / \phi_i \rangle$ | $2(\underline{S}^{-1})_{ii}$ | Diagonal<br>Contribution | Re-alloc.<br>Contribution | Nuclear<br>Contribution | PLMO<br>Moment |
|----------------------|---------------------------------------|------------------------------|--------------------------|---------------------------|-------------------------|----------------|
| $k_{N1}$             | 0.0021                                | 2.0010                       | -0.0042                  | -0.0036                   | -                       | -0.0036        |
| $k_{N2}$             | 5.2696                                | 2.0010                       | -10.5445                 | -10.5395                  | 10.5432                 | 0.0037         |
| $\lambda_{N1}$       | -1.2261                               | 2.0479                       | 2.5109                   | 2.6406                    | -                       | 2.6406         |
| $\lambda_{N2}$       | 6.4979                                | 2.0479                       | -13.3070                 | -13.1840                  | 10.5432                 | -2.6408        |
| $\mu_{NN}$           | 2.6358                                | 2.0000                       | -5.2716                  | -5.2716                   | 5.2716                  | 0.0000         |
| $\pi_1$              | 2.6359                                | 2.0000                       | -5.2718                  | -5.2718                   | 5.2716                  | -0.0002        |
| $\pi_2$              | 2.6359                                | 2.0000                       | -5.2718                  | -5.2718                   | 5.2716                  | -0.0002        |
| Total Dipole         |                                       |                              |                          |                           |                         | -0.0005        |

| PLMO<br>( $\phi_i$ ) | PLMO<br>( $\phi_j$ ) | $\langle \phi_i / z / \phi_j \rangle$ | $4(\underline{S}^{-1})_{ji}$ | Off-Diagonal<br>Contribution |
|----------------------|----------------------|---------------------------------------|------------------------------|------------------------------|
| $k_{N1}$             | $\lambda_{N1}$       | -0.0599                               | 0.0086                       | 0.0005                       |
| $k_{N1}$             | $\lambda_{N2}$       | 0.0074                                | -0.0922                      | 0.0007                       |
| $k_{N2}$             | $\lambda_{N1}$       | 0.1124                                | -0.0916                      | 0.0103                       |
| $k_{N2}$             | $\lambda_{N2}$       | 0.0718                                | 0.0048                       | -0.0003                      |
| $\lambda_{N1}$       | $\lambda_{N2}$       | 0.3988                                | -0.6196                      | 0.2471                       |
| $\lambda_{N1}$       | $\mu_{NN}$           | 1.2069                                | -0.0012                      | 0.0014                       |
| $\lambda_{N2}$       | $\mu_{NN}$           | -1.2051                               | -0.0012                      | -0.0014                      |
| Total Dipole         |                      |                                       |                              | 0.2583                       |

(a) All units in Debyes

TABLE 6.6 DIPOLE MOMENT ANALYSIS IN TERMS OF PLMOs FOR H<sub>2</sub>O (z COMPONENT) (STO-3G BASIS) (a)  
(for explanation see narrative)

| PLMO<br>( $\phi_i$ )     | $\langle \phi_i / z / \phi_i \rangle$ | $2(\underline{S}^{-1})_{ii}$ | Diagonal<br>Contribution | Re-alloc<br>Contribution | Nuclear<br>Contribution | PLMO<br>Moment |
|--------------------------|---------------------------------------|------------------------------|--------------------------|--------------------------|-------------------------|----------------|
| k <sub>O</sub>           | -0.0011                               | 2.0001                       | 0.0022                   | 0.0006                   | -                       | 0.0006         |
| $\lambda_O$              | 0.7578                                | 2.0019                       | -1.5170                  | -1.6120                  | -                       | -1.6020        |
| $\mu_{OH_1}$             | -1.4299                               | 2.0368                       | 2.9124                   | 2.7429                   | -2.8140                 | -0.0711        |
| $\mu_{OH_2}$             | -1.4299                               | 2.0368                       | 2.9124                   | 2.7429                   | -2.8140                 | -0.0711        |
| Total Dipole (Component) |                                       |                              |                          |                          |                         | -1.7436        |

| PLMO<br>( $\phi_i$ ) | PLMO<br>( $\phi_j$ ) | $\langle \phi_i / z / \phi_j \rangle$ | $4(\underline{S}^{-1})_{ji}$ | Off-Diagonal<br>Contribution |
|----------------------|----------------------|---------------------------------------|------------------------------|------------------------------|
| k <sub>O</sub>       | $\mu_{OH_1}$         | -0.0866                               | -0.0188                      | -0.0016                      |
| k <sub>O</sub>       | $\mu_{OH_2}$         | -0.0866                               | -0.0188                      | -0.0016                      |
| $\lambda_O$          | $\mu_{OH_1}$         | -1.0417                               | -0.0817                      | -0.0851                      |
| $\lambda_O$          | $\mu_{OH_2}$         | -1.0417                               | -0.0817                      | -0.0851                      |
| $\mu_{OH_1}$         | $\mu_{OH_2}$         | -0.4677                               | -0.5392                      | -0.2522                      |
|                      |                      |                                       |                              | -0.4256                      |

(a) All units in Debyes

TABLE 6.7 DIPOLE MOMENT ANALYSIS IN TERMS OF PLMOs FOR H<sub>2</sub>O (x COMPONENT) (STO-3G BASIS) (a)  
(for explanation see narrative)

| PLMO<br>( $\phi_i$ )   | $\langle \phi_i / x / \phi_i \rangle$ | $2(\underline{\underline{S}}^{-1})_{ii}$ | Diagonal<br>Contribution | Re-alloc.<br>Contribution | Nuclear<br>Contribution | PLMO<br>Moment |
|------------------------|---------------------------------------|--|--------------------------|---------------------------|-------------------------|----------------|
| $k_0$                  | 0.0000                                | 2.0001                                   | -                        | -                         | -                       | 0.0000         |
| $\lambda_0$            | 0.0000                                | 2.0019                                   | -                        | -                         | -                       | 0.0000         |
| $\mu_{OH_1}$           | 1.6947                                | 2.0368                                   | -3.4518                  | -3.4092                   | 3.6356                  | 0.2264         |
| $\mu_{OH_2}$           | -1.6947                               | 2.0368                                   | 3.4518                   | 3.4092                    | -3.6356                 | -0.2264        |
| Total Dipole Component |                                       |  |                          |                           |                         | 0.0000         |

| PLMO<br>( $\phi_i$ )   | PLMO<br>( $\phi_j$ ) | $\langle \phi_i / x / \phi_i \rangle$ | $4(\underline{\underline{S}}^{-1})_{ji}$ | Off-Diagonal<br>Contribution |
|------------------------|----------------------|---------------------------------------|--|------------------------------|
| $k_0$                  | $\mu_{OH_1}$         | 0.0708                                | -0.0188                                  | 0.0014                       |
| $k_0$                  | $\mu_{OH_2}$         | -0.0708                               | -0.0188                                  | -0.0014                      |
| $\lambda_0$            | $\mu_{OH_1}$         | 1.0272                                | -0.0816                                  | 0.0838                       |
| $\lambda_0$            | $\mu_{OH_2}$         | -1.0272                               | -0.0816                                  | -0.0838                      |
| Total Dipole Component |                      |                                       |  | 0.0000                       |

(a) All units in Debyes

TABLE 6.8 DIPOLE MOMENT ANALYSIS IN TERMS OF PLMOs FOR  $\text{NH}_3$  (z COMPONENT) (STO-3G BASIS) (a)

(For explanation see narrative)

| PLMO<br>( $\phi_i$ )     | $\langle \phi_i / z / \phi_i \rangle$ | $2(\underline{\underline{S}}^{-1})_{ii}$ | Diagonal<br>Contribution | Re-alloc.<br>Contribution | Nuclear<br>Contribution | PLMO<br>Moment |
|--------------------------|---------------------------------------|--|--------------------------|---------------------------|-------------------------|----------------|
| $k_N$                    | -0.0014                               | 2.0007                                   | -0.0028                  | -0.0086                   | -                       | -0.0086        |
| $\lambda_N$              | 1.7402                                | 2.0039                                   | -3.4874                  | -3.5487                   | -                       | -3.5487        |
| $\mu_{\text{NH}_1}$      | -1.2851                               | 2.0878                                   | 2.6831                   | 2.2898                    | -1.7794                 | 0.5104         |
| $\mu_{\text{NH}_2}$      | -1.2851                               | 2.0878                                   | 2.6831                   | 2.2898                    | -1.7794                 | 0.5104         |
| $\mu_{\text{NH}_3}$      | -1.2851                               | 2.0878                                   | 2.6831                   | 2.2898                    | -1.7794                 | 0.5104         |
| Total Dipole (Component) |                                       |  |                          |                           |                         | -2.0261        |

| PLMO<br>( $\phi_i$ )     | PLMO<br>( $\phi_j$ ) | $\langle \phi_i / z / \phi_j \rangle$ | $4(\underline{\underline{S}}^{-1})_{ji}$ | Off-Diagonal<br>Contribution |         |
|--------------------------|----------------------|---------------------------------------|--|------------------------------|---------|
| $k_N$                    | $\lambda_N$          | 0.1022                                | 0.0288                                   | -0.0029                      |         |
| $k_N$                    | $\mu_{\text{NH}_1}$  | -0.0816                               | -0.0356                                  | -0.0029                      |         |
| $k_N$                    | $\mu_{\text{NH}_2}$  | -0.0816                               | -0.0356                                  | -0.0029                      |         |
| $k_N$                    | $\mu_{\text{NH}_3}$  | -0.0816                               | -0.0356                                  | -0.0029                      |         |
| $\lambda_N$              | $\mu_{\text{NH}_1}$  | -0.4511                               | -0.0888                                  | -0.0400                      |         |
| $\lambda_N$              | $\mu_{\text{NH}_2}$  | -0.4511                               | -0.0888                                  | -0.0400                      |         |
| $\lambda_N$              | $\mu_{\text{NH}_3}$  | -0.4511                               | -0.0888                                  | -0.0400                      |         |
| $\mu_{\text{NH}_1}$      | $\mu_{\text{NH}_2}$  | -0.6671                               | -0.5574                                  | -0.3718                      |         |
| $\mu_{\text{NH}_1}$      | $\mu_{\text{NH}_3}$  | -0.6671                               | -0.5574                                  | -0.3718                      |         |
| $\mu_{\text{NH}_2}$      | $\mu_{\text{NH}_3}$  | -0.6671                               | -0.5574                                  | -0.3718                      |         |
| Total Dipole (Component) |                      |                                       |  |                              | -1.2470 |

(a) All units in Debyes



TABLE 6.9 DIPOLE MOMENT ANALYSIS IN TERMS OF PLMOs FOR  $\text{NH}_3$  (x COMPONENT) (STO-3G BASIS) (a)

(For explanation see narrative)

| PLMO<br>( $\phi_i$ )   | $\langle \phi_i / x / \phi_i \rangle$ | $2(\underline{S}^{-1})_{ii}$ | Diagonal<br>Contribution | Re-alloc.<br>Contribution | Nuclear<br>Contribution | PLMO<br>Moment |
|------------------------|---------------------------------------|------------------------------|--------------------------|---------------------------|-------------------------|----------------|
| $k_N$                  | 0.0000                                | 2.0007                       | -                        | -                         | -                       | 0.0000         |
| $\lambda_N$            | 0.0000                                | 2.0039                       | -                        | -                         | -                       | 0.0000         |
| $\mu_{\text{NH}_1}$    | 2.4945                                | 2.0878                       | -5.2080                  | -5.0266                   | 4.5026                  | -0.5240        |
| $\mu_{\text{NH}_2}$    | -1.2472                               | 2.0878                       | 2.6040                   | 2.5133                    | -2.2513                 | 0.2620         |
| $\mu_{\text{NH}_3}$    | -1.2472                               | 2.0878                       | 2.6040                   | 2.5133                    | -2.2513                 | 0.2620         |
| Total Dipole Component |                                       |                              |                          |                           |                         | 0.0000         |

| PLMO<br>( $\phi_i$ )   | PLMO<br>( $\phi_j$ ) | $\langle \phi_i / x / \phi_j \rangle$ | $4(\underline{S}^{-1})_{ji}$ | Off-Diagonal<br>Contribution |        |
|------------------------|----------------------|---------------------------------------|------------------------------|------------------------------|--------|
| $k_N$                  | $\mu_{\text{NH}_1}$  | 0.0942                                | -0.0356                      | 0.0034                       |        |
| $k_N$                  | $\mu_{\text{NH}_2}$  | -0.0471                               | -0.0356                      | -0.0017                      |        |
| $k_N$                  | $\mu_{\text{NH}_3}$  | -0.0471                               | -0.0356                      | -0.0017                      |        |
| $\lambda_N$            | $\mu_{\text{NH}_1}$  | 1.1254                                | -0.0888                      | 0.1000                       |        |
| $\lambda_N$            | $\mu_{\text{NH}_2}$  | -0.5627                               | -0.0888                      | -0.0500                      |        |
| $\lambda_N$            | $\mu_{\text{NH}_3}$  | -0.5627                               | -0.0888                      | -0.0500                      |        |
| $\mu_{\text{NH}_1}$    | $\mu_{\text{NH}_2}$  | 0.2327                                | -0.5574                      | 0.1297                       |        |
| $\mu_{\text{NH}_1}$    | $\mu_{\text{NH}_3}$  | 0.2327                                | -0.5574                      | 0.1297                       |        |
| $\mu_{\text{NH}_2}$    | $\mu_{\text{NH}_3}$  | -0.4654                               | -0.5574                      | -0.2594                      |        |
| Total Dipole Component |                      |                                       |                              |                              | 0.0000 |

(a) All units in Debyes

TABLE 6.10 DIPOLE MOMENT ANALYSIS IN TERMS OF PLMOs FOR  $\text{NH}_3$  (Y COMPONENT) (STO-3G BASIS) (a)

(For explanation see narrative)

| PLMO<br>( $\phi_i$ )   | $\langle \phi_i / y / \phi_i \rangle$ | $2(\underline{S}^{-1})_{ii}$ | Diagonal<br>Contribution | Re-alloc.<br>Contribution | Nuclear<br>Contribution | PLMO<br>Moment |
|------------------------|---------------------------------------|------------------------------|--------------------------|---------------------------|-------------------------|----------------|
| $k_N$                  | 0.0000                                | 2.0007                       | -                        | -                         | -                       | 0.0000         |
| $\lambda_N$            | 0.0000                                | 2.0039                       | -                        | -                         | -                       | 0.0000         |
| $\mu_{\text{NH}_1}$    | 0.0000                                | 2.0878                       | -                        | -                         | -                       | 0.0000         |
| $\mu_{\text{NH}_2}$    | 2.1603                                | 2.0878                       | -4.5103                  | -4.3533                   | 3.8993                  | -0.4540        |
| $\mu_{\text{NH}_3}$    | -2.1603                               | 2.0878                       | 4.5103                   | 4.3533                    | -3.8993                 | 0.4540         |
| Total Dipole Component |                                       |                              |                          |                           |                         | 0.0000         |

| PLMO<br>( $\phi_i$ )   | PLMO<br>( $\phi_j$ ) | $\langle \phi_i / y / \phi_j \rangle$ | $4(\underline{S}^{-1})_{ji}$ | Off-Diagonal<br>Contribution |
|------------------------|----------------------|---------------------------------------|------------------------------|------------------------------|
| $k_N$                  | $\mu_{\text{NH}_1}$  | 0.0000                                | -0.0356                      | -                            |
| $k_N$                  | $\mu_{\text{NH}_2}$  | 0.0816                                | -0.0356                      | 0.0028                       |
| $k_N$                  | $\mu_{\text{NH}_3}$  | -0.0816                               | -0.0356                      | -0.0028                      |
| $\lambda_N$            | $\mu_{\text{NH}_1}$  | 0.0000                                | -0.0888                      | -                            |
| $\lambda_N$            | $\mu_{\text{NH}_2}$  | 0.9746                                | -0.0888                      | 0.0866                       |
| $\lambda_N$            | $\mu_{\text{NH}_3}$  | -0.9746                               | -0.0888                      | -0.0866                      |
| $\mu_{\text{NH}_1}$    | $\mu_{\text{NH}_2}$  | 0.4030                                | -0.5574                      | 0.2246                       |
| $\mu_{\text{NH}_1}$    | $\mu_{\text{NH}_3}$  | -0.4030                               | -0.5574                      | -0.2246                      |
| $\mu_{\text{NH}_2}$    | $\mu_{\text{NH}_3}$  | 0.0000                                | -0.5574                      | -                            |
| Total Dipole Component |                      |                                       |                              | 0.0000                       |

(a) All units in Debyes

TABLE 6.11 DIPOLE MOMENT ANALYSIS IN TERMS OF PLMOs FOR CH<sub>4</sub> (z COMPONENT) (STO-3G BASIS) (a)

(For explanation see narrative)

| PLMO<br>( $\phi_i$ )          | $\langle \phi_i / z / \phi_i \rangle$ | $2(\underline{S}^{-1})_{ii}$ | Diagonal<br>Contribution | Re-alloc<br>Contribution | Nuclear<br>Contribution | PLMO<br>Moment |
|-------------------------------|---------------------------------------|------------------------------|--------------------------|--------------------------|-------------------------|----------------|
| k <sub>C</sub>                | 0.0000                                | 2.0009                       | -                        | -                        | -                       | -              |
| <sup>1</sup> H <sub>CH1</sub> | 2.0994                                | 2.0877                       | -4.3829                  | -4.1851                  | 3.0226                  | -1.1625        |
| <sup>1</sup> H <sub>CH2</sub> | 2.0994                                | 2.0877                       | -4.3829                  | -4.1851                  | 3.0226                  | -1.1625        |
| <sup>1</sup> H <sub>CH3</sub> | -2.0994                               | 2.0877                       | 4.3829                   | 4.1851                   | -3.0226                 | -1.1625        |
| <sup>1</sup> H <sub>CH4</sub> | -2.0994                               | 2.0877                       | 4.3829                   | 4.1851                   | -3.0226                 | 1.1625         |
| Total Dipole Component        |                                       |                              |                          |                          |                         | 0.0000         |

| PLMO<br>( $\phi_i$ )          | PLMO<br>( $\phi_j$ )          | $\langle \phi_i / z / \phi_j \rangle$ | $4(\underline{S}^{-1})_{ji}$ | Off Diagonal<br>Contribution |
|-------------------------------|-------------------------------|---------------------------------------|------------------------------|------------------------------|
| k <sub>C</sub>                | <sup>1</sup> H <sub>CH1</sub> | 0.0721                                | -0.0354                      | 0.0026                       |
| k <sub>C</sub>                | <sup>1</sup> H <sub>CH2</sub> | 0.0721                                | -0.0354                      | 0.0026                       |
| k <sub>C</sub>                | <sup>1</sup> H <sub>CH3</sub> | -0.0721                               | -0.0354                      | -0.0026                      |
| k <sub>C</sub>                | <sup>1</sup> H <sub>CH4</sub> | -0.0721                               | -0.0354                      | -0.0026                      |
| <sup>1</sup> H <sub>CH1</sub> | <sup>1</sup> H <sub>CH2</sub> | 0.8965                                | -0.4384                      | 0.3930                       |
| <sup>1</sup> H <sub>CH3</sub> | <sup>1</sup> H <sub>CH4</sub> | -0.8965                               | -0.4384                      | -0.3930                      |
| Total Dipole Component        |                               |                                       |                              | 0.0000                       |

(a) All units in Debyes

TABLE 6.12 DIPOLE MOMENT ANALYSIS IN TERMS OF PLMOs FOR CH<sub>4</sub> (x COMPONENT) (STO-3G BASIS) (a)  
(for explanation see narrative)

| PLMO<br>( $\phi_i$ )         | $\langle \phi_i / x / \phi_i \rangle$ | $2(\underline{S}^{-1})_{ii}$ | Diagonal<br>Contribution | Re-alloc.<br>Contribution | Nuclear<br>Contribution | PLMO<br>Moment |
|------------------------------|---------------------------------------|------------------------------|--------------------------|---------------------------|-------------------------|----------------|
| k <sub>C</sub>               | 0.0000                                | 2.0009                       | -                        | -                         | -                       | 0.0000         |
| <sup>1</sup> CH <sub>1</sub> | 2.0092                                | 2.0877                       | -4.3825                  | -4.1848                   | 3.0221                  | -1.1627        |
| <sup>1</sup> CH <sub>2</sub> | -2.0992                               | 2.0877                       | 4.3825                   | 4.1848                    | -3.0221                 | 1.1627         |
| <sup>1</sup> CH <sub>3</sub> | -2.0992                               | 2.0877                       | 4.3825                   | 4.1848                    | -3.0221                 | 1.1627         |
| <sup>1</sup> CH <sub>4</sub> | 2.0992                                | 2.0877                       | -4.3825                  | -4.1848                   | 3.0221                  | -1.1627        |
| Total Dipole Component       |                                       |                              |                          |                           |                         | 0.0000         |

| PLMO<br>( $\phi_i$ )         | PLMO<br>( $\phi_j$ )         | $\langle \phi_i / x / \phi_j \rangle$ | $4(\underline{S}^{-1})_{ji}$ | Off-Diagonal<br>Contribution |
|------------------------------|------------------------------|---------------------------------------|------------------------------|------------------------------|
| k <sub>C</sub>               | <sup>1</sup> CH <sub>1</sub> | 0.0721                                | -0.0354                      | 0.0026                       |
| k <sub>C</sub>               | <sup>1</sup> CH <sub>2</sub> | -0.0721                               | -0.0354                      | -0.0026                      |
| k <sub>C</sub>               | <sup>1</sup> CH <sub>3</sub> | -0.0721                               | -0.0354                      | -0.0026                      |
| k <sub>C</sub>               | <sup>1</sup> CH <sub>4</sub> | 0.0721                                | -0.0354                      | 0.0026                       |
| <sup>1</sup> CH <sub>1</sub> | <sup>1</sup> CH <sub>4</sub> | 0.8964                                | -0.4382                      | 0.3928                       |
| <sup>1</sup> CH <sub>2</sub> | <sup>1</sup> CH <sub>3</sub> | -0.8964                               | -0.4382                      | -0.3928                      |
| 0.0000                       |                              |                                       |                              |                              |

(a) All units in Debyes

TABLE 6.13 DIPOLE MOMENT ANALYSIS IN TERMS OF PLMOs FOR CH<sub>4</sub> (y COMPONENT) (STO-3G BASIS) (a)

(for explanation see narrative)

| PLMO<br>( $\phi_i$ )   | $\langle \phi_i / y / \phi_i \rangle$ | $2(\underline{S}^{-1})_{ii}$ | Diagonal<br>Contribution | Re-alloc.<br>Contribution | Nuclear<br>Contribution | PLMO<br>Moment |
|------------------------|---------------------------------------|------------------------------|--------------------------|---------------------------|-------------------------|----------------|
| k <sub>C</sub>         | 0.0000                                | 2.0009                       | -                        | -                         | -                       | 0.0000         |
| $\mu_{CH_1}$           | -2.0993                               | 2.0877                       | 4.3827                   | 4.1849                    | -3.0224                 | 1.1625         |
| $\mu_{CH_2}$           | 2.0993                                | 2.0877                       | -4.3827                  | -4.1849                   | 3.0224                  | -1.1625        |
| $\mu_{CH_3}$           | -2.0993                               | 2.0877                       | 4.3827                   | 4.1849                    | -3.0224                 | 1.1625         |
| $\mu_{CH_4}$           | 2.0993                                | 2.0877                       | -4.3827                  | -4.1849                   | 3.0224                  | -1.1625        |
| Total Dipole Component |                                       |                              |                          |                           |                         | 0.0000         |

| PLMO<br>( $\phi_i$ )   | PLMO<br>( $\phi_j$ ) | $\langle \phi_i / y / \phi_j \rangle$ | $4(\underline{S}^{-1})_{ji}$ | Off-Diagonal<br>Contribution |
|------------------------|----------------------|---------------------------------------|------------------------------|------------------------------|
| k <sub>C</sub>         | $\mu_{CH_1}$         | -0.0721                               | -0.0354                      | -0.0026                      |
| k <sub>C</sub>         | $\mu_{CH_2}$         | 0.0721                                | -0.0354                      | 0.0026                       |
| k <sub>C</sub>         | $\mu_{CH_3}$         | -0.0721                               | -0.0354                      | -0.0026                      |
| k <sub>C</sub>         | $\mu_{CH_4}$         | 0.0721                                | -0.0354                      | 0.0026                       |
| $\mu_{CH_1}$           | $\mu_{CH_3}$         | -0.8965                               | -0.4384                      | -0.3930                      |
| $\mu_{CH_2}$           | $\mu_{CH_4}$         | 0.8965                                | -0.4384                      | 0.3930                       |
| Total Dipole Component |                      |                                       |                              | 0.0000                       |

(a) All units in Debyes

are re-allocated amongst the inner shells, bonds and lone pairs by dividing each off-diagonal term equally between the overlapping PLMOs in question, following the second term in equation (6.5). The resulting "reallocated" electronic moment is shown in column five in the upper part of the table. To this must be added the moment arising from the associated positive nuclear charges that have been assigned to the PLMOs after Appendix I (Section 5). This is presented in the sixth column. The final total dipole moment component for each inner shell, bond and lone pair described by the PLMOs is hence produced in the last column of the table. The sign convention used is that if a dipole has its negative end in the direction of the positive co-ordinate axis, the moment has a negative sign.

The total bond and lone pair moments (in Debyes) for the example molecules are expressed in diagrammatic form in Figures 6.1 to 6.6. The arrows in the figures point towards the negative end of the dipole in each case. In water and ammonia the bonding hybrids on oxygen and nitrogen in the PLMOs do not point directly towards the hydrogen atoms (see Chapter 8) and hence produce "bent" bonds. This means that the centroids of electron charge in the NH and OH bonds do not lie on the internuclear lines. For this reason the bond moments in these molecules have been expressed in the figures as a vector pointing from the centroid of positive charge (midpoint between the nuclei) to the centroid of negative charge. The direction of this vector is defined relative to the line joining the nuclei (Figures 6.4 and 6.5). The CH bond moments in methane point towards the hydrogen atoms by symmetry (Figure 6.6).

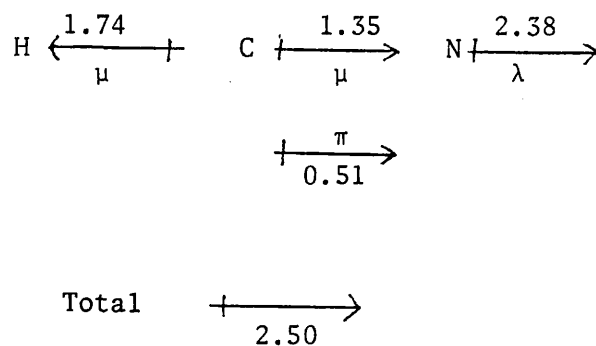


Figure 6.1. Bond and lone pair moments for HCN (STO-3G basis) (a)

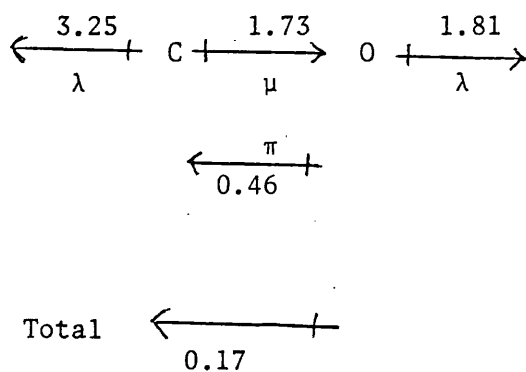


Figure 6.2 Bond and lone pair moments for CO (STO-3G basis) (a)

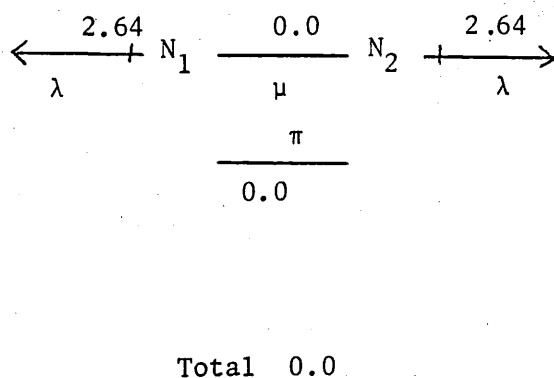


Figure 6.3 Bond and lone pair moments for N<sub>2</sub> (STO-3G basis) (a)

(a) All in Debyes

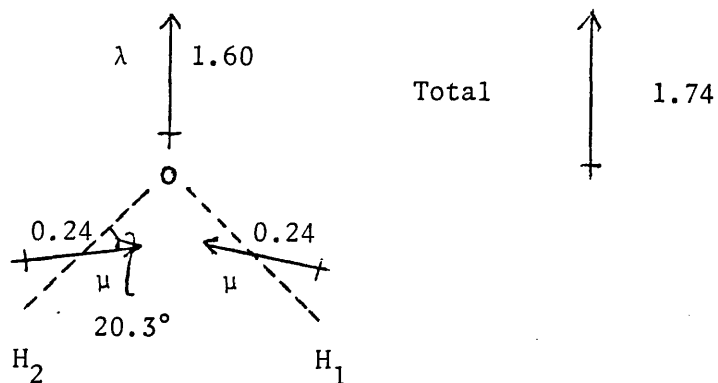


Figure 6.4 Bond and lone pair moments for  $\text{H}_2\text{O}$  (STO-3G basis) <sup>(a)</sup>

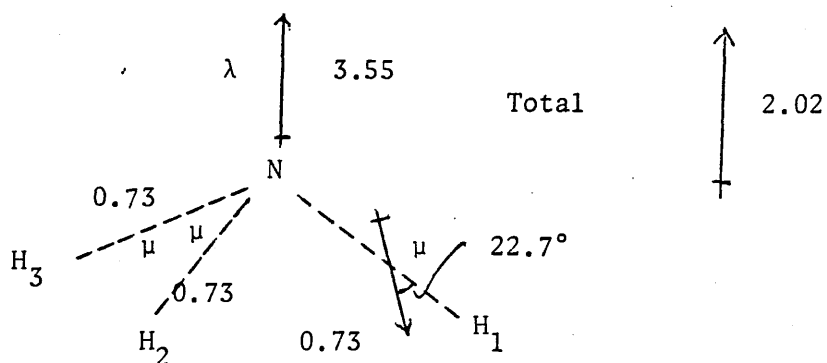


Figure 6.5 Bond and lone pair moments for  $\text{NH}_3$  (STO-3G basis) <sup>(a)</sup>

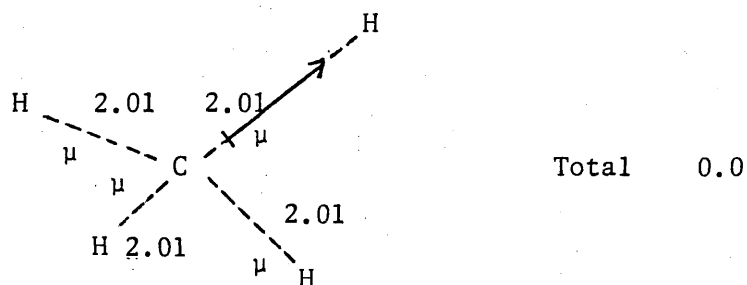


Figure 6.6 Bond moments for  $\text{CH}_4$  (STO-3G basis) <sup>(a)</sup>

(a) All in Debyes.



A discussion of the results presented here, their physical significance, and a comparison to the results of other authors is reserved for Chapter 9.

PART C

DISCUSSION AND INTERPRETATION OF RESULTS

- POPULATION ANALYSIS

CHAPTER SEVEN

ENERGY DIAGRAMS

7.1 INTRODUCTION

The manner in which the energy diagrams were constructed for a molecule has been described in Chapter 4. The energies represent the minimum value obtained by imposing the corresponding arrangement of lone pairs and bonds on the transformed MOs. All possible arrangements of lone pairs and bonds were considered for each molecule. As was said in Chapter 4, not all of these structures converged to an energy minimum, but of those which did converge, the lowest energy structures are shown in the energy diagrams (Figures 4.1 to 4.3 and 5.1 to 5.5). Some aspects of these energy diagrams are discussed in this chapter.

7.2 COMPOSITION OF THE DIAGRAMS

7.2(a) Significance of the Energies

For all the structures considered, the manner in which the MOs are transformed and truncated does influence the shape of the energy surface that is searched, and hence the value of the energy minimum obtained (Section 4.7). This point is exemplified in water (Figure 5.3) where the  $2\mu_{OH_a} \mu_{OH_b}$  structure could be generated by forming suitable linear combinations of the endpoint LMOs found in the lower energy  $\lambda_0 \mu_{OH_1} \mu_{OH_2}$  structure. The wavefunction for water thus obtained would give an energy of 0.00625H above the canonical energy - since a one-determinant wavefunction is invariant to linear combinations of its constituent MOs - rather than the 0.00644H found from the PLMO procedure. Similar situations arise in the

$(3\mu_{\text{OH}_a})$ ,  $(\lambda_0 2\mu_{\text{OH}_a})$ ,  $(2\lambda_0 \mu_{\text{OH}_a})$  structures in water and the  $(\lambda_N \mu_{\text{NH}_1} \mu_{\text{NH}_2} \mu_{\text{NH}_3})$   
 $(2\mu_{\text{NH}_a} \mu_{\text{NH}_b} \mu_{\text{NH}_c})$  and  $(3\mu_{\text{NH}_a} \mu_{\text{NH}_b})$ ,  $(2\mu_{\text{NH}_a} 2\mu_{\text{NH}_b})$ ,  $(2\lambda_N \mu_{\text{NH}_a} \mu_{\text{NH}_b})$ ,  
 $(\lambda_N 2\mu_{\text{NH}_a} \mu_{\text{NH}_b})$  structures in ammonia (Figure 5.4). Clearly the search  
 for an energy minimum for each structure is constrained by the  
 procedures of the PLMO method.

In view of this, what significance can be ascribed to the energy  
 value on the diagrams (The energy difference between  $\Psi_{\text{DMO}}$  and  $\Psi_{\text{CMO}}$ )  
 corresponding to a particular arrangement of lone pairs and bonds?

For the PLMO structure, the energy difference is to be inter-  
 preted as a delocalisation energy. This is the energy that has to  
 be sacrificed in order to localise the MOs (hence electrons) into  
 two-centre bonds and one-centre lone pairs; or equivalently; the  
 energy lowering that would result if the PLMOs were allowed to  
 delocalise over all the AOs in the molecule. This energy value is  
 discussed further in Section 7.3.

Structures similar to the PLMO structure, but in which a PLMO  
 lone pair has been replaced by a bond involving the same atom,  
 should represent a partial delocalisation and therefore be found  
 at an energy lower than the PLMOs. This is true in HCN (Fig. 4.1)  
 but not so in water and ammonia where the relevant structures occur  
 at higher energies. These energy values are imposed by the shape of  
 the energy surface generated by the PLMO method and have already  
 been discussed above. In CO and  $\text{N}_2$  (Figures 5.1 and 5.2) all such  
 structures span the Hartree-Fock function space (with the inner  
 shells left untruncated) and therefore give the canonical energy,  
 while in methane (Figure 5.5) no structures representing partial  
 delocalisation are possible since only two-centre bonds are considered.

It would seem dangerous, then, to attach much significance to the relative energy values of the non-PLMO low energy structures.

For structures further up each energy scale attempts at interpretation become even more dangerous because the relative energy values occurring here are generally of the same order as the dissociation energies of the individual bonds; for example  $D(\text{CH}_3 - \text{H}) = 0.166\text{H}$ ; <sup>243</sup>  $D(\text{H} - \text{OH}) = 0.190\text{H}$ ; <sup>244</sup>  $D(\text{N} - \text{N}) = 0.360\text{H}$ . <sup>245</sup> It is unlikely that any of the high energy structures correspond to excited states because of the large overlap that exists between the generated wavefunctions and the Hartree-Fock canonical ground state wavefunction. In appearance, these "unusual" structures are reminiscent of Valence Bond resonance structures, though of a type that would not normally be expected to make any appreciable contribution to the ground state molecular wavefunction. This is, of course, exactly where the significance of the high energy structures lies. The structures are significant in that they do occur at relatively high energies and are therefore not candidates for a single representation of the electronic organisation of the molecule in question.

#### 7.2(b) Overlaps with CMO Wavefunction

The overlap between the wavefunction constructed from the LMOs for each structure,  $\psi_{\text{LMO}}$  and the wavefunction constructed from the CMOs,  $\psi_{\text{CMO}}$ , is also shown on the energy diagrams. For the PLMO structures the overlaps are all close to unity ( $>0.98$ ) and in CO and  $\text{N}_2$  (Figures 5.1 and 5.2) are exactly equal to one. These figures reflect the closeness of the PLMO descriptions of the molecules to the original CMO descriptions.

For each molecule, the overlaps generally increase as the relative energies decrease, though there are a couple of exceptions.

These occur in water and ammonia (Figures 5.3 and 5.4) in the structures that represent a partial delocalisation of the PLMO structure. In these cases the wavefunction overlaps show the expected increase in value where the energy does not show the expected decrease. That strict linearity is not maintained between energy and overlap is demonstrated in the INDO approximation by other LMO work.<sup>246</sup>

The individual values of wavefunction overlap seem to have little significance and provide limited scope for comparison to other work in the literature. For this reason further discussion and comparison of the wavefunction properties exhibited in the energy diagrams are restricted to the relative energy values.

### 7.3 PLMO DELOCALISATION ENERGY - COMPARISON TO OTHER METHODS

The arrangement of lone pairs and bonds chosen to yield the PLMOs for each example molecule corresponds to those generated by other LMO methods. In some methods such arrangements are fixed by a priori assumptions concerning the valence descriptions of molecules, while in others they are generated (with LMO "tails") by imposing different localising criteria on the MOs (see Chapter 2). When such methods yield LMOs that are strictly localised (either by a direct calculation or by deleting orbital "tails") a comparison may be made between the energy sacrifice required in those methods and that necessary in the PLMO method. Such a comparison should be an aid in judging the success of the approach to one and two-centre localisation adopted in this work.

The energy sacrifices necessary in different LMO methods are compared in Tables 7.1 to 7.5 for the molecules investigated by the

PLMO method. No results are available for comparison for  $N_2$ . The values for the PLMOs include a contribution from the truncation of the inner shells. Such information is available for HCN, and for the other molecules an allowance of 0.0005H has been made for each inner shell in the molecule. This allowance is based on the results for HCN where two inner shell truncations gave an increase of 0.0007H (see Chapter 4) and in carbon monoxide (obtained in supplementary calculations) where an increase of 0.00085H was obtained.

It can be seen from the tables that the accuracy of the Hartree-Fock calculations to which the LMO energies are compared, vary from author to author. The minimal STO-3G basis employed in this work is the same as that used in the recent work of Stoll, Wagenblast and Preuss,<sup>38</sup> but is less accurate than those employed by all the other authors. This disadvantage to the PLMO wavefunctions should be borne in mind when comparing the delocalisation energies.

The results of Newton, Switkes and Lipscomb<sup>93</sup> are the only ones obtained by a transformation relocalisation LMO method, in this case that of Edmiston & Ruedenberg.<sup>70, 83-85</sup> The energy sacrifice in methane (Table 7.5) and HCN (Table 7.1) when deleting the LMO "tails" is significantly greater than that in the PLMO wavefunctions and in view of the general similarity of LMO orbital forms obtained by most transformation methods,<sup>96-98, 124,125,247,248</sup> this difference would presumably still be evident when comparing the truncated LMOs obtained by the methods of Boys,<sup>71,72</sup> Magnasco & Perico,<sup>124,125</sup> and Von Niessen<sup>96-98</sup> for example.

Hoyland<sup>48</sup> and Petke & Whitten<sup>180</sup> obtain one and two-centre localised orbitals constructed from HAOs. The hybrid expansion co-

TABLE 7.1 COMPARISON OF PLMO DELOCALISATION ENERGY IN HCN WITH THAT SACRIFICED IN OTHER METHODS THAT YIELD ONE AND TWO-CENTRE LMOs

| Author                                      | Type of Basis         | HF Energy (H) | LMO Energy (H) | Difference (H) |
|---|-----------------------|---------------|----------------|----------------|
| Petke & Whitten <sup>180</sup>              | Minimal HFAO-Gaussian | -92.7203      | -92.7188       | 0.0015         |
| This work                                   | Minimal STO-3G        | -91.6752      | -91.6713       | 0.0039         |
| Newton, Switkes <sup>93</sup><br>& Lipscomb | Minimal STO           | -92.6095      | -92.5684       | 0.0411         |

TABLE 7.2 COMPARISON OF PLMO DELOCALISATION ENERGY IN CO WITH THAT SACRIFICED IN OTHER METHODS THAT YIELD ONE AND TWO-CENTRE LMOs

| Author  | Type of Basis       | HF Energy (H) | LMO Energy (H) | Difference (H) |
|---|---------------------|---------------|----------------|----------------|
| This work   | Minimal STO-3G      | -111.2246     | -111.2236      | 0.0010         |
| Stoll, Wagenblast <sup>154</sup><br>& Preuss (1978) | Contracted Gaussian | -112.5643     | -112.4917      | 0.0726         |



TABLE 7.3 COMPARISON OF PLMO DELOCALISATION ENERGY IN  $H_2O$  WITH THAT SACRIFICED IN OTHER METHODS THAT YIELD ONE AND TWO-CENTRE LMOs

| Author   | Type of Basis                          | HF Energy (H) | LMO Energy (H) | Difference (H) |
|--|--|---------------|----------------|----------------|
| Stoll, Wagenblast <sup>38</sup><br>& Preuss (1980) | Minimal STO-3G                         | -74.9629      | -74.9598       | 0.0031         |
| This work  | Minimal STO-3G                         | -74.9629      | -74.9561       | 0.0068         |
| Wilhite & Whitten <sup>151</sup>                   | "Frozen" Gaussian                      | -75.9670      | -75.9598       | 0.0072         |
|  | "Split" Gaussian                       | -75.9893      | -75.9810       | 0.0083         |
| Petke & Whitten <sup>180</sup>                     | Minimal HFAO-Gaussian                  | -75.9734      | -75.9646       | 0.0088         |
| Payne <sup>37</sup>                                | Extended 4-31G                         | -75.9032      | -75.8879       | 0.0153         |
| Matsuoka <sup>146</sup>                            | Contracted Gaussian<br>('double zeta') | -85.1985 (a)  | -85.1617 (a)   | 0.0368         |

(a) Electronic energy only.

TABLE 7.4 COMPARISON OF PLMO DELOCALISATION ENERGY IN  $\text{NH}_3$  WITH THAT SACRIFICED IN OTHER METHODS THAT YIELD ONE AND TWO-CENTRE LMOs

| Author   | Type of Basis         | HF Energy (H) | LMO Energy (H) | Difference (H) |
|--|-----------------------|---------------|----------------|----------------|
| Stoll, Wagenblast<br>& Preuss (1980) <sup>38</sup> | Minimal STO-3G        | -55.4540      | -55.4493       | 0.0047         |
| Payne <sup>37</sup>                                | Extended 4-31G        | -56.0983      | -56.0869       | 0.0114         |
| Wilhite & Whitten <sup>151</sup>                   | "Split" Gaussian      | -56.1542      | -56.1403       | 0.0139         |
|  | "Frozen" Gaussian     | -56.1262      | -56.1105       | 0.0157         |
| This work  | Minimal STO-3G        | -55.4534      | -55.4344       | 0.0190         |
| Petke & Whitten <sup>180</sup>                     | Minimal HFA0-Gaussian | -56.1415      | -56.1206       | 0.0209         |

TABLE 7.5 COMPARISON OF PLMO DELOCALISATION ENERGY IN CH<sub>4</sub> WITH THAT SACRIFICED IN OTHER METHODS THAT YIELD ONE AND TWO-CENTRE LMOs

| Author  | Type of Basis                          | HF Energy (H) | LMO Energy (H) | Difference (H) |
|---|--|---------------|----------------|----------------|
| Hoyland <sup>48</sup>                               | Contracted Gaussian                    | -40.1329      | -40.1327       | 0.0002         |
| Stoll, Wagenblast <sup>38</sup><br>& Preuss (1980)  | Minimal STO-3G                         | -39.7269      | -39.7213       | 0.0056         |
| Payne <sup>37</sup>                                 | Extended 4-31G                         | -40.1369      | -40.1298       | 0.0071         |
| Matsuoka <sup>146</sup>                             | Contracted Gaussian<br>("double zeta") | -53.5741 (a)  | -53.5659 (a)   | 0.0082         |
| This work   | Minimal STO-3G                         | -39.7267      | -39.7111       | 0.0156         |
| Newton, Switkes <sup>93</sup><br>& Lipscomb         | Minimal STO                            | -40.1281      | -40.0976       | 0.0305         |
| Stoll, Wagenblast <sup>154</sup><br>& Preuss (1978) | Contracted Gaussian                    | -39.7445      | -39.6867       | 0.0578         |
| Peters <sup>150</sup>                               | Minimal STO                            | -53.3516 (a)  | -53.2509 (a)   | 0.1007         |

(a) Electronic energy only.

efficients and polarity parameters in bonds in each case are variationally optimised to give an energy minimum. The Petke & Whitten delocalisation energies in  $\text{NH}_3$  (Table 7.4),  $\text{H}_2\text{O}$  (Table 7.3) and  $\text{HCN}$  are close to those of the PLMOs while Hoyland's calculation on methane yields an energy very near to that of a full SCF Hartree-Fock calculation.

All the remaining LMO methods yield localised orbitals without "tails" by direct solution of eigenvalue equations involving localisation operators. Peters<sup>150</sup> in his calculation on methane (Table 7.5) used a minimal STO basis while Wilhite & Whitten<sup>151</sup> using essentially Peters' method employed two different gaussian bases in both water and ammonia (Tables 7.3 and 7.4). The energy sacrifices found by Wilhite & Whitten are similar to those of the PLMOs, but the value obtained by Peters in methane is much larger. Such a big difference between methane and ammonia from essentially the same method probably highlights the danger in comparing results obtained using dissimilar basis sets.

Stoll et al<sup>154</sup> obtain LMOs in a partitioned gaussian basis for methane and carbon monoxide (Table 7.2). The energy sacrificed is much greater than that for the PLMO wavefunctions, though the main aim of their method is to reduce computational effort rather than obtain variationally exact calculations.<sup>153</sup>

The work of Matsuoka<sup>146</sup> and (to a lesser extent) Payne<sup>37</sup> owes much to the eigenvalue equations of Adams and Gilbert.<sup>135,136,138</sup> One and two-centre LMOs are found in gaussian bases. Stoll et al.<sup>38</sup> modify the Payne method and obtain LMO eigenfunctions in a minimal STO-3G basis. The delocalisation energies found by Payne in methane

and ammonia and by Matsuoka in methane are less than those of the PLMOs; in water however the reverse is true. The improved method of Stoll et al.<sup>38</sup> needs only a very small energy sacrifice, which is smaller than that shown by the PLMOs even in water.

Generally speaking, the delocalisation energies in the PLMO wavefunctions compare favourably to those of the other methods (though this is less true in ammonia). It is not surprising that the energy sacrificed by the PLMOs is less than that when deleting the LMO "tails" of Edmiston and Ruedenberg (and presumably of similar transformation methods), because the very criterion fixing the orthogonal transformation of the CMOs in the PLMO method is that the energy sacrifice after truncation be a minimum. As much encouragement may be derived from the fact that the energy sacrificed by the PLMOs is at least comparable to the delocalisation energies from the remaining methods. In particular, those involving the direct variational optimisation of wavefunctions, and those based on the solution of variationally optimised eigenvalue equations, often using more accurate basis sets. This is especially true in CO (and N<sub>2</sub>) where only the inner shells are deemed to contribute to a PLMO delocalisation energy in the tables.

In summary, it would seem that the first desired property of the PLMOs (Section 1.3(b)) is satisfied because the energy sacrifice relative to the canonical wavefunction is indeed small. The exact situation is clouded, however, by the use of different basis sets in computations by different workers.

CHAPTER EIGHTFORMS OF PLMOs AND POPULATION ANALYSIS

This chapter is concerned with an analysis of the forms of the PLMOs and their overlap integrals which are further described in Sections 8.2 and 8.3. As an aid to interpretation, the results of an electron population analysis (introduced in Section 8.1) are also shown. In section 8.4 the significance of the results, and a comparison to the forms of the LMOs of other methods, is discussed.

8.1 ELECTRON POPULATION ANALYSIS

The method of Mulliken<sup>118-121</sup> and McWeeny<sup>122,123</sup> for calculating AO electronic populations, adapted for the case of non-orthogonal MOs, is outlined in Section 6 of Appendix I. The electron populations so obtained are expected to aid the analysis of aspects of the electronic structure of the molecules considered.

It is important, however, to keep certain reservations in mind when dealing with Mulliken populations. Firstly, the concept of the electronic population of an atom or atomic orbital has no exact physical significance and which part of the overall electron density is to be assigned to any particular atom or AO is, to an extent, arbitrary. Secondly, arising from the first point, there exist many alternative methods of defining electronic populations which attempt to overcome the deficiencies in Mulliken's procedure.<sup>249-253</sup>

It is certainly true however, that despite the well known drawbacks the Mulliken method is still useful in the analysis of electronic structure by its power to condense the sometimes difficult concepts of the quantum mechanical valence theory into

easily understandable concepts and numerical values. It seems to be generally true that there is less significance in the absolute value of the electron populations for a single molecule, than in the relative populations along a series of molecules. Such comparisons remain an invaluable tool in the characterisation of structural trends. In this work, the method is used mainly to support conclusions drawn from the sizes of AO coefficients and bond polarity parameters.

## 8.2 HYBRIDISATION AND POPULATION ANALYSIS OF MOLECULES

### 8.2(a) HCN

The forms of the PLMOs obtained for three different cases for HCN have been shown in Tables 4.4, 4.5 and 4.6 of Chapter 4. Since they are all quite similar, this discussion will concentrate on the STO-3G basis set results in Table 4.4.

The results of the population analysis is shown in Table 8.1. The table shows for each PLMO, the individual AO populations and the sum for each atom and for all AOs. The AO and atom populations summed over all PLMOs are shown on the bottom line. The grand total (i.e. the number of electrons in the molecule) is shown in the bottom right-hand corner. For a particular bond, the polarities may be obtained from the atom populations in the bond PLMO by allocating +1.0e nuclear charge from each bonded atom (as in the bond moment calculations, Appendix I). The 2s AO in all the population tables is the STO and is hence not orthogonal to the 1s STO. This means that these populations are not exactly applicable to the tables of PLMOs in Chapters 4 and 5 where the Schmidt-orthogonalised 2s<sup>or</sup> AO was used. However the difference is not great, and since only the gross features are to be noted, the

TABLE 8.1 ELECTRON POPULATIONS OF AOs IN PLMOs FOR HCN (STO-3G BASIS)

(For explanation see narrative)

|                        | 1s <sub>H</sub> | 1s <sub>C</sub> | 2s <sub>C</sub> | 2p <sub>xC</sub> | 2p <sub>yC</sub> | 2p <sub>zC</sub> | C<br>TOTAL | 1s <sub>N</sub> | 2s <sub>N</sub> | 2p <sub>xN</sub> | 2p <sub>yN</sub> | 2p <sub>zN</sub> | N<br>TOTAL | Total<br>over<br>AOs |
|------------------------|-----------------|-----------------|-----------------|------------------|------------------|------------------|------------|-----------------|-----------------|------------------|------------------|------------------|------------|----------------------|
| k <sub>N</sub>         | -               | -               | -0.001          | -                | -                | -0.002           | -0.003     | 1.998           | 0.015           | -                | -                | -                | 2.003      | 2.000                |
| k <sub>C</sub>         | -0.001          | 1.998           | 0.015           | -                | -                | -                | 2.003      | -               | -0.002          | -                | -                | -                | -0.002     | 2.000                |
| λ <sub>N</sub>         | -               | -0.001          | -0.002          | -                | -                | 0.001            | -0.002     | 0.009           | 1.773           | -                | -                | 0.220            | 2.002      | 2.000                |
| μ <sub>CH</sub>        | 0.851           | 0.003           | 0.574           | -                | -                | 0.577            | 1.154      | -               | -               | -                | -                | -0.005           | -0.005     | 2.000                |
| μ <sub>CN</sub>        | -0.004          | 0.004           | 0.447           | -                | -                | 0.437            | 0.888      | 0.001           | -0.020          | -                | -                | 1.135            | 1.116      | 2.000                |
| π <sub>1</sub>         | -               | -               | -               | 0.702            | 0.270            | -                | 0.972      | -               | -               | 0.743            | 0.285            | -                | 1.028      | 2.000                |
| π <sub>2</sub>         | -               | -               | -               | 0.270            | 0.702            | -                | 0.972      | -               | -               | 0.285            | 0.743            | -                | 1.028      | 2.000                |
| Total<br>Over<br>PLMOs | 0.846           | 1.994           | 1.033           | 0.972            | 0.972            | 1.011            | 5.984      | 1.998           | 1.766           | 1.028            | 1.028            | 1.350            | 7.170      | 14.000               |



distinction is not important.

The results for HCN may be analysed as follows. The inner shells,  $k_N$  and  $k_C$ , in Table 4.4 are the original CMOs obtained from Gaussian 70. They are composed almost exclusively of the 1s AO of the appropriate atom. This is reflected by the 1s AO populations in Table 8.1 being close to 2.0. This localisation of the inner shell CMOs was the reason these MOs were not included in the subsequent localising process of the method. The very small values of 1s AO coefficients and populations in the rest of the PLMOs shows how little this inner shell "core" has penetrated the valence region and supports the idea of core/valence separability (Section 4.7).

The nitrogen lone pair,  $\lambda_{N_1}$  can be seen to be very largely  $2s^{or}$  in character but with a small contribution from the 2p AO which directs the electron density away from the rest of the molecule.

The carbon-hydrogen bond,  $\mu_{CH_1}$  is polar in the sense  $C^-H^+$ , both from the size of the polarity parameters in the PLMO and also from the population analysis. The actual values in the latter are approximately + and - 0.15e and follows the usually expected electronegativity properties of the atoms concerned. The carbon hybrid in this PLMO is heavily hybridised with roughly equal contributions from the  $2s^{or}$  and 2p AOs, this is reflected by nearly equal s and p AO populations on carbon (approximately 0.6 electrons). The carbon hybrid in the C-N sigma bond,  $\mu_{CN_1}$ , is similarly hybridised with almost equal weights of  $2s^{or}$  and 2p AOs. The nitrogen hybrid in this bond is very little hybridised however and is composed

of a nearly pure nitrogen 2p orbital with very small amounts of  $2s^{\text{or}}$  (though unusually of negative sign). This bond is also polar in the sense expected by electronegativity,  $C^+N^-$ , but to a lesser extent than the C-H bond. The relevant electron charges here are approximately  $+ 0.1$ .

The  $\pi$  bonds between carbon and nitrogen are those CMOs found by Gaussian 70. From the orbital forms and the population analysis they can be seen to be slightly polar in the sense  $C^+N^-$ .

A simple analysis of this kind can be applied to the PLMOs of the other molecules studied. This is carried out in the following subsections where only exceptions to the general pattern manifested in HCN will be dealt with in any detail.

#### 8.2(b) CO

The PLMOs for CO may be seen in Table 5.11, Chapter 5. The population analysis results are in Table 8.2.

The CMO inner shells on carbon and oxygen,  $k_C$  and  $k_O$ , are again almost entirely made up of the relevant 1s orbital. The valence PLMOs can also be seen to contain very little 1s contribution. The lone pair on oxygen,  $\lambda_O$ , and the carbon lone pair,  $\lambda_C$ , both have a similar form. Each has a large  $2s^{\text{or}}$  contribution and a smaller contribution from the 2p AO which directs the lone pair electron density away from the internuclear region. The polarity of the C-O sigma bond,  $\mu_{CO}$ , from the polarity parameters and the populations can be seen to be in the sense  $C^+O^-$ . The charges are approximately  $+ 0.35e$  from Table 8.2. The hybrids on carbon and oxygen that form this bond are approximately pure 2p atomic orbital. The  $\pi$  orbitals are again the CMOs. Here however, by dividing the remaining

TABLE 8.2 ELECTRON POPULATIONS OF AOs IN PLMOs FOR CO (STO-3G BASIS)

(For explanation see narrative)

|                        | 1s <sub>C</sub> | 2s <sub>C</sub> | 2p <sub>xC</sub> | 2p <sub>yC</sub> | 2p <sub>zC</sub> | C<br>TOTAL | 1s <sub>O</sub> | 2s <sub>O</sub> | 2p <sub>xO</sub> | 2p <sub>yO</sub> | 2p <sub>zO</sub> | O<br>TOTAL | Total<br>Over<br>AOs |
|------------------------|-----------------|-----------------|------------------|------------------|------------------|------------|-----------------|-----------------|------------------|------------------|------------------|------------|----------------------|
| k <sub>O</sub>         | -               | -0.001          | -                | -                | -0.001           | -0.002     | 1.988           | 0.014           | -                | -                | -                | 2.002      | 2.000                |
| k <sub>C</sub>         | 1.987           | 0.015           | -                | -                | -                | 2.002      | -               | -0.001          | -                | -                | 0.001            | -0.002     | 2.000                |
| λ <sub>C</sub>         | 0.010           | 1.687           | -                | -                | 0.324            | 2.020      | -               | -0.027          | -                | -                | 0.007            | -0.020     | 2.000                |
| λ <sub>O</sub>         | -               | -0.042          | -                | -                | 0.020            | -0.021     | 0.009           | 1.861           | -                | -                | 0.151            | 2.021      | 2.000                |
| H <sub>CO</sub>        | 0.002           | 0.018           | -                | -                | 0.635            | 0.655      | -               | 0.008           | -                | -                | 1.336            | 1.345      | 2.000                |
| π <sub>1</sub>         | -               | -               | 0.003            | 0.570            | -                | 0.573      | -               | -               | 0.008            | 1.419            | -                | 1.427      | 2.000                |
| π <sub>2</sub>         | -               | -               | 0.570            | 0.003            | -                | 0.573      | -               | -               | 1.419            | 0.008            | -                | 1.427      | 2.000                |
| Total<br>Over<br>PLMOs | 1.998           | 1.677           | 0.573            | 0.573            | 0.978            | 5.799      | 1.998           | 1.854           | 1.427            | 1.427            | 1.495            | 8.201      | 14.000               |

unallocated nuclear charges on carbon and oxygen between the two  $\pi$  orbitals, the populations show a polarity of  $C^-O^+$ . The charges are about  $\pm 0.1e$ .

#### 8.2(c) $N_2$

The PLMOs of  $N_2$  are shown in Table 5.12; the population analysis in Table 8.3.

As expected, the PLMOs and population analysis reflect the symmetry of the molecule. As already stated, the inner shell orbitals shown are in fact the renormalised sum and difference of the inner shell CMOs. This procedure has clearly localised the orbitals. The overall form of the PLMOs in this molecule is similar to that of CO with which it is isoelectronic. There is slight hybridisation in the lone pairs while the hybrids forming the sigma bond are almost pure 2p in character.

#### 8.2(d) $H_2O$

Table 5.13 exhibits the PLMOs of  $H_2O$ . The population analysis of this molecule is shown in Table 8.4.

The oxygen inner shell,  $k_0$ , is almost solely composed of a doubly occupied 1s atomic orbital on oxygen. The two O-H bonds are equivalent, each being polar in the sense  $O^-H^+$ . The populations on the atoms reveal this polarity to be approximately  $-0.2e$  on oxygen and  $+0.2e$  on hydrogen in each bond. The oxygen hybrid has little  $2s^{or}$  contribution and is composed largely of the  $2p_x$  and  $2p_z$  AOs, the small  $2s^{or}$  coefficient is unusual however in being negative in sign. The relative sizes of the p orbital coefficients may be used to calculate at which angle in the xz plane the oxygen hybrids point. This is shown in Figure 8.1. It can be seen that the hybrids

TABLE 8.3 ELECTRON POPULATIONS OF AOs IN PLMOs FOR N<sub>2</sub> (STO-3G BASIS)

(For explanation see narrative)

|                        | 1s <sub>N1</sub> | 2s <sub>N1</sub> | 2p <sub>xN1</sub> | 2p <sub>yN1</sub> | 2p <sub>zN1</sub> | N <sub>1</sub><br>TOTAL | 1s <sub>N2</sub> | 2s <sub>N2</sub> | 2p <sub>xN2</sub> | 2p <sub>yN2</sub> | 2p <sub>zN2</sub> | N <sub>2</sub><br>TOTAL | Total<br>Over<br>AOs |
|------------------------|------------------|------------------|-------------------|-------------------|-------------------|-------------------------|------------------|------------------|-------------------|-------------------|-------------------|-------------------------|----------------------|
| k <sub>N1</sub>        | 1.988            | 0.014            | -                 | -                 | -                 | 2.002                   | -                | -0.002           | -                 | -                 | -                 | -0.002                  | 2.000                |
| k <sub>N2</sub>        | -                | -0.002           | -                 | -                 | -                 | -0.002                  | 1.987            | 0.015            | -                 | -                 | -                 | 2.002                   | 2.000                |
| λ <sub>N1</sub>        | 0.009            | 1.755            | -                 | -                 | 0.260             | 2.024                   | -                | -0.040           | -                 | -                 | 0.016             | -0.024                  | 2.000                |
| λ <sub>N2</sub>        | -                | -0.040           | -                 | -                 | 0.016             | -0.024                  | 0.009            | 1.755            | -                 | -                 | 0.260             | 2.024                   | 2.000                |
| μ <sub>NN</sub>        | 0.001            | 0.015            | -                 | -                 | 0.984             | 1.000                   | 0.001            | 0.015            | -                 | -                 | 0.984             | 1.000                   | 2.000                |
| π <sub>1</sub>         | -                | -                | 0.607             | 0.393             | -                 | 1.000                   | -                | -                | 0.607             | 0.393             | -                 | 1.000                   | 2.000                |
| π <sub>2</sub>         | -                | -                | 0.393             | 0.607             | -                 | 1.000                   | -                | -                | 0.393             | 0.607             | -                 | 1.000                   | 2.000                |
| Total<br>Over<br>PLMOs | 1.998            | 1.743            | 1.000             | 1.000             | 1.259             | 7.000                   | 1.998            | 1.743            | 1.000             | 1.000             | 1.259             | 7.000                   | 14.000               |

TABLE 8.4 ELECTRON POPULATIONS OF AOs IN PLMOs FOR H<sub>2</sub>O (STO-3G BASIS)

(For explanation see narrative)

|                             | 1s <sub>O</sub> | 2s <sub>O</sub> | 2p <sub>xO</sub> | 2p <sub>yO</sub> | 2p <sub>zO</sub> | O<br>TOTAL | 1s <sub>H<sub>1</sub></sub> | 1s <sub>H<sub>2</sub></sub> | Total<br>Over<br>AOs |
|-----------------------------|-----------------|-----------------|------------------|------------------|------------------|------------|-----------------------------|-----------------------------|----------------------|
| k <sub>O</sub>              | 1.987           | 0.014           | -                | -                | -                | 2.002      | -0.001                      | -0.001                      | 2.000                |
| λ <sub>O</sub>              | 0.010           | 1.874           | -                | -                | 0.124            | 2.009      | -0.004                      | -0.004                      | 2.000                |
| μ <sub>OH<sub>1</sub></sub> | -               | -0.025          | 0.585            | -                | 0.622            | 1.182      | 0.825                       | -0.007                      | 2.000                |
| μ <sub>OH<sub>2</sub></sub> | -               | -0.025          | 0.585            | -                | 0.622            | 1.182      | -0.007                      | 0.825                       | 2.000                |
| π                           | -               | -               | -                | 2.000            | -                | 2.000      | -                           | -                           | 2.000                |
| Total<br>Over<br>PLMOs      | 1.998           | 1.837           | 1.170            | 2.000            | 1.368            | 8.374      | 0.813                       | 0.813                       | 10.000               |

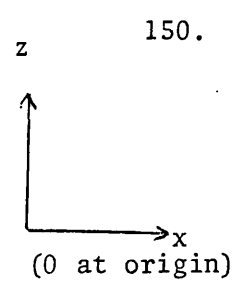
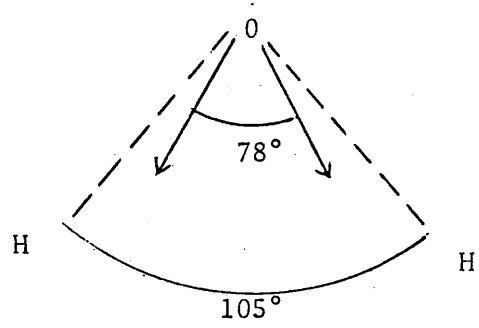


Figure 8.1 Direction of bonding hybrids of oxygen in water

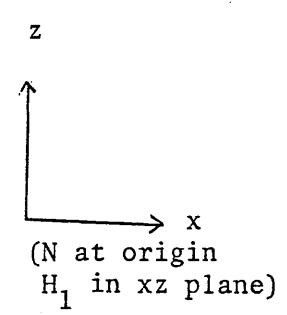
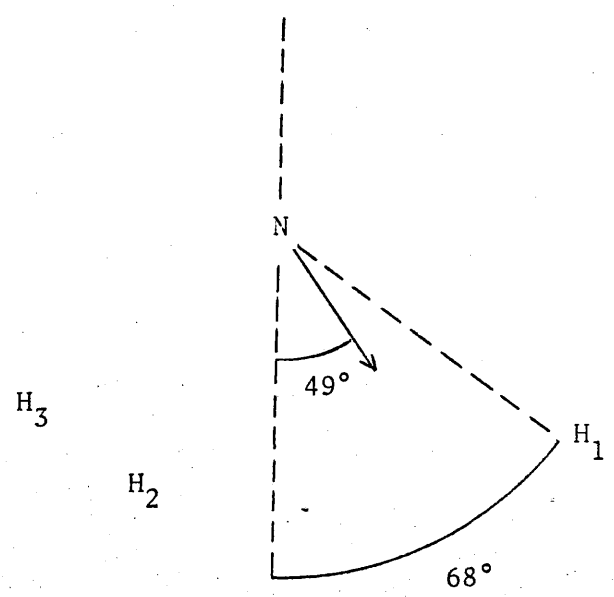


Figure 8.2 Direction of bonding hybrids of nitrogen in ammonia<sup>(a)</sup>

(a) in the xy plane of ammonia the angle between bonding hybrids is 120°.

point not at the hydrogen atoms but at an angle significantly smaller than that formed by the internuclear lines. The bonds formed from such hybrids are often termed "bent" bonds. Of the two oxygen lone pairs, one lies in a doubly occupied  $2p_y$  orbital perpendicular to the plane of the molecule, and the other is shown in Table 5.13. This has only a small  $2p$  coefficient which directs the electron density away from the two hydrogen atoms.

#### 8.2(e) $\underline{\text{NH}}_3$

The PLMOs are in Table 5.14 and the population numbers in Table 8.5.

The nitrogen inner shell,  $k_N$ , is of the usual form and the nitrogen lone pair,  $\lambda_N$ , again points away from the internuclear region. The lone pair is slightly more hybridised than those seen before but the population analysis still attributes two-thirds of the electron charge to the  $2s$  orbital. The three equivalent N-H bonds are polar, each roughly having charges of  $+0.15e$  and  $+0.15e$  on nitrogen and hydrogen respectively. As in water the bonding nitrogen hybrids do not point directly at the hydrogen atoms but form an angle smaller than that formed by the internuclear lines. The directions are shown in Figure 8.2. In the  $xy$  plane the hybrids form an angle of  $120^\circ$ , identical to that of the molecular geometry.

#### 8.2(f) $\underline{\text{CH}}_4$

The PLMOs for this last molecule are in Table 5.15 and the population analysis is in Table 8.6.

The high symmetry of methane helps to fix the transformation of the CMOs needed in the localising method and also ensures that the carbon hybrids point directly towards the hydrogen atoms. The



TABLE 8.5 ELECTRON POPULATIONS OF AOs IN PLMOs FOR NH<sub>3</sub> (STO-3G BASIS)

(For explanation see narrative)

|                             | 1s <sub>N</sub> | 2s <sub>N</sub> | 2p <sub>xN</sub> | 2p <sub>yN</sub> | 2p <sub>zN</sub> | N<br>TOTAL | 1s <sub>H<sub>1</sub></sub> | 1s <sub>H<sub>2</sub></sub> | 1s <sub>H<sub>3</sub></sub> | Total<br>Over<br>AOs |
|-----------------------------|-----------------|-----------------|------------------|------------------|------------------|------------|-----------------------------|-----------------------------|-----------------------------|----------------------|
| k <sub>N</sub>              | 1.986           | 0.017           | -                | -                | -                | 2.003      | -0.001                      | -0.001                      | -0.001                      | 2.000                |
| λ <sub>N</sub>              | 0.009           | 1.362           | -                | -                | 0.640            | 2.011      | -0.004                      | -0.004                      | -0.004                      | 2.000                |
| μ <sub>NH<sub>1</sub></sub> | -               | 0.053           | 0.775            | -                | 0.333            | 1.161      | 0.858                       | -0.009                      | -0.009                      | 2.000                |
| μ <sub>NH<sub>2</sub></sub> | -               | 0.053           | 0.194            | 0.581            | 0.333            | 1.161      | -0.009                      | 0.858                       | -0.009                      | 2.000                |
| μ <sub>NH<sub>3</sub></sub> | -               | 0.053           | 0.194            | 0.581            | 0.333            | 1.161      | -0.009                      | -0.009                      | 0.858                       | 2.000                |
| Total<br>Over<br>PLMOs      | 1.995           | 1.539           | 1.162            | 1.162            | 1.638            | 7.496      | 0.835                       | 0.835                       | 0.835                       | 10.000               |

TABLE 8.6 ELECTRON POPULATIONS OF AOs IN PLMOs FOR CH<sub>4</sub> (STO-3G BASIS)

(For explanation see narrative)

|                             | 1s <sub>C</sub> | 2s <sub>C</sub> | 2p <sub>xC</sub> | 2p <sub>yC</sub> | 2p <sub>zC</sub> | C<br>TOTAL | 1s <sub>H<sub>1</sub></sub> | 1s <sub>H<sub>2</sub></sub> | 1s <sub>H<sub>3</sub></sub> | 1s <sub>H<sub>4</sub></sub> | Total<br>Over<br>AOs |
|-----------------------------|-----------------|-----------------|------------------|------------------|------------------|------------|-----------------------------|-----------------------------|-----------------------------|-----------------------------|----------------------|
| k <sub>C</sub>              | 1.988           | 0.017           | -                | -                | -                | 2.005      | -0.001                      | -0.001                      | -0.001                      | -0.001                      | 2.000                |
| h <sub>CH<sub>1</sub></sub> | 0.001           | 0.238           | 0.273            | 0.273            | 0.273            | 1.056      | 0.972                       | -0.009                      | -0.009                      | -0.009                      | 2.000                |
| h <sub>CH<sub>1</sub></sub> | 0.001           | 0.238           | 0.273            | 0.273            | 0.273            | 1.056      | -0.009                      | 0.972                       | -0.009                      | -0.009                      | 2.000                |
| h <sub>CH<sub>3</sub></sub> | 0.001           | 0.238           | 0.273            | 0.273            | 0.273            | 1.056      | -0.009                      | -0.009                      | 0.972                       | -0.009                      | 2.000                |
| h <sub>CH<sub>4</sub></sub> | 0.001           | 0.238           | 0.273            | 0.273            | 0.273            | 1.056      | -0.009                      | -0.009                      | -0.009                      | 0.972                       | 2.000                |
| Total<br>Over<br>PLMOs      | 1.991           | 0.968           | 1.090            | 1.090            | 1.090            | 6.229      | 0.943                       | 0.943                       | 0.943                       | 0.943                       | 10.000               |

four equivalent bonds shown in Table 5.15 are each slightly polar, with carbon proving the more electronegative element. The bond contributions at carbon are heavily hybridised and are in fact quite close to the classical  $sp^3$  hybrids.

#### 8.2(g) Summary

For the molecules described above, the following summary may be made.

Inner shells - the inner shells of all the molecules were well localised onto the relevant atomic centre(s). The separation of the core and valence regions as manifested in the sizes of the 1s AO coefficients was almost complete.

Valence sigma bonds and lone pairs - these are summarised in terms of normalised hybrids in Figure 8.3. The arrows point in the direction of the hybrids; a single headed arrow represents a bonding hybrid, a double headed arrow represents a lone pair. The numbers in the figure are the percentage  $2s^{or}$  or 2p content of the hybrids and are defined in the footnote of the figure.

From the figure it will be noticed that the lone pairs are all largely  $2s^{or}$  in character with between 7% and 30% 2p character. The nitrogen lone pair in ammonia is significantly more hybridised than all the other lone pairs. The bonding hybrids are of two kinds. The "internal" atoms exhibit a high degree of hybridisation (carbon hybrids in HCN and methane) while "end" atoms (all the other bonding hybrids) have between 97 and 100% p character, i.e. use almost pure p AOs for bonding.

The polarities of all the sigma bonds studied were found to be in the sense expected on electronegativity grounds. "Bent" bonds

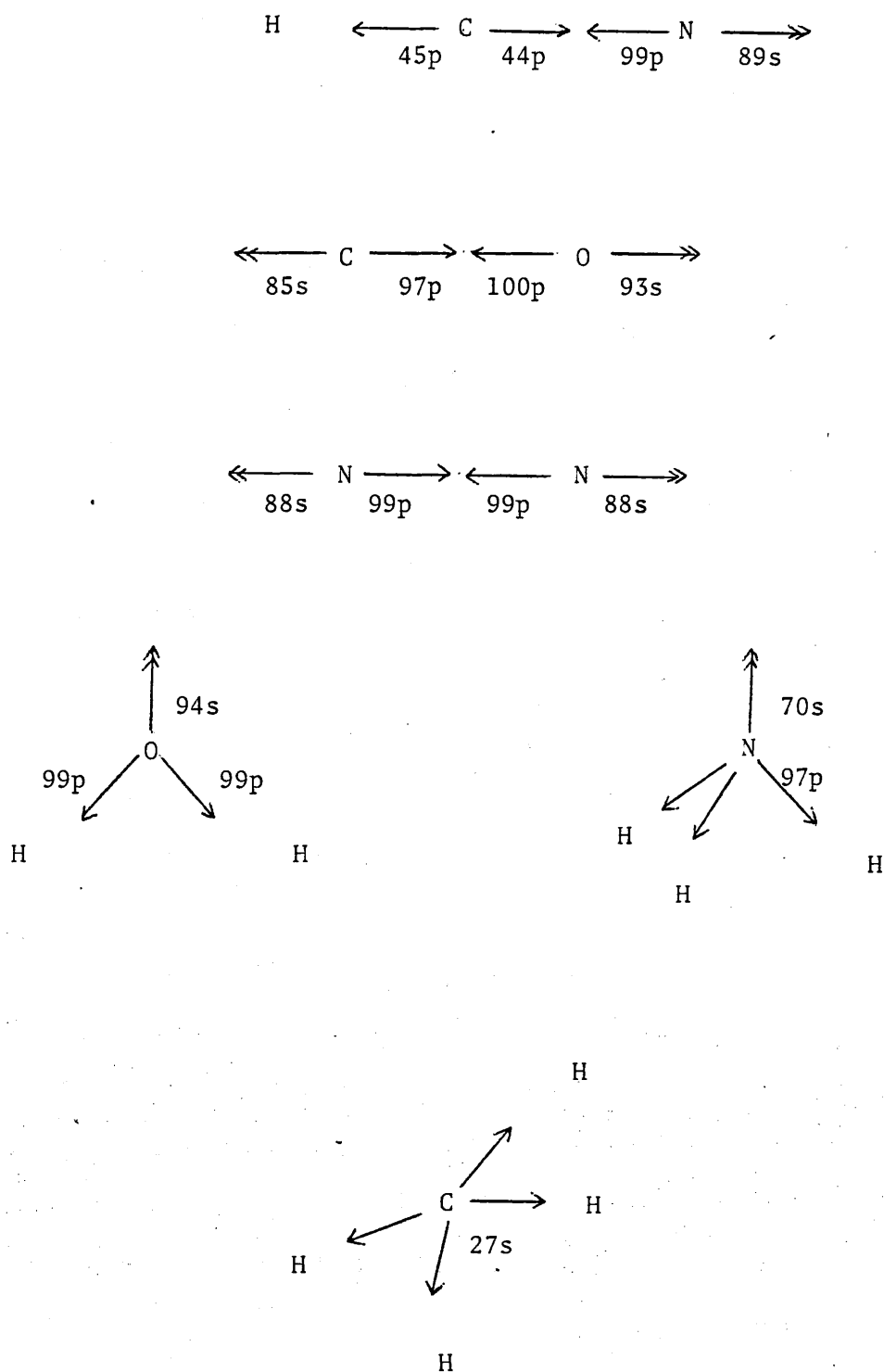


Figure 8.3 Valence sigma HAOs in the PLMOs of the example molecules<sup>(a)</sup>

- (a) In a normalised valence HAO:  $a(1s) + b(2s^{\text{or}}) + c(2px) + d(2py) + e(2pz)$   
 the %  $2s^{\text{or}}$  character is  $100b^2$  - written 27s for example  
 the % 2p character is  $100(c^2 + d^2 + e^2)$  - written 97p for example  
 the % 1s character is negligible.

were found in water and ammonia.

$\pi$  orbitals - noteworthy in the forms of these MOs and also revealed by the population analysis were the polarities.  $\pi_{\text{CO}}$  in CO and  $\pi_{\text{CN}}$  in HCN were both less polar than the corresponding sigma bonds.  $\pi_{\text{CN}}$  was polar in the same sense as the sigma bond ( $\text{C}^+\text{N}^-$ ) while  $\pi_{\text{CO}}$  was the reverse ( $\text{C}^-\text{O}^+$ ).

### 8.3 PLMO OVERLAP INTEGRALS

The absolute values of the non-orthogonality integrals between the PLMOs for the example molecules have already been shown in Tables 4.7, 4.8, 4.9 and 5.16 to 5.20 along with a total measure of their non-orthogonality,  $\Delta$ . The main features of these tables will be highlighted here. A discussion of their significance will be left to the next section.

For the sigma PLMOs of HCN, Tables 4.7, 4.8, and 4.9, all the overlap integrals are smaller than about 0.03 except for that between the two bonds which is 0.1. The  $\Delta$  value, 0.03, shows that overall the PLMOs are not far from orthogonal.

Tables 5.16 (CO) and 5.17 ( $\text{N}_2$ ) are similar in appearance and may be taken together. As in HCN, all the integrals are below about 0.03 in value except one in each case. This is the overlap between the lone pairs on different centres which is 0.14 in CO and 0.15 in  $\text{N}_2$ . In both molecules the lone pairs are each almost exactly orthogonal to the sigma bond. In both molecules the value of  $\Delta$  is 0.05 which is low.

The figures for water and ammonia (Table 5.18 and 5.19 respectively) may also be taken as a pair. The only overlaps greater than 0.03 in each case are those between the bonds which are 0.13 in

water and 0.15 in ammonia. As before, the lone pairs have only small overlap integrals with the bonds.

Finally, in methane (Table 5.20) the non-orthogonality of the bonds is again clear. The resulting six overlap integrals pushes up  $\Delta$  to 0.1, larger than that for the other molecules.

The main observations on the tables may be summarised as follows. The overlap integrals between the inner shells and valence shell PLMOs are always very small, and remain so when the inner shells are truncated (Table 4.9). The  $\pi$  orbitals are orthogonal to the sigma MOs by symmetry. Among the sigma PLMOs, the overlap integrals between two or more bonds or, in CO and N<sub>2</sub>, between two lone pairs on different atoms, are not negligible and are found to lie between 0.1 and 0.15. Lone pairs are found to be very nearly orthogonal to adjoining bonds however. A rough guide to the general magnitude of the overlaps,  $\Delta$ , is usually small. Four of the molecules have values of the order of 0.05 for  $\Delta$ , which rises to 0.08 in ammonia and 0.10 in methane as the number of overlapping bonds increases.

#### 8.4 DISCUSSION AND COMPARISON WITH OTHER WORK

##### 8.4(a) Overall Significance of PLMO Results

The general forms of the PLMOs, the bond polarities and the electron populations are attractively self-consistent. The overall level of hybridisation is low, especially in the bonding hybrids of "end" atoms, and is only extensive for carbon when this is an "internal" atom. The bond polarities found can be matched with the relative electronegativities of the atoms concerned. The only variance with normal valence ideas occurs in the bonding hybrids of nitrogen in HCN and oxygen in water where negative hybrids<sup>254</sup> are utilised. In both cases the negative  $2s^{or}$  coefficient is small (-0.05 on N and -0.10 on O) so that the almost pure 2p bonding is affected only to a small extent.

The justification of chemical valence ideas by the results of the PLMO method is not exceptional or novel. All the LMO methods described in Chapter 2 achieve to a greater or lesser extent such a bridge between classical chemical ideas of valence and quantum mechanics. In particular, the results of the early work of Peters<sup>104-106</sup> show a clear resemblance to the overall orbital forms found here. The PLMOs however are without delocalised "tails" so that the concepts of two-centre bonds and one-centre lone pairs apply exactly. Once again, it should be emphasised that the PLMOs are not constrained to be orthogonal and are expressed in terms of HAOs which are not orthogonal among themselves on an atom.

The descriptions of the example molecules offered by the PLMOs are instructive in themselves, but a better understanding of these descriptions may be sought by a comparison to the results of other LMO methods. In particular the effect of the lack of orthogonality requirements in the PLMOs may be gauged by comparing the results with other LMO methods that have orthogonality restrictions of one sort or another.

#### 8.4(b) Comparison of PLMOs to LMOs Obtained by Other Methods

##### 8.4(b)(i) Forms of LMOs

The PLMOs and corresponding LMOs obtained by the methods of Magnasco & Perico,<sup>124,125</sup> Polak<sup>126,128</sup> and Roby<sup>132</sup> are shown in Tables 8.7 to 8.12.

In these tables the LMOs of the other authors have been expressed in the same format, co-ordinate system and STO basis set as the PLMOs (except for the 2s AO in Polak's work - see below). When equivalent LMOs occur (e.g.  $\mu_{OH}$  in  $H_2O$ ) only one example is shown.

TABLE 8.7 COMPARISON OF VALENCE SIGMA PLMOs OF HCN (STO-3G BASIS) to LMOs OF OTHER METHODS

(For explanation see narrative)

| LMO             | Author (a) | 1s <sub>H</sub> | 1s <sub>C</sub> | 2s <sup>or</sup> (b) <sub>C</sub> | 2p <sub>zC</sub> | 1s <sub>N</sub> | 2s <sup>or</sup> (b) <sub>N</sub> | 2p <sub>zN</sub> |
|-----------------|------------|-----------------|-----------------|-----------------------------------|------------------|-----------------|-----------------------------------|------------------|
| λ <sub>N</sub>  | This work  |                 |                 |                                   |                  |                 |                                   |                  |
|                 | M & P      | 0.0648          | -0.0249         | -0.1784                           | -0.1140          | 1.0530          | 0.9442                            | 0.3288           |
|                 | Polak      |                 |                 |                                   |                  | -               | 0.8653                            | 0.4899           |
| μ <sub>CH</sub> | This work  | 0.4729          | 0.6141          | 0.7388                            | -0.6711          |                 |                                   |                  |
|                 | M & P      | 0.4198          | 0.6459          | 0.7034                            | -0.7085          | 0.0055          | -0.0165                           | 0.0392           |
|                 | Polak      | 0.4280          | 0.6431          | 0.6948                            | -0.7192          |                 |                                   |                  |
| μ <sub>CN</sub> | This work  |                 |                 |                                   |                  |                 |                                   |                  |
|                 | M & P      | -0.0388         | 0.4965          | 0.7130                            | 0.7010           | 0.5729          | 0.4842                            | -0.8750          |
|                 | Polak      |                 | 0.5316          | 0.7192                            | 0.6948           | 0.5627          | 0.2861                            | -0.9582          |

(a) M & P - Magnasco & Perico, reference 125. (b) Symmetrically orthogonalised in Polak's LMOs  
Polak, reference 128.



TABLE 8.8 COMPARISON OF VALENCE SIGMA PLMOs OF CO (STO-3G BASIS) TO LMOs OF OTHER METHODS

(For explanation see narrative)

| LMO         | Author <sup>(a)</sup> | 1s <sub>C</sub> | 2s <sub>C</sub> <sup>or</sup> | 2p <sub>zC</sub> | 1s <sub>O</sub> | 2s <sub>O</sub> <sup>or</sup> | 2p <sub>zO</sub> |
|-------------|-----------------------|-----------------|-------------------------------|------------------|-----------------|-------------------------------|------------------|
| $\lambda_C$ | This work             | -0.0201         | 0.9227                        | -0.3851          |                 |                               |                  |
|             | M & P                 | ( 0.1048        | 0.8865                        | -0.4506)         | -0.0160         | -0.1120                       | 0.1176           |
|             | Roby                  | 0.0001          | 0.9255                        | -0.3787          |                 |                               |                  |
| $\lambda_O$ | This work             |                 |                               |                  | -0.0161         | 0.9642                        | 0.2647           |
|             | M & P                 | -0.0126         | -0.1078                       | -0.1263          | ( 0.1065        | 0.8584                        | 0.5018)          |
|             | Roby                  |                 |                               |                  | 0.0000          | 0.9629                        | 0.2697           |
| $\mu_{CO}$  | This work             | 0.4638          | 0.0688                        | 0.9863)          | 0.7486          | 0.0231                        | -0.9983)         |
|             | M & P                 | 0.3961          | 0.4638                        | 0.8854)          | 0.6889          | 0.5031                        | -0.8637)         |
|             | Roby                  | 0.4597          | 0.0701                        | 0.9888)          | 0.7565          | 0.0202                        | -0.9985)         |

(a) M &amp; P - Magnasco &amp; Perico, reference 124.

Roby, reference 132.

TABLE 8.9 COMPARISON OF VALENCE SIGMA PLMOs OF N<sub>2</sub> (STO-3G BASIS) TO LMOs OF OTHER METHODS

(For explanations see narrative)

| LMO                        | Author (a) | 1s <sub>N<sub>1</sub></sub> | 2s <sub>N<sub>1</sub></sub> <sup>or</sup> | 2p <sub>zN<sub>1</sub></sub> | 1s <sub>N<sub>2</sub></sub> | 2s <sub>N<sub>2</sub></sub> <sup>or</sup> | 2p <sub>zN<sub>2</sub></sub> |
|----------------------------|------------|-----------------------------|---|------------------------------|-----------------------------|---|------------------------------|
| λ <sub>N<sub>1</sub></sub> | This work  | -0.0181                     | 0.9386                                    | -0.3444                      |                             |   |                              |
|                            | M & P      | 1.0377 ( 0.1069             | 0.8681                                    | -0.4847)                     | - 0.0151                    | -0.1163                                   | 0.1311                       |
| μ <sub>NN</sub>            | This work  | 0.6122 (-0.0905             | 0.0408                                    | 0.9942)                      | 0.6122 (-0.0905             | 0.0408                                    | -0.9942)                     |
|                            | M & P      | 0.5388 ( 0.0035             | 0.4909                                    | 0.8712)                      | 0.5388 ( 0.0035             | 0.4909                                    | -0.8712)                     |

(a) M &amp; P - Magnasco &amp; Perico, reference 124.

TABLE 8.10 COMPARISON OF VALENCE SIGMA PLMOs OF H<sub>2</sub>O (STO-3G BASIS) TO LMOs OF OTHER METHODS  
(For explanation see narrative)

| LMO                         | Author (a) | 1s <sub>O</sub> | 2s <sub>O</sub> <sup>or</sup> (b) | 2p <sub>xO</sub> | 2p <sub>zO</sub> | 1s <sub>H<sub>1</sub></sub> | 1s <sub>H<sub>2</sub></sub> |
|-----------------------------|------------|-----------------|-----------------------------------|------------------|------------------|-----------------------------|-----------------------------|
| λ <sub>O</sub>              | This work  | -0.0212         | 0.9712                            | -                | 0.2375           |                             |                             |
|                             | M & P      | 1.0445          | ( 0.0926                          | -                | 0.6470)          | -0.1535                     | -0.1535                     |
|                             | Polak      | -               | 0.9768                            | -                | 0.2142           |                             |                             |
| μ <sub>OH<sub>1</sub></sub> | This work  | 0.6841          | (-0.0384                          | 0.6240           | -0.7735)         | 0.5382                      |                             |
|                             | M & P      | 0.6457          | ( 0.0479                          | 0.5944           | -0.5427)         | 0.5429                      | -0.2329                     |
|                             | Polak      | 0.6398          | ( -                               | 0.7071           | -0.6907)         | 0.5457                      |                             |

(a) M & P - Magnasco & Perico, reference 125. Polak, reference 128.

(b) Symmetrically orthogonalised in Polak's LMOs.

TABLE 8.11 COMPARISON OF VALENCE SIGMA PLMOs OF NH<sub>3</sub> (STO-3G BASIS) TO LMOs OF OTHER METHODS

(For explanation see narrative)

| LMO                         | Author (a) | 1s <sub>N</sub> | 2s <sub>N</sub> <sup>or(b)</sup> | 2p <sub>xN</sub> | 2p <sub>yN</sub> | 2p <sub>zN</sub> | 1s <sub>H<sub>1</sub></sub> | 1s <sub>H<sub>2</sub></sub> | 1s <sub>H<sub>3</sub></sub> |
|-----------------------------|------------|-----------------|----------------------------------|------------------|------------------|------------------|-----------------------------|-----------------------------|-----------------------------|
| λ <sub>N</sub>              | This work  | -0.0232         | 0.8347                           | -                | -                | 0.5501           |                             |                             |                             |
|                             | M & P      | 1.0185 (        | 0.4958                           | -                | -                | 0.8662)          |                             |                             |                             |
|                             | Polak      | -               | 0.7723                           | 0.0428           | 0.0002           | 0.6638           |                             |                             |                             |
| μ <sub>NH<sub>1</sub></sub> | This work  | 0.6450 (-       | 0.1729                           | 0.7397           | -                | -0.6492)         | 0.5100                      |                             |                             |
|                             | M & P      | 0.6355 (        | 0.5355                           | 0.8139           | -                | -0.2213)         | 0.5146                      | -0.0927                     | -0.0927                     |
|                             | Polak      | 0.6133 (        | 0.3393                           | 0.8158           | -                | -0.4686)         | 0.5115                      |                             |                             |

(a) M &amp; P - Magnasco &amp; Perico, reference 125.

Polak, reference 126.

(b) Symmetrically orthogonalised in Polak's LMOs.

TABLE 8.12 COMPARISON OF VALENCE SIGMA PLMOs FOR CH<sub>4</sub> (STO-3G BASIS) TO LMOs OF OTHER METHODS

(For explanation see narrative)

| LMO                   | Author (a) | 1s <sub>C</sub> | 2s <sub>C</sub> <sup>or(b)</sup> | 2p <sub>xC</sub> | 2p <sub>yC</sub> | 2p <sub>zC</sub> | 1s <sub>H<sub>1</sub></sub> | 1s <sub>H<sub>2</sub></sub> | 1s <sub>H<sub>3</sub></sub> | 1s <sub>H<sub>4</sub></sub> |
|-----------------------|------------|-----------------|----------------------------------|------------------|------------------|------------------|-----------------------------|-----------------------------|-----------------------------|-----------------------------|
| $\mu$ CH <sub>1</sub> | This work  | 0.5694          | (-0.0557                         | 0.5239           | 0.4909           | -0.4907          | 0.4907)                     | 0.5311                      |                             |                             |
|                       | M & P      | 0.6085          | ( 0.0437                         | 0.5318           | 0.4883           | -0.4883          | 0.4883)                     | 0.5062                      | -0.0638                     | -0.0638                     |
|                       | Polak      | 0.5881          | ( -                              | 0.5000           | 0.5000           | -0.5000          | 0.5000)                     | 0.5017                      |                             |                             |

(a) M & P - Magnasco & Perico, reference 125.  
Polak, reference 126.

(b) Symmetrically orthogonalised in Polak's LMOs.

It is generally accepted that the main reallocation LMO methods of Edmiston & Ruedenberg,<sup>83-85</sup> Boys<sup>71,72</sup> Von Niessen<sup>96-98</sup> and Magnasco & Perico yield similar LMOs.<sup>96-98,124,125,247,248</sup> The orthogonal LMOs obtained by Magnasco & Perico (M & P) by their "uniform localisation" criterion are therefore taken as an example of these methods. The results of M & P are chosen because all the molecules investigated by the PLMO method were also studied by M & P in a minimal STO basis while maintaining sigma-pi separability. For ease of comparison the M & P LMOs are shown with the 2s AO Schmidt-orthogonalised to the 1s AO in each case.

The most obvious aspect of the orthogonal M & P LMOs shown in the tables is that they are not perfectly localised. There are non-negligible orbital "tails" on secondary centres in every molecule. In the bond LMOs in water (Table 8.10) the secondary AO coefficients get as large as 0.2. The bond LMOs of M & P usually have similar polarity parameters to those of the PLMOs, but the hybridisations in the HAOs are generally quite different. The amount of hybridisation in the M & P results is usually higher than in the PLMOs. This is true in all the lone pairs and also in all the bonding hybrids except those on carbon in HCN and CH<sub>4</sub> (Tables 8.7 and 8.12) where hybridisation is also marked for the PLMOs.

Polak<sup>126,128</sup> obtains non-orthogonal "strictly localised orbitals" (SLOs) having contributions from one or two centres only that represent sigma lone pairs and bonds. The AO coefficients of the directed hybrids and the polarity parameters in the bonds are optimised so as to give the largest possible projection onto the Hartree-Fock manifold. For a comparison with other LMOs however,

two points should be noted. Firstly the 1s and 2s STOs in Polak's work have been symmetrically orthogonalised<sup>255</sup> and not Schmidt-orthogonalised. Since this procedure leads to well localised AOs<sup>83,114</sup> the inner shells are represented by the resulting pure 1s AOs and the valence hybrids contain only 2s and 2p AOs. Secondly, the hybrids on each atomic centre are constrained to be mutually orthogonal. The difference to the PLMO method contained in the first point is not expected to invalidate a comparison, since the penetration of 1s AO into the valence PLMOs was very low (Section 8.2). The second point may be utilised when contrasting the LMO results to gauge the effect of hybrid orthogonality.

The SLOs of HCN, H<sub>2</sub>O, NH<sub>3</sub> and CH<sub>4</sub> are shown in the Tables. A pattern does seem to emerge in those four examples available for comparison. It appears that while the polarities of the bond orbitals are similar, the hybridisation in the SLOs is often intermediate in character between the M & P LMOs and the PLMOs. Furthermore, it may be seen that a higher level of hybridisation than in the PLMOs, is imposed on the hybrids in the SLOs by virtue of their orthogonality at each atom. For example, in HCN (Table 8.7) the nitrogen lone pair SLO is little hybridised and is similar to the PLMO. In order to maintain hybrid orthogonality however, the bonding nitrogen hybrid in the  $\mu_{\text{CN}}$  SLO contains more 2s character than the corresponding PLMO hybrid, though not as much as the M & P LMO. (The hybrids on carbon in HCN have roughly equal 2s and 2p coefficients in the LMOs of all three methods). An analogous situation occurs in H<sub>2</sub>O (Table 8.10) where the lone pair SLO closely resembles the PLMO but to satisfy hybrid orthogonality, the bonding oxygen hybrid in the SLO contains a larger 2s coefficient than occurs in

the equivalent PLMO. In ammonia (Table 8.11) the extent of hybridisation in the SLOs of both the bonds and the lone pair (which does not apparently point exactly along the z axis) lies between that shown by the M & P LMOs and the PLMOs. In methane (Table 8.12) Polak's carbon hybrids are classically  $sp^3$  hybridised which corresponds to a slightly smaller 2s content than is found from the other two methods.

For carbon monoxide, non-orthogonal LMOs in a minimal STO basis have also been obtained by a projection operator technique by Roby.<sup>132</sup> These LMOs in Table 8.8 are shown with the 2s AO Schmidt-orthogonalised to the 1s STO.\* In this method the HAOs on each atom are not restricted to be mutually orthogonal. When Roby generates LMOs he searches for vectors in the occupied MO manifold having maximum projection onto the relevant one or two-centre subspaces. For CO he finds that the resulting inner shell and lone pair LMOs have complete projection on their particular atomic subspaces and therefore have no "tails". The CO bond occupies the complete MO manifold already. Thus Roby finds by his method what is revealed at least for the valence PLMOs in this work. That is, in CO (and  $N_2$ <sup>104</sup>) it is possible to generate completely localised MOs without tails in the CMO manifold (i.e. at the canonical energy) providing LMO and HAO orthogonality is not imposed.

It is not surprising then that the LMOs of Roby in Table 8.8 show a very close resemblance to the corresponding PLMOs. In fact the differences in the AO coefficients and polarity parameters are

---

\* The LMOs in Table 7 of reference 132 are not shown in terms of a Schmidt-orthogonalised  $2s^{0T}$  STO despite a reference in the text to that effect. This may be seen most easily by calculating the self-overlap integrals of the carbon and oxygen lone pairs from reference 132.



only generally manifest in the third decimal place.

In order to be able to gauge the effect of orthogonality requirements in these molecules, the values of the overlap integrals between valence HAOs are required. Absolute values for the overlap integrals between normalised valence HAOs on the same atom for the example molecules are shown in Table 8.13. Overlaps are exhibited for the hybrids in the PLMOs, the M & P LMOs and the LMOs of Roby. All such values are zero for the SLOs of Polak. The overlaps found in the PLMOs are all significantly greater than those in the M & P LMOs, except in methane where both sets of values are very small and in the bonding hybrids of water where the M & P HAOs have a large overlap. In fact, apart from the water molecule, the hybrids found by M & P on an atom are very nearly mutually orthogonal. The overlaps in CO found by Roby are almost identical with the PLMO results as is expected from the closeness of the orbital forms.

#### 8.4(b)(ii) Summary

From the discussion above it does seem that the orthogonality properties of the LMOs or HAOs do influence the LCAO form of the LMOs of the different methods. However, the effect of such mathematical constraints cannot be understood independently of the particular LMO method in question, rather, the orthogonality properties satisfied by LMOs or HAOs, and the way, in turn, that these constraints effect the orbital forms, are dependent on the way the LMOs are generated. The above remarks and discussion may be systematised therefore as follows.

The PLMOs and the LMOs of Roby show a similarity of form: non-orthogonal LMOs without "tails" are composed of non-orthogonal,

TABLE 8.13 ABSOLUTE VALUES OF OVERLAP INTEGRALS BETWEEN NORMALISED VALENCE HAOS ON THE SAME ATOM FOR THE EXAMPLE MOLECULES

| Molecule         | Integral (a) (b)  | This Work | M & P <sup>(c)</sup> | Roby <sup>(c)</sup> |
|------------------|---|-----------|----------------------|---------------------|
| HCN              | $\langle \lambda_{\text{N}}/h_{\text{N}(\text{C})} \rangle$         | 0.3679    | 0.0090               |                     |
|                  | $\langle h_{\text{C}(\text{H})}/h_{\text{C}(\text{N})} \rangle$     | 0.1031    | 0.0058               |                     |
| CO               | $\langle \lambda_{\text{C}}/h_{\text{C}(\text{O})} \rangle$         | 0.3133    | 0.0090               | 0.3096              |
|                  | $\langle \lambda_{\text{O}}/h_{\text{O}(\text{C})} \rangle$         | 0.2411    | 0.0018               | 0.2498              |
| N <sub>2</sub>   | $\langle \lambda_{\text{N}_1}/h_{\text{N}_1(\text{N}_2)} \rangle$   | 0.2601    | 0.0043               |                     |
| H <sub>2</sub> O | $\langle \lambda_{\text{O}}/h_{\text{O}(\text{H}_1)} \rangle$       | 0.2837    | 0.1010               |                     |
|                  | $\langle h_{\text{O}(\text{H}_1)}/h_{\text{O}(\text{H}_2)} \rangle$ | 0.2212    | 0.2934               |                     |
| NH <sub>3</sub>  | $\langle \lambda_{\text{N}}/h_{\text{N}(\text{H}_1)} \rangle$       | 0.2119    | 0.0765               |                     |
|                  | $\langle h_{\text{N}(\text{H}_1)}/h_{\text{N}(\text{H}_2)} \rangle$ | 0.1793    | 0.0064               |                     |
| CH <sub>4</sub>  | $\langle h_{\text{C}(\text{H}_1)}/h_{\text{C}(\text{H}_2)} \rangle$ | 0.0370    | 0.0463               |                     |

(a)  $\lambda_{\text{X}}$  - lone pair HAO on atom X.

$h_{\text{X}(\text{Y})}$  - bonding HAO on atom X, pointing to atom Y.

(b) For equivalent overlap integrals in N<sub>2</sub>, H<sub>2</sub>O, NH<sub>3</sub> and CH<sub>4</sub> only one example is shown.

(c) For references see Tables 8.7 to 8.12.

little hybridised HAOs with appreciable overlap integrals.

(A similar level of hybridisation and hybrid overlap is shown in the orthogonal LMOs of Peters.<sup>104,106</sup>)

Polak obtains non-orthogonal SLOs without "tails" (with a corresponding sacrifice in the accuracy of the molecular wavefunction) but imposes hybrid orthogonality at each atom, which forces greater hybridisation in some or all HAOs at that centre. (In fact removing such orthogonality constraints leads to a more accurate wavefunction but this yields HAOs in water with an overlap integral as high as 0.7.<sup>127</sup>)

In the M & P method (and in the other transformation methods of Edmiston & Ruedenberg and Boys) the LMO orthogonality imposed also yields very nearly orthogonal HAOs (in contrast to Peters method<sup>104,106</sup>), leading to orbital "tails" and a degree of hybridisation even greater than that of Polak. Even when the LMO orthogonality requirement is relaxed in these transformation methods, the LMO forms are hardly altered<sup>192</sup> and the LMO overlaps remain very small.<sup>189,192</sup>

The "condition of the atom in the molecule" [Section 3.2] revealed by the PLMO method can hence be understood in terms of the mathematical freedom allowed the PLMOs. The resulting condition consists of a significant amount of non-orthogonality among the HAOs (Table 8.13) and a corresponding low level of hybridisation in all but "internal" carbon hybrids.

#### 8.4(b)(iii) "Bent" bonds

The bonding hybrids in the PLMOs of water and ammonia were found not to point directly along the O-H or N-H internuclear lines

(Figures 8.1 and 8.2). Such "bent" bonds were discussed in Section 3.2 where it was concluded that the orthogonality properties of hybrids at an atomic centre seem to have little clear correlation with the appearance of "bent" bonds. This conclusion is borne out by Table 8.14 where the angles between bonding hybrids in water and ammonia are shown for some LMO methods. In all cases except one, the angles between hybrids are smaller than the angle between the corresponding internuclear axes.

This result is expected, and simply reflects the fact that in order to maintain molecular stability, electronic charge has to be accumulated in the binding regions in water and ammonia which lie between the nuclei.<sup>256</sup> In a theoretical treatment of bonding in the water molecule, Bader<sup>256</sup> suggests that in order to concentrate the maximum possible electronic charge in the binding region (and to place as little charge as possible in the strongly antibinding region) each bonding hybrid at oxygen should be directed about 15 or 20 degrees inside the internuclear axis (giving an overall hybrid angle of about 65-75 degrees) and that the oxygen sigma lone pair should be almost pure 2s AO in character. These properties are clearly exhibited by the PLMOs.

#### 8.4(c) Hybridisation Trends

As well as a description of individual molecules, chemistry is also concerned with the search for similarities and trends in "related" molecules. In this respect trends along groups or periods of the periodic table are often considered. If a LMO description of such a series of molecules is to truly be in chemical terms such trends should be apparent in the LMO-LCAO forms and in particular

TABLE 8.14 "BENT BONDS" IN WATER AND AMMONIA FROM DIFFERENT  
LMO METHODS

| Author                                   | Angle between bonding hybrids |                 | Orthogonality Properties <sup>(a)</sup> |              |
|--|-------------------------------|-----------------|---|--------------|
|  | H <sub>2</sub> O              | NH <sub>3</sub> | LMOs                                    | HAOs         |
| Duncan (1957) <sup>103</sup>             | -                             | 94°             | Orthog.                                 | Non-orthog.  |
| Peters (1963) <sup>106</sup>             | 69°                           | 83°             | Orthog.                                 | Non-orthog.  |
| Edmiston & Rudenberg(1966) <sup>85</sup> | 90°                           | 105°            | Orthog.                                 | Near-orthog. |
| Magnasco & Perico (1968) <sup>125</sup>  | 95°                           | -               | Orthog.                                 | Non-orthog.  |
| Magnasco & Perico (1968) <sup>125</sup>  | -                             | 113°            | Orthog.                                 | Near-orthog. |
| Petke & Whitten (1969) <sup>180</sup>    | 95°                           | 102°            | Non-Orthog.                             | Orthog.      |
| Polak (1970.72) <sup>126,128</sup>       | 91°                           | 97°             | Non-Orthog.                             | Orthog.      |
| Von Niessen (1973) <sup>98</sup>         | 93°                           | 100°            | Orthog.                                 | Near-orthog. |
| This work                                | 78°                           | 82°             | Non-Orthog.                             | Non-orthog.  |
| Angle between internuclear lines         | 104.5°                        | 107°            |   |              |

(a) A general guide to the size of the overlap integrals between the LMOs and between the HAOs in the different methods:

"Orthog." - Integrals are zero

"Near-Orthog." - Integrals about 0.05 or less

"Non-Orthog." - Integrals about 0.1 or more.

in the bond polarities, electron populations and HAO hybridisations. For the limited number of molecules tackled in this work, trends may be noted in the bonding and non-bonding hybrids found for the series carbon, nitrogen and oxygen. The PLMOs for the ten-electron hybrids methane, ammonia and water; and for the fourteen-electron diatomics CO and N<sub>2</sub> are to be considered. The relevant PLMOs, HAOs and populations are reproduced in Tables 8.15, 8.16 and 8.17.

The data for the bonds in CH<sub>4</sub>, NH<sub>3</sub> and H<sub>2</sub>O (Table 8.15), shows a gradation in going along the row of the periodic table. The weight of hydrogen in the bonds is approximately the same in all three cases but the weight of central atom, and hence bond polarity, increases from carbon to oxygen. This is also shown by the atomic populations. Hybridisation is only really marked for carbon in CH<sub>4</sub> where the hybrids have 27% 2s<sup>OR</sup> character. For nitrogen in ammonia this figure is 3% and for oxygen in water, one per cent. The carbon atom in methane is sp<sup>2.63</sup> hybridised, close to the classical sp<sup>3</sup>, while for nitrogen and oxygen in the other molecules it is the lone pairs in each case (Tables 8.10 and 8.11) and not the bonds that exploit the 2s<sup>OR</sup> AO.

The lone pairs in CO and N<sub>2</sub> (Table 8.16) are also predominantly 2s<sup>OR</sup> AO, but a gradual decrease in the slight 2p admixture in going from carbon to oxygen is also evident. This trend has its reflection in the hybrids found in the bonds in these molecules (Table 8.17) where the large 2p content increases slightly from carbon to oxygen.

The above trends may be summarised by noting that in going from carbon to oxygen, the lone pairs contain less and less 2p character and the bonding hybrids less and less 2s<sup>OR</sup> character. This gradation across the periodic table in bond polarities and atomic hybridisation

TABLE 8.15 COMPARISON OF BOND PLMOs IN CH<sub>4</sub>, NH<sub>3</sub> AND H<sub>2</sub>O

| Molecule         | PLMO            | 1s <sub>X</sub> | 2s <sub>X</sub> <sup>or</sup> | 2p <sub>xx</sub> | 2p <sub>yx</sub> | 2p <sub>zx</sub> <sup>(a)</sup> | 1s <sub>H</sub> | %2s <sup>or</sup> (b) | Atomic Populations |      |
|------------------|-----------------|-----------------|-------------------------------|------------------|------------------|---------------------------------|-----------------|-----------------------|--------------------|------|
|                  |                 |                 |                               |                  |                  |                                 |                 |                       | X                  | H    |
| CH <sub>4</sub>  | μ <sub>CH</sub> | 0.5694          | (-0.0557                      | 0.5239           | 0.4909           | 0.4909                          | 0.5311          | 27                    | 1.06               | 0.97 |
| NH <sub>3</sub>  | μ <sub>NH</sub> | 0.6450          | (-0.0389                      | 0.1729           | 0.7397           | -                               | 0.5100          | 3                     | 1.16               | 0.86 |
| H <sub>2</sub> O | μ <sub>OH</sub> | 0.6841          | (-0.0384                      | -0.1038          | 0.6240           | -                               | 0.5382          | 1                     | 1.18               | 0.83 |

TABLE 8.16 COMPARISON OF LONE PAIR PLMOs IN CO AND N<sub>2</sub>

| Molecule       | PLMO           | 1s <sub>X</sub> | 2s <sub>X</sub> <sup>or</sup> | 2p <sub>zx</sub> <sup>(a)</sup> | %2s <sup>or</sup> (b) |
|----------------|----------------|-----------------|-------------------------------|---------------------------------|-----------------------|
|                |                |                 |                               |                                 |                       |
| N <sub>2</sub> | λ <sub>N</sub> | -0.0818         | 0.9386                        | 0.3444                          | 88                    |
| CO             | λ <sub>O</sub> | -0.0161         | 0.9642                        | 0.2647                          | 93                    |

(a) The signs of the 2p<sub>z</sub> coefficients have been made the same in the different molecules.

(b) In a normalised valence HAO:

$$a(1s) + b(2s^{\text{or}}) + c(2p_x) + d(2p_y) + 2(2p_z)$$

the % 2s<sup>or</sup> character is 100b<sup>2</sup>

the % 2p character is 100(c<sup>2</sup> + d<sup>2</sup> + e<sup>2</sup>)

the % 1s character is negligible.

TABLE 8.17 COMPARISON OF BONDING HAOs IN CO AND N<sub>2</sub>

| Molecule       | HAO (c)                                   | 1s <sub>X</sub> | 2s <sub>X</sub> <sup>or</sup> | 2p <sub>ZX</sub> <sup>(a)</sup> | %2p <sup>(b)</sup> |
|----------------|---|-----------------|-------------------------------|---------------------------------|--------------------|
| CO             | h <sub>C(O)</sub>                         | -0.1496         | 0.0688                        | 0.9863                          | 97                 |
| N <sub>2</sub> | h <sub>N<sub>1</sub>(N<sub>2</sub>)</sub> | -0.0905         | 0.0408                        | 0.9942                          | 99                 |
| CO             | h <sub>O(C)</sub>                         | -0.0553         | 0.0231                        | 0.9982                          | 100                |

(a) The signs of the 2p<sub>z</sub> coefficients have been made the same in the different molecules.

(b) In a normalised valence HAO:  $a(1s) + b(2s^{\text{or}}) + c(2p_x) + d(2p_x) + e(2p_z)$   
 the %2s<sup>or</sup> character is  $100b^2$   
 the %2p character is  $100(c^2 + d^2 + e^2)$   
 the %1s character is negligible.

(c) h<sub>X(Y)</sub> - bonding HAO on atom X, pointing to atom Y.



is familiar. The level of hybridisation is usually expected<sup>214,257</sup> to be greater for elements on the left of the first row of the periodic table in view of the trend in the relative separation of 2s and 2p energy levels.<sup>258</sup> Such trends are noted in HAOs having appreciable non-orthogonality by Roby in CO<sup>132</sup> and by Peters<sup>104,106</sup> in all the example hybrids of Tables 8.15, 8.16 and 8.17 and also in the diatomic hydrides of the 1st row.

A different method for systematising the different degrees of hybridisation in simple molecules has been introduced by Edmiston & Ruedenberg.<sup>84</sup> To each atom in a molecule is assigned a value of "Population Ratio" which is defined as "the ratio obtained by dividing the total number of bonding electrons of the neutral atom in the particular valence situation by the total number of its lone pair electrons." This definition has more recently been slightly modified by Aufderheide<sup>259</sup> so that the ratio ranges from 0 to 1 rather than 0 to infinity. Using this method, based on an earlier analysis of Ruedenberg et al,<sup>260,261</sup> as the Population Ratio (PR) increases, the s character of the bonding hybrids at an atom and the p character of lone pair hybrids at an atom should also increase.<sup>84,259</sup> The reverse trends should be observed as PR decreases along a series of atoms in molecules. To adequately explain the observed hybridisations by PR however, a description in terms of mutually orthogonal (or nearly orthogonal) HAOs at each centre is necessary. In this way, trends exhibited by the LMOs of Edmiston & Ruedenberg<sup>84,85</sup> Boys<sup>98</sup> and Von Niessen<sup>98</sup> and by the exactly orthogonal HAOs of Ruedenberg,<sup>260,261</sup> Aufderheide<sup>181,182,259</sup> and Rives & Weinhold<sup>188</sup> are those expected from the PR of the atom in the molecule.

The Population Ratio of the 1st row atoms decreases going from left to right across the periodic table in methane, ammonia and water and also in the series of diatomic hydrides LiH to FH; hence the same trends are observed in these molecules by the PLMOs and the LMOs of Peters<sup>104,106</sup> as are shown by the methods involving orthogonal HAOs. In CO and N<sub>2</sub> however, the PR of each atom increases from carbon to oxygen and therefore the trends in the PLMOs, and the LMOs of Peters<sup>104</sup> and Roby<sup>132</sup> are completely the reverse in both the bonding and lone pair hybrids, of those found by Magnasco & Perico (Tables 8.8 and 8.9), Edmiston and Ruedenberg<sup>84</sup> and Rives & Weinhold<sup>188</sup> etc.

Although the appearance of a greater degree of hybridisation at oxygen than at carbon in CO might seem somewhat surprising in classical terms,<sup>262</sup> the PR method clearly has a firm foundation. The method has been used extensively to order and explain the degree of hybridisation in many simple polyatomic molecules.<sup>259</sup> Rather than describing different patterns of electronic organisation, the results of the PLMO method and the Edmiston & Ruedenberg method for example, may be explained by the differences in the orthogonality properties of the constituent HAOs. It was noted in section 8.4(b) that the occurrence of nearly orthogonal hybrids in the Edmiston & Ruedenberg and similar transformation methods is a particular property of these methods. That these properties of HAOs are necessary for a description using the PR formalism is supported by the fact that in the Magnasco & Perico LMOs for CH<sub>4</sub>, NH<sub>3</sub> and H<sub>2</sub>O (Tables 8.12, 8.11 and 8.10) the gradation in hybridisation in the bonds is the reverse of that expected by the PR calculation. It is in just this series of molecules that the HAOs depart further and further from orthogonality (Table 8.13).

The trends in bond polarity (which are shared by all the other LMO methods mentioned) and in hybridisation found in the PLMOs in Tables 8.15, 8.16 and 8.17, hence reinforce the self-consistency already noted in the PLMO results. This pattern is also clearly dependent on the "condition of the atom in the molecule" revealed by the PLMO method and in particular the non-orthogonality of the constituent HAOs.

#### 8.4(d) PLMO Overlap Integrals

The non-orthogonality of the PLMOs and constituent HAOs has been referred to repeatedly in the present section. In fact, unlike the hybrid AOs, the PLMOs are not far from orthogonal, as is demonstrated by the small value of  $\Delta$  for each molecule (Section 8.3(b)). This was one of the desired properties of the PLMOs (Section 1.3(b)). No linear dependence problems were therefore encountered with the PLMOs of any molecule, though some high energy structures failed to yield an energy minimum for this reason. The effect of this near orthogonality on the decomposition of the total dipole moment into PLMO contributions is shown in the next chapter.

It was mentioned in Chapter one that the inherent (irremovable) delocalisation of electrons in a molecule means that restricting LMOs to be perfectly localised usually leads to LMO non-orthogonality and/or introduces inaccuracies into the molecular wavefunction. The PLMO overlap integrals are therefore related to the delocalisation of electrons out of two-centre bonds and one-centre lone pairs. This may be seen from the fact that the large intra-atomic HAO overlap integrals (Table 8.13) bear no relationship to the overlap integrals between valence PLMOs formed from such hybrids (Tables

4.7, 5.16 to 5.20). The valence PLMO overlaps are hence connected to the small electron delocalisations - in the orthogonal MO Hartree-Fock manifold expressed as orbital "tails" - residing on secondary atomic centres that have been deleted from orthogonal LMOs,  $\phi^R$  in the PLMO method at the truncation stage (Section 4.3(d)). Non-negligible overlap integrals therefore arise between PLMOs in which one LMO contained an orbital "tail" on an atom contained in the other LMO before truncation. Similarly, near zero PLMO overlap integrals arise from LMOs that had little or no "tails" on relevant secondary atomic centres before truncation. In this way, the characteristics of the wavefunctions composed of the orthogonally transformed MOs of the example molecules,  $\phi^R$ , before removal of LMO "tails", can be gauged from the final PLMO overlap integrals.

The values of the PLMO overlaps in the example molecules were discussed in Section 8.3. There it was noted that the non-negligible overlap integrals occurred between two or more adjacent bonds, or, in CO and N<sub>2</sub>, between the two lone pairs on different atoms. The lone pairs in all the molecules were found to be very nearly orthogonal to adjoining bonds however.

Thus, apart from the diatomic molecules in which only the lone pairs are able to delocalise, a characteristic pattern emerges from the above description. This is one in which the untruncated lone pair LMOs have little or no tails, but the bond LMOs have non-negligible tails. Therefore it seems that the orthogonally transformed LMO wavefunction is in a form most energetically near to that of one and two-centre PLMOs when the lone pairs are almost completely localised onto their atomic centre but the bond LMOs are delocalised.

This result is in contrast to the type of wavefunction that emerges from the orthogonal transformation methods of Edmiston & Ruedenberg<sup>83-85</sup> and Boys,<sup>71,72</sup> where in general the lone pair LMOs, for all but halogen atoms, are more delocalised than the bond LMOs.<sup>43,76,93,263-265</sup> Such a result is in agreement however, with the wavefunctions generated by the method of Peters<sup>104,106</sup> and by other intuitive "cut-off" criteria (see Section 2.2(c)) where the localisation transformation of the CMOs is usually fixed by the requirement that the lone pair LMOs have no delocalisation tails. In view of this contrast, it is not surprising that in the molecules studied, the overall PLMO forms are similar to the primary contributions to Peters orthogonal LMOs but are at variance to the other transformation methods (Sections 8.4(b) and 8.4(c)).

In CO and N<sub>2</sub> the link between PLMO overlaps, electron delocalisation and "cut-off" localising criteria is even more apparent. In these molecules, truncation of the molecular wavefunction to give the PLMOs does not lead to an energy sacrifice and hence all the inherent electron delocalisation at the Hartree-Fock level is expressed in the PLMO overlap integrals. For CO, Peters demonstrates<sup>104</sup> that it is possible to apply orthogonal transformations to the CMOs such that a lone pair LMO at one centre is completely localised, but that it is necessary for the lone pair LMO at the other centre to be delocalised. There are hence two possible sets of LMOs corresponding to the two possible "cut-off" criteria. As mentioned by Peters<sup>104</sup>, shown by Roby<sup>132</sup> and demonstrated by the PLMOs for both CO and N<sub>2</sub>; it is only necessary to allow the lone pair LMOs to become non-orthogonal to each other and the delocalisation tails may be deleted completely with no sacrifice in the accuracy of the wavefunction.

The description of the electronic structure of the example molecules by a molecular wavefunction constructed from PLMOs hence depends in a methodical way on the non-orthogonality of the PLMOs.

## CHAPTER NINE

### BOND AND LONE PAIR MOMENTS

The electric dipole moments of the molecules studied and the division of the totals into PLMO bond and lone pair contributions were set out in Chapter 6. Although these bond and lone pair moments are not directly observable they can nevertheless serve as an aid in the understanding of the structure of molecules in chemistry where the properties of any given molecule are invariably broken down into the properties of its constituent parts. Specific examples of the usefulness of these moments were given in Chapter 6. In this chapter the results will be analysed and interpreted and some conclusions drawn.

#### 9.1 TOTAL DIPOLE MOMENTS AND PLMO COMPONENTS

The total dipole moments calculated from the canonical wavefunction of Gaussian 70, from the PLMO wavefunction, and the experimental<sup>235</sup> values are shown in Table 9.1. The dipoles of nitrogen and methane are necessarily zero by symmetry.

Calculations carried out in a minimal Slater AO basis (including the STO-kG type basis) are generally expected to underestimate the total dipole.<sup>266</sup> This characteristic is revealed in HCN and H<sub>2</sub>O. In NH<sub>3</sub> the dipole is overestimated however and in CO the small experimental moment is quite well reproduced. Ammonia proves to be a genuine exception to the general rule since a moment close to that found from Gaussian 70 was obtained in the original STO-kG work of Hehre, Stewart and Pople.<sup>223</sup> The agreement between theory and experiment in CO, whilst pleasing, is probably fortuitous. Truncation of the LMOs to give the PLMOs leads to an increase in the

TABLE 9.1 NON-ZERO TOTAL DIPOLE MOMENTS OF THE EXAMPLE MOLECULES (STO-3G BASIS) (a) (b)

| Molecule         | CMO Wavefunction | PLMO Wavefunction | Experimental <sup>235</sup>           |
|------------------|------------------|-------------------|---------------------------------------|
| HCN              | 2.45             | 2.50              | 2.95 (N <sup>-</sup> H <sup>+</sup> ) |
| CO               | 0.17             | 0.17              | 0.13 (C <sup>-</sup> O <sup>+</sup> ) |
| H <sub>2</sub> O | 1.73             | 1.74              | 1.82 (O <sup>-</sup> H <sup>+</sup> ) |
| NH <sub>3</sub>  | 1.76             | 2.03              | 1.47 (N <sup>-</sup> H <sup>+</sup> ) |

a) All units in Debyes

b) The polarity of the total dipole is the same as that shown experimentally in each case.



total dipole in all cases except CO, where the CMO and PLMO wavefunctions are identical. The difference between the CMO and PLMO dipole moments is only substantial in ammonia which also had the largest energy sacrifice in the PLMO wavefunction (Chapter 7). Why an increase in total dipole moment is obtained when the LMOs are truncated is not clear, although the same effect is found with Boys LMOs<sup>72</sup> in a series of carbocyclic compounds<sup>43</sup> and also in the individual Edmiston & Ruedenberg LMOs<sup>70,83-85</sup> in a series of molecules.<sup>93</sup>

It is shown in Appendix I (and Chapter 6) that for non-orthogonal LMOs the electronic contribution to the total dipole moment is made up of "diagonal" terms arising from each LMO, and "off-diagonal" terms arising from the overlap between LMOs (equation 6.3). In Chapter 1 it was hoped that the off-diagonal terms would be relatively small so that the physical interpretation of the PLMO moments, after re-allocation of the off-diagonal terms, would be straightforward. The figures to show that this is indeed the case are exhibited in Tables 9.2 and 9.3. In Table 9.2 the contributions to the total dipole moments, collated from the tables of Chapter 6, are featured. It can be seen firstly that the total dipole is usually the difference of two much larger numbers, the electronic and nuclear components. Secondly, the electronic component is almost entirely composed of the diagonal terms, the off-diagonal terms generally being small by comparison. However, by collecting the PLMO terms of Chapter 6 together in Table 9.2 some cancellation of terms of opposite sign has occurred. This is most obvious in CH<sub>4</sub> where the origin of co-ordinates is at the centre of symmetry.

TABLE 9.2 CONTRIBUTIONS TO THE TOTAL DIPOLE MOMENTS OF THE PLMO WAVEFUNCTIONS OF THE EXAMPLE MOLECULES  
(STO-3G BASIS) (a) (b)

| Molecule                       | Diagonal<br>Electronic | Off-Diagonal<br>Electronic | Total<br>Electronic | Nuclear | Total |
|--------------------------------|------------------------|----------------------------|---------------------|---------|-------|
| HCN                            | -36.14                 | -0.01                      | -36.15              | 33.64   | -2.50 |
| CO                             | -43.44                 | 0.26                       | -43.18              | 43.35   | 0.17  |
| N <sub>2</sub>                 | -37.16                 | 0.26                       | -36.90              | 36.90   | 0.00  |
| H <sub>2</sub> O (z component) | 4.31                   | -0.43                      | 3.88                | -5.63   | -1.74 |
| NH <sub>3</sub> (z component)  | 4.56                   | -1.25                      | 3.31                | -5.34   | -2.03 |
| CH <sub>4</sub> (z component)  | 0.00                   | 0.00                       | 0.00                | 0.00    | 0.00  |

a) All units in Debyes

b) The sign convention is the same as that used in Chapter 6

TABLE 9.3 SUM OF ABSOLUTE VALUES OF DIAGONAL AND OFF-DIAGONAL ELECTRONIC CONTRIBUTIONS TO THE DIPOLE MOMENTS OF THE PLMO WAVEFUNCTIONS OF THE EXAMPLE MOLECULES (STO-3G BASIS) (a)

| Molecule                       | Diagonal Electronic | Off-Diagonal Electronic | Off-Diagonal as a Percentage of Diagonal |
|--------------------------------|---------------------|-------------------------|--|
| HCN                            | 49.84               | 0.07                    | 0.13                                     |
| CO                             | 49.68               | 0.26                    | 0.53                                     |
| N <sub>2</sub>                 | 42.18               | 0.26                    | 0.62                                     |
| H <sub>2</sub> O (z component) | 7.34                | 0.43                    | 5.79                                     |
| NH <sub>3</sub> (z component)  | 11.54               | 1.25                    | 10.81                                    |
| CH <sub>4</sub> (z component)  | 17.53               | 0.80                    | 4.54                                     |

(a) All units in Debyes

For this reason, and to show the relative sizes of diagonal and off-diagonal contributions more clearly, the absolute sum of these terms together with their ratio expressed as a percentage are produced in Table 9.3. Only in ammonia do the off-diagonal terms contribute 10% of the diagonal terms. In water and methane the figure is about 5%, and in the other molecules it is less than 1%. Clearly, it is generally safe to assign the calculated PLMO moments to specific bonds and lone pairs.

The individual bond and lone pair moments found in Chapter 6 have been shown in diagrammatic form in Figures 6.1 to 6.6. Several points can be made about them. Taking the lone pair moments first it can be seen that they are generally larger than the bond moments. The lone pair moments lie in the range 1.60D (oxygen in H<sub>2</sub>O) to 3.55D (nitrogen in NH<sub>3</sub>) which is comparable to the largest total dipole moment of these molecules. The lone pair moments are due entirely to the hybridisation dipole resulting from the admixture of 2p atomic orbital with the 2s<sup>OR</sup> AO which directs the electron density in the lone pair away from the rest of the molecule in each case. The nature of the atom bearing a lone pair sensibly effects the value of the dipole moment. In going from carbon to nitrogen to oxygen we see a gradual reduction in the moment in line with the electronegativity of the atom concerned. The values are 3.25D ( $\lambda_C$  in CO); 2.64D ( $\lambda_N$  in N<sub>2</sub>) and 2.38D ( $\lambda_N$  in HCN); 1.81D ( $\lambda_O$  in CO) and 1.60D ( $\lambda_O$  in H<sub>2</sub>O). The nitrogen lone pair in ammonia is anomalous, but this high value of 3.55D is also found by other workers (see next subsection) and reflects the basic nature of ammonia.

Referring now to the sigma bond moments, these vary from 0.24D ( $\mu_{\text{OH}}$  in water) to 2.01D ( $\mu_{\text{CH}}$  in methane). As expected there is no general connection between the bond moments and the bond polarities (populations) already noted. Bond moments opposite in direction to that expected from the PLMO polarities are found in  $\mu_{\text{CH}}$  (HCN,  $\text{CH}_4$ ) and  $\mu_{\text{NH}}$  ( $\text{NH}_3$ ) for example. This is due to the fact that each bond moment has contributions from the hybridisation dipoles of the two atoms joined by the bond and also a homopolar dipole arising from non-symmetric overlap of the two atomic hybrids, besides the charge dipole due to the slight positive and negative charges on the bonding atoms. As already mentioned, the bond moments in water and ammonia do not point directly along the internuclear lines but diverge by  $20^\circ$  and  $23^\circ$  respectively. This reflects the fact that the centroid of electron charge is forced off the internuclear line by the "bent" bonds found in these molecules.

The  $\pi$  bond moments in HCN and CO are of roughly the same magnitude but are of opposite direction relative to the carbon atoms. This is in line with the  $\pi$  atomic charges (Tables 8.1 and 8.2) although the unusual partitioning of nuclear charge in  $\pi_{\text{CO}}$  should be noted.

The total molecular dipole has thus been broken down into bond and lone pair contributions insofar as these are adequately represented by the non-orthogonal PLMOs. Since these moments may not be directly compared to experimental quantities the acceptability of these results will be measured by a comparison to the bond and lone pair moments obtained by other workers.

## 9.2 COMPARISON TO OTHER AUTHORS

Bond and lone pair moments from LMOs are reported in the literature for many molecules using many different LMO methods. An alternative approach is to calculate bond moments from dipole moment derivatives with respect to symmetry co-ordinates obtained from infra-red spectroscopic data.<sup>237-240</sup> The results of the two approaches are not generally closely matched since while an LMO method assigns static moments to distinct bonds and lone pairs, bond moments from infra-red intensity data contain factors arising from the mutual interaction of different bonds and lone pairs during vibration.<sup>271,275-277</sup> Thus the PLMO moments must be compared to the bond and lone pair moments of other LMO methods.

The bond and lone pair moments obtained for all the molecules studied (except  $N_2$  for which no comparison can be found) in this work and selected other works are shown in Tables 9.4 to 9.8. The inner shell contributions, which are in any case normally very small, have been neglected in all instances. The sign convention for the moments are the same as in Chapter 6 and, where necessary, the conventions used in other works have been changed accordingly. For ease of comparison only the z component of the bond moments are shown in water and ammonia. No allowance has been made for different molecular geometries employed by various authors but the difference is small and certainly not large enough to effect any conclusions drawn.

A large variety of levels of approximation, basis functions and localisation criteria are exhibited in the tables and it is clear from only a brief study that the PLMO moments found in Chapter 6

TABLE 9.4 COMPARISON OF PLMO BOND AND LONE PAIR MOMENTS OF HCN TO THOSE OF OTHER METHODS (a) (b)  
 (For explanation see narrative)

| Author                     | $D_{CH}$ | $D_{CN}$ (c) | $D_N$ | Total | Basis/Wavefunction                         | Localising Criterion                  |
|----------------------------|----------|--------------|-------|-------|--|---------------------------------------|
| This work                  | 1.74     | -1.85        | -2.38 | -2.50 | Minimal STO-3G                             | See Chapter 4                         |
|                            | 1.74     | -1.87        | -2.37 | -2.52 | Minimal STO-5G                             | See Chapter 4                         |
|                            | 1.74     | -1.86        | -2.38 | -2.51 | Minimal STO-3G<br>(inner shells truncated) | See Chapter 4                         |
| Newton et al <sup>93</sup> | 1.60     | -0.54        | -3.22 | -2.14 | Minimal STO                                | Edmiston & Ruedenberg<br>70, 83-85    |
| Gey et al <sup>170</sup>   | 1.64     | -0.54        | -3.38 | -2.48 | Minimal STO (LMO<br>"tails" deleted)       | Edmiston & Ruedenberg<br>70, 83-85    |
|                            | 1.40     | -0.68        | -2.83 | -2.11 | Minimal STO                                | Maximum Hybrid Overlap <sup>169</sup> |

a) All units in Debyes

b)  $D_X$  - lone pair moment of atom X.

$D_{XY}$  - bond moment between atoms X and Y.

c) Combined  $\sigma$  and  $\pi$  moment.

(a) (b)

TABLE 9.5 COMPARISON OF PLMO BOND AND LONE PAIR MOMENTS OF CO TO THOSE OF OTHER METHODS

(For explanation see narrative)

| Author                    | $D_O$ | $D_C$ | $D_{CO}(c)$ | Total | Basis/Wavefunction   | Localising Criterion                       |
|---------------------------|-------|-------|-------------|-------|----------------------|--|
| This work                 | 1.81  | -3.25 | 1.27        | -0.17 | Minimal STO-3G       | See Chapter 4                              |
| Peters <sup>105</sup>     | 2.13  | -3.26 | -0.16       | -1.29 | Valence STO          | $\lambda_C$ free from oxygen AOs           |
| Robb et al <sup>267</sup> | 1.67  | -3.31 | 1.04        | -0.60 | Valence STO          | $\lambda_O$ free from carbon AOs           |
|                           | 2.92  | -4.00 | 1.49        | 0.41  | Large Gaussian basis | Edmiston & Ruedenberg <sup>70, 83-85</sup> |

a) All units in Debyes

b)  $D_X$  - lone pair moment of atom X. $D_{XY}$  - bond moment between atoms X and Y.c) Combined  $\sigma$  and  $\pi$  moment.



TABLE 9.6 COMPARISON OF PLMO BOND AND LONE PAIR MOMENTS OF H<sub>2</sub>O TO THOSE OF OTHER METHODS (a) (b)

(For explanation see narrative)

| Author                          | D <sub>O</sub> (c) (d) | D <sub>OH</sub> (c) | Total | Basis/Wavefunction           | Localising Criterion   |
|---------------------------------|------------------------|---------------------|-------|------------------------------|--|
| This work                       | -1.60                  | -0.07               | -1.74 | Minimal STO-3G               | See Chapter 4  |
| Pople <sup>100</sup>            | -1.67                  | 0.09                | -1.51 | Minimal STO                  | $\lambda_O$ free from 1s <sub>H</sub> AOs                              |
| Ellison & Shull <sup>101</sup>  | -1.69                  | 0.09                | -1.52 | Minimal STO                  | " " " "  |
| Duncan & Pople <sup>117</sup>   | -3.03                  | 0.60                | -1.84 | Valence STO                  | LMOs matched to exptl. dipole. Bonding Oxygen HAOs point to hydrogens. |
| Amos et al <sup>268</sup>       | -3.40                  | 0.43                | -2.54 | Floating spherical Gaussians | Von Niessen <sup>96-98</sup>   |
| Kapuy & Kozmutza <sup>269</sup> | -2.88                  | 0.73                | -1.43 | Minimal STO                  | Edmiston & Ruedenberg <sup>70,83-85</sup>                              |
| Peters <sup>105</sup>           | -3.18                  | 0.27                | -2.64 | Contracted Gaussian          | Edmiston & Ruedenberg <sup>70,83-85</sup>                              |
|                                 | -3.20                  | 0.48                | -1.76 | Valence STO                  | Bonding oxygen HAOs point to hydrogens                                 |
|                                 | -1.69                  | 0.09                | -1.52 | Valence STO                  | $\lambda_O$ free from 1s <sub>H</sub> AOs.                             |

a) All units in Debyes

b) D<sub>X</sub> - lone pair moment of atom X.

D<sub>XY</sub> - bond moment between atoms X and Y

c) z component of moment

d) combined moment of both lone pairs.

TABLE 9.7 COMPARISON OF PLMO BOND AND LONE PAIR MOMENTS OF NH<sub>3</sub> TO THOSE OF OTHER METHODS (a) (b)

(For explanation see narrative)

| Author                                | D <sub>N</sub> (c) | D <sub>NH</sub> (c) | Total | Basis/Wavefunction           | Localising Criterion                         |
|---------------------------------------|--------------------|---------------------|-------|------------------------------|--|
| This work                             | -3.55              | 0.51                | -2.03 | Minimal STO-3G               | See Chapter 4.                               |
| Peters <sup>106</sup>                 | -3.52              | 0.43                | -2.24 | Valence STO                  | Bonding nitrogen HAOs point to hydrogens.    |
|                                       | -3.56              | 0.42                | -2.30 | Valence HFAO                 | " " "  |
| Robb et al <sup>267</sup>             | -3.41              | 0.21                | -2.78 | Valence HFAO                 | λ <sub>N</sub> free from 1s <sub>H</sub> AOs |
| Amos et al <sup>268</sup>             | -3.53              | 0.39                | -2.36 | Large gaussian basis         | Edmiston & Ruedenberg 70, 83-85              |
|                                       | -3.93              | 0.53                | -2.34 | Floating spherical gaussians | Von Niessen 96-98                            |
| Figeys et al <sup>270</sup>           | -3.32              | 0.61                | -1.49 | Minimal STO                  | Edmiston & Ruedenberg 70, 83-85              |
| Gey et al <sup>170</sup>              | -3.33              | 0.52                | -1.79 | Minimal STO-3G               | Edmiston & Ruedenberg 70, 83-85              |
| Smit & Van Dam <sup>273</sup>         | -3.66              | 0.63                | -1.76 | Minimal STO                  | Maximum Hybrid overlap <sup>169</sup>        |
| Schmeidekamp <sup>274</sup><br>et al. | -2.74              | 0.35                | -1.69 | Contracted gaussian basis    | Magnasco & Perico <sup>124, 125</sup>        |
|                                       | -3.64              | 0.56                | -1.95 | Contracted gaussian basis    | Boys <sup>71, 72</sup>                       |

a) All units in Debyes

b) D<sub>X</sub> - lone pair moment of atom X.

D<sub>XY</sub> - bond moment between atoms X and Y.

c) z component of moment.

TABLE 9.8 COMPARISON OF PLMO BOND MOMENTS OF CH<sub>4</sub> TO THOSE OF OTHER METHODS (a) (b)

(For explanation see narrative)

| Author                     | D <sub>CH</sub> | Basis/Wavefunction                | Localising Criterion                      |
|----------------------------|-----------------|-----------------------------------|---|
| This work                  | 2.01            | Minimal STO-3G                    | See Chapter 4                             |
| Peters <sup>150</sup>      | 1.67            | Minimal STO (CH LMOs truncated)   | (Direct determination of LMOs             |
| Newton et al <sup>93</sup> | 1.89            | Minimal STO (CH LMOs delocalised) | (by eigenvalue equation                   |
|                            | 2.02            | Minimal STO                       | Edmiston & Ruedenberg <sup>70,83-85</sup> |
| Amos et al <sup>268</sup>  | 2.06            | Minimal STO (LMO "tails" deleted) | Edmiston & Ruedenberg <sup>70,83-85</sup> |
|                            | 2.08            | Floating spherical gaussians      | Von Niessen <sup>96-98</sup>              |
| Burke et al <sup>248</sup> | 2.02            | Minimal STO                       | Edmiston & Ruedenberg <sup>70,83-85</sup> |
|                            | 1.93            | Minimal STO-3G                    | Boys <sup>71,72</sup>                     |
|                            | 1.78            | Extended 4-31G                    | Boys <sup>71,72</sup>                     |
| Gey et al <sup>170</sup>   | 1.67            | Contracted gaussian "double zeta" | Boys <sup>71,72</sup>                     |
|                            | 1.84            | Minimal STO                       | Maximum Hybrid Overlap <sup>169</sup>     |

a) All units in Debyes

b) D<sub>XY</sub> - bond moment between atoms X and Y.

are quite comparable to those obtained by other methods, despite a large variation in the total molecular dipole moment predicted in many cases.

Probably the largest discrepancy in the LMO moments occurs in the carbon-nitrogen bonds in HCN (Table 9.4). The value obtained for the sigma and pi PLMO moments combined is clearly greater than that found by Gey et al, and also greater than that found in the combined "banana" bonds of the Edmiston & Ruedenberg procedure. This is compensated for in that procedure by the higher moment found in the nitrogen lone pair in line with the higher degree of hybridisation already noted in the Edmiston & Ruedenberg method (Chapter 8) so that, in the truncated case at least, a similar total dipole is obtained. The  $\mu_{\text{CH}}$  moments are similar in all examples.

In CO (Table 9.5) the Edmiston & Ruedenberg criterion again gives larger lone pair moments but here the carbon-oxygen "banana" bonds yield a moment similar in magnitude to the PLMOs. The two alternative localisation "routes" employed by Peters both yield lone pair moments more in line with the PLMOs although  $D_{\text{CO}}$  varies widely giving different totals.

In Table 9.6 to aid comparison to the PLMOs the combined lone pair moments are shown in cases where two equivalent oxygen lone pairs are generated by the particular method used. Despite the large variation in total dipole moment for water (1.4-2.6D) two distinct values for the lone pair moment are discernable in the various methods. The first value is in the range 1.6-1.7D is accompanied by a z component in the bonds of around zero, and apparently occurs in methods where the localising criterion is such that the lone pairs have no "tails". The second value is in the

range 2.9-3.4D, is accompanied by a bond component in the range 0.3-0.7D and seems to occur in instances where the localisation criterion either generates slightly delocalised lone pairs and/or demands that the oxygen hybrids point directly along the O-H internuclear line. This is neatly exemplified by the results from the two different criteria employed by Peters. The distinction between the molecular wavefunctions generated on the one hand both by the PLMO method and by "cut-off" methods requiring that lone pairs have no "tails", and on the other hand by transformation methods yielding delocalised lone pairs has already been noted in Section 8.4(d). The different values of the total lone pair moment in these cases could be seen as evidence of this.

Similar features are not displayed in the examples of ammonia however (Table 9.7). In fact the degree of agreement in the LMO moments across the different methods is quite remarkable. The LMO moment ranges are:  $D_N$  (except Smit & Van Dam) 3.3-3.9D and  $D_{NH}$  0.2-0.6D. The PLMO moments lie near the middle of the range in each case.

The total dipole moment of methane (Table 9.8) is always zero by symmetry, and there is again a large measure of agreement among the different LMO methods on the value of the bond moment. The values in Table 9.8 lie in the range 1.7-2.1D which clearly includes the PLMO value of 2.0D. This value of the C-H bond moment is found in LMO analyses of many different molecules and basis sets<sup>272</sup> but is in disagreement with a value of about 0.4D obtained in early work by Coulson<sup>57</sup> and in much spectroscopic and empirical work. This disparity is well known and has been discussed in the literature.<sup>193,194,271</sup> Apart from the inaccurate early wavefunction

of Coulson, the difference between LMO C-H moments and those obtained from other methods is probably one of definition.

To summarise then, the conclusion that emerges from the present study of bond and lone pair LMO moments is that perfectly sensible figures are produced for these moments by the non-orthogonal PLMOs. The figures are directly comparable to those generated by a variety of other methods and criteria, and show sensible trends from atom to atom in the lone pairs. Further, identical lone pairs and bonds in different molecules have similar moments (see next chapter). A criticism sometimes levelled against the use of non-orthogonal LMOs is that molecular one-electron properties can no longer be expressed as a sum of LMO contributions. This is, of course, strictly true, but it has been shown in this work that by partitioning the electronic moment arising from the overlap of LMOs - the off-diagonal terms - amongst the contributions arising from the LMOs themselves - the diagonal terms - sensible moments, attributable to the bonds and lone pairs and summing to the total dipole moment, result.

CHAPTER TEN  
TRANSFERABILITY

10.1 INTRODUCTION

In the present work, as in most such work, the ability to transfer bond or lone pair properties between "similar chemical environments" in different, but related, molecules, is one of the proposed aims. The idea of transferability was introduced in Chapter One, and it was mentioned there that, based on an original suggestion by Adams,<sup>46</sup> some authors seem to feel that completely localised and non-orthogonal LMOs are best suited for possible transfer between molecules.<sup>47-49</sup> Some problems of definition arise at this point however.

Most workers expect that transfer will succeed only between "similar chemical environments", although quite what these are is rarely precisely defined. A common example that is used is the transfer of C-C and C-H sigma bonds between small and larger molecules up the paraffin series of hydrocarbons, although in this context it may be mentioned that Trindle & Sinanoglu<sup>230</sup> conclude that  $-\text{CHF}_2$  and  $-\text{CH}_3$  count as different environments. In view of this situation, and because only a few molecules have been analysed in this work, it is not possible to test the potential transferability of the PLMOs (or to test the accuracy of Adams suggestions) anything other than superficially. A more detailed test must wait upon the results from more, and larger, molecules. In this short chapter, therefore, the close similarity of only a few selected PLMOs in different molecules will be demonstrated.

## 10.2 TRANSFERABILITY IN THE PLMOs

The transferability of inner shell CMOs is well known,<sup>53</sup> and is demonstrated for the CMOs of Gaussian 70, after truncation and renormalisation, in Table 10.1. Such "automatic" localisation of the inner shell CMOs is the reason why they were not included in the localisation procedure of Chapter 4.

The oxygen and nitrogen lone pair PLMOs in different molecules are compared in Table 10.2. The lone pair on the carbon atom in CO is also included for completeness. It can be seen that the PLMO coefficients are very similar for the nitrogen lone pairs in N<sub>2</sub> and HCN, and for the oxygen lone pairs in CO and H<sub>2</sub>O. The nitrogen lone pair in ammonia is anomalous as has been found in numerous other studies.<sup>98</sup> This similarity in the lone pairs is evident, despite the fact that in such small molecules the rest of the molecule would be expected to have a marked characteristic influence in each case, and hence the molecular environments might not have been thought similar. (It should be remembered that in H<sub>2</sub>O a second oxygen lone pair lies in a pure 2p<sub>y</sub> AO perpendicular to the first. Only by distinguishing between the oxygen lone pairs in this way is a comparison to the sigma lone pair in CO possible). The lone pair moments in Table 10.2 are not transferable to the same extent and it is noticeable how sensitive the moments are to the degree of hybridisation. Indeed the dependence of the moment on the percentage of 2s<sup>or</sup> character in all the molecules (except ammonia) is almost linear. This is to be expected over this short range of high 2s character.<sup>278</sup>

The same high degree of equivalence in the LMO coefficients is found in the principal contributions to the Magnasco & Perico nitrogen lone pairs in N<sub>2</sub> and HCN (Tables 8.9 and 8.7) but not in the oxygen lone pairs of CO and water (Tables 8.8 and 8.10). In all cases the



TABLE 10.1 TRUNCATED AND RENORMALISED INNER SHELL CMOs OF THE EXAMPLE MOLECULES (STO-3G BASIS)

| CMO            | Molecule         | 1s <sub>X</sub> | 2s <sub>X</sub> <sup>or</sup> | 2p <sub>ZX</sub> <sup>(a)</sup> |
|----------------|------------------|-----------------|-------------------------------|---------------------------------|
| k <sub>C</sub> | HCN              | 0.9995          | 0.0301                        | 0.0019                          |
|                | CO               | 0.9997          | 0.0255                        | 0.0070                          |
|                | CH <sub>4</sub>  | 0.9993          | 0.0367                        | -                               |
| k <sub>N</sub> | HCN              | 0.9995          | 0.0290                        | -0.0088                         |
|                | N <sub>2</sub>   | 0.9996          | 0.0273                        | 0.0084                          |
|                | NH <sub>3</sub>  | 0.9995          | 0.0313                        | -0.0049                         |
| k <sub>O</sub> | CO               | 0.9996          | 0.0270                        | -0.0068                         |
|                | H <sub>2</sub> O | 0.9997          | 0.0258                        | -0.0043                         |

(a) No allowance for the different co-ordinate systems in the different molecules has been made in the signs of the 2p<sub>Z</sub> coefficient.

TABLE 10.2 LONE PAIR PLMOs OF THE EXAMPLE MOLECULES (STO-3G BASIS)

| PLMO        | Molecule         | $1s_X$  | $2s_X$ <sup>or</sup> | $2p_{ZX}$ <sup>(a)</sup> | % $2s$ <sup>or</sup> (b) | Moment (D) |
|-------------|------------------|---------|----------------------|--------------------------|--------------------------|------------|
| $\lambda_C$ | CO               | -0.0201 | 0.9227               | 0.3851                   | 85                       | 3.25       |
| $\lambda_N$ | N <sub>2</sub>   | -0.0181 | 0.9386               | 0.3444                   | 88                       | 2.64       |
|             | HCN              | -0.0187 | 0.9442               | 0.3288                   | 89                       | 2.38       |
|             | NH <sub>3</sub>  | -0.0232 | 0.8347               | 0.5501                   | 70                       | 3.55       |
| $\lambda_O$ | CO               | -0.0161 | 0.9642               | 0.2647                   | 93                       | 1.81       |
|             | H <sub>2</sub> O | -0.0212 | 0.9712               | 0.2375                   | 94                       | 1.60       |

(a) All  $2p_z$  coefficients have been made positive. The lone pair is directed away from the rest of the molecule in each case.

(b) In a normalised lone pair PLMO:  $a(1s) + b(2s^{\text{or}}) + c(2p_x) + d(2p_y) + e(2p_z)$

- the %  $2s^{\text{or}}$  character is  $100b^2$
- the %  $2p$  character is  $100(c^2 + d^2 + e^2)$
- the %  $1s$  character is negligible.

delocalised "tails" of course complicate matters. Furthermore, in a wide study of various relocalisation transforming criteria,<sup>98</sup> the orthogonal lone pair LMOs of these molecules, as revealed in 2s and 2p type populations, are not as transferable as the lone pair PLMOs. To this limited extent, this work may therefore be counted in support of Adams<sup>46</sup> original suggestion.

It is not possible to discuss the transferability of bond PLMOs in the framework of the present investigation because there is only one example to hand, the C-H bond in HCN and CH<sub>4</sub>. Even here the LMO forms are not expected to be the same since classically the hybrids at carbon are sp<sup>3</sup> in methane and sp in HCN. This is indeed revealed by the PLMOs in Table 10.3. All that can be said is that the bond polarity is the same in both cases (C<sup>-</sup>H<sup>+</sup>) and that the bond moment is of the same magnitude and in the same sense (C<sup>+</sup>H<sup>-</sup>). A similar state of affairs is found elsewhere.<sup>93</sup>

A final attempt to find transferable entities from molecule to molecule is expressed in Table 10.4 where the bonding hybrids on nitrogen in N<sub>2</sub> and HCN are compared. The sigma bonding is to roughly equivalent atoms (carbon and nitrogen) and underlies a π bond or bonds. The closeness of the hybrid forms would be remarkable were it not for the negative hybridisation in HCN. The 2s<sup>or</sup> AO coefficient is very small however and should not influence the almost pure 2p bonding in these hybrids.

In summary, where comparisons have been possible in these few molecules - noticeably in the oxygen and nitrogen lone pairs and also in the bonding nitrogen hybrids in HCN and N<sub>2</sub> - the PLMO coefficients and to a lesser extent PLMO moments, have been found transferable

TABLE 10.3 C-H BOND PLMOs IN THE EXAMPLE MOLECULES (STO-3G BASIS)

| PLMO       | Molecule        | $1s_C$ | $2s_C^{or}$ | $2p_{xC}$ | $2p_{yC}$ | $2p_{zC}$ | $1s_H$ | % $2s^{or}$ (b) | Moment (D) |
|------------|-----------------|--------|-------------|-----------|-----------|-----------|--------|-----------------|------------|
| $\mu_{CH}$ | HCN             | 0.6140 | (-0.0611    | 0.7388    | -         | -0.6712)  | 0.4730 | 55              | 1.74       |
|            | CH <sub>4</sub> | 0.5694 | (-0.0557    | 0.5239    | 0.4909    | -0.4907)  | 0.5311 | 27              | 2.01       |

TABLE 10.4 BONDING NITROGEN HAOS IN N<sub>2</sub> AND HCN (STO-3G BASIS)

| HAO        | Molecule       | $1s_N$  | $2s_N^{or}$ | $2p_{zN}^{(a)}$ | % $2p^{(b)}$ |
|------------|----------------|---------|-------------|-----------------|--------------|
| $h_{N(N)}$ | N <sub>2</sub> | -0.0905 | 0.0408      | 0.9942          | 99           |
| $h_{N(C)}$ | HCN            | -0.0935 | -0.0454     | 0.9946          | 99           |

(a) Both  $2p_z$  coefficients have been made positive. The hybrid is directed towards the other atom in each case.

(b) In a normalised valence PLMO or HAO:  $a(1s) + b(2s^{or}) + c(2p_x) + d(2p_y) + e(2p_z)$

- the % $2s^{or}$  character is  $100b^2$

- the %  $2p$  character is  $100(c^2 + d^2 + e^2)$

- the %  $1s$  character is negligible.

between molecules. The fact that the PLMOs have no delocalised "tails" and are hence non-orthogonal, is felt to enhance their potential transferability. Before any firm conclusions can be drawn however it is clearly necessary for further work to be done on other molecules with the transferability question in mind.

PART D

THE BEHAVIOUR OF THE PLMO WAVEFUNCTION

CHAPTER ELEVEN \*BOND AND ANGLE DEFORMATION IN WATER11.1 INTRODUCTION

All the results quoted and conclusions drawn so far in this work have applied to the experimental equilibrium geometry of each molecule. (Always bearing in mind of course, the slight variation in experimental geometries found from different sources). If such results and conclusions are to be of use in explaining the electronic structure of the isolated or unperturbed molecule, such an investigation is all that is required. However, the analysis of molecular wavefunctions for other geometries besides the experimental one can lead to information, not only about the characteristics of the wavefunction itself, but also about the behaviour of a molecule during vibration. Such an approach is reported in this short chapter which describes the study of the Gaussian 70 CMO and PLMO wavefunctions at various geometries of the water molecule. The investigation was undertaken with the following points in mind.

Firstly, quantum mechanical calculations on molecules at the Hartree-Fock level usually produce an absolute energy minimum at a different molecular geometry to that observed experimentally. It would therefore be of interest to compare the energy minimum geometries of the CMO wavefunction and PLMO wavefunction to the equilibrium geometry and to each other. The difference in energy between the two wavefunctions at these non-equilibrium geometries may further reveal the accuracy of the previous calculations.

Secondly, the appropriateness of the PLMOs as a description of the electronic structure of a molecule may be tested by a) examining the force constants obtained through simulating bond stretching and

---

\* The computations in this chapter were carried out as part of a one-term research project by an undergraduate student, Mark J. Foster, under the author's supervision.

bending from the PLMO wavefunction, and comparing these to those obtained from the CMO wavefunction and from experiment, and b) noting the change in the form of the PLMOs during the stretch of a bond. If the PLMO description is indeed useful, it is expected that the LCAO form of a bond that is extended would change, whilst the PLMOs representing the static parts of the molecule would remain approximately constant.

## 11.2 ENERGY MINIMA AND FORCE CONSTANTS

### 11.2(a) Energy Minima

The positions and values of the energy minima for the CMO and PLMO wavefunctions (STO-3G) are shown in Table 11.1. The corresponding values at the experimental equilibrium geometry are also shown. It can be seen that the position of energy minimum for the CMOs and the PLMOs are quite close. The difference in the bond length is only  $0.004\text{\AA}$  and the difference in the bond angle is  $0.6^\circ$ . There is also a close similarity in the total energy values and in their difference. These geometries differ from the experimental geometry by a larger amount although the total energy values here are only  $0.003/4$  H above those of the minima. The energy surface as a function of geometry for these wavefunctions therefore, is apparently quite "shallow" in this area. It is also noticeable that at the absolute energy minima, the delocalisation energy has been reduced by about 20% of its value at the experimental geometry. This is quite a substantial reduction considering how small, in relative terms, the delocalisation energy is.

It may be concluded from these few observations that the canonical wavefunction and the PLMO wavefunction seem to have a



TABLE 11.1 POSITIONS AND VALUES OF ENERGY MINIMA IN THE CMO AND PLMO WAVEFUNCTIONS OF H<sub>2</sub>O (STO-3G BASIS)

|                    | Geometry <sup>(a)</sup>   | CMO energy (H) | PLMO energy (H) | Difference (H) |
|--------------------|---------------------------|----------------|-----------------|----------------|
| Position of energy | R <sub>1</sub> = 0.989 Å  | -74.96590      | -74.96075       | 0.00515        |
| Minimum for CMO    | R <sub>2</sub> = 0.989 Å  |                |                 |                |
| Wavefunction       | θ = 100.04°               |                |                 |                |
| Position of energy | R <sub>1</sub> = 0.993 Å  | -74.96582      | -74.96085       | 0.00497        |
| Minimum for PLMO   | R <sub>2</sub> = 0.993 Å  |                |                 |                |
| Wavefunction       | θ = 99.41°                |                |                 |                |
| Experimental       | R <sub>1</sub> = 0.9572 Å | -74.96293      | -74.95668       | 0.00625        |
| Equilibrium        | R <sub>2</sub> = 0.9572 Å |                |                 |                |
| Geometry           | θ = 104.52°               |                |                 |                |

(a) R<sub>1</sub> = R(O - H<sub>1</sub>), R<sub>2</sub> = R(O - H<sub>2</sub>), θ = ∠HOH.

similar behaviour as a function of molecular geometry, at least near their energy minima. Further, in view of the reduction in delocalisation energy already noted, it might be hoped that with a more accurate canonical wavefunction, having its potential minimum nearer to the experimental geometry, the creation of the corresponding PLMO wavefunction will entail a smaller loss in accuracy than is required at the equilibrium geometry here.

#### 11.2(b) Force Constants

Force constants for bond and angle deformation in water can be obtained by calculating the total energy of the molecule at various geometries. Bond force constants were found by keeping the HOH angle and one bond length fixed, while the second bond length was varied either side of a likely energy minimum value. The total energy was calculated at each geometry from the CMO wavefunction and, assuming that the resulting potential function had the form:

$$E_{\text{TOT}} = E_0 + \frac{1}{2} k_R (\delta R)^2 \quad (11.1)$$

where

$E_0$  is the energy minimum

$\delta R$  is the displacement from the bond length at the energy minimum

$k_R$  is the bond force constant ( $\text{Nm}^{-1}$ ).

The energy data created was fitted to a quadratic curve by a standard quadratic plotter computer program. This revealed the energy minimum  $E_0$ , the corresponding value of the variable bond length, and hence the force constant  $k_R$ . This procedure was repeated for the energy values calculated from the PLMO wavefunction in each case, and also for different values of the fixed bond length.

The force constant for angle deformation was obtained in an analogous fashion, from the CMO and PLMO wavefunctions, by keeping both OH bond lengths fixed at the appropriate absolute energy minimum values,  $R_e$ , and varying the bond angle. In this case, the assumed potential function:

$$E_{TOT} = E_0 + \frac{1}{2} k_{\theta} (\delta\theta)^2 \quad (11.2)$$

where

$\delta\theta$  is the change in angle from its value at the energy minimum

$k_{\theta}$  is the angular force constant ( $Jrad^{-2}$ )

can be rewritten in the form:

$$E_{TOT} = E_0 + \frac{k_{\theta}}{2R_e^2} (R_e \delta\theta)^2 \quad (11.3)$$

which becomes:

$$E_{TOT} = E_0 + \frac{1}{2} k_{\theta}' (R_e \delta\theta)^2 \quad (11.4)$$

where

$k_{\theta}'$  is a modified force constant and now has the more manageable units of  $Nm^{-1} rad^{-2}$ .

The results of this process are displayed in Table 11.2.

Calculations 1 to 3 yielded a bond force constant for both the CMO and PLMO wavefunctions while calculations 4 and 5 provided an angular force constant from the PLMO and CMO wavefunctions respectively.

The experimental<sup>279</sup> bond and angular force constants obtained from Infra Red spectra, assuming a valence force field, are  $845 Nm^{-1}$  and  $76.1 Nm^{-1} rad^{-2}$ .

TABLE 11.2 FORCE CONSTANTS FOR BOND AND ANGLE DEFORMATION IN H<sub>2</sub>O (STO-3G BASIS)

(For explanation see narrative)

| Calculation | Geometries used (a) |                   |                   | Force constants calculated            |                                       |  |
|-------------|---------------------|-------------------|-------------------|---------------------------------------|---------------------------------------|--|
|             | $\theta^\circ$      | $R_2(\text{\AA})$ | $R_1(\text{\AA})$ | CMO Wavefunction                      | PLMO Wavefunction                     |  |
| 1           | 104.52              | 0.9572            | 0.950             | 943 Nm <sup>-1</sup>                  | 955 Nm <sup>-1</sup>                  |  |
|             | 104.52              | 0.9572            | 1.000             |                                       |                                       |  |
|             | 104.52              | 0.9572            | 1.050             |                                       |                                       |  |
| 2           | 104.52              | 0.970             | 0.920             | 1133 Nm <sup>-1</sup>                 | 1144 Nm <sup>-1</sup>                 |  |
|             | 104.52              | 0.970             | 0.970             |                                       |                                       |  |
|             | 104.52              | 0.970             | 1.020             |                                       |                                       |  |
| 3           | 104.52              | 0.993             | 0.950             | 972 Nm <sup>-1</sup>                  | 983 Nm <sup>-1</sup>                  |  |
|             | 104.52              | 0.993             | 0.993             |                                       |                                       |  |
|             | 104.52              | 0.993             | 1.050             |                                       |                                       |  |
| 4           | 98.5                | 0.993             | 0.993             | -                                     | 65 Nm <sup>-1</sup> rad <sup>-2</sup> |  |
|             | 100.0               | 0.993             | 0.993             |                                       |                                       |  |
|             | 101.5               | 0.993             | 0.993             |                                       |                                       |  |
| 5           | 98.5                | 0.989             | 0.989             | 66 Nm <sup>-1</sup> rad <sup>-2</sup> |                                       |  |
|             | 100.0               | 0.989             | 0.989             |                                       |                                       |  |
|             | 101.5               | 0.989             | 0.989             |                                       |                                       |  |

(a)  $R_1 = R(\text{O}-\text{H}_1)$ ,  $R_2 = R(\text{O}-\text{H}_2)$ ,  $\theta = \angle\text{HOH}$

Of the bond force constant calculations it is clear that the calculation 2 results are furthest from those obtained experimentally. In fact calculation 2 is the least reliable since none of the three variable bond lengths are very close to the energy minimum values (Table 11.1) and hence fitting the three points to a quadratic curve is likely to give a less accurate result than those of calculations 1 and 3. These two latter calculations correspond to quite different fixed bond lengths. The results from 1 deviate by almost 12% from the experimental value, and those from 3 by almost 16%. This is not as bad as would seem at first sight when it is remembered how crude the method is, and that we are dealing with Hartree-Fock ~~wavefunctions~~ <sup>force constants</sup> that are in any case only normally within approximately 10% of the experimental values.<sup>280</sup> The agreement between the results from the CMO and PLMO wavefunctions are close in each case. A similar situation exists in calculations 4 and 5 where the angular force constants obtained from the canonical and PLMO wavefunctions are very close and are within about 13% of the experimental value.

From these results it can be seen once again that the wavefunction constructed from the non-orthogonal PLMOs has a satisfactory behaviour as the molecular geometry is varied and is close to that shown by the canonical wavefunction. It remains to be seen whether the PLMOs themselves reveal a behaviour appropriate to localised bonds and lone pairs - which the CMOs obviously cannot - when the molecule geometry is distorted.

### 11.3 CHANGES IN PLMOs

The LCAO form of the PLMOs - with the Slater 2s, A0 orthogonalised to the 1s A0 as usual - and the bond and lone pair moments corresponding to different geometries are shown in Tables 11.3 and 11.4.

In Table 11.3 the stretch of one O-H bond is simulated as in calculation 3 above. In Table 11.4 the HOH bond angle is varied as in calculation 4. Changes in the total molecular dipole moment are shown in Tables 11.5 and 11.6. In Table 11.6 the angle between bonding hybrids is also shown.

In Table 11.3 it is  $\mu_{\text{OH}_1}$  which encompasses the proton whose position is changed. It is within this PLMO then, where the most variation is expected. This is indeed the case. That the LCAO coefficients in  $\mu_{\text{OH}_1}$  change more rapidly than those in  $\mu_{\text{OH}_2}$  can most clearly be seen in the oxygen 2p and hydrogen 1s coefficients. On stretching the bond  $\mu_{\text{OH}_1}$  there is a shift of negative charge to the hydrogen atom and away from oxygen in that PLMO. This is manifest in the size of the  $1s_{\text{H}}$  coefficient and the oxygen hybrid polarity parameter. This shift is not reflected in a change in the total bond moment which remains constant. It is probable therefore that the electron charge follows the moving proton so as to keep the centroids of positive and negative charge in the same relative positions in the bond. Although of course, the presence of atomic dipoles do complicate the analysis. During the stretch the form of  $\mu_{\text{OH}_2}$  remains roughly constant although the  $1s_{\text{H}}$  coefficient increases very slightly as does the oxygen hybrid polarity parameter. This effect is permissible due to the slight change in the form of the hybrids on oxygen. The oxygen lone pair becomes slightly less hybridised on increasing the O-H<sub>1</sub> distance which leads to a decrease in the lone pair moment. Since the lone pair is the greatest contributor to the total dipole moment this too decreases (Table 11.5).

TABLE 11.3 PLMOs and PLMO MOMENTS DURING STRETCH OF O-H<sub>1</sub> BOND IN H<sub>2</sub>O (STO-3G BASIS)

(For explanation see narrative)

| PLMO              | (a)                |                 |                               |                  |                  |                             |                             |         |         |       | PLMO Moment (b) (c) |  |  |
|-------------------|--------------------|-----------------|-------------------------------|------------------|------------------|-----------------------------|-----------------------------|---------|---------|-------|---------------------|--|--|
|                   | R <sub>1</sub> (Å) | 1s <sub>O</sub> | 2s <sup>or</sup> <sub>O</sub> | 2p <sub>xO</sub> | 2p <sub>zO</sub> | 1s <sub>H<sub>1</sub></sub> | 1s <sub>H<sub>2</sub></sub> | z comp. | x comp. | total |                     |  |  |
| λ <sub>O</sub>    | 0.950              | -0.0211         | 0.9721                        | -0.0031          | 0.2336           | -                           | -                           | -1.57   | -       | 1.57  |                     |  |  |
|                   | 0.993              | -0.0209         | 0.0735                        | -                | 0.2274           | -                           | -                           | -1.53   | -       | 1.53  |                     |  |  |
|                   | 1.050              | -0.0207         | 0.9755                        | 0.0042           | 0.2200           | -                           | -                           | -1.48   | -       | 1.48  |                     |  |  |
| H <sub>2</sub> OH | 0.950              | 0.6802          | -0.0354                       | -0.1019          | -0.6279          | -                           | 0.5467                      | -0.071  | -0.224  | 0.235 |                     |  |  |
|                   | 0.993              | 0.6807          | -0.0364                       | -0.1097          | -0.6265          | -                           | 0.5479                      | -0.080  | -0.233  | 0.246 |                     |  |  |
|                   | 1.050              | 0.6819          | -0.0387                       | -0.1230          | -0.6257          | -                           | 0.5494                      | -0.086  | -0.244  | 0.259 |                     |  |  |
| H <sub>1</sub> OH | 0.950              | 0.6855          | -0.0398                       | -0.1103          | 0.6222           | 0.5374                      | -                           | -0.073  | 0.235   | 0.246 |                     |  |  |
|                   | 0.993              | 0.6807          | -0.0364                       | -0.1097          | 0.6265           | 0.5479                      | -                           | -0.080  | 0.233   | 0.246 |                     |  |  |
|                   | 1.050              | 0.6758          | -0.0324                       | -0.1068          | 0.6317           | 0.5605                      | -                           | -0.085  | 0.230   | 0.245 |                     |  |  |

(a)  $\theta = 104.52^\circ$ ,  $R_2 = 0.993 \text{ \AA}$  throughout.  $R_1 = R(\text{O-H}_1)$ ,  $R_2 = R(\text{O-H}_2)$ ,  $\theta = \angle\text{HOH}$ .

(b) Sign convention as in Chapter 6.

(c) The total is shown positive. The total bond moments are not colinear with the internuclear lines.

TABLE 11.4 PLMOs and PLMO MOMENTS DURING ANGLE DEFORMATION IN H<sub>2</sub>O (STO-3G BASIS)

(For explanation see narrative)

| PLMO         | $\theta^\circ$ (a) | PLMO Moment (c) (d) |                 |                  |                  |                             |                             |         |         |       |
|--------------|--------------------|---------------------|-----------------|------------------|------------------|-----------------------------|-----------------------------|---------|---------|-------|
|              |                    | 1s <sub>O</sub>     | 2s <sub>O</sub> | 2p <sub>xO</sub> | 2p <sub>zO</sub> | 1s <sub>H<sub>1</sub></sub> | 1s <sub>H<sub>2</sub></sub> | z comp. | x comp. | total |
| $\lambda_0$  | 98.5               | -0.0209             | 0.9777          | -                | 0.2088           | -                           | -                           | -1.42   | -       | 1.42  |
|              | 100.0              | -0.0208             | 0.9767          | -                | 0.2133           | -                           | -                           | -1.45   | -       | 1.45  |
|              | 101.5              | -0.0209             | 0.9758          | -                | 0.2179           | -                           | -                           | -1.48   | -       | 1.48  |
| $\mu_{OH_1}$ | 98.5               | 0.6792              | (-0.0367        | -0.1328          | 0.6374           | -0.7581)                    | 0.5528                      | -0.149  | 0.209   | 0.257 |
|              | 100.0              | 0.6795              | (-0.0365        | -0.1272          | 0.6346           | -0.7614)                    | 0.5516                      | -0.132  | 0.215   | 0.252 |
|              | 101.5              | 0.6799              | (-0.0365        | -0.1215          | 0.6318           | -0.7646)                    | 0.5504                      | -0.115  | 0.221   | 0.249 |

(a)  $R_1 = R_2 = 0.993 \text{ \AA}$  throughout.  $R_1 = R(O-H_1)$ ,  $R_2 = R(O-H_2)$ ,  $\theta = \angle HOH$ .(b)  $\mu_{OH_2}$  is equivalent to  $\mu_{OH_1}$ , but with negative values of  $2p_{xO}$  coefficient and x component of the PLMO moment.

(c) Sign convention as in Chapter 6.

(d) The total is shown positive. The total bond moments are not colinear with the internuclear lines.



TABLE 11.5 MOLECULAR DIPOLE MOMENT DURING STRETCH OF O-H<sub>1</sub> BOND  
IN H<sub>2</sub>O (STO-3G BASIS)

| $R_1$ (Å) (a) | Molecular Dipole Moment <sup>(b)</sup> |         |
|---------------|--|---------|
|               | z comp.                                | x comp. |
| 0.950         | -1.718                                 | 0.026   |
| 0.993         | -1.692                                 | -       |
| 1.050         | -1.650                                 | -0.038  |

(a)  $\theta = 104.52^\circ$ ,  $R_2 = 0.993\text{Å}$  throughout.  $R_1 = R(\text{O-H}_1)$ ,  $R(\text{O-H}_2)$ ,  $\theta = \angle\text{HOH}$ .

(b) Sign convention as in Chapter 6.

TABLE 11.6 MOLECULAR DIPOLE MOMENT AND DIRECTION OF BONDING HYBRIDS  
DURING ANGLE DEFORMATION IN H<sub>2</sub>O (STO-3G BASIS)

| $\theta$ (a) | Molecular Dipole Moment <sup>(b)</sup> |         | Angle Between Bonding Hybrids |
|--------------|--|---------|-------------------------------|
|              | z comp.                                | x comp. |                               |
| 98.5°        | -1.718                                 | -       | 80.1°                         |
| 100.0°       | -1.711                                 | -       | 79.6°                         |
| 101.5°       | -1.705                                 | -       | 79.1°                         |

(a)  $R_1 = R_2 = 0.993\text{Å}$  throughout.  $R_1 = R(\text{O-H}_1)$ ,  $R_2 = R(\text{O-H}_2)$ ,  $\theta = \angle\text{HOH}$ .

(b) Sign convention as in Chapter 6.

In Tables 11.4 and 11.6 the effect of opening up the HOH angle may be described as follows. The hybridisation in the lone pair increases very slightly giving a very small increase in the lone pair moment. The polarity of the O-H bonds remains almost constant (a tiny shift to oxygen may be detected) although the z component of the associated bond moment decreases while the x component increases as expected. The angle formed by the oxygen hybrids varies slightly in the opposite sense to the internuclear angle. The total molecular dipole becomes smaller as would be expected from the movement of the bonds, although this decrease is not so large as it would otherwise be due to the associated increase in the lone pair moment.

This description of "bending" in water hence produces a sensible outcome as did the previous description of bond stretching. The two O-H bonds are largely unaffected by angle deformation (even in their orientation) and the lone pair is only little altered in appearance.<sup>281</sup> What slight change there is in the hybrid angle at oxygen, is in the opposite sense to the change in the internuclear angle, and has been noted in a minimal basis in other investigations.<sup>256,282,283</sup>

To a first degree then, the proposed aim of this section has been attained. That is, it was required to show that the localised description of the water molecule was still possible at molecular geometries other than the experimental one, and that only PLMOs describing bonds and lone pairs on atoms that actually change their relative positions should vary in form. This latter conclusion is not completely true of course, since changes in geometry in one part of a small molecule such as water must have an effect on other

parts. What other changes in PLMO forms were found have been relatively small, though not negligible. (The contribution of the lone pair moment to the total dipole on angle deformation is rarely taken into account for example). It can further be concluded from the discussion of the previous section that in attaining a description of the water molecule in terms of Perfectly Localised MOs, little sacrifice need be made in the accuracy or behaviour of the wavefunction at non-equilibrium geometries.

PART E

SUMMARY AND CONCLUSIONS

CHAPTER TWELVESUMMARY AND CONCLUSIONS

The objectives of the present work were outlined in Chapter One (Section 1.3). It was stated there that a preliminary investigation of a new LMO method was to be presented and applied to some simple example molecules. Drawing from these examples it was attempted "to investigate the extent to which the electronic structure of simple molecules - obtained via the one-determinant Hartree-Fock MO-LCAO scheme in a minimal AO basis - may be expressed in terms of two-centre bond and one-centre lone pair PLMOs".

In this chapter the overall success of the new LMO method (the PLMO method) will be assessed and therefore the extent to which the one and two-centre PLMOs represent the electronic structure of the example molecules can be gauged. Arising from a comparison of the PLMO results to those of other LMO methods which has already been made, it will also be possible to draw wider conclusions about the way certain LMO methods describe electronic structure.

12.1 THE PLMO METHOD12.1(a) General Points

The simple chemical view of the electronic description of molecules is that they consist of two-centre bonds and one-centre lone pairs. Thus the rationale of the PLMO method is to impose this description on a previously determined one-determinant MO wavefunction and to minimise the energy sacrificed in doing so. This is done by searching the function space generated by a truncation of orthogonally transformed CMOs. The PLMO method is hence a relocalisation LMO method

(Chapter 2) and it is closely related to the LMO methods that orthogonally transform a starting set of CMOs depending on other criteria.<sup>70-72, 83-85, 96-98, 104-113, 124,125.</sup>

The present method is a simple, easily understandable procedure that yields unique PLMOs (except where there is more than one bond between a pair of atoms or more than one lone pair on an atom). However, certain constraints are required in order for the method (at least in its current form) to function satisfactorily and to yield unique sigma LMOs. These are the separation of core and valence regions and the separation of sigma and pi electrons. Both of these constraints have been discussed in section 4.7.

#### 12.1(b) Desired Properties

Some desired properties of the localised orbitals were described in Chapter One (subsection 1.3(b)) as an aid in judging the overall success of the method. It is useful to go through them here one by one.

##### 12.1(b)(i) Small energy sacrifice

The energy sacrificed in forming the PLMOs from the CMO wave-function i.e. the delocalisation energy of the PLMOs, has been compared to that sacrificed in other LMO methods in Chapter 7. Since the PLMOs are generated by minimising the energy sacrificed in deleting the "tails" of an orthogonal transformation of the CMOs. This sacrifice is obviously less than that when deleting the "tails" of any other set of orthogonal LMOs generated by this procedure. The energy sacrifice in the PLMOs is found in Chapter 7 to be at least comparable to that in many direct or hybrid LMO methods (though the use of different AO basis sets by different workers does cloud the picture

somewhat). Hence it seems that producing one and two-centre LMOs by deleting the inherent delocalisations in orthogonal LMOs constituting a previously determined Hartree-Fock MO wavefunction is at least justifiable energetically as starting with one and two-centre LMOs and variationally optimising the wavefunction constructed from them. This is especially true in the examples of  $N_2$  and CO.

The size of the energy sacrifice in absolute terms may be judged by comparing the delocalisation energy per bond in  $H_2O$  and  $CH_4$  with the values of the dissociation energies of these bonds (Chapter 7). In both cases the delocalisation energy is under  $2\frac{1}{2}\%$  of the dissociation energy. Furthermore, the energy sacrifice in water,  $0.007H$ , is of the same order as the energetic penalty to the PLMO wavefunction in using the experimental equilibrium geometry rather than the energy minimum geometry,  $0.004H$  (Chapter 11).

From these comparisons it can be seen that the energy sacrifice necessary in the PLMO method is indeed small.

#### 12.1(b)(ii) Near orthogonality

The PLMOs were expected to be non-orthogonal but for practical computational reasons it was hoped they would not be too far from orthogonal (Chapter One). The method itself should have ensured this to a certain extent, since obtaining the PLMOs by deleting the energetically least significant "tails" from orthogonal LMOs was unlikely to move the PLMOs far away from orthogonality. This was found to be the case.

The overall measure of the non-orthogonality of the PLMOs in the trial molecules,  $\Delta$ , was small (Chapters 4 and 5) and the calculation of PLMO moments and electronic populations by the non-orthogonal

formalisms of Appendix I led to sensible results. In particular, it was demonstrated in Chapter 9 that the "diagonal" terms of the dipole moment expression arising from the individual PLMOs were far greater than the "off-diagonal" terms arising from the overlap of the PLMOs.

While the general near-orthogonality of the PLMOs may be demonstrated, it is also true that the individual values of the non-negligible PLMO overlap integrals give an indication of the kind of LMO wavefunction selected by the PLMO procedure (see below).

#### 12.1(b)(iii) Sensible bond and lone pair moments

The theoretical difficulties of breaking down one-electron molecular properties into non-orthogonal LMO contributions <sup>were</sup> ~~was~~ mentioned in Chapter one. That in practice no difficulty was encountered with the PLMOs in this respect has been explained in the previous subsection.

Essentially through reasons of the definition of bond and lone pair moments in different instances (Chapter 9), it is only possible to test the "sensiblyness" of the PLMO moments by a comparison to the results of other LMO work. In Chapter 9 it was shown that for all the trial molecules where results were available for comparison, the PLMO moments were indeed compatible with those from a wide variety of different LMO methods. Where differences did occur with certain of the methods they were consistent with the general differences in the degree of hybridisation found by the different procedures. Clearly the PLMO method may usefully be used to assign local moments to bonds and lone pairs.

#### 12.1(b)(iv) Close connection to classical valence concepts

The bridge between classical chemical ideas and quantum mechanics which any LMO method is meant to provide must clearly be justified by



its ability to reproduce the normal chemical descriptions of bonding and valence. For chemists this is the most important test that may be applied to such methods.

The PLMOs in the example molecules, expressed in terms of normalised HAOs on each atom, were found to have a consistent make-up. The descriptions have been summarised in subsection 8.2(g) and in Figure 8.3, and clearly reflect a normal valence description in which the lone pairs are largely  $2s^{\text{or}}$  in character and the bonding HAOs, except for "internal" carbon hybrids, largely  $2p$  in character. The carbon atom in HCN is  $sp$  hybridised and in methane is nearly  $sp^3$  hybridised. Furthermore, the hybridisation trends in the PLMOs were found to straightforwardly reflect the nature of the atom upon which the HAOs reside.

Unlike the classical hybrids of Slater<sup>155</sup> and Pauling<sup>156,157</sup> however, the HAOs in the PLMOs are non-orthogonal. In fact, the "condition of the atom in the molecule" that emerges from the results includes substantial non-orthogonality among the hybrids on each atom (Table 8.13). It is this which allows the HAOs to be very little hybridised, unlike some other LMO methods which either impose hybrid orthogonality or in which hybrid near-orthogonality arises automatically (subsection 8.4(b)). Thus despite the non-orthogonality of the HAOs in the PLMO method (or perhaps more accurately, because of it) the valence description of the molecules studied is clearly compatible with the usual chemists description of these molecules.

#### 12.1(b)(v) Transferability

The potential transferability of the PLMOs between "similar chemical environments" cannot really be gauged satisfactorily by the

present study because of the small number of examples to hand. However, the few entities that could be compared in the trial molecules, notably the lone pairs on nitrogen and oxygen, were found to be roughly transferable. No clear conclusion about the possible advantages in this respect of non-orthogonal and completely localised LMOs can be made with any confidence, though some comparisons made to the literature would seem to support that view (see Chapter 10). It can at least be said of the present study that there were no instances in the trial molecules where similarities were expected but not found.

#### 12.1(c) Conclusions

Judged by the extent to which the present method matched the above requirements, it can be said to have been successful. Also, the behaviour of the PLMO wavefunction, and the forms of the PLMOs themselves, at non-experimental geometries of the water molecule has been shown to be completely satisfactory (Chapter 11). It may be concluded therefore that a single determinant of one and two-centre PLMOs in a minimal AO basis offers a very good approximation to the electronic structure of the example molecules. The small sacrifice in accuracy necessary to completely localise the LMOs in this way is certainly not large enough to outweigh the advantages of dealing with one and two-centre PLMOs, to which the bonds and lone pairs of classical valence theory have exact application.

#### 12.2 RELATED LMO METHODS

The substantial non-orthogonality of the HAOs in the PLMO method, and the resulting low level of hybridisation, is not shown by the HAOs in all other LMO methods. Methods in which the HAOs are

substantially non-orthogonal include those of Peters<sup>104-113</sup> and Roby,<sup>132</sup> while examples of methods which have orthogonal or near-orthogonal hybrids at each atom are those of Edmiston & Ruedenberg,<sup>70,83-85</sup> Boys<sup>71,72</sup> and Aufderheide<sup>181,182</sup> (section 8.4). It was found, when comparing the hybridisation trends of these two groups of methods, that a further contrast was apparent (subsection 8.4(c)). Those methods using orthogonal or near-orthogonal hybrids at each centre showed trends that could be rationalised using the Population Ratio (PR) formalism,<sup>84,259</sup> while in  $N_2$  and CO the completely opposite trends were encountered in the PLMOs and in the other methods utilising substantially non-orthogonal HAOs.

Arising from the discussion of the sizes of the PLMO overlap integrals (subsection 8.4(d)) it is possible to understand the source of this dichotomy, at least in the transformation relocalisation LMO methods to which the PLMO method is closely related.

Because the PLMO overlap integrals are related to the "tails" of the orthogonal LMOs that were deleted during truncation, it can be said of the transformed LMOs that those representing lone pairs were almost completely localised onto their atomic centres while those representing bonds were more delocalised (subsection 8.4(d)). (Since the PLMOs are found at an energy minimum, the orthogonally transformed LMOs, from which the PLMOs are obtained, are most near energetically to one and two-centre LMOs in this state). The orthogonal transformation matrix fixed by the PLMO method that generates localised lone pair LMOs and delocalised bond LMOs is hence similar to those matrices selected by the methods of Peters<sup>104-113</sup> and by other "cut-off" methods in which the criterion fixing the trans-

formation is usually that lone pair LMOs have no "tails". From the examples discussed in this work, the attendant properties of the resulting LMOs are that the constituent HAOs are substantially non-orthogonal and the overall level of hybridisation is low.

Within the similar intrinsic transformation LMO methods of Edmiston & Ruedenberg,<sup>70,83-85</sup> Boys<sup>71,72</sup> and Von Niessen<sup>96-98</sup> and in the population method of Magnasco + Perico,<sup>124,125</sup> the orthogonal transformation of the CMOs is significantly different from that selected above. In these methods the relative amounts of delocalisation in the bonds and lone pairs is the reverse of that in the PLMO method. It is found here that the lone pair LMOs (for all except halogen atoms) are generally more delocalised than the bonds.<sup>43,76,93,263-265</sup>

The properties of the constituent HAOs in these cases consist of near-orthogonality at each centre and greater hybridisation than in the PLMOs (section 8.4).

These two alternative descriptions of the electronic structure of a molecule via LMOs are obviously equivalent (since both could be obtained from the same molecular wavefunction) and the one chosen would seem to be a matter of preference. In order to keep close to the chemical ideas of two-centre bonds and one-centre lone pairs however, the LMOs need to be completely localised. (These types are likely to be better suited for transfer between molecules for example).<sup>46-49</sup> These orthogonal LMOs most energetically near to one and two-centre LMOs are those with localised lone pairs. The one and two-centre LMOs themselves are the PLMOs, constructed for a number of molecules in this work.

APPENDICES

APPENDIX I  
BASIC THEORY

The approach taken in the main body of this work has been a chemical one, and in the text the equations have been kept to a minimum. The bulk of the mathematical development is therefore reproduced here in the first appendix.

Most of the equations used in the computations are present in Sections I.4 to I.7, but in order to lay the foundations for these and to introduce the MO method and the density matrix formalism, the earlier parts are necessary. Though these earlier sections repeat very basic theory that is available in many standard texts, they serve to define the notation in a methodical way and are therefore kept. Not in the readily available sources however, except in fragmented form, is much of the development concerning non-orthogonal orbitals which is present throughout this appendix. This has obvious application to the main body of this work.

The density matrix formalism has proved very helpful throughout and the notation used in this respect, as in the rest of the appendix, is based to a large extent on McWeeny & Sutcliffe.<sup>19</sup>

I.1. MOLECULAR WAVEFUNCTIONS

The properties of a molecular system in a stationary state consisting of a set of interacting electrons and nuclei may be determined in principle by solution of Schrodinger's (time-independent) equation.<sup>1</sup> If it is assumed that  $N$  electrons move in a field due to  $L$  stationary nuclei<sup>284</sup> then Schrodinger's equation takes the form (in atomic units)

$$\hat{H}(X_1, X_2, X_3 \dots X_N) \Psi (X_1, X_2, \dots X_N) = E \Psi (X_1, X_2 \dots X_N) \quad (\text{I.1})$$

where

$\hat{H}(X_1, X_2, X_3 \dots X_N)$  is the Hamiltonian operator.

$$\hat{H} = \sum_{p=1}^N \hat{h}(p) + \frac{1}{2} \sum_{p=1}^N \sum_{q=1}^N \hat{g}(p, q) \quad (\text{I.2})$$

$$\text{where } \hat{h}(p) = \frac{1}{2} \hat{\nabla}^2(p) + \hat{V}(p) \quad (\text{I.3})$$

is the one-electron Hamiltonian operator for electron  $p$

while

$$\hat{g}(p, q) = \frac{1}{r_{pq}} \quad (\text{I.4})$$

is the electrostatic interaction between electrons  $p$  and  $q$ .

$\hat{h}(p)$  consists of two parts: the kinetic energy operator which, in cartesian co-ordinates is

$$\hat{\nabla}^2(p) = \left( \frac{\partial^2}{\partial x_p^2} + \frac{\partial^2}{\partial y_p^2} + \frac{\partial^2}{\partial z_p^2} \right) \quad (\text{I.5})$$

and the potential energy of electron  $p$  in the field of the fixed nuclei

$$\hat{V}(p) = - \sum_{a=1}^L \frac{Z_a}{r_{ap}} \quad (\text{I.6})$$

The electronic wavefunction  $\Psi(X_1, X_2 \dots X_N)$  describes the electronic state of the molecule and is a function of the space-spin co-ordinates of the  $N$  electrons.

If  $\Psi$  is normalised then we have

$$\int \Psi^*(X_1 \dots X_N) \Psi (X_1 \dots X_N) dx_1 \dots dx_N \quad (\text{I.7})$$

$$= \int |\Psi(X_1 \dots X_N)|^2 dx_1 \dots dx_N = 1$$

Here,  $|\Psi(x_1 \dots x_N)|^2$  is a probability density with the physical interpretation that

$$|\Psi(x_1 \dots x_N)|^2 dx_1 dx_2 \dots dx_N = \left( \begin{array}{l} \text{probability of finding} \\ \text{electrons 1, 2, \dots N} \\ \text{simultaneously in space-} \\ \text{spin elements} \\ dx_1 dx_2 \dots dx_N \end{array} \right) \quad (\text{I.8})$$

Since electrons are indistinguishable, permutating any two electrons should not affect the probability density  $|\Psi|^2$ . This leads to the requirement that the wavefunction is antisymmetric. This can be formulated as

$$\hat{P}(p,q) \Psi(x_1 \dots x_N) = -\Psi(x_1 \dots x_N) \quad (\text{I.9})$$

where  $\hat{P}(p,q)$  is a permutation operator which interchanges the co-ordinates of electrons  $p$  and  $q$ .

The electronic energy  $E$  in equation (I.1) is the energy of the  $N$  electrons moving in the field provided by the nuclei. Equation (I.1) is an eigenvalue equation and possesses acceptable solutions  $\Psi_k$  only for certain values of the eigenvalue  $E_k$ . The values  $E_k$  are the quantised energies of the allowed states  $\Psi_k$  of the electronic system.

#### I.1(a) Method of Molecular Orbitals

The orbital approach to solutions of the many-electron Schrodinger equation is an attempt to construct a satisfactory wavefunction from a combination of functions each dependent upon the co-ordinates of one electron only. To do this we may associate with the  $N$  electrons,  $N$  wavefunctions  $\psi_1, \psi_2 \dots \psi_g$  each dependent upon the space-spin co-ordinates of one electron. These functions are called spin-orbitals.

A wavefunction constructed from spin-orbitals must satisfy the antisymmetry requirement (Equ. (I.9)) and this leads to a wavefunction



of the form:

$$\Psi(X_1 \dots X_N) = \sum_k C_k \Phi_k(X_1 \dots X_N) \quad (\text{I.10})$$

where  $C_k$  is a numerical coefficient and  $\Phi_k$  is an "antisymmetrised spin-orbital product" which is formed from a linear combination of all the possible permutations of the electron co-ordinates amongst the ordered set of  $N$  spin-orbitals  $\psi_1 \dots \psi_\ell$ . The sum in equation (I.10) is over all distinct ordered configurations of spin-orbitals that may be selected from a complete set of spin-orbitals.

The definition of the "antisymmetrised spin-orbital product" is that of a determinant of the form:

$$\Phi_k = N_k \begin{vmatrix} \psi_1(X_1) & \psi_2(X_1) & \dots & \psi_\ell(X_1) \\ \psi_1(X_2) & \psi_2(X_2) & \dots & \psi_\ell(X_2) \\ \cdot & \cdot & & \cdot \\ \cdot & \cdot & & \cdot \\ \cdot & \cdot & & \cdot \\ \psi_1(X_N) & \psi_2(X_N) & \dots & \psi_\ell(X_N) \end{vmatrix} \quad (\text{I.11})$$

called a "Slater determinant".<sup>285</sup> The wavefunction is hence expressed in equation (I.10) as a linear combination of determinants, each containing a different selection of spin-orbitals.

#### I.1(b) The One-Determinant Approximation

An exact expansion of a wavefunction in terms of Slater determinants (equation (I.10)) requires an infinite sum of such determinants. However, a good approximate wavefunction, based on an intelligent choice of spin-orbitals, may be constructed from only a small number of terms in the expansion. Indeed, the wavefunction



$$\begin{aligned}\delta_{\alpha\beta} &= 1 \quad \text{if} \quad \alpha = \beta \\ \delta_{\alpha\beta} &= 0 \quad \text{if} \quad \alpha \neq \beta\end{aligned}\tag{I.15}$$

This means that integration of spin-orbitals will yield zero if they are of different spin, or the relevant integral over MOs if they are the same spin.

The single-determinant wavefunction of MOs has the property that it is invariant (besides a "phase-factor") to any linear transformation of the MOs.<sup>54</sup> This can be seen to arise from the property of a determinant that the multiple of any row (or column) may be added to, or subtracted from, any other row (or column) without changing the value of the determinant.

## I.2 DENSITY MATRIX FORMALISM<sup>2-8</sup>

### I.2(a) Definitions and Properties\*

If  $\hat{\theta}$  is a Hermitian operator representing a physical quantity, then the expectation value of  $\hat{\theta}$  in state  $\Psi(X_1 \dots X_N)$  is given by

$$\langle \theta \rangle = \int \Psi^*(X_1 \dots X_N) \hat{\theta} \Psi(X_1 \dots X_N) dX_1 \dots dX_N\tag{I.16}$$

when  $\Psi$  is normalised according to equation (I.7).

Now  $\hat{\theta}$  may be written in the form

$$\hat{\theta} = \hat{\theta}(0) + \sum_{p=1}^N \hat{\theta}(p) + \frac{1}{2} \sum_{p=1}^N \sum_{\substack{q=1 \\ (p \neq q)}}^N \hat{\theta}(p,q) + \dots\tag{I.17}$$

and also

---

\* The symbols for 1st and 2nd order density functions ( $\rho_1, \rho_2, P_1, P_2$ ) and normalisation employed, are those of McWeeny. 5

Only when the functions are expanded in terms of MO or AO bases are the representatives called "matrices".

$$\langle \theta \rangle = \langle \theta_0 \rangle + \langle \theta_1 \rangle + \langle \theta_2 \rangle + \dots \quad (\text{I.18})$$

where the terms are zero, one, two ... particle operators and expectation values respectively, and are symmetrical in the indices of the electrons.

Now, considering the one-electron term only we have

$$\langle \theta_1 \rangle = \int \Psi^*(X_1 \dots X_N) \left[ \sum_{p=1}^N \hat{\theta}(p) \right] \Psi(X_1 \dots X_N) dX_1 \dots dX_N \quad (\text{I.19})$$

from the symmetry of the electron co-ordinates this becomes

$$\langle \theta_1 \rangle = N \int \Psi^*(X_1 \dots X_N) [\hat{\theta}(1)] \Psi(X_1 \dots X_N) dX_1 \dots dX_N \quad (\text{I.20})$$

The operator  $\hat{\theta}(1)$ , which operates only on the factor following it, may, nevertheless, be separated from the wavefunction product by the following artifice. By changing the variable  $X_1$  in  $\Psi^*$  to  $X_1'$  it becomes immune from the effect of  $\hat{\theta}(1)$ . Equation (I.20) now becomes

$$\langle \theta_1 \rangle = N \int [\hat{\theta}(1) \Psi^*(X_1', X_2 \dots X_N) \Psi(X_1 \dots X_N)]_{X_1'=X_1} dX_1 \dots dX_N \quad (\text{I.21})$$

where  $X_1' = X_1$  after operating with  $\hat{\theta}(1)$ , but before completing the integration. This may be written

$$\langle \theta_1 \rangle = \int [\hat{\theta}(1) \rho_1(X_1'/X_1)]_{X_1'=X_1} dX_1 \quad (\text{I.22})$$

where

$$\rho_1(X_1'/X_1) = N \int \Psi^*(X_1', X_2 \dots X_N) \Psi(X_1 \dots X_N) dX_2 \dots dX_N \quad (\text{I.23})$$

is called the 1st order density function.<sup>3,6</sup>

Similarly, for the two-electron terms in equations (I.17) and (I.18) we may write

$$\langle \theta_2 \rangle = \frac{1}{2} \int [\hat{\theta}(1,2) \rho_2(x_1' x_2' / x_1 x_2)]_{x_1'=x_1, x_2'=x_2} dx_1 dx_2 \quad (\text{I.24})$$

where

$$\rho_2(x_1' x_2' / x_1 x_2) = N(N-1) \int \Psi^*(x_1', x_2', x_3 \dots x_N) \Psi(x_1 \dots x_N) dx_3 \dots dx_N \quad (\text{I.25})$$

is called the 2nd order density function.<sup>3,6</sup>

All one-electron properties may hence be described in terms of  $\rho_1(x_1' / x_1)$  and all two-electron properties in terms of  $\rho_2(x_1' x_2' / x_1 x_2)$ †.

If the operator in question is simply a multiplier, for example a function of cartesian co-ordinates, the distinction between primed and unprimed co-ordinates is no longer necessary since the order of operation does not matter. We may write:

$$\rho_1(x_1' / x_1) = \rho_1(x_1 / x_1) = \rho_1(x_1) \quad (\text{I.26})$$

$$\rho_2(x_1' x_2' / x_1 x_2) = \rho_2(x_1 x_2 / x_1 x_2) = \rho_2(x_1 x_2) \quad (\text{I.27})$$

these "diagonal elements" may be interpreted as follows.<sup>2</sup>

$$\rho_1(x_1) dx_1 = \left( \begin{array}{l} \text{Probability of finding any of the } N \\ \text{electrons in space-spin element } dx_1 \end{array} \right) \quad (\text{I.28})$$

$$\rho_2(x_1 x_2) dx_1 dx_2 = \left( \begin{array}{l} \text{Probability of finding any 2} \\ \text{of the } N \text{ electrons simultaneously} \\ \text{in space-spin elements } dx_1 \text{ and} \\ dx_2 \end{array} \right) \quad (\text{I.29})$$

Hence the expectation values of operators may be directly related to the electron distribution.

---

†  $x_1, x_2$  etc. on the left hand side of equations (I.23) and (I.25) refer to "points 1 and 2 and no longer specifically to the "co-ordinates of electrons 1 and 2".

For many observables, spinless operators are used. The spinless counterparts of the density functions defined in equations (I.23) and (I.25) can be obtained by integrating over spins.

We obtain:

$$P_1(r'_1/r_1) = \int [\rho_1(X'_1/X_1)]_{s'_1=s_1} ds_1 \quad (I.30)$$

$$P_2(r'_1 r'_2 / r_1 r_2) = \int [\rho_2(X'_1 X'_2 / X_1 X_2)]_{s'_1=s_1, s'_2=s_2} ds_1 ds_2 \quad (I.31)$$

The "diagonal elements" of which may be interpreted in terms analogous to definitions (I.28) and (I.29). When operators are spinless, the expressions for observables found above may simply be rewritten with  $\rho$  replaced by  $P$  and  $X$  replaced by  $r$ .

In the one-determinant approximation the 2nd order density function (and all higher order density functions) may be factorised in terms of the 1st order density function.<sup>7</sup> We obtain

$$\rho_2(X'_1 X'_2 / X_1 X_2) = \rho_1(X'_1 / X_1) \rho_1(X'_2 / X_2) - \rho_1(X'_1 / X_2) \rho_1(X'_2 / X_1) \quad (I.32)$$

This means that in this approximation the whole physical situation is determined by the fundamental invariant  $\rho_1(X'_1 / X_1)$  the "Fock-Dirac density function."<sup>54,286,287.</sup>

## I.2(b) Expansion of Density Functions in Terms of an Orbital Basis

### I.2(b)(i) Spin-orbital basis

Generally,  $\rho_1(X'_1 / X_1)$  may be expanded in terms of an arbitrary basis of the  $N$ -particle wavefunction. For a one-determinant wavefunction of spin-orbitals we have:

$$\rho_1(X'_1 / X_1) = \sum_{k=1}^N \sum_{\ell=1}^N \psi_k^*(X'_1) \psi_\ell(X_1) \rho_{\ell k} \quad (I.33)$$

where the elements  $\rho_{\ell k}$  form a square Hermitian  $N \times N$  matrix  $\underline{\rho}$  which is the matrix representation of  $\rho_1(X_1'/X_1)$  in this basis.

For a non-orthogonal (but linearly independent) set of spin-orbitals, this expression may be found<sup>6</sup> explicitly from equation (I.23) by replacing the determinant  $\Psi^*$  by its leading diagonal and expanding  $\Psi$  by its cofactors and integrating the terms to get:

$$\rho_1(X_1'/X_1) = \sum_{k=1}^N \sum_{\ell=1}^N \psi_k^*(X_1') \psi_{\ell}(X_1) \underline{V}^{-1}_{\ell k} \quad (\text{I.34})$$

which is

$$\rho_1(X_1'/X_1) = \sum_{k=1}^N \sum_{\ell=1}^N \psi_k^*(X_1') \psi_{\ell}(X_1) (\underline{V}^{-1})_{\ell k} \quad (\text{I.35})$$

$$\text{hence } \rho_{\ell k} = (\underline{V}^{-1})_{\ell k} \quad (\text{I.36})$$

where  $\underline{V}^{-1}$  is the inverse of  $\underline{V}$  which is the ( $N \times N$ ) matrix of overlap integrals between spin-orbitals.

$$V_{\ell k} = \int \psi_{\ell}^*(X_1) \psi_k(X_1) dX_1 \quad (\text{I.37})$$

$$\text{For orthonormal spin-orbitals } V_{\ell k} = (\underline{V}^{-1})_{\ell k} = \delta_{\ell k} \quad (\text{I.38})$$

and hence we obtain

$$\rho_1(X_1'/X_1) = \sum_{k=1}^N \psi_k^*(X_1') \psi_k(X_1) \quad (\text{I.39})$$

We may obtain the second order density function for the orthonormal case from equations (I.39) and (I.32):

$$\rho_2(X_1' X_2' / X_1 X_2) = \sum_{k=1}^N \sum_{\ell=1}^N [\psi_k^*(X_1') \psi_k(X_1) \psi_{\ell}^*(X_2') \psi_{\ell}(X_2) - \psi_k^*(X_1') \psi_{\ell}(X_1) \psi_{\ell}^*(X_2') \psi_k(X_2)] \quad (\text{I.40})$$

I.2(b)(ii) Doubly occupied MO basis

The first order density function in a non-orthogonal MO basis may be obtained from equation (I.35) by integrating over spins.

$$P_1(r_1'/r_1) = 2 \sum_{i=1}^n \sum_{j=1}^n \phi_i^*(r_1') \phi_j(r_1) (\underline{S}^{-1})_{ji} \quad (\text{I.41})$$

where  $\underline{S}^{-1}$  is the inverse of  $\underline{S}$  which is the (nxn) matrix of overlap integrals between MOs.

The expression in the case of orthonormal MOs follows since

$$(\underline{S}^{-1})_{ji} = \delta_{ji} \quad (\text{I.42})$$

we have

$$P_1(r_1'/r_1) = 2 \sum_{i=1}^n \phi_i^*(r_1') \phi_i(r_1) \quad (\text{I.43})$$

Integrating equation (I.40) over spins gives

$$P_2(r_1' r_2' / r_1 r_2) = \sum_{i=1}^n \sum_{j=1}^n [ 4 \phi_i^*(r_1') \phi_i(r_1) \phi_j^*(r_2') \phi_j(r_2) - 2 \phi_i^*(r_1') \phi_j(r_1) \phi_j^*(r_2') \phi_i(r_2) ] \quad (\text{I.44})$$

where the second term occurs with reduced weight because spin integration gives 0 or 1 depending on whether  $\psi_k$  and  $\psi_\ell$  have like or unlike spins.

From (I.43) and (I.44) we obtain

$$P_2(r_1' r_2' / r_1 r_2) = P_1(r_1'/r_1) P_1(r_2'/r_2) - \frac{1}{2} P_1(r_1'/r_2) P_1(r_2'/r_1) \quad (\text{I.45})$$

I.2(b)(iii) Non-orthogonal atomic orbital basis

The N-particle wavefunction may be expanded further in a basis of m atomic orbitals

$$\chi_1 \cdots \chi_m$$

hence



$$P_1(r_1'/r_1) = \sum_{\mu=1}^m \sum_{\nu=1}^m \chi_{\mu}^*(r_1') \chi_{\nu}(r_1) P_{\nu\mu} \quad (1.46)$$

Each MO may be expressed as a linear combination of atomic orbitals (LCAO)

$$\phi_i(r_1) = \sum_{\mu=1}^m c_{\mu i} \chi_{\mu}(r_1) \quad (1.47)$$

hence for orthonormal MOs we obtain from equations (I.43) and (I.47)

$$P_1(r_1'/r_1) = \sum_{\mu=1}^m \sum_{\nu=1}^m \left\{ 2 \sum_{i=1}^n c_{\mu i}^* c_{\nu i} \right\} \chi_{\mu}^*(r_1') \chi_{\nu}(r_1) \quad (1.48)$$

and from equation (I.46) it can be seen that

$$P_{\nu\mu} = 2 \sum_{i=1}^n c_{\mu i}^* c_{\nu i} \quad (1.49)$$

where  $P_{\nu\mu}$  is an element of the (mxm) matrix representation of  $P_1$  in the atomic orbital basis. From equations (I.46) and (I.45) we can obtain an expression for  $P_2$  in this basis, we have:

$$\begin{aligned} P_2(r_1'r_2'/r_1r_2) &= \sum_{\mu=1}^m \sum_{\nu=1}^m \sum_{\lambda=1}^m \sum_{\sigma=1}^m P_{\nu\mu} P_{\sigma\lambda} [\chi_{\mu}^*(r_1') \chi_{\nu}(r_1) \chi_{\lambda}^*(r_2') \chi_{\sigma}(r_2) \\ &- \frac{1}{2} \chi_{\mu}^*(r_1') \chi_{\sigma}(r_1) \chi_{\lambda}^*(r_2') \chi_{\nu}(r_2)] \end{aligned} \quad (1.50)$$

### 1.3 ENERGY OF A CLOSED SHELL SYSTEM

The electronic energy of a system described by  $\Psi(X_1 \dots X_N)$  is given by:

$$\langle E \rangle = \int \Psi^*(X_1 \dots X_N) \hat{H} \Psi(X_1 \dots X_N) dX_1 \dots dX_N \quad (1.51)$$

where the Hamiltonian  $\hat{H}$  is defined by equations (I.2) to (I.6).

If the terms are grouped into one-electron and two-electron parts

this expression may be written in terms of first order and second order density functions thus

$$\langle E \rangle = \int_{r_1=r_1} [\hat{h}(1) P_1(r_1'/r_1)] dr_1 + \frac{1}{2} \int \hat{g}(1,2) P_2(r_1 r_2) dr_1 dr_2 \quad (\text{I.52})$$

$$\langle E \rangle = E_{\text{one}} + E_{\text{two}} \quad (\text{I.53})$$

The primes in  $P_2$  have been dropped since  $\hat{g}(1,2)$  is simply a function of co-ordinates ( $\frac{1}{r_{12}}$ ) but they have been retained in  $P_1$  since the kinetic energy part of  $\hat{h}(1)$  contains the differential operator  $\hat{\nabla}^2$ .

The energy may be expressed in terms of doubly occupied orthogonal MOs using equations (I.43) and (I.44):

$$\begin{aligned} \langle E \rangle &= 2 \sum_{i=1}^n \langle \phi_i / h / \phi_i \rangle \\ &+ \sum_{i=1}^n \sum_{j=1}^n [ 2 \langle \phi_i \phi_i / g / \phi_j \phi_j \rangle - \langle \phi_i \phi_j / g / \phi_j \phi_i \rangle ] \end{aligned} \quad (\text{I.54})$$

$$\text{where } \langle \phi_a / h / \phi_b \rangle = \int \phi_a^*(r_1) \hat{h}(1) \phi_b(r_1) dr_1 \quad (\text{I.55})$$

$$\text{and } \langle \phi_a \phi_b / g / \phi_c \phi_d \rangle = \int \phi_a^*(r_1) \phi_b(r_1) \hat{g}(1,2) \phi_c^*(r_2) \phi_d(r_2) dr_1 dr_2 \quad (\text{I.56})$$

equation (I.54) is sometimes written:

$$\langle E \rangle = 2 \sum_{i=1}^n h_{ii} + \sum_{i=1}^n \sum_{j=1}^n [ 2J_{ij} - K_{ij} ] \quad (\text{I.57})$$

where  $J_{ij}$  is a "coulomb integral" and represents the interaction between the charge distributions  $\phi_i^* \phi_i$  and  $\phi_j^* \phi_j$  while  $K_{ij}$  is an "exchange integral" and represents an interaction due to the correlation between electrons of the same spin in different MOs.

When the orthonormal MOs are expanded in an AO basis we obtain for the energy expression from equations (I.46), (I.50) and (I.52):

$$\begin{aligned}
 \langle E \rangle &= \sum_{\mu=1}^m \sum_{\nu=1}^m P_{\nu\mu} \langle \chi_{\mu}/h/\chi_{\nu} \rangle \\
 &+ \frac{1}{2} \sum_{\mu=1}^m \sum_{\nu=1}^m \sum_{\lambda=1}^m \sum_{\sigma=1}^m P_{\nu\mu} P_{\sigma\lambda} [ \langle \chi_{\mu}\chi_{\nu}/g/\chi_{\lambda}\chi_{\sigma} \rangle \\
 &- \frac{1}{2} \langle \chi_{\mu}\chi_{\sigma}/g/\chi_{\lambda}\chi_{\nu} \rangle ] \quad (I.58)
 \end{aligned}$$

where the notation of (I.55) and (I.56) is used with  $\chi$  replacing  $\phi$

#### I.4 SCF SOLUTIONS TO SCHRODINGERS EQUATION

##### I.4(a) Hartree-Fock MOs

Using the expression (I.57) for the energy of the system and by applying the variational method, a set of differential equations for the optimum forms of the orthogonal MOs that minimise the energy, may be obtained. These are called the Hartree-Fock equations:<sup>54,288,289</sup>

$$\left\{ \hat{h}(i) + \sum_{j=1}^n (2\hat{J}_j - \hat{K}_j) \right\} \phi_i(r_1) = \sum_{j=1}^n \epsilon_{ij} \phi_j(r_1) \quad i=1,2, \dots, n \quad (I.59)$$

$$\text{where } \hat{J}_j \phi_i(r_1) = \left\{ \int \phi_j^*(r_2) \phi_j(r_2) \hat{g}(1,2) dr_2 \right\} \phi_i(r_1) \quad (I.60)$$

$$\text{and } \hat{K}_j \phi_i(r_1) = \left\{ \int \phi_j^*(r_2) \phi_i(r_2) \hat{g}(1,2) dr_2 \right\} \phi_j(r_1) \quad (I.61)$$

equation (I.59) may be abbreviated to:

$$\hat{F} \phi_i(r_1) = \sum_{j=1}^n \epsilon_{ij} \phi_j(r_1) \quad i = 1,2, \dots, n \quad (I.62)$$

or in matrix notation:

$$\hat{F} \underline{\phi} = \underline{\phi} \cdot \underline{\epsilon} \quad (I.63)$$

where  $\underline{\phi}$  is a row vector of MOs.

$\underline{\epsilon}$  is a (n x n) Hermitian matrix of elements  $\epsilon_{ij}$ . Any set of orthonormal MOs satisfying the set of equations (I.62) are hence optimum MOs that minimise the energy.

All the possible sets of orthonormal MOs satisfying equation (I.62) are related to some fixed set  $\underline{\phi}$  by a general unitary transformation  $\underline{U}$ . For example the set  $\underline{\phi}'$  is given by:

$$\underline{\phi}' = \underline{\phi} \cdot \underline{U} \quad (\text{I.64})$$

since  $\hat{F}$  is invariant to a unitary transformation, the new set  $\underline{\phi}'$  still satisfy equation (I.63), the only difference being the matrix  $\underline{\epsilon}$  which is now  $\underline{\epsilon}'$  and is given by:

$$\underline{\epsilon}' = \underline{U}^{-1} \cdot \underline{\epsilon} \cdot \underline{U} \quad (\text{I.65})$$

This indeterminacy may be removed by choosing the set  $\underline{\phi}^c$  for which  $\underline{\epsilon}$  is diagonal. This set is called the canonical MOs (CMOs) and equation (I.62) becomes an eigenvalue equation:

$$\hat{F} \phi_i = \epsilon_i \phi_i \quad i = 1, 2 \dots n \quad (\text{I.66})$$

these equations cannot be easily solved directly however except in a one-centre problem.

#### I.4(b) LCAO-MO approximation

Solutions of the Hartree-Fock equations (I.66) may be obtained by expanding each MO as a LCAO involving the constituent atoms in the molecule.<sup>290,291</sup> Equation (I.47) may be expressed in matrix notation:

$$\phi_i = \sum c_j \chi_j \quad (\text{I.67})$$

where  $\underline{\chi}$  is a row vector of AOs and  $\underline{c}_i$  is a column vector of expansion coefficients.

Applying the calculus of variations to the energy expression (equation (I.58)) we obtain equations for the AO coefficients in the  $i$ th CMO.

$$\sum_{\nu=1}^m F_{\mu\nu} c_{\nu i} = \sum_{\nu=1}^m \epsilon_i c_{\nu i} M_{\mu\nu} \quad \mu = 1, 2 \dots m \quad (\text{I.68})$$

or

$$\sum_{\nu=1}^m (F_{\mu\nu} - \epsilon_i M_{\mu\nu}) c_{\nu i} = 0 \quad \mu = 1, 2 \dots m \quad (\text{I.69})$$

where  $F_{\mu\nu}$  is the matrix element of the Hartree-Fock Hamiltonian  $\hat{F}$  over AOs, and is given by:

$$\begin{aligned} F_{\mu\nu} = & \langle \chi_{\mu} / h / \chi_{\nu} \rangle \\ & + \sum_{\lambda=1}^m \sum_{\sigma=1}^m P_{\sigma\lambda} [\langle \chi_{\mu} \chi_{\nu} / g / \chi_{\lambda} \chi_{\sigma} \rangle \\ & - \frac{1}{2} \langle \chi_{\mu} \chi_{\sigma} / g / \chi_{\lambda} \chi_{\nu} \rangle] \end{aligned} \quad (\text{I.70})$$

(notation as in equation (I.58))

and  $M_{\mu\nu}$  is the overlap integral:

$$M_{\mu\nu} = \int \chi_{\mu}^*(r_1) \chi_{\nu}(r_1) dr_1 \quad (\text{I.71})$$

In matrix notation (I.68) becomes

$$\underline{F} \underline{c}_i = \underline{M} \underline{c}_i \epsilon_i \quad (\text{I.72})$$

the values  $\epsilon_i$  will be the  $n$  lowest roots of the corresponding secular equation:

$$|\underline{F} - \epsilon \underline{M}| = 0 \quad (\text{I.73})$$

and for each root  $\epsilon_i$  the coefficients  $\underline{c}_i$  can be obtained from substitution into equation (I.72)

Since  $F_{\mu\nu}$  is itself dependent on the AO coefficients in  $P_{\sigma\lambda}$  (equations (I.70) and (I.49)) the process of solving for the  $c_i$  is iterative involving cycles of the form:

- 1) start with AO coefficients in  $c_i$   $i = 1, 2 \dots n$
  - 2) generate density matrix via equation (I.49)
  - 3) generate  $\underline{F}$  matrix from equation (I.70) and energy from equation (I.58)
  - 4) solve secular equation (I.73) for  $n$  eigenvalues and hence produce new set of AO coefficients  $c_i$   $i = 1, 2 \dots n$
  - 5) generate density matrix via equation (I.49) ...
- ... and so on.

The cycles are continued until the AO coefficients (or density matrix) at successive cycles are the same to the required accuracy. The energy should also have converged to its minimum value. Where convergence is slow, or oscillatory behaviour occurs, special interpolation procedures may be required.

#### I.4(c) The forms of the atomic orbitals

The basis functions into which the MOs may be expanded can be of many different types. One popular set of basis functions comprise the atomic orbitals of the constituent atoms in the molecule. The number of atomic orbitals  $m$  used in the expansion must be greater than  $n$ , the number of doubly occupied MOs, but otherwise can take any value. Generally the larger the value of  $m$  then the more accurate will the expansion of the MO into a LCAO be. Two specific sizes of basis set may be distinguished:

- a) A "minimal basis set" comprises those atomic orbitals up to and including the orbitals of the valence shell of each atom in the molecule, and

- b) An "extended basis set" amounts to a minimal basis set plus any number of AOs lying outside the valence shell for each atom.

Rather than using hydrogenic atomic orbitals which are solutions of the Schrodinger equation for one-electron atomic systems, approximations to these, called Slater-type orbitals<sup>292</sup> (STOs) may be used. The STOs have a simpler analytical form for the radial part of the AO function which makes many of the integrals required in MO calculations easier to evaluate. They have the form

$$R(r) = (2\zeta)^{\left\{ \frac{n_p+1}{2} \right\}} \left[ (2n_p)! \right]^{-\frac{1}{2}} r^{\left\{ n_p-1 \right\}} \exp(-\zeta r) \quad (\text{I.74})$$

where  $n_p$  is the principal quantum number, and  $\zeta$  is the orbital exponent which is ideally treated as a further variational parameter in a LCAO-MO SCF calculation but can alternatively be given an empirical value using certain well known rules.<sup>292</sup> The form of  $R(r)$  given in equation (I.74) means that STOs have no radial nodes and hence that certain AOs on the same atom are no longer orthogonal to each other, e.g. the 1s and 2s functions. This may be overcome in the case of the 1s and 2s AOs by leaving the 1s function unaltered and then constructing a 2s<sup>or</sup> function orthogonal to it by the Schmidt procedure (section I.7).

Even more attractive than STOs in the evaluation of integrals, are gaussian functions,<sup>293</sup> although these do not have such a clear chemical interpretation as STOs when used as a basis set. A compromise may therefore be reached if each STO (of a minimal basis set say) is replaced by a linear combination of a small number of gaussian-type orbitals at all points in an SCF MO

calculation.<sup>294</sup> The representations of STOs could, for example, be obtained using gaussian functions by a least squares method,<sup>295,296</sup> and will become more accurate as the size of the gaussian set increases.<sup>223</sup>

For example, the expansion could be of the form:

$$\chi_{\mu}^{\text{STO}} = \sum_{k=1}^K d_{\mu k} g_{\mu}(\alpha_k, r) \quad (\text{I.75})$$

where (in this equation only)  $K$  is the number of gaussian functions in the expansion,  $d_{\mu k}$  is a linear coefficient,  $g_{\mu}$  is a gaussian function and  $\alpha_k$  is a gaussian exponent. This sort of basis set may be used in the Gaussian 70<sup>222</sup> computer programme for the calculation of SCF MOs.

#### I.5 DIPOLE MOMENTS

Classically, the electrical dipole moment for a set of discrete charges  $q_i$  is:

$$\underline{D} = \sum_i q_i \underline{r}_i \quad (\text{I.76})$$

where  $\underline{r}_i$  is the position vector of the  $i$ th charge. Quantum mechanically, the dipole moment operator for a system of  $N$  electrons and  $L$  nuclei is

$$\hat{\underline{D}} = - \sum_{p=1}^N \hat{\underline{r}}(p) + \sum_{a=1}^L Z_a \hat{\underline{r}}(a) \quad (\text{I.77})$$

Both the electronic and nuclear contributions may be separated into  $x$ ,  $y$  and  $z$  components. We obtain:

$$\begin{aligned} \hat{\underline{D}} &= \underline{i} \hat{D}_x + \underline{j} \hat{D}_y + \underline{k} \hat{D}_z \\ \hat{\underline{r}}(p) &= \underline{i} \hat{x}(p) + \underline{j} \hat{y}(p) + \underline{k} \hat{z}(p) \\ \hat{\underline{r}}(a) &= \underline{i} \hat{x}(a) + \underline{j} \hat{y}(a) + \underline{k} \hat{z}(a) \end{aligned} \quad (\text{I.78})$$



Now, since in the quantum mechanical description the nuclei are considered fixed while the electrons are described by the wavefunction  $\Psi$  we obtain (via equations (I.16) (I.17) and (I.22)) for the z component of the total dipole moment:

$$\langle D_z \rangle = -\int \hat{z}(1) P_1(r_1) dr_1 + \sum_{a=1}^L Z_a z(a) \quad (\text{I.79})$$

where the primes in the density function have been dropped since we are dealing with a co-ordinate operator only.

Hence

$$\langle D_z \rangle = \langle D_z \rangle_{\text{elec}} + D_z \text{ nuclear} \quad (\text{I.80})$$

the other components may be expressed similarly.

We may express  $\langle D_z \rangle_{\text{elec}}$  in terms of MOs. Using equation (I.41) we have:

$$-\langle D_z \rangle_{\text{elec.}} = 2 \sum_{i=1}^n \sum_{j=1}^n \langle \phi_i / z / \phi_j \rangle (\underline{S}^{-1})_{ji} \quad (\text{I.81})$$

$$\text{where } \langle \phi_a / z / \phi_b \rangle = \int \phi_a^*(r_1) \hat{z}(1) \phi_b(r_1) dr_1 \quad (\text{I.82})$$

equation (I.81) may be written

$$\begin{aligned} -\langle D_z \rangle_{\text{elec.}} &= 2 \sum_{i=1}^n \langle \phi_i / z / \phi_i \rangle (\underline{S}^{-1})_{ii} \\ &+ 4 \sum_{i=1}^n \sum_{\substack{j=1 \\ (i < j)}}^n \langle \phi_i / z / \phi_j \rangle (\underline{S}^{-1})_{ji} \end{aligned} \quad (\text{I.83})$$

where the first sum could be called the "diagonal terms" and the second (double) sum the "off-diagonal terms". For orthonormal molecular orbitals equation (I.83) becomes

$$-\langle D_z \rangle_{\text{elec}} = 2 \sum_{i=1}^n \langle \phi_i / z / \phi_i \rangle \quad (\text{I.84})$$

or

$$-\langle D_z \rangle_{\text{elec}} = \sum_{i=1}^n z^i_{\text{elec}} \quad (\text{I.85})$$

where the  $z$  component of the electronic moment is simply a sum of contributions each arising from one of the  $n$  occupied MOs.

The expression (I.83) for non-orthogonal MOs may be put in the form (I.85) by defining:

$$z^i_{\text{elec}} = 2 \langle \phi_i / z / \phi_i \rangle (\underline{S}^{-1})_{ii} + 2 \sum_{\substack{j=1 \\ (j \neq i)}}^n \langle \phi_i / z / \phi_j \rangle (\underline{S}^{-1})_{ji} \quad (\text{I.86})$$

where the "off-diagonal terms" have been allocated amongst the "diagonal terms" such that the overlap contribution arising from two MOs has been divided equally between them.

The total dipole moment  $\underline{D}$  and each of the  $x$ ,  $y$  and  $z$  components are independent of the choice of origin for a neutral molecule. However, the electronic contribution alone and each of the MO contributions  $z^i_{\text{elec}}$  are origin dependent.

It is possible to partition the total nuclear charge among the  $n$  MOs so that the expression (I.79) for the total  $z$  component of the dipole moment becomes

$$\langle D_z \rangle = - \sum_{i=1}^n z^i_{\text{elec}} + \sum_{a=1}^L \sum_{i=1}^n Z_{ai} z(a) \quad (\text{I.87})$$

where  $Z_{ai}$  is the amount of positive charge of nucleus  $a$  allocated to the  $i$ th MO.

Obviously

$$\sum_{i=1}^n Z_{ai} = Z_a \quad (\text{I.88})$$

Equation (I.87) may be written

$$\langle D_z \rangle = \sum_{i=1}^n \left[ z^i_{elec} + \sum_{a=1}^L z_{ai} z(a) \right] \quad (I.89)$$

$$\text{or } \langle D_z \rangle = \sum_{i=1}^n z^i \quad (I.90)$$

where  $z^i$  is the total moment of the  $i$ th MO and its corresponding nuclear charge. This is independent of the origin of co-ordinates provided there is no net positive or negative charge associated with  $z^i$ . Since each MO is doubly occupied this means that:

$$\sum_{a=1}^L z_{ai} = 2 \quad (I.91)$$

When the MOs are LMOs corresponding to two-centre bonds or lone pairs the  $z^i$  may be called bond or lone pair moments. In this case the allocation of nuclear charge satisfying (I.91) is usually taken to be.<sup>30,200,297,298</sup>

$$\begin{aligned} z_{ai} = 2 \quad \text{when } \phi_i \text{ is a lone pair on atom a} & \quad ) \\ & \quad ) \\ z_{ai} = z_{bi} = 1 \quad \text{when } \phi_i \text{ is a bond between atoms a and b} & \quad ) \end{aligned} \quad (I.92)$$

although many other allocation schemes not necessarily satisfying equation (I.91) are of course possible.<sup>193</sup> Using this formalism the expression for the  $z$  component of the dipole moment of the  $i$ th MO becomes:

$$z^i = 2 \langle \phi_i / z / \phi_i \rangle (\underline{S}^{-1})_{ii} + 2 \sum_{\substack{j=1 \\ (j \neq i)}}^n \langle \phi_i / z / \phi_j \rangle (\underline{S}^{-1})_{ji} + 2z(a) \quad (I.93)$$

when  $\phi_i$  is a lone pair or inner shell on atom  $a$ , and:

$$z^i = 2 \langle \phi_i / z / \phi_i \rangle (\underline{S}^{-1})_{ii} + 2 \sum_{\substack{j=1 \\ (j \neq i)}}^n \langle \phi_i / z / \phi_j \rangle (\underline{S}^{-1})_{ji} + z(a) + z(b) \quad (I.94)$$

when  $\phi_i$  is a bond between atoms  $a$  and  $b$ . The total  $z$  component is then given from equation (I.90). The  $x$  and  $y$  components are defined entirely analogously.

## I.6 ELECTRON POPULATION ANALYSIS

From the definition of the 1st order density function, equation (I.23), and the normalisation condition of  $\Psi$ , equation (I.7), it can be seen that:

$$\int \rho_1(X_1) dX_1 = N \quad (\text{I.95})$$

or, by integrating over spin:

$$\int P_1(r_1) dr_1 = N \quad (\text{I.96})$$

By expanding  $P_1$  in terms of an MO or AO basis set and integrating, the total number of electrons,  $N$ , can be broken up into "electron populations" associated with MOs, AOs or both. This procedure of "Population Analysis" can help give insights into the electronic structure of molecules. 118-123.

For MOs not necessarily orthogonal (but linearly independent) we may proceed as follows:

From equation (I.41) and the expansions:

$$\begin{aligned} \phi_i(r_1) &= \sum_{\mu=1}^m c_{\mu i} \chi_{\mu}(r_1) \\ \phi_j(r_1) &= \sum_{\nu=1}^m c_{\nu j} \chi_{\nu}(r_1) \end{aligned} \quad (\text{I.97})$$

we obtain

$$P_1(r_1) = 2 \sum_{i=1}^n \sum_{j=1}^n \sum_{\mu=1}^m \sum_{\nu=1}^m c_{\mu i}^* c_{\nu j} (\underline{S}^{-1})_{ji} \chi_{\mu}^*(r_1) \chi_{\nu}(r_1) \quad (\text{I.98})$$

by integrating:

$$N = 2 \sum_{i=1}^n \sum_{j=1}^n \sum_{\mu=1}^m \sum_{\nu=1}^m c_{\mu i}^* c_{\nu j} (\underline{S}^{-1})_{ji} M_{\mu\nu} \quad (\text{I.99})$$

where  $M_{\mu\nu}$  is defined in equation (I.71).

Equation (I.99) may be manipulated to give (for real functions)

$$N = \sum_{i=1}^n N(i) = \sum_{i=1}^n \left\{ \sum_{\mu=1}^m \sum_{\nu=1}^m 2 c_{\mu i} c_{\nu i} (\underline{S}^{-1})_{ii} M_{\mu\nu} + \sum_{\substack{j=1 \\ (j \neq i)}}^n \sum_{\mu=1}^m \sum_{\nu=1}^m 2 c_{\mu i} c_{\nu j} (\underline{S}^{-1})_{ji} M_{\mu\nu} \right\} \quad (\text{I.100})$$

this becomes in the orthonormal MO case

$$N = \sum_{i=1}^n N(i) = \sum_{i=1}^n \left\{ \sum_{\mu=1}^m 2 c_{\mu i}^2 + \sum_{\mu=1}^m \sum_{\nu=1}^m 4 c_{\mu i} c_{\nu i} M_{\mu\nu} \right\} \quad (\text{I.101})$$

( $\mu > \nu$ )

where  $N(i)$  is what Mulliken<sup>118</sup> defines "the total population in MO  $\phi_i$ ". Alternatively we may obtain from equation (I.99)

$$N = \sum_{\mu=1}^m N(\mu) = \sum_{\mu=1}^m \left\{ \sum_{i=1}^n \sum_{j=1}^n 2 c_{\mu i} c_{\mu j} (\underline{S}^{-1})_{ji} + \sum_{\substack{\nu=1 \\ (\nu \neq \mu)}}^m \sum_{i=1}^n \sum_{j=1}^n 2 c_{\mu i} c_{\nu j} (\underline{S}^{-1})_{ji} M_{\mu\nu} \right\} \quad (\text{I.102})$$

which for orthonormal MOs reduces to:

$$N = \sum_{\mu=1}^m N(\mu) = \sum_{\mu=1}^m \left\{ \sum_{i=1}^n 2 c_{\mu i}^2 + \sum_{i=1}^n \sum_{\substack{\nu=1 \\ (\nu \neq \mu)}}^m 2 c_{\mu i} c_{\nu i} M_{\mu\nu} \right\} \quad (\text{I.103})$$

where  $N(\mu)$  may be defined<sup>118</sup> as "the total gross population in

AO  $\chi_{\mu}$ ". We may now go on to define a population  $N(i, \mu)$  such that:

$$N = \sum_{i=1}^n \sum_{\mu=1}^m N(i, \mu) \quad (\text{I.104})$$

$N(i, \mu)$  may be defined<sup>118</sup> as "the partial gross population in AO

$\chi_{\mu}$  in MO  $\phi_i$ ". From reference 118 we obtain for the orthonormal MO

case (in our notation):

$$N = \sum_{i=1}^n \sum_{\mu=1}^m N(i,\mu) = \sum_{i=1}^n \sum_{\mu=1}^m \left\{ 2c_{\mu i}^2 + \sum_{\substack{v=1 \\ (v \neq \mu)}}^m 2c_{\mu i} c_{v i} M_{\mu v} \right\} \quad (\text{I.105})$$

For non-orthogonal MOs in a non-orthogonal AO basis two different expressions for  $N(i,\mu)$  are obtained depending on which AO index is associated with each MO index in the expansions (I.97).

A more general expression that circumvents this problem may be obtained by using, instead of equation (I.99), the equation:

$$N = N/2 + N/2 = \sum_{i=1}^n \sum_{j=1}^n \sum_{\mu=1}^m \sum_{v=1}^m (\underline{S}^{-1})_{ji} M_{\mu v} (c_{\mu i} c_{vj} + c_{vi} c_{\mu j}) \quad (\text{I.106})$$

This equation leads to identical expressions for all the populations defined above, and we obtain for  $N(i,\mu)$

$$\begin{aligned} N(i,\mu) = & 2 c_{\mu i}^2 (\underline{S}^{-1})_{ii} + \sum_{\substack{v=1 \\ (v \neq \mu)}}^m 2c_{\mu i} c_{v i} (\underline{S}^{-1})_{ii} M_{\mu v} \\ & + \sum_{\substack{j=1 \\ (j \neq i)}}^n 2c_{\mu i} c_{\mu j} (\underline{S}^{-1})_{ji} + \sum_{\substack{j=1 \\ (j \neq i)}}^n \sum_{\substack{v=1 \\ (v \neq \mu)}}^m (c_{\mu i} c_{vj} + c_{vi} c_{\mu j}) (\underline{S}^{-1})_{ji} M_{\mu v} \end{aligned} \quad (\text{I.107})$$

where the terms have been collected into four groups for clarity.

This reduces to equation (I.105) for orthonormal MOs.

All the definitions above satisfy the relations:

$$\sum_{i=1}^n \sum_{\mu=1}^m N(i,\mu) = \sum_{i=1}^n N(i) = \sum_{\mu=1}^m N(\mu) = N \quad (\text{I.108})$$

## I.7 METHODS OF ORTHOGONALISATION

It is sometimes necessary, and was so in this work, to generate an orthonormal set of functions from a non-orthogonal but linearly independent (LI) set of functions. The methods which may be used have been reviewed by Lowdin<sup>299</sup> and one is shown below.

The general problem may be formulated in the following way.

A non-orthogonal, LI, normalised set of  $n$  real functions

$\gamma_1, \gamma_2 \dots \gamma_n$ , generate a square ( $n \times n$ ) matrix of overlap integrals  $\underline{S}$  with elements  $S_{ij}$

$$S_{ij} = \int \gamma_i(r) \gamma_j(r) dr = \langle \gamma_i / \gamma_j \rangle \quad (\text{I.109})$$

In matrix notation where  $\underline{\gamma}$  is a row vector of functions, this is

$$\underline{S} = \langle \underline{\gamma} / \underline{\gamma} \rangle \quad (\text{I.110})$$

A real, orthonormal set of  $n$  functions  $\underline{\theta}$  may be formed by a linear transformation of the set  $\underline{\gamma}$  by a square  $n \times n$  matrix  $\underline{A}$ . This is written

$$\underline{\theta} = \underline{\gamma} \cdot \underline{A} \quad (\text{I.111})$$

The problem is hence to find a matrix of coefficients  $\underline{A}$  such that

$$\begin{aligned} \langle \underline{\theta} / \underline{\theta} \rangle &= \langle \underline{\gamma} \underline{A} / \underline{\gamma} \underline{A} \rangle \\ &= \tilde{\underline{A}} \langle \underline{\gamma} / \underline{\gamma} \rangle \underline{A} \\ &= \tilde{\underline{A}} \cdot \underline{S} \cdot \underline{A} = \underline{I}_n \end{aligned} \quad (\text{I.112})$$

where  $\underline{I}_n$  is the unit matrix of order  $n$  and  $\tilde{\underline{A}}$  is the transpose of  $\underline{A}$ . There is no unique solution to equation (I.112) so that many sets of orthogonal functions can be obtained from the non-orthogonal set  $\underline{\gamma}$ .

If the non-orthogonal set  $\underline{\gamma}$  are the constituent functions of a one-determinant wavefunction then the wavefunction will be unchanged for computational purposes if the set  $\underline{\theta}$  replace the set  $\underline{\gamma}$ .

This is because the two sets are linked by a linear transformation (I.111) and, as was explained in Section I.1(b) a one-determinant wavefunction is invariant (besides a "phase-factor") to a linear

transformation amongst its constituent MOs.

The simplest orthogonalising procedure to apply is the Schmidt method in which each member of the set, in order, is orthogonalised against all the previous members and subsequently normalised. The method may be expressed as follows. For a non-orthogonal pair of functions  $\gamma_1$  and  $\gamma_2$ , an orthogonal pair,  $\theta_1$  and  $\theta_2$ , are obtained by:

$$\begin{aligned} \theta_1 &= \gamma_1 && ) \\ & && ) \\ \theta_2 &= N_{12} \{ \gamma_2 - \gamma_1 \langle \gamma_1 / \gamma_2 \rangle \} && ) \end{aligned} \quad (\text{I.113})$$

where  $N_{12}$  is a normalising constant and  $\theta_2$  is the component of  $\gamma_2$  orthogonal to  $\gamma_1$ . The method is easily extended to obtain an orthonormal set of  $n$  functions from a non-orthogonal set  $\gamma_1^\circ, \gamma_2^\circ, \dots, \gamma_n^\circ$  in a step-wise process. Firstly,  $\gamma_2^\circ \dots \gamma_n^\circ$  are made orthogonal to  $\gamma_1^\circ$  in a series of changes of the type given by (I.113). The superscript denotes the number of times the function has been changed. The new functions are

$$\gamma_i^1 = N_{1i} \{ \gamma_i^\circ - \gamma_1^\circ \langle \gamma_1^\circ / \gamma_i^\circ \rangle \} \quad i = 2 \dots n \quad (\text{I.114})$$

Since  $\gamma_2^1 \dots \gamma_n^1$  are now all orthogonal to  $\gamma_1^\circ$  they may be combined linearly without losing orthogonality to  $\gamma_1^\circ$ . The functions  $\gamma_3^1 \dots \gamma_n^1$  are now made orthogonal to  $\gamma_2^1$  in a similar series of changes

$$\gamma_i^2 = N_{2i} \{ \gamma_i^1 - \gamma_2^1 \langle \gamma_2^1 / \gamma_i^1 \rangle \} \quad i=3, \dots, n \quad (\text{I.115})$$

This process is repeated until all functions are mutually orthogonal.

The resulting set is  $\gamma_1^\circ, \gamma_2^1 \dots \gamma_n^{n-1}$ . It can be seen that  $\gamma_1^\circ$  is left unchanged by the method,  $\gamma_2^1$  is changed once, and later functions in the



series are changed to greater and greater extents.

This fact has led to the search for other methods of orthogonalisation in cases when the forms of the final orthogonal set are important.<sup>299</sup> This was not the case in this work, so that the straightforward Schmidt procedure was used.

This procedure corresponds to a solution of equation (I.112) in which the matrix  $\underline{A}$  is triangular. Although the individual elements of  $\underline{A}$  become rather cumbersome for increasing  $n$ , the method is easy to use in the computer programme.

## APPENDIX II    COMPUTATIONAL DETAILS

All the computer programmes employed in this work were written in FORTRAN and were run on the CDC 7600 and 6600 machines at the University of London Computer Centre (ULCC).

### II.1 Gaussian Seventy

Gaussian 70, originally written by W.J. Hehre et al.<sup>222</sup> and modified for implementation on the ULCC CDC 7600 by P. Mallinson,<sup>224</sup> was used to generate a suitable starting set of CMOs and for the evaluation of integrals over AOs for each molecule considered. The geometry for each molecule was defined for Gaussian 70 by specifying bond lengths and angles, except in the case of methane, where in order to remove CMO degeneracies, the geometry was defined by direct input of the atomic co-ordinates.

To ensure that strict convergence was achieved in each SCF calculation, the iterative procedure was continued until a change of less than  $10^{-7}$  was obtained in the density matrix on successive cycles. Where slight oscillatory behaviour was encountered during the iteration to an energy minimum, for example in CO, a version<sup>300</sup> of Gaussian 70 using the technique of "level shifting"<sup>301</sup> was used.

For each molecule, the output file produced by Gaussian 70 that contained the AO coefficients in the CMOs was written to disc storage along with the files containing the following integrals over AOs: the kinetic and potential energy integrals, the two-electron integrals, the AO overlap integrals and the x, y and z dipole moment integrals. Only those two-electron integrals greater than  $10^{-6}$  and the lower triangle of each matrix of one-electron integrals were

stored. For the technique used to economically store the two-electron integrals and associated AO indices into integer words see ULCC Bulletin B5/10.2.<sup>224</sup>

## II.2 ENLOC7

A computer programme called ENLOC7 was written in order to generate the many possible bond and lone pair "structures" and associated LMOs using the method of Chapter 4. From such LMOs the programme also calculated other functions. A flow-diagram representing the components of the programme is shown in Figures II.1 and II.2.

### II.2(a) Preliminaries

The starting CMOs and integrals over AOs were read into ENLOC7 from disc, and other data specifying the calculation, including the atoms in the molecule, their co-ordinates, the number of basis AOs, the starting values of the transforming parameters and other parameters required in library subroutines, were read in from punched cards. The AO coefficients and one-electron integrals were read into two-dimensional arrays while the two-electron integrals and indices were read into a one-dimensional array of length 3200. This length was sufficient since in none of the molecules studied did the number of two-electron integrals of the required size exceed 1600.

The structure imposed on the CMOs to be transformed was specified in two stages. Firstly, the numbers of lone pairs (MOs having contributions from one atom only) and two-centre bonds (MOs having contributions from two atoms only) were fixed. This part definition of the structure was referred to as a specific "case". Secondly,

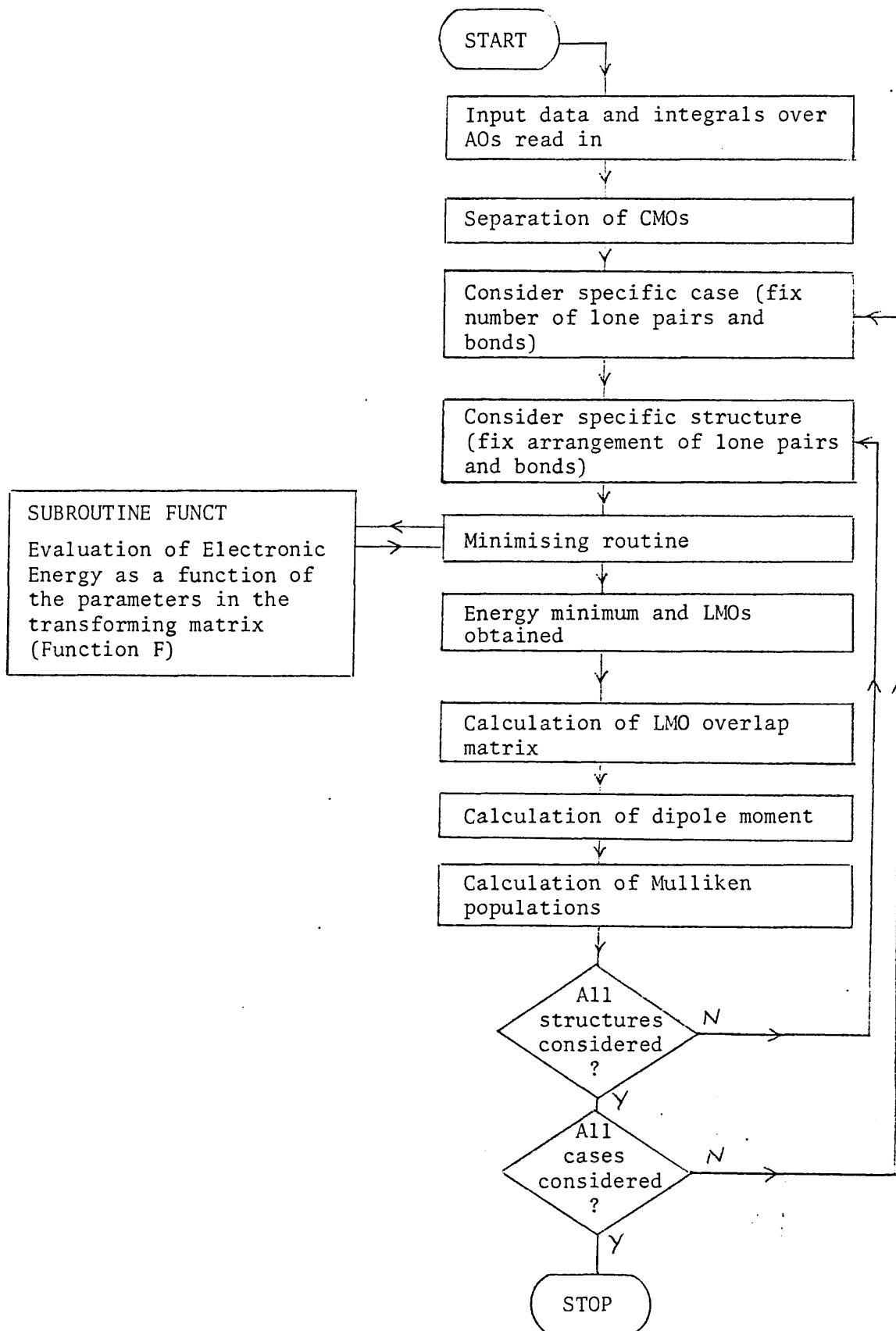


Figure II.1 Flow-diagram of ENLOC7

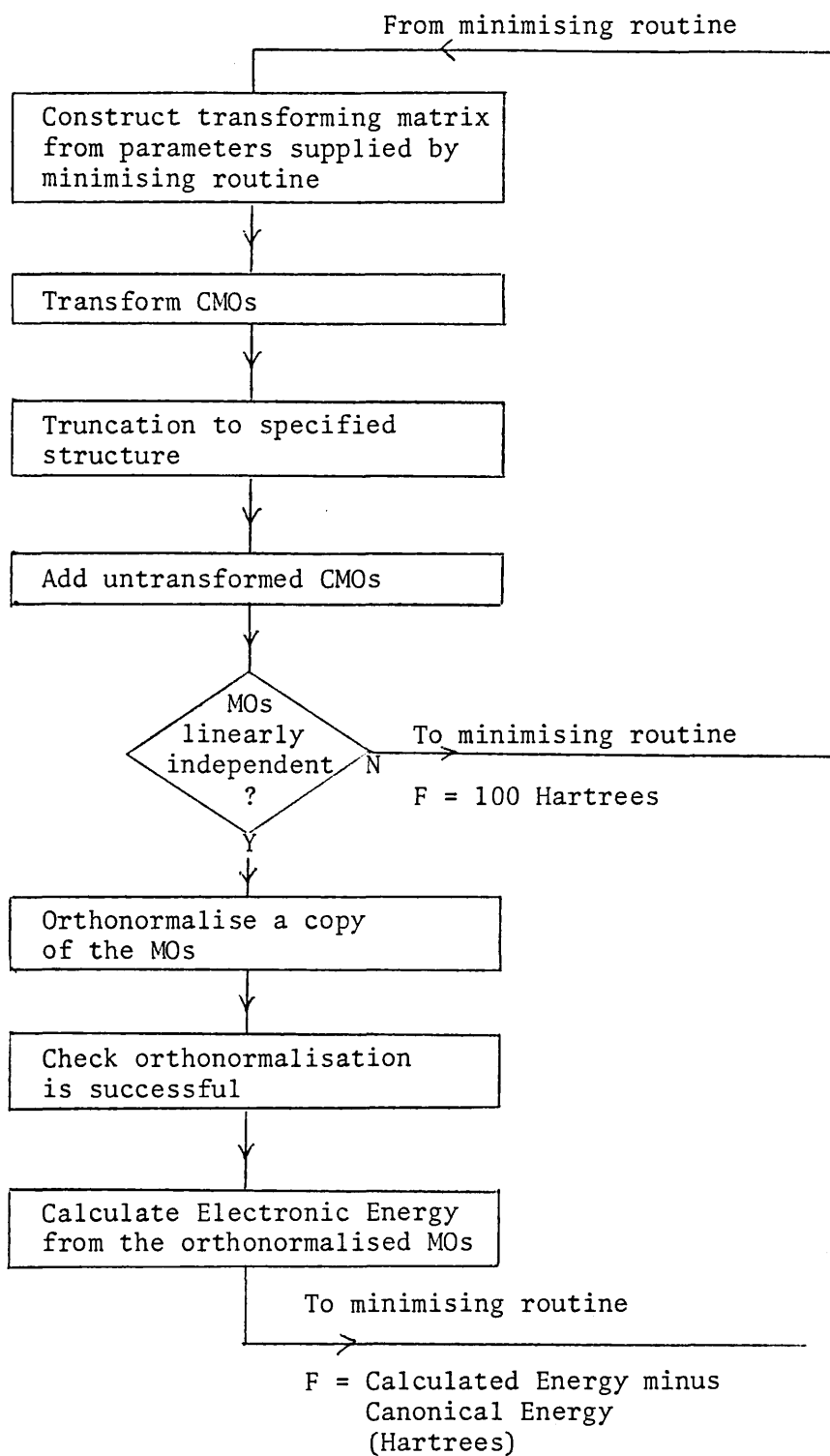


Figure II.2 Flow-diagram of subroutine FUNCT.

within each "case" the structure was completely defined by fixing the arrangement of the lone pairs and bonds amongst the atoms. The programme looped over all possible structures within each case and then over all possible cases. In the first version of ENLOC7 the lone pairs and bonds comprising a structure were permuted amongst the MOs to be transformed. In order to save computer time in a second version of the programme, this interchanging of the MO labels was not carried out since the different permutations gave the same energy and LMOs on all but rare occasions. The variation in the starting values of the transformation parameters in any case ensured that the endpoint LMOs were not dependent on the character of individual CMOs.

Another source of potential time-wasting, encountered in  $\text{NH}_3$  and  $\text{CH}_4$ , was the large number of "equivalent" structures that differed only in hydrogen atom labels. This problem was circumvented by performing an initial loop over all the structures in each molecule - without undertaking any computation - to identify the equivalent ones. A selection of these were then chosen at random for energy minimisation.

#### II.2(b) Energy minimisation

Once a structure consisting of lone pairs and bonds was fixed then the programme ENLOC7 entered a minimising subroutine, E04CCF, from Mark 6 of the NAG (Numerical Algorithms Group Ltd.) library. This subroutine minimised an energy function,  $F$  (the electronic energy minus the canonical electronic energy) of several independent variables (the transforming matrix parameters) by the Simplex method.<sup>302,303</sup> This method tends to be slow (derivatives of the

function with respect to the variables were not supplied) but it is robust. In early work, a different minimising subroutine, VA04A, from the Harwell Subroutine Library was used. This routine employed a different method which again did not require derivatives.<sup>304</sup> Results from the two methods were identical, and while both used a similar amount of computer time, the NAG subroutine was able to locate an energy minimum for higher energy structures on occasions when the Harwell subroutine could not. E04CCF was hence the preferred routine and was used in all subsequent work.

After the minimising routine was supplied with an arbitrary starting set of independent variables, it iterated to a minimum of the function  $F$  by employing another subroutine FUNCT which calculated the value of  $F$  for any set of values of the parameters.

For the larger molecules examined it was found that a disproportionate amount of computer time was being spent on the energy minimisation of 'bizarre' high energy structures. To help correct this situation in a later version of ENLOC7, the value of the energy function  $F$  after forty iterations was compared with a predetermined threshold value (say  $0.6H$ ) and if a reduction to this function value had not been achieved, energy minimisation for this structure was abandoned and the next structure was considered.

The computational procedures required in order to return a value of  $F$  to subroutine FUNCT are outlined below.

#### II.2(b)(i) Transformation, Truncation and Testing

A general orthogonal matrix was constructed by the successive multiplication of  $\frac{1}{2}R(R-1)$  orthogonal matrices, each being a function

of one independent variable only, as shown in section 4.3(c).<sup>225</sup> This orthogonal matrix was then used to transform the relevant CMOs by simple matrix multiplication. The rotated MOs were then truncated, according to the structure previously specified, by copying the required AO coefficients into a second array. They were then normalised.

The untransformed CMOs were next recombined with the truncated MOs and the resulting matrix of AO coefficients tested for linear dependence. This test was performed using subroutine MFGR from the SSP (Scientific subroutine package) library, which used the standard Gaussian elimination technique to find the rank (the number of linearly independent columns) of the matrix. When the rank was less than the total number of columns, a large function value, F, was returned to the minimising routine and no further operations in the function evaluation were executed,

When the MOs were linearly independent, a copy of them was orthonormalised by the Schmidt procedure<sup>299</sup> (see Part 7 of Appendix I). This was carried out in subroutine ORTHOG. The success of the orthonormalisation was checked by forming the matrix of overlap integrals between the MOs and ensuring that this was the unit matrix.

#### II.2(b)(ii) Energy calculation

Having obtained an orthonormal set of MOs expressed in LCAO form, corresponding to the non-orthogonal truncated MOs, the electronic energy was calculated. This was undertaken by using equation (I.58) of Appendix I and the one-electron kinetic and potential energy integrals and the two-electron integrals. The



actual procedure adopted involved the construction of the first order density matrix from the AO coefficients as in equation (I.49) followed by the computation of the one-electron contribution to the electronic energy from the density matrix and the one-electron integrals according to the first term in equation (I.58). The two-electron contribution to the energy was computed in two stages.

In the first stage, the two-electron part of the matrix representation  $\underline{F}$  of the Hartree-Fock Hamiltonian in the AO basis was constructed using the second term of equation (I.70). (Subroutine FOFCL0 of Gaussian 70 which adds the various contributions from each two-electron integral to the relevant elements of  $\underline{F}$  was utilised at this stage). The two-electron energy calculation was completed by adding the products of corresponding elements of the density matrix and the two-electron part of the  $\underline{F}$  matrix following the second term in equation (I.58). The total electronic energy was the sum of the one and two-electron parts.

The function F (the electronic energy minus the canonical energy) was thus returned to the minimising routine.

### II.2(c) Endpoint LMOs

When the minimising subroutine had iterated to an energy minimum, the non-orthogonal truncated LMOs (obtained immediately before orthonormalisation) became the endpoint LMOs for that structure. Besides displaying the LMOs and the corresponding electronic energy, other calculations using the LMOs were undertaken.

Firstly, in subroutine WAVEFN, the matrix of overlap integrals between the LMOs was computed, the determinantal wavefunction comprising the LMOs was normalised and the overlap with the canonical wave-

function was found. (NAG library subroutine F03AAF was used to take the determinant of a matrix using the factorisation method of Crout.<sup>305</sup>) Secondly, the electrical dipole moment was calculated both from the density matrix formed from orthonormal AO coefficients in subroutine DOMOS, and directly from the non-orthogonal LMOs in subroutine DLMOS using the x, y and z dipole moment integrals obtained from Gaussian 70. The dipole moment integrals over LMOs were also displayed so that the total dipole moment could be partitioned into LMO components after part 5 of Appendix I. Finally, the population analysis of the LMO wavefunction was undertaken in subroutine POPAN using the equations in part 6 of Appendix I.

The programme ENLOC7 repeated the above procedures for all possible structures (or a selection for the larger molecules) and hence allowed an energy diagram (Chapters 4 and 5) to be constructed, from which the PLMO structure, PLMOs and associated properties could be obtained.

#### II.2(d) Computing time

Approximate figures for the number of energy calculations required to achieve an energy minimum and the corresponding processing time taken are shown in Table II.1. These numbers refer to the PLMO structure for each molecule. The time includes that taken for the computation of Mulliken populations and dipole moments etc., and is the Central Processing Unit (CPU) time of the ULCC CDC 7600 machine.

TABLE II.1 PROCESSING RESOURCES REQUIRED TO OBTAIN AN ENERGY  
MINIMUM FOR THE PLMOs OF EACH MOLECULE

(For explanation, see narrative)

| Molecule         | Number of Energy Calculations | CPU Time(s) |
|------------------|-------------------------------|-------------|
| HCN              | 150                           | 2.5         |
| N <sub>2</sub>   | 150                           | 1.5         |
| CO               | 150                           | 1.5         |
| H <sub>2</sub> O | 150                           | 1.0         |
| NH <sub>3</sub>  | 800                           | 8.0         |
| CH <sub>4</sub>  | 800                           | 11.0        |

The number of energy calculations required for other structures for these molecules varied from 50 to 2000. To complete a thorough search of all structures for the larger molecules hence took several minutes.

### II.3 BOND AND ANGLE DEFORMATION IN WATER

The investigation of different geometries of the water molecule (Chapter 11) followed much the same lines as the investigation of the different example molecules. For every geometry chosen for H<sub>2</sub>O the Gaussian 70 programme was run to yield a set of CMOs, a total energy value and the various integrals over AOs. Using the CMOs and the integrals, the ENLOC7 programme was run (for the PLMO structure only) to generate the PLMOs, a value of the total energy corresponding to the PLMOs, and the dipole moment etc. calculated from them.

The geometries used for H<sub>2</sub>O were chosen to simulate slight bond and angle deformation. Hence by fitting the values of the total energy obtained for the CMOs and for the PLMOs to quadratic curves (using a standard graph plotter programme), it was possible to find the energy minimum geometries and to calculate force constants.

The computing time required to generate the PLMOs at the various geometries was close to the value in Table II.1 in each case.

APPENDIX III ABBREVIATIONS AND SYMBOLS USED

|       |  |
|-------|--|
| AO    | atomic orbital                             |
| AG    | Adams-Gilbert (formalism)                  |
| CI    | configuration interaction                  |
| CMO   | canonical molecular orbital                |
| CPU   | central processing unit                    |
| HAO   | hybrid atomic orbital                      |
| H-F   | Hartree-Fock                               |
| INDO  | incomplete neglect of differential overlap |
| LCAO  | linear combination of atomic orbitals      |
| LMO   | localised molecular orbital                |
| LAO   | localised atomic orbital                   |
| MO    | molecular orbital                          |
| M & P | Magnasco and Perico                        |
| NAG   | Numerical Algorithms Group Ltd.,           |
| PLMO  | perfectly localised molecular orbital      |
| PR    | population ratio                           |
| SCF   | self consistent field                      |
| SLO   | strictly localised orbital                 |
| STO   | Slater-type (atomic) orbital               |
| SSP   | Scientific Subroutine Package              |
| ULCC  | University of London Computer Centre       |
| VB    | valence bond                               |
| VSEPR | valence shell electron pair repulsion      |
| Å     | Angstrom unit                              |
| D     | Debye unit                                 |
| e     | electron (charge) unit                     |
| H     | Hartree unit                               |

|                                 |  |
|---------------------------------|--|
| $R(X-Y)$                        | bond length of X-Y bond                                      |
| $R_1, R_2$                      | $R(O-H_1)$ and $R(O-H_2)$ respectively in $H_2O$             |
| $R_e$                           | equilibrium bond length (energy minimum value)               |
| $\theta$                        | internuclear angle (in $H_2O$ )                              |
| $k_R$                           | bond force constant  |
| $\delta R$                      | displacement from equilibrium bond length                    |
| $k_\theta$                      | angular force constant                                       |
| $\delta \theta$                 | displacement from equilibrium internuclear angle             |
| $\phi$                          | molecular orbital  |
| $\underline{\phi}$              | row vector of molecular orbitals                             |
| $\underline{\phi}^C$            | row vector of canonical molecular orbitals                   |
| $\underline{\phi}^R$            | row vector of transformed CMOs                               |
| $\underline{\phi}^T$            | row vector of truncated and renormalised MOs                 |
| $k_X$                           | inner shell MO on atom X                                     |
| $\sigma$                        | sigma MO   |
| $\pi$                           | pi MO  |
| $\lambda_X$                     | lone pair LMO on atom X                                      |
| $\mu_{XY}$                      | bond LMO between atoms X and Y                               |
| X-Y                             | a two-centre bond LMO between atoms X and Y                  |
| $X \approx Y$                   | two two-centre bond LMOs between atoms X and Y               |
| $X \overset{\lambda}{\times}$   | a lone pair LMO on atom X                                    |
| $X \overset{\mu}{\text{---}} Y$ | a two-centre bond LMO between non-neighbouring atoms X and Y |
| $\chi$                          | atomic orbital   |
| $\underline{\chi}$              | row vector of atomic orbitals                                |
| $1s_X, 2s_X, 2p_X$              | specific Slater-type AOs on atom X                           |

|   |  |
|---|--|
| $2s_X^{\text{or}}$                                      | a $2s_X$ AO orthogonalised to the $1s_X$ AO                        |
| $h_{X(Y)}$  | bonding HAO on atom X, pointing to atom Y                          |
| R   | number of CMOs to be transformed                                   |
| $\underline{T}$   | orthogonal transforming matrix (RxR)                               |
| $\gamma_{ij}$   | general independent parameter in a transforming matrix             |
| $C_{ij}$  | $\text{Cos } \gamma_{ij}$  |
| $\Delta$  | measure of the non-orthogonality of the PLMOs,<br>equation (4.5)   |
| $n\sigma$   | number of sigma PLMOs (including inner shells)                     |
| $D(X-Y)$  | dissociation energy of the X-Y bond                                |
| $\Psi$  | electronic wavefunction  |
| $\Psi_{\text{CMO}}$                                     | wavefunction constructed from the CMOs                             |
| $\Psi_{\text{LMO}}$                                     | wavefunction constructed from the LMOs                             |
| $\langle \Psi_{\text{CMO}} / \Psi_{\text{LMO}} \rangle$ | overlap of the wavefunctions constructed from the<br>CMOs and LMOs |
| $\hat{H}$   | Hamiltonian operator   |
| E   | electronic energy  |
| $X_1$   | Space-Spin Co-ordinate of electron 1 (or point 1)                  |
| $s_1$   | spin co-ordinate of electron 1 (or point 1)                        |
| $r_1$   | spatial co-ordinate of electron 1 (or point 1)                     |
| N   | number of electrons  |
| $n(= N/2)$  | number of doubly occupied molecular (spatial) orbitals             |
| p,q   | indices over electrons   |
| k, l  | indices over spin-orbitals   |
| i,j   | indices over molecular orbitals                                    |
| $\mu, \nu, \lambda, \sigma$                             | indices over atomic orbitals                                       |

|                               |   |
|-------------------------------|---|
| $a, b$                        | indices over atoms  |
| $K$                           | index over distinct ordered configurations of spin-orbitals |
| $L$                           | number of atoms   |
| $\hat{h}(p)$                  | one-electron Hamiltonian operator                           |
| $\hat{g}(p, q)$               | two-electron Hamiltonian operator                           |
| $\hat{v}^2(p)$                | kinetic energy operator                                     |
| $\hat{V}(p)$                  | potential energy operator                                   |
| $\vec{r}_p$                   | position vector of $p$                                      |
| $r_{pq}$                      | distance between $p$ and $q$                                |
| $x, y, z$                     | cartesian co-ordinates                                      |
| $Z_a$                         | atomic number of atom $a$                                   |
| $\hat{P}(p, q)$               | permutation operator  |
| $\Phi$                        | general Slater determinant                                  |
| $N$                           | normalising constant  |
| $\psi$                        | spin-orbital  |
| $\alpha(s), \beta(s)$         | spin functions  |
| $\delta_{\alpha\beta}$        | Kronecker delta, properties in equation (I.15)              |
| $\hat{\Theta}$                | general hermitian operator                                  |
| $\langle \Theta \rangle$      | expectation value of $\hat{\Theta}$                         |
| $\hat{\Theta}(0)$             | general zero-particle operator                              |
| $\hat{\Theta}(p)$             | general one-particle operator                               |
| $\hat{\Theta}(p, q)$          | general two-particle operator                               |
| $\rho_1(x'_1/x'_1)$           | 1st order density function                                  |
| $\rho_2(x'_1 x'_2/x'_1 x'_2)$ | 2nd order density function                                  |
| $P_1(r'_1/r_1)$               | spinless 1st order density function                         |
| $P_2(r'_1 r'_2/r_1 r_2)$      | spinless 2nd order density function                         |



|  |   |
|--|---|
| $\rho_{k\ell}$   | an element of the matrix representation of $\rho_1$ in a spin-orbital basis   |
| $\underline{\rho}$   | matrix of representative coefficients $\rho_{k,\ell}$   |
| $P_{ij}$   | an element of the matrix representation of $P_1$ in a molecular orbital basis   |
| $P_{\mu\nu}$   | an element of the matrix representation of $P_1$ in an atomic orbital basis   |
| $M_{\mu\nu}$   | overlap integral between atomic orbitals $\chi_\mu, \chi_\nu$   |
| $c_{\mu i}$  | the coefficient of $\chi_\mu$ in $\phi_i$   |
| $S_{ij}$   | overlap integral between molecular orbitals $\phi_i, \phi_j$  |
| $V_{k\ell}$  | overlap integral between spin-orbitals $\psi_k, \psi_\ell$  |
| $m$  | number of basis atomic orbitals   |
| $\underline{\underline{M}}$                                      | mxm matrix of atomic orbital overlap integrals  |
| $\underline{\underline{S}}$                                      | nxn matrix of molecular orbital overlap integrals   |
| $\underline{\underline{V}}$                                      | NxN matrix of spin-orbital overlap integrals  |
| $ \underline{\underline{M}} $                                    | determinant of matrix elements of $\underline{\underline{M}}$   |
| $ \underline{\underline{S}} $                                    | determinant of matrix elements of $\underline{\underline{S}}$   |
| $ \underline{\underline{V}} $                                    | determinant of matrix elements of $\underline{\underline{V}}$   |
| $V^{k,\ell}$   | cofactor of (k, $\ell$ ) element of $ \underline{\underline{V}} $   |
| $S^{i,j}$  | cofactor of (i, j) element of $ \underline{\underline{S}} $   |
| $\underline{\underline{V}}^{-1}, \underline{\underline{S}}^{-1}$ | inverse matrices of $\underline{\underline{V}}$ and $\underline{\underline{S}}$ respectively  |
| $(\underline{\underline{V}}^{-1})_{\ell k}$                      | ( $\ell, k$ ) element of $\underline{\underline{V}}^{-1}$   |
| $(\underline{\underline{S}}^{-1})_{ij}$                          | (i, j) element of $\underline{\underline{S}}^{-1}$  |
| $h_{ii}$   | self integral = $\langle \phi_i   h   \phi_i \rangle = \int \phi_i^*(r_1) \hat{h}(1) \phi_i(r_1) dr_1$  |
| $J_{ij}$   | coulomb integral = $\langle \phi_i \phi_i   g   \phi_j \phi_j \rangle$<br>$= \int \phi_i^*(r_1) \phi_i(r_1) \hat{g}(1,2) \phi_j^*(r_2) \phi_j(r_2) dr_1 dr_2$ |

|   |  |
|---|--|
| $K_{ij}$                                      | exchange integral = $\langle \phi_i \phi_j / g / \phi_j \phi_i \rangle$<br>$= \int \phi_i^*(r_1) \phi_j(r_1) \hat{g}(1,2) \phi_j^*(r_2) \phi_i(r_2) dr_1 dr_2$ |
| $\hat{J}_j$                                   | Coulomb operator, see equation (I.60)  |
| $\hat{K}_j$                                   | exchange operator, see equation (I.61)   |
| $\hat{F}$                                     | Hartree-Fock hamiltonian operator  |
| $\epsilon_i$                                  | energy eigenvalue for $\phi_i$   |
| $\epsilon_{ij}$                               | expansion coefficient in the Hartree-Fock equation<br>(I.59)   |
| $\underline{\epsilon}$                        | $n \times n$ matrix of elements $\epsilon_{ij}$  |
| $\underline{U}$                               | a unitary matrix (transformation)  |
| $\underline{c}_i$                             | column vector of coefficients $c_{\mu i}$  |
| $F_{\mu\nu}$                                  | Hartree-Fock integral over atomic orbitals<br>$= \langle \chi_\mu / \hat{F} / \chi_\nu \rangle$  |
| $\underline{F}$                               | $m \times m$ matrix of elements $F_{\mu\nu}$   |
| $\zeta$                                       | atomic orbital exponent  |
| $n_p$   | principal quantum number   |
| $g_\mu$                                       | gaussian function  |
| $d_{\mu k}$                                   | linear expansion coefficient for a gaussian function   |
| $\underline{D}$                               | dipole moment  |
| $\hat{D}$                                     | dipole moment operator   |
| $\langle \underline{D} \rangle$               | expectation value of the dipole moment   |
| $q$   | charge   |
| $\hat{r}(p)$                                  | position vector operator   |
| $\underline{i}, \underline{j}, \underline{k}$ | unit co-ordinate vectors   |
| $\hat{D}_x, \hat{D}_y, \hat{D}_z$             | $x, y, z$ dipole moment operators  |
| $\hat{x}(p), \hat{y}(p), \hat{z}(p)$          | cartesian co-ordinate operators  |
| $z^i_{elec.}$                                 | part of the $z$ component of electronic moment allocated<br>to the $i$ th molecular orbital  |

|                      |  |
|----------------------|--|
| $z_{ai}$             | part of the atomic charge of atom a allocated to the $i$ th molecular orbital.           |
| $z^i$                | part of the z component of total dipole moment allocated to the $i$ th molecular orbital |
| $D_{XY}$             | dipole moment contribution of the XY sigma bond  |
| $D_X$                | dipole moment contribution of the X lone pair  |
| $N(i)$               | total population in molecular orbital $\phi_i$   |
| $N(\mu)$             | total gross population in atomic orbital $\chi_\mu$                                      |
| $N(i,\mu)$           | partial gross population in atomic orbital $\chi_\mu$ in molecular orbital $\phi_i$      |
| $\gamma$             | general real function  |
| $\underline{\gamma}$ | row vector of $\gamma$   |

REFERENCES

1. E. Schrodinger, Ann. Physik 79, 361 (1926)
2. R. McWeeny, Proc. Roy. Soc. London A223, 63 (1954)
3. R. McWeeny, Proc. Roy. Soc. London A232, 114 (1955)
4. R. McWeeny, Proc. Roy. Soc. London A235, 496 (1956)
5. R. McWeeny, Rev. Mod. Phys. 32, 335 (1960)
6. P.O. Lowdin, Phys. Rev. 97, 1474 (1955)
7. P.O. Lowdin, Phys. Rev. 97, 1490 (1955)
8. P.O. Lowdin, Phys. Rev. 97, 1509 (1955)
9. For a recent comment on bonding and quantum mechanics see  
G. Berthier, Int. J. Quantum Chem. 19, 985 (1981)
10. R.F.W. Bader, P.M. Beddall, & P.E. Cade, J. Amer. Chem. Soc. 93,  
3095 (1971)
11. R.F.W. Bader & P.M. Beddall, Chem. Phys. Lett. 8, 29 (1971)
12. R.F.W. Bader & P.M. Beddall, J. Chem. Phys. 56, 3320 (1972)
13. R.F.W. Bader, P.M. Beddall & J. Peslak, J. Chem. Phys. 58, 557  
(1973)
14. R.F.W. Bader & P.M. Beddall, J. Amer. Chem. Soc. 95, 305 (1973)
15. R.F.W. Bader, A.J. Duke & R.R. Messer, J. Amer. Chem. Soc. 95,  
7715 (1973)
16. S. Srebrenik & R.F.W. Bader, J. Chem. Phys. 61, 2536 (1974)
17. R.F.W. Bader in "Localisation and delocalisation in quantum  
chemistry. Vol. 1" Ed. O. Chalvet et al., D. Reidel, Holland  
(1975), p.15
18. see references in R. Daudel, in "Localisation and delocalisation  
in quantum chemistry. Vol. 1" Ed. O. Chalvet et al., D. Reidel,  
Holland (1975) p. 3

19. see R. McWeeny & B.T. Sutcliffe, "Methods of molecular quantum mechanics" Academic Press, London (1969)
20. M. Simonetta, "Forty years of valence bond theory" in "Structural chemistry and molecular biology" Eds. A. Rich & N. Davidson, Freeman, San Fransisco (1968)
21. W. Heitler & F. London, Z. Phys. 44, 455 (1927)
22. J. Gerratt, Spec. Per. Rep. Chem. Soc. - Theoret. Chem. 1, 60 (1974)
23. D.M. Chipman, B. Kirtman & W.E. Palke, J. Chem. Phys. 65, 2556 (1976)
24. D.M. Chapman, W.E. Palke & B. Kirtman, J. Amer. Chem. Soc. 102, 3377 (1980)
25. T. Koopmans, Physica 1, 104 (1933)
26. R.S. Mulliken, J. Chim. Phys. 46, 497 (1949)
27. J.P. Daudey, J.P. Malrieu & O. Rojas in "Localisation and de-localisation in quantum chemistry. Vol. 1" Ed. O. Chalvet et al., D. Reidel, Holland (1975) p. 155
28. W. Von Niessen, Theoret. Chim. Acta 38, 9 (1975)
29. G. Del Re, Int. J. Quantum Chem: -Symp. 7, 193 (1973)
30. W. England & M.S. Gordon, J. Amer. Chem. Soc. 93, 4649 (1971)
31. see discussion and references at end of section 3.1
32. D. Caldwell & H. Eyring, Adv. Quantum Chem. 11, 93 (1978)
33. see references in Chapter 9.
34. B. O'Leary, B.J. Duke & J.E. Eilers, Adv. Quantum Chem. 9, 1 (1975)
35. A.C. Hurley, "Electron correlation in small molecules", Academic Press, London (1977)
36. R. Polak, Theoret. Chim. Acta 14, 163 (1969)
37. P.W. Payne, J. Amer. Chem. Soc. 99, 3787 (1977)
38. H. Stoll, G. Wagenblast & H. Preuss, Theoret. Chim. Acta 57, 169 (1980)

39. R. Ponec, J. Mol. Struct. (Theochem) 86, 285 (1982)
40. C. Trindle & O. Sinanoglu, J. Amer. Chem. Soc. 91, 853 (1969)
41. D.A. Kleier, J. Hall, T. Halgren & W.N. Lipscomb, Proc. Nat. Acad. Sci. U.S.A. 71, 2265 (1974)
42. L.D. Brown, D.A. Kleier & W.N. Lipscomb, J. Amer. Chem. Soc. 99, 6787 (1977)
43. R. Bonaccorsi, C. Ghio, E. Scrocco & J. Tomasi, Isr. J. Chem. 19, 109 (1980)
44. R. Daudel in "Localisation and delocalisation in quantum chemistry. Vol. 1" Ed. O. Chalvet et al., D. Reidel, Holland (1975) p. 111
45. For example, W.N. Lipscomb, Acc. Chem. Res. 6, 257 (1973)
46. W.H. Adams, J. Chem. Phys. 42, 4030 (1965)
47. J.R. Hoyland, J. Amer. Chem. Soc. 90, 2227 (1968)
48. J.R. Hoyland, J. Chem. Phys. 50, 473 (1969)
49. W.H. Fink, J. Chem. Phys. 60, 402 (1974)
50. W. England, L.S. Salmon & K. Ruedenberg, Topics in Current Chem. 23, 31 (1971)
51. R. Daudel, M.E. Stephens, E. Kapuy & C. Kozmutza, Chem. Phys. Lett. 40, 194 (1976)
52. H. Weinstein & R. Pauncz, Adv. Atomic & Mol. Phys. 7, 97 (1971)
53. P. Millie, B. Levy & G. Berthier in "Localisation and delocalisation in quantum chemistry. Vol. 1" Ed. O. Chalvet et al., D. Reidel, Holland (1975), p. 59.
54. V. Fock, Z. Physik, 61, 126 (1930)
55. F. Hund, Z. Physik 73, 1 (1931)
56. F. Hund, Z. Physik 73, 565 (1932)

57. C.A. Coulson, *Trans. Farad. Soc.* 38, 433 (1942)
58. C.A. Coulson, *J. Chim. Phys.* 46, 198 (1949)
59. J.E. Lennard-Jones, *Proc. Roy. Soc. London A* 198, 1 (1949)
60. J.E. Lennard-Jones, *Proc. Roy. Soc. London A* 198, 14 (1949)
61. G.G. Hall & J.E. Lennard-Jones, *Proc. Roy. Soc. London A* 202, 155 (1950)
62. J.E. Lennard-Jones & J.A. Pople, *Proc. Roy. Soc. London A* 202, 166 (1950)
63. J.A. Pople, *Proc. Roy. Soc. London A* 202, 323 (1950)
64. G.G. Hall, *Proc. Roy. Soc. London A* 202, 336 (1950)
65. G.G. Hall & J.E. Lennard-Jones, *Proc. Roy. Soc. London A* 205, 357 (1951)
66. J.E. Lennard-Jones & J.A. Pople, *Proc. Roy. Soc. London A* 210, 190 (1951)
67. J.E. Lennard-Jones, *J. Chem. Phys.* 20, 1024 (1952)
68. A.C. Hurley, "On orbital theories of molecular structure". Thesis, Trinity College, Cambridge (1952)
69. J.A. Pople, *Quart. Rev. Chem. Soc.* 11, 273 (1957)
70. K. Ruedenberg in "Modern quantum chemistry. Part 1" Ed. O. Sinanoglu, Academic Press, N.Y. (1965) p. 85.
71. S.F. Boys & J.M. Foster, *Rev. Mod. Phys.* 32, 300 (1960)
72. S.F. Boys in "Quantum theory of atoms, molecules and the solid state" Ed. P.O. Lowdin, Academic Press, N.Y. (1966) p. 253
73. R.K. Nesbet, *J. Chem. Phys.* 36, 1518 (1962)
74. R. Bonaccorsi, C. Petrongolo, E. Scrocco & J. Tomassi, *J. Chem. Phys.* 48, 1500 (1968)
75. R. Bonaccorsi, C. Petrongolo, E. Scrocco & J. Tomassi, *Theoret. Chim. Acta* 15, 332 (1969)

76. R. Bonaccorsi, E. Scrocco & J. Tomasi, J. Chem. Phys. 52, 5270 (1970)
77. For example, R.C. Haddon & G.R. Williams, Chem. Phys. Lett. 42, 453 (1976) and reference 43.
78. R.S. Mulliken, Phys. Rev. 40, 55 (1932)
79. R.S. Mulliken, Phys. Rev. 41, 49 (1932)
80. R.S. Mulliken, Phys. Rev. 41, 751 (1932)
81. R.S. Mulliken, Phys. Rev. 43, 279 (1933)
82. R.S. Mulliken, J. Chem. Phys. 1, 492 (1933)
83. C. Edmiston & K. Ruedenberg, Rev. Mod. Phys. 35, 457 (1963)
84. C. Edmiston & K. Ruedenberg, J. Chem. Phys. 43, S97 (1965)
85. C. Edmiston & K. Ruedenberg in "Quantum theory of atoms, molecules and the solid state" Ed. P.O. Lowdin, Academic Press, N.Y. (1966) p. 263
86. R.M. Pitzer, J. Chem. Phys. 41, 2216 (1964)
87. R.M. Pitzer, J. Chem. Phys. 46, 4871 (1967)
88. U. Kaldor, J. Chem. Phys. 46, 1981 (1967)
89. W.J. Taylor, J. Chem. Phys. 48, 2385 (1968)
90. E. Switkes, R.M. Stevens, W.N. Lipscomb & M.D. Newton, J. Chem. Phys. 51, 2085 (1969)
91. E. Switkes, W.N. Lipscomb & M.D. Newton J. Amer. Chem. Soc. 92, 3837 (1970)
92. E. Switkes, W.N. Lipscomb & M.D. Newton, J. Amer. Chem. Soc. 92, 3847 (1970)
93. M.D. Newton, E. Switkes & W.N. Lipscomb, J. Chem. Phys. 53, 2645 (1970)
94. W. England, J. Chem. Phys. 58, 5182 (1973)
95. R. Barr & H. Basch, Chem. Phys. Lett. 32, 537 (1975)



96. W. Von Niessen, J. Chem. Phys. 56, 4290 (1972)
97. W. Von Niessen, Theoret. Chim. Acta 27, 9 (1972)
98. W. Von Niessen, Theoret. Chim. Acta 29, 29 (1973)
99. R.C. Sahni, Trans. Farad. Soc. 49, 1246 (1953)
100. J.A. Pople, J. Chem. Phys. 21, 2234 (1953)
101. F. Ellison & H. Shull, J. Chem. Phys. 23, 2348 (1955)
102. L. Burnelle & C.A. Coulson, Trans. Farad. Soc. 53, 403 (1957)
103. A.B.F. Duncan, J. Chem. Phys. 27, 423 (1957)
104. D. Peters, J. Chem. Soc., 2003 (1963)
105. D. Peters, J. Chem. Soc., 2015 (1963)
106. D. Peters, J. Chem. Soc., 4017 (1963)
107. D. Peters, J. Chem. Soc., 2901 (1964)
108. D. Peters, J. Chem. Soc., 2908 (1964)
109. D. Peters, J. Chem. Soc., 2916 (1964)
110. D. Peters, J. Chem. Soc., 3026 (1965)
111. D. Peters, J. Chem. Soc. A, 644 (1966)
112. D. Peters, J. Chem. Soc. A, 652 (1966)
113. D. Peters, J. Chem. Soc. A, 656 (1966)
114. R. Polak, Coll. Czech. Chem. Comm. 33, 2765 (1968)
115. W.S. Verwoerd, Chem. Phys. 44, 151 (1979)
116. T.A. Claxton, Chem. Phys. 52, 23 (1980)
117. A.B.F. Duncan & J.A. Pople, Trans. Farad. Soc. 49, 217 (1953)
118. R.S. Mulliken, J. Chem. Phys. 23, 1833 (1955)
119. R.S. Mulliken, J. Chem. Phys. 23, 1841 (1955)
120. R.S. Mulliken, J. Chem. Phys. 23, 2338 (1955)
121. R.S. Mulliken, J. Chem. Phys. 23, 2343 (1955)

122. R. McWeeny, J. Chem. Phys. 19, 1614 (1951)
123. R. McWeeny, J. Chem. Phys. 20, 920 (1951)
124. V. Magnasco & A. Perico, J. Chem. Phys. 47, 971 (1967)
125. V. Magnasco & A. Perico, J. Chem. Phys. 48, 800 (1968)
126. R. Polak, Int. J. Quantum Chem. 4, 271 (1970)
127. R. Polak, Chem. Phys. Lett. 9, 630 (1971)
128. R. Polak, Int. J. Quantum Chem. 6, 1077 (1972)
129. R. Polak, Theoret. Chim. Acta 24, 107 (1972)
130. R. Polak, Coll. Czech. Chem. Comm. 38, 1450 (1973)
131. R. Polak & J. Kavan, Coll. Czech. Chem. Comm. 40, 3743 (1975)
132. K.R. Roby, Mol. Phys. 28, 1441 (1974)
133. R. Polak, Coll. Czech. Chem. Comm. 43, 3292 (1978)
134. D. Caldwell, P. Redington & H. Eyring, Proc. Nat. Acad. Sci. U.S.A. 76, 3042 (1979)
135. W.H. Adams, J. Chem. Phys. 34, 89 (1961)
136. W.H. Adams, J. Chem. Phys. 37, 2009 (1962)
137. W.H. Adams, Chem. Phys. Lett. 12, 295 (1971)
138. T.L. Gilbert in "molecular orbitals in chemistry, physics and biology" Ed. P.O. Lowdin & B. Pullman, Academic Press, N.Y. (1964) p. 405.
139. P.W. Anderson, Phys. Rev. Lett. 21, 13 (1968)
140. P.W. Anderson, Phys. Rev. 181, 25 (1969)
141. J.D. Weeks, P.W. Anderson & A.G. Davidson, J. Chem. Phys. 58, 1388 (1973)
142. a) A.B. Kunz & T.L. Gilbert, Phys. Rev. B10, 3706 (1974)  
and references therein.  
b) H. Schlosser & T.L. Gilbert, J. Chem. Phys. 56, 8 (1972)  
and references therein.

- c) D.W. Bullett, *Solid State Phys.* 35, 129 (1980)
143. a) T.L. Gilbert, *Phys. Rev.* A6, 580 (1972)
- b) T.L. Gilbert, *J. Chem. Phys.* 60, 3835 (1974)
- c) H. Schlosser, *J. Chem. Phys.* 57, 4332 (1972)
- d) H. Schlosser, *J. Chem. Phys.* 57, 4342 (1972)
- e) H. Schlosser, *Chem. Phys. Lett.* 23, 545 (1973)
- f) H. Schlosser, *J. Chem. Phys.* 61, 2814 (1974)
- g) H. Schlosser, *Chem. Phys. Lett.* 35, 239 (1975)
- h) H. Schlosser, *Chem. Phys. Lett.* 44, 563 (1976)
144. T. Kambara, *J. Phys. Soc. Japan* 39, 187 (1975)
145. T. Kambara, *Prog. Theoret. Phys.* 55, 1335 (1976)
146. O. Matsuoka, *J. Chem. Phys.* 66, 1245 (1977)
147. E.L. Mehler, *J. Chem. Phys.* 67, 2728 (1977)
148. E.L. Mehler, *J. Chem. Phys.* 74, 6298 (1981)
149. D. Peters, *J. Chem. Phys.* 51, 1559 (1969)
150. D. Peters, *J. Chem. Phys.* 51, 1566 (1969)
151. D.L. Wilhite & J.L. Whitten, *J. Chem. Phys.* 58, 948 (1973)
152. J.M. Carpenter & D. Peters in "Localisation and delocalisation in quantum chemistry. Vol. 1" Ed. O. Chalvet et al., D. Reidel, Holland (1975) p. 99
153. H. Stoll & H. Preuss, *Theoret. Chim. Acta* 46, 11 (1977)
154. H. Stoll, G. Wagenblast & H. Preuss, *Theoret. Chim. Acta* 49, 67 (1978)
155. J.C. Slater, *Phys. Rev.* 37, 481 (1931)
156. L. Pauling, *J. Amer. Chem. Soc.* 53, 1367 (1931)
157. L. Pauling, "The nature of the chemical bond" 3rd edn., Cornell University Press (1960)
158. M. Randic & Z.B. Maksic, *Chem. Rev.* 72, 43 (1972)

159. D. Peters, *Trans. Farad. Soc.* 60, 1193 (1964)
160. J.N. Murrell, *J. Chem. Phys.* 32, 767 (1960)
161. A. Golebiewski, *Trans. Farad. Soc.* 57, 1849 (1961)
162. T.L. Gilbert & P.G. Lykos, *J. Chem. Phys.* 34, 2199 (1961)
163. P.G. Lykos & H.N. Schmeising, *J. Chem. Phys.* 35, 288 (1961)
164. P. Pelikan & L. Valko, *J. Mol. Struct.* 28, 229 (1975)
165. G. Del Re, *Theoret. Chim. Acta* 1, 188 (1963)
166. A. Veillard & G. Del Re, *Theoret. Chim. Acta* 2, 55 (1964)
167. C.A. Coulson & T.H. Goodwin, *J. Chem. Soc.*, 2851 (1962)  
[errata *J. Chem. Soc.*, 3161 (1963)]
168. G. Del Re, U. Esposito & M. Carpentieri, *Theoret. Chim. Acta*  
6, 36 (1966)
169. J.G. Stamper & N. Trinajstic, *J. Chem. Soc.* A, 782 (1967)
170. E. Gey, Z.B. Maksic & N. Trinajstic, *J. Mol. Struct.* 3, 21 (1969)
171. R. Boca, P. Pelikan, L. Valko & S. Miertus *Chem. Phys.* 11, 229  
(1975)
172. R. Boca, P. Pelikan, L. Valko & S. Miertus, *Chem. Phys.* 11, 237  
(1975)
173. R. Boca, *Chem. Zvesti* 30 13 (1976)
174. R. Boca, P. Pelikan & L. Valko, *Chem. Zvesti* 33, 289 (1979)
175. R. Boca, *Chem. Zvesti* 34, 18 (1980)
176. R. McWeeny & G. Del Re, *Theoret. Chim. Acta* 10, 13 (1968)
177. J.H. Letcher & T.H. Dunning, *J. Chem. Phys.* 48, 4538 (1968)
178. M.L. Unland, T.H. Dunning & J.R. Van Wazer, *J. Chem. Phys.*  
50, 3208 (1969)
179. J.H. Letcher, *J. Chem. Phys.* 54, 3215 (1971)
180. J.D. Petke & J.L. Whitten, *J. Chem. Phys.* 51, 3166 (1969)

181. K.H. Aufderheide, J. Chem. Phys. 73, 1777 (1980)
182. a) K.H. Aufderheide & A. Chung-Phillips, J. Chem. Phys. 73, 1789 (1980)  
b) K.H. Aufderheide & A.Chung-Phillips, J. Chem. Phys. 76. 1885 (1982)
183. W.H. Flygare & V.W. Weiss, J. Chem. Phys. 45, 2785 (1966)
184. G. Del Re, Int. J. Quantum Chem. 1, 293 (1967)
185. H. Weinstein & R. Pauncz, Symp. Farad. Soc. 2, 23 (1968)
186. H. Weinstein & R.Pauncz, Chem. Phys. Lett. 14, 161 (1972)
187. J.P. Foster & F. Weinhold, J. Amer. Chem. Soc. 102, 7211 (1980)
188. A.B. Rives & F. Weinhold, Int. J. Quantum Chem.Symp. 14, 201 (1980)
189. K.R. Sundberg, J. Bicerano & W.N. Lipscomb, J. Chem. Phys. 71, 1515 (1979)
190. M. Levy, T.S. Nee & R.G. Parr, J. Chem. Phys. 63, 316 (1975)
191. P.A. Christiansen & W. Palke, Chem. Phys. Lett. 31, 462 (1975)
192. M. Levy, J. Chem. Phys. 65, 2473 (1976)
193. S. Rothenberg, J. Chem. Phys. 51, 3389 (1969)
194. S. Rothenberg, J. Amer. Chem. Soc. 93, 68 (1971)
195. M.S. Gordon & W. England, J. Amer. Chem. Soc. 94, 5168 (1972)
196. E. Kapuy, C. Kozmutza, R. Daudel & M.E, Stephens, Theoret. Chim. Acta 53, 147 (1979)
197. E. Kapuy, C. Kozmutza & R. Daudel, Theoret. Chim. Acta 56, 259 (1980)
198. W. England, M.S. Gordon & K. Ruedenberg, Theoret. Chim. Acta 37, 177 (1975)
199. M.S. Gordon & W. England, J. Amer. Chem. Soc. 95, 1753 (1973)
200. K. Ruedenberg, Rev. Mod. Phys. 34, 326 (1962)

201. V. Magnasco & G.F. Musso, J. Chem. Phys. 46, 4015 (1967)
202. V. Magnasco & G.F. Musso, J. Chem. Phys. 47, 1723 (1967)
203. V. Magnasco G.F. Musso & R. McWeeny, J. Chem. Phys. 47,  
4617 (1967)
204. V. Magnasco & G.F. Musso, J. Chem. Phys. 47, 4629 (1967)
205. V. Magnasco, Theoret. Chim. Acta 21, 267 (1971)
206. V. Magnasco & G.F. Musso, Theoret. Chim. Acta 21, 280 (1971)
207. V. Magnasco & G.F. Musso, J. Chem. Phys. 54, 2925 (1971)
208. V. Magnasco & G.F. Musso, Chem. Phys. Lett. 9, 433 (1971)
209. V. Magnasco & G.F. Musso, J. Chem. Phys. 60, 3744 (1974)
210. V. Magnasco, G.F. Musso & M.P. Giardina, J. Chem. Phys. 60,  
3749 (1974)
211. V. Magnasco & G.F. Musso, J. Chem. Phys. 60, 3754 (1974)
212. H.A. Bent, Chem. Rev. 61, 275 (1961)
213. A.D. Walsh, Discuss. Farad. Soc. 2, 18 (1947)
214. R. McWeeny, "Coulson's Valence" 3rd edn., Oxford University  
Press (1979)
215. D. Peters, Tetrahedron 19, supp. 2, 143 (1963)
216. C.A. Coulson, comment following reference 215.
217. T.A. Halgren, L.D. Brown, D.A. Kleier, & W.N. Lipscomb,  
J. Amer. Chem. Soc. 99, 6793 (1977)
218. N.V. Sidgwick & H.E. Powell, Proc. Roy. Soc. London A 176, 153  
(1940)
219. R.J. Gillespie & R. Nyholm, Quart. Rev. Chem. Soc. 11, 339  
(1957)
220. R.J. Gillespie "Molecular Geometry" Van Nostrand-Rheinhold,  
London (1972)

221. A.E. Douglas & D. Sharma, J. Chem. Phys. 21, 448 (1953)
222. W.J. Hehre, W.A. Latham, R. Ditchfield, M.D. Newton & J.A. Pople, "Gaussian 70" Programme 236, Quantum Chemistry Package Exchange, Indiana University (1971)
223. W.J. Hehre, R.F. Stewart & J.A. Pople, J. Chem. Phys. 51, 2657 (1969)
224. P. Mallinson & D. Peters, University of London Computer Centre Bulletins B5. 10/1, B5. 10/2 (1976)
225. R.C. Raffanetti & K. Ruedenberg, Int. J. Quantum Chem. -Symp. 3, 625 (1970)
226. W.J. Hehre, R.F. Stewart & J.A. Pople, Symp. Farad. Soc. 2,15 (1968)
227. P. Politzer & R.G. Parr, J. Chem. Phys. 64, 4634 (1976)
228. R.N. Dixon & I.L. Robertson, Spec. Per. Rep. Chem. Soc. -Theoret. Chem. 3, 100 (1978)
229. J.C. Barthelat & P. Durand, Chem. Phys. Lett. 16, 63 (1972)
230. C. Trindle & O. Sinanoglu, J. Chem. Phys. 49, 65 (1968)
231. O.R. Gilliam, C. Johnson & W.Gordy, Phys. Rev. 78, 140 (1950)
232. "Handbook of Chemistry and Physics" 56th edition., Ed. R.C. Weast, CRC Press, Cleveland, Ohio (1975)
233. W.S. Benedict, N. Gailar & E.K. Plyler, J. Chem. Phys. 24,1139, (1956)
234. For example
- a) D. Neumann & J.M. Moskowitz, J. Chem. Phys. 49, 2056 (1968)
- b) D. Neumann & J.M. Moskowitz, J. Chem. Phys. 50, 2216 (1969)
235. A.L. McClellan, "Tables of Experimental Dipole Moments" Freeman, San Fransisco (1963)
236. R.D. Nelson, D.R. Lide & A.A. Maryott, "Selected Values of Electric Dipole Moments for Molecules in the Gas Phase" Nat. Bureau Standards (U.S.), Govt. Printing Office, Washington D.C. (1967)

237. L.A. Gribov, "Intensity Theory for Infrared Spectra of Polyatomic Molecules" Consultants Bureau, New York (1964)
238. L.M. Sverdlov, M.A. Kovner & E.P. Krainov, "Vibrational Spectra of Polyatomic Molecules" John Wiley & Sons, New York (1974)
239. "Vibrational Spectroscopy - Modern Trends" Eds. A.J. Barnes & W.J. Orville-Thomas, Elsevier, Amsterdam (1977) Chap. 13.
240. W. Person & D. Steele, Spec. Per. Rep. Chem. Soc. -Mol. Spectros. 2, 357 (1974)
241. E.M. Lassetre & L.B. Dean, J. Chem. Phys. 17, 317 (1949)
242. L. Radom, W.J. Hehre & J.A. Pople, J. Amer. Chem. Soc. 94, 2371 (1972)
243. D.M. Golden & S.W. Benson, Chem. Rev. 69, 125 (1969)
244. J.A. Kerr, Chem. Rev. 66, 465 (1966)
245. R. Dixon & H. Lambertson, J. Mol. Spectros. 25, 12 (1968)
246. R. Polak, Coll. Czech. Chem. Comm. 39, 2877 (1974)
247. D.A. Kleier, T.A. Halgren, J.H. Hall & W.N. Lipscomb, J. Chem. Phys. 61, 3905 (1974)
248. L.A. Burke, G. Leroy, R. Daudel & M.E. Stephens, Chem. Phys. Lett. 57, 15 (1978)
249. K.R. Roby, Mol. Phys. 27, 81 (1974) and references therein.
250. R. Heinzmann & R. Ahlrichs, Theoret. Chim. Acta 42, 33 (1976)
251. S. Iwata, Chem. Phys. Lett. 69, 305 (1980)
252. R. Polak, Theoret. Chim. Acta 50, 21 (1978)
253. S. Huzinaga & S. Narita, Isr. J. Chem. 19, 242 (1980)
254. R.S. Mulliken, J. Chem. Phys. 19, 900 (1951)
255. P.O. Lowdin, J. Chem. Phys. 18, 365 (1950)



256. R.F.W. Bader, J. Amer. Chem. Soc. 86, 5070 (1964)
257. A.G. Massey, "The Typical Elements" 1st edn., Penguin Books (1972)
258. See for example, Figure 14, page 27 of reference 257.
259. K.H. Aufderheide, J. Chem. Phys. 76, 1897 (1982)
260. E.M. Layton & K. Ruedenberg, J. Phys. Chem. 68, 1654 (1964)
261. R.R. Rue & K. Ruedenberg, J. Phys. Chem. 68, 1676 (1964)
262. See for example, pages 151-153 of reference 214.
263. M.F. Guest, I.H. Hillier & V.R. Saunders, J. Chem. Soc. Farad. Trans. II 68, 866 (1972)
264. M.F. Guest & I.H. Hillier, Int. J. Quantum Chem. 6, 967 (1972)
265. M.E. Stephens, E. Kapuy & C. Kozmutza, Theoret. Chim. Acta 45, 111 (1977)
266. A. Hinchliffe & D.G. Bounds, Spec. Per. Rep. Chem. Soc. -Theoret. Chem. 3, 80 (1978)
267. M.A. Robb, W.J. Haines & I.G. Csizmadia, J. Amer. Chem. Soc. 95, 42 (1973)
268. A.T. Amos, R.J. Crispin & R.A. Smith, Theoret. Chim. Acta 39, 7 (1975)
269. E. Kapuy & C. Kozmutza, Theoret. Chim. Acta 43, 175 (1976)
270. H.P. Figeys, D. Berckmans & P. Geerlings, J. Mol. Struct. 57, 271 (1979)
271. G. Riley, S. Suzuki, W.J. Orville-Thomas & B. Galabov, J. Chem. Soc. Farad. Trans. II 74, 1947 (1978)
272. A. Hinchliffe & I.F. Kidd, J. Chem. Soc. Farad. Trans. II 76, 172 (1980)
273. W.M.A. Smit & T. Van dam, J. Chem. Phys. 72, 3658 (1980)

274. A. Schmiedekamp, S. Skaarup, P. Pulay & J.E. Boggs,  
J. Chem. Phys. 66, 5769 (1977)
275. R.E. Bruns, A. Bassi & P. Kuznesof, J. Amer. Chem. Soc. 98,  
3432 (1976)
276. H.P. Figeys, P. Geerlings & C. Van Alsenoy, J. Chem. Soc.  
Farad. Trans. II 75, 528 (1979)
277. B. Galabov & W.J. Orville-Thomas, J. Chem. Phys. 71, 4716 (1979)
278. See figure 6.20 page 172 of reference 214.
279. K. Kuchitsu & Y. Morino, Bull. Chem. Soc. Japan 38, 814 (1965)
280. for example, T.H. Dunning, R.M. Pitzer & S. Aung, J. Chem.  
Phys. 57, 5044 (1972)
281. A similar conclusion for a number of molecules is reached in  
reference 24
282. C.A. Naleway & M.E. Schwartz, J. Amer. Chem. Soc. 95, 8235 (1973)
283. R.G. Maclagen & G.W. Schnuelle, Theoret. Chim. Acta 46, 165  
(1977)
284. M. Born & J.R. Oppenheimer, Ann. Physik 84, 457 (1927)
285. J.C. Slater, Phys. Rev. 34, 1293 (1929)
286. P. Dirac, Proc. Cambridge Phil. Soc. 26, 376 (1930)
287. J.E. Lennard-Jones. Proc. Cambridge Phil. Soc. 27, 469 (1931)
288. a) D.R. Hartree, Proc. Cambridge Phil. Soc. 24, 89 (1928)  
b) D.R. Hartree, Proc. Cambridge Phil. Soc. 24, 111 (1928)
289. J.C. Slater, Phys. Rev. 35, 210 (1930)
290. G.G. Hall, Proc. Roy. Soc. London A 205, 541 (1951)
291. C.C.J. Roothaan, Rev. Mod. Phys. 23, 69 (1951)
292. J.C. Slater, Phys. Rev. 36, 57 (1930)

293. S.F. Boys, Proc. Roy. Soc. London A 200, 542 (1950)
294. J.M. Foster & S.F. Boys, Rev. Mod. Phys. 32, 303 (1960)
295. C.M. Reeves & R. Fletcher, J. Chem. Phys. 42, 4073 (1965)
296. K. Oohata, H. Taketa & S. Huzinaga, J. Phys. Soc. Japan 21,  
2306 (1966)
297. R.H. Pritchard & C.W. Kern, J. Amer. Chem. Soc. 91, 1631 (1969)
298. R. Bonaccorsi, E. Scrocco & J. Tomasi, J. Amer. Chem. Soc.  
98, 4049 (1976)
299. P.O. Lowdin, Adv. Quantum Chem. 5, 185 (1970)
300. R. Overill, King's College London, Computer Unit Bulletin K5.10/1  
(1977)
301. I.H. Hillier & V.R. Saunders, Int. J. Quantum Chem. 7, 699 (1973)
302. J.A. Nelder & R. Mead, Computer J. 7, 308 (1965)
303. J.M. Parkinson & D. Hutchinson, "An Investigation into the  
Efficiency of Variants of the Simplex Method" in "Numerical Methods  
for Non-Linear Optimization" Ed. F.A. Lootsma, Academic Press  
(1972)
304. M.J.D. Powell, Computer, J. 7, 155 (1964)
305. J.H. Wilkinson & C. Reinsch, "Handbook for Automatic  
Computation. Vol. II Linear Algebra" Springer-Verlag (1971)  
pp. 93-110